



**Elucidating bioadhesive processes in nasal drug  
delivery systems**

**By**

**Michelle Armstrong**

A thesis submitted to the Strathclyde Institute of Pharmacy and  
Biomedical Sciences, University of Strathclyde, in fulfilment of the  
requirement for degree of Doctor of Philosophy

2014

## **Declaration of authenticity and author's rights**

‘This thesis is the result of the author’s original research. It has been composed by the author and has not been previously submitted for examination which has led to the award of a degree.’

‘The copyright of this thesis belongs to the author under the terms of the United Kingdom Copyright Acts as qualified by University of Strathclyde Regulation 3.50. Due acknowledgement must always be made of the use of any material contained in, or derived from, this thesis.’

Signed:

Date:

This thesis is dedicated to the loving memory of Peter John Davis Armstrong and  
David Leslie Haird. Two wonderful and heroic men taken from us too soon.

## **Acknowledgements**

I would like to begin by thanking Prof. Clive Wilson for his continued support, advice and encouragement throughout my PhD. You are an amazing mentor and I am so grateful for everything you have done for me. Huge thanks also go to Dr. Fiona McInnes for sparking my interest in the field of nasal drug delivery and to Dr. Gavin Bone, from GlaxoSmithKline, for his input and industrial insight during the course of this research. Special thanks also goes out to Dr. Anne Boyter for her words of encouragement throughout.

From the University of Strathclyde I would like to thank Dr. Niall McAlinden, from the Institute of Photonics, for his help with the microrheology and to the technical staff, especially Anne Goudie, for always being there whenever I required a helping hand. I am also very grateful for the help and encouragement I received from Dr Ibrahim Khadra, you helped me so much when all I wanted to do was run away.

To the beautiful friends I have made throughout the course of my PhD; Lisa, Kelly, Ruairidh, Joe, Munerah, Gracie and Stewart, thank you for always being there and for the all good times we have shared. Sincere thanks goes to my wonderful mentor and friend Dr Jen Mains, thanks for pushing me further and for making me a better person. Your enthusiasm and drive inspires me. To three of the most fabulous people I have ever met; Jen, Shonagh and Gemma. You made each and every day of my PhD an absolute joy and I am eternally grateful – “that’s what makes you beautiful!” To Claire and Louise, my lifelong friends, thank you for sticking by me when I decided to go back to studying and thank you for reminding me that there is a life outside of a PhD!

I would like to also thank my loving family. To my amazing Mum and Dad, thank you for your support over the years and for always believing in me. You are both so inspirational and I cannot thank you enough for everything you have both done for me. To my granny, you are a woman who believes in hard work and this has inspired me from an early age. Thank you for instilling this attitude into me, I think I would have given up a long time ago without it! To Sandie, my wonderful Mother-in-Law, thank you for your limitless encouragement and words of wisdom. You are just fabulous. Thanks also to Nicola and Laura, the sisters I never had. You have the infectious laughter and energy that reminds me to smile and be grateful for everything in life.

Finally, a very special thank you to Neil for being my rock throughout this whole process. Thank you for putting up with my tantrums and dramas and for always supporting me, no matter what. Your unconditional love has inspired me to always aim higher and I strive to always make you proud. I could not have done it without you.

## Table of Contents

Declaration of authenticity and author's rights .....	i
Acknowledgements .....	iii
Table of Contents .....	1
Abstract .....	1
Chapter 1 General introduction .....	1
1.1 Introduction .....	1
1.2 Anatomy and physiology of the nasal cavity .....	3
1.2.1 Nasal cavity .....	3
1.2.2 Mucus .....	7
1.3 Factors influencing nasal absorption .....	10
1.3.1 Physiological factors affecting drug absorption .....	11
1.3.1.1 Mucociliary clearance .....	11
1.3.1.2 Vasculature in the nasal cavity .....	12
1.3.1.3 Enzymatic degradation .....	13
1.3.2 Drug and formulation factors affecting absorption .....	13
1.3.2.1 Molecular weight .....	13
1.3.2.2 Lipophilicity .....	14
1.3.2.3 pH of drug formulation .....	15
1.4 Mucoadhesion .....	16
1.4.1 Theories of mucoadhesion .....	17
1.4.1.1 The wettability theory .....	18
1.4.1.2 The electronic theory .....	19
1.4.1.3 The fracture theory .....	19
1.4.1.4 The adsorption theory .....	20

1.4.1.5	The diffusion theory .....	20
1.4.1.6	The mechanical theory .....	21
1.4.2	Factors affecting mucoadhesion.....	21
1.4.2.1	Molecular weight and chain length .....	21
1.4.2.2	Crosslinking and swelling .....	22
1.4.2.3	pH and charge .....	22
1.4.2.4	Concentration .....	23
1.4.2.5	Viscosity.....	23
1.4.3.	Mucoadhesive polymers.....	24
1.4.3.1	Cellulose derivatives .....	25
1.4.3.2	Carbomers .....	29
1.4.3.3	Chitosan .....	30
1.5	Mucoadhesive testing.....	31
1.5.1	Texture analyser .....	31
1.5.2	Rheology .....	34
1.5.3	Atomic force microscopy.....	38
1.5.3	Other techniques.....	39
1.7	Project aim and objectives .....	41
Chapter 2	Rheological analysis of mucoadhesive polymeric nasal formulations .	42
2.1	Introduction .....	42
2.2	Materials.....	43
2.2.1	Apparatus .....	43
2.2.2	Chemicals.....	43
2.3	Methods.....	44
2.3.1	Preparation of mucoadhesive polymeric nasal formulations .....	44
2.3.2	Preparation of placebo nasal formulation .....	45

2.3.3	Preparation of mucin solution .....	46
2.3.4	Rheological flow behaviour of mucoadhesive polymeric nasal formulations .....	46
2.3.5	Analysis of viscoelasticity of mucoadhesive polymeric nasal formulations .....	48
2.4	Statistical analysis .....	49
2.5	Results and discussion.....	49
2.5.1	Rheological flow behaviour of mucoadhesive polymeric nasal formulations and mucin formulations .....	49
2.5.2	Analysis of viscoelasticity of mucoadhesive polymeric nasal formulations .....	75
2.6	Conclusion.....	100
Chapter 3 Investigation into mucus/polymer interfacial interactions using rheology and microrheology .....		102
3.1	Introduction .....	102
3.2	Materials.....	106
3.2.1	Apparatus .....	106
3.2.2	Chemicals.....	107
3.3	Methods.....	107
3.3.1	Preparation of mucoadhesive polymeric nasal formulations .....	107
3.3.2	Preparation of placebo nasal formulation .....	108
3.3.3	Preparation of mucin solution .....	108
3.3.4	Preparation of samples for rheological analysis.....	108
3.3.5	Preparation of samples for microrheological analysis .....	109
3.3.6	Assessment of interfacial interactions of mucoadhesive polymeric nasal formulations using rheology .....	109

3.3.7	Assessment of interfacial interactions of mucoadhesive polymeric nasal formulations using microrheology .....	110
3.4	Statistical analysis .....	112
3.5	Results and discussion.....	112
3.5.1	Assessment of interfacial interactions of polymeric nasal formulations and mucin using rheology.....	112
3.5.2	Assessment of interfacial interactions of mucoadhesive polymeric nasal formulations and mucin using microrheology .....	118
3.6	Conclusion.....	123
Chapter 4	Adhesion studies of mucoadhesive polymeric nasal formulations....	125
4.1	Introduction .....	125
4.2	Materials.....	126
4.2.1	Apparatus .....	126
4.2.2	Chemicals.....	127
4.3	Methods.....	128
4.3.1	Preparation of mucoadhesive polymeric nasal formulations .....	128
4.3.2	Preparation of placebo nasal formulations.....	128
4.3.3	Preparation of Krebs Bicarbonate Ringer solution .....	128
4.3.4	Preparation of porcine nasal tissue.....	129
4.3.7	Measurement of mucoadhesive strength of polymeric nasal formulations and placebo nasal formulations .....	132
4.4	Results and discussion.....	134
4.4.1	Measurement of mucoadhesive strength of polymeric nasal formulations .....	134
4.5	Conclusion.....	143
Chapter 5	The impact of spray device actuation on the rheological behaviour of mucoadhesive polymeric nasal formulations	146

5.1	Introduction .....	146
5.2	Materials.....	149
5.2.1	Apparatus .....	149
5.2.2	Chemicals.....	150
5.3	Methods.....	150
5.3.1	Preparation of mucoadhesive polymeric nasal formulations .....	150
5.3.2	Rheological investigation into the effect of spray device actuation on the flow behaviour of mucoadhesive polymeric nasal formulations ....	151
5.4	Statistical Analysis .....	152
5.5	Results and discussion.....	152
5.5.1	The effect of spray device actuation on the rheological flow behaviour of mucoadhesive polymeric nasal formulations.....	152
5.6	Conclusion.....	182
Chapter 6 Summary and future work.....		184
References .....		192
Abbreviations .....		205
List of figures .....		207
List of tables.....		215
List of equations.....		217
Publications and presentations .....		218

## **Abstract**

Mucoadhesive formulations have been used to increase the residence time and improve bioavailability of nasal dosage forms. The exact nature of the interplay between formulations and the mucus layer has not been defined, although theories have been proposed suggesting that certain characteristics are required for optimum mucoadhesivity. This thesis presents an investigation into the effects of the properties of excipients in nasal formulations on their mucoadhesive performance. The main factors that were investigated included molecular weight, concentration, crosslinking density, charge, and viscosity.

It was established using rotational and oscillation rheology that the polymeric formulations with the highest molecular weight expressed the highest viscosity. Thixotropy, a vital property in mucoadhesion, was also assessed. The greatest thixotropy was found with polymers of increasing molecular weight whereas low molecular weight polymers exhibited little or no thixotropy. As expected, high molecular weight polymers produced strongly gelled networks; a requirement for mucoadhesion. Mucoadhesive interactions between polymers and mucin were analysed using standard rheology and microrheology. Greater synergy was found with high molecular weight, linear, ionic polymers; factors which allow for improved chain interactions. Texture analysis of the formulations confirmed that the adhesive forces increased for higher molecular weight, ionic polymers.

In conclusion, it was found that a combination of a high molecular weight, increased viscosity, charge, and a moderate level of crosslinking are all favourable properties in a polymeric nasal spray. The formulation of a mucoadhesive dosage form with these characteristics may improve the retention time of the formulation within the nose, resulting in an increased opportunity for drug absorption and thus greater bioavailability.

## **Chapter 1 General introduction**

### **1.1 Introduction**

The administration of drugs through the nasal cavity has become established in recent decades as an inexpensive and non-invasive technique for the local and systemic delivery of drugs which might require parenteral administration to attain efficacy (Pires *et al.*, 2009, Privalova *et al.*, 2012). Intranasal drug delivery offers direct access to the systemic circulation, avoiding first pass hepatic extraction. The delivery route is facile and drug formulations are thus easily administered without the need for extensive training, making intranasal delivery highly desirable for both patients and medical practitioners (Costantino *et al.*, 2007). These factors coupled with the potential large surface area (150 cm<sup>2</sup>, (Illum *et al.*, 1987)), the porous endothelial membrane, and highly vascularised sub-epithelial layer offer an attractive alternative of non-parenteral administration for therapeutic compounds (Turker *et al.*, 2004). In particular, the nose provides an effective route for the delivery of systemically active drugs, including peptides susceptible to acidic degradation in the stomach, such as oxytocin and calcitonin. Nasal drug delivery may be desirable in crisis treatments, for example accidental overdose with opiates. The advantages of this method of administration within emergency treatment environments have been illustrated by many authors (Kerr *et al.*, 2008, Merlin *et al.*, 2010, Sibley *et al.*, 2013).

It can be said that drug delivery via the nasal cavity has a promising future but it is not without its disadvantages. The major limitations of nasal drug delivery include

limited capacity from conventional spray systems, the mucociliary clearance of instilled or sprayed solutions (Kim, 2008, Storms and Farrar, 2009) and the fragile nature of the mucosa; however, developments in nasal delivery technology, such as ViaNase<sup>®</sup>, may be able to exploit the benefits of moderated viscosified solutions to sustain delivery of large instilled volumes (Figure 1.1).

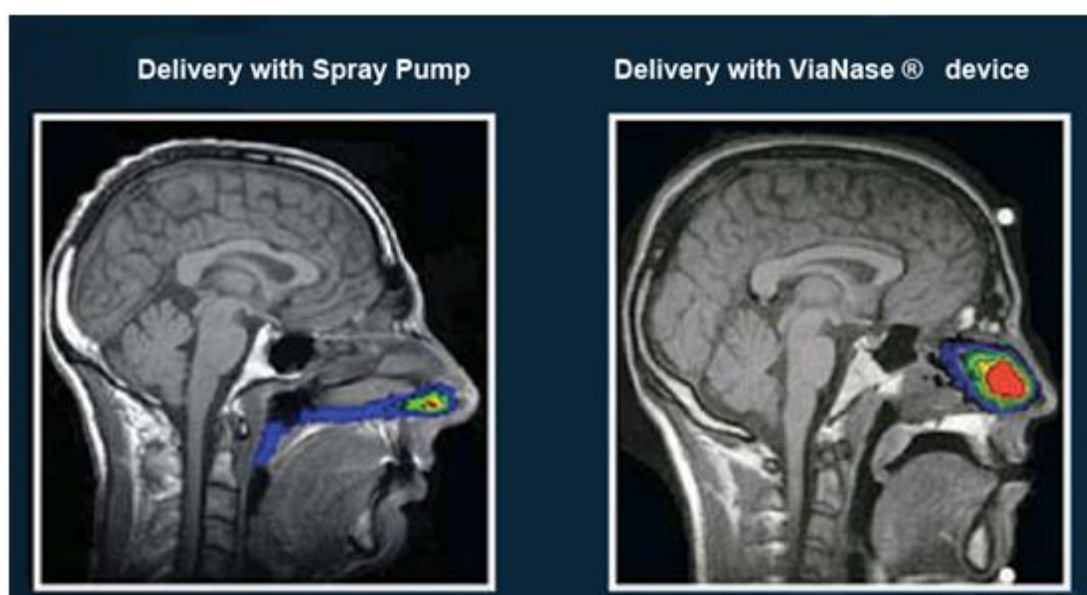


**Figure 1.1** Illustrating the difference in nasal deposition achieved with the use of different delivery devices.

The addition of mucoadhesive polymers allows for additional contact of the formulation, facilitating drug absorption and maximising bioavailability.

The mucosa of the nose is particularly complex, covered by different types of epithelium with protective (squamous), respiratory (ciliated) and olfactory functions, together with numerous goblet cells. In order to relate the deposition of a

formulation to likely outcomes, it is necessary to consider the anatomical and physiological aspects of the human nasal apparatus.

## **1.2 Anatomy and physiology of the nasal cavity**

### **1.2.1 Nasal cavity**

The nose is a complex, multifunctional organ positioned on the face between the eyes. It is the doorway to the respiratory system and runs posteriorly to the nasopharynx, further leading to the trachea and oesophagus. The nasal cavity is separated into two symmetrical halves by the median septum which stretches posteriorly to the nasopharynx (Harkema *et al.*, 2006). The majority of the nasal cavity is occupied by the respiratory region and the turbinates, which are also known as the nasal conchae. Lateral walls divide the respiratory region into three (or four) sections (Figure 1.2 and Figure 1.3); the superior nasal turbinate and meatus at the top, the middle nasal turbinate and meatus below and the inferior turbinate and meatus at the base, which are all important for maintaining the facilitation of temperature regulation and humidification of inspired air by sustaining a slit-like cavity. A fourth, much smaller turbinate, known as the supreme turbinate, is present in approximately 60% of the population and is located above the three more common turbinates (Gizurason, 2012). Spongy mucosa covers the thin, skeletal turbinates. One function of the turbinates is to prepare the inspired air prior to it reaching the lungs. The spaces between the turbinates are known as meatus and are essentially

flues which the inhaled air flows through. Swell bodies, located within the septum and turbinates, can adjust the width of the normally tight spaces. A tight spacing is always maintained which results in the inhaled air being in constant close proximity to the moist mucus lining of the nasal cavity. Rich vasculature through the arteriovenous anastomoses in the turbinates facilitates the heating and humidifying of the air. Another aid to this process comes from the anterior serous glands, seromucous glands and goblet cells which secrete fluid to sustain the humidification of the air. The presence of these folded turbinates, along with approximately 300 microvilli present on each cell, also provides the nasal cavity with an increased surface area.

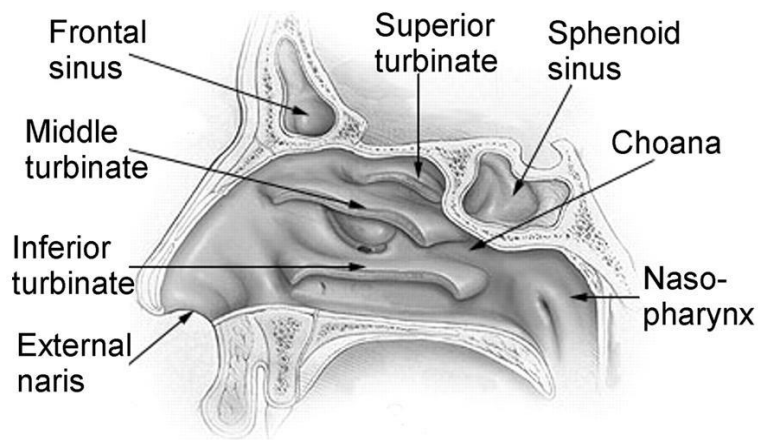


**Figure 1.2** Sagittal section of the nasal cavity (Liu et al., 2009).

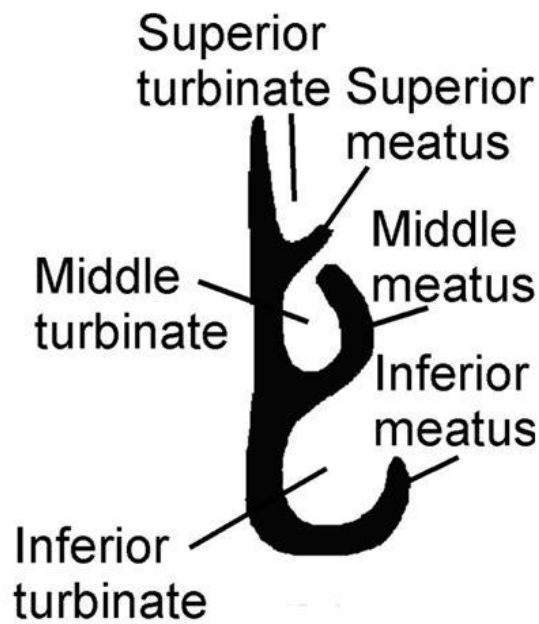


**Figure 1.3** Frontal plane midway through the nasal cavity (Liu et al., 2009).

The nasal passage possesses three individual functional regions; the vestibular region, the respiratory region and the olfactory region. The nasal vestibule is the most anterior part of the nasal cavity, which is adjacent to the atrium (Kim, 2008), and opens through the nostrils to the face. It acts as a baffle system and possesses numerous vibrissae (nasal hairs) which aid in the filtration of large airborne particles. This region of the nasal cavity contains stratified and squamous epithelial cells which are keratinised with sebaceous glands. The nasal vestibule can withstand the harmful effects of noxious environmental materials and is very resistant to dehydration. However, it allows limited permeation of substances and is therefore not a preferred site for the administration and absorption of drugs (Csaba *et al.*, 2009).

The highly vascularised respiratory region constitutes approximately 80 to 90% of the total area of the nasal cavity (Lochhead and Thorne, 2012) and consists of pseudostratified columnar cells with approximately 100 cilia covering each ciliated cell and approximately 300 microvilli covering each ciliated and nonciliated cell. The microvilli further increase the surface area of the nasal cavity making the respiratory region ideal for drug absorption. Goblet cells are interspersed with the pseudostratified columnar cells of the respiratory region but it has been recorded that compared with the submucosal glands, the volume of mucus produced by the goblet cells is insignificant (Mygind and Dahl, 1998). The mucus layer is formed from secretions of the submucosal glands and works in collaboration with the actively beating cilia to trap and remove any foreign particles before transporting them towards the nasopharynx, where they are then swallowed ahead of destruction by the gastrointestinal tract. This is termed mucociliary clearance and is an important defence mechanism of the body, preventing noxious substances from reaching the lungs. It is therefore imperative that any drug formulation does not interfere with mucociliary clearance as any changes in this process can lead to an increased risk of respiratory disease (Lansley, 1993).

The olfactory region is concerned with the process of olfaction, the prime function of the nose, and is located at the uppermost region of the nasal cavity. It covers approximately 10-20 cm<sup>2</sup> of the nasal cavity (Ali *et al.*, 2010) and is predominantly lined with a mucous membrane, however a small area is lined by neuroepithelium. The neuroepithelium possess dendritic fibres which project into the nasal cavity.

Bowman's glands produce a mucus secretion which thinly covers the dendritic fibres. The secretion acts as a solvent and dissolves odours from the air which chemically stimulates the nerve cells of the olfactory region and registers a smell. The neuroepithelium is the only part of the central nervous system that is fully exposed to the external environment (Pires *et al.*, 2009). It is for this reason that many researchers have exploited the olfactory region in an effort to deliver drugs direct to the central nervous system (CNS) and thus bypassing the blood brain barrier. Many reported investigations have used animal models to deliver such drugs as siRNA (Renner *et al.*, 2012a), insulin (Renner *et al.*, 2012b), recombinant iduronidase (Wolf *et al.*, 2012) and nerve growth factor (Zhu *et al.*, 2011). The olfactory region in animals is generally much larger and more accessible compared to humans and in general the bioavailability of the drug within the CNS is less than 1% (Illum, 2012). There are many major challenges to overcome when attempting intranasal delivery of drugs to the CNS of humans. In order to improve their bioavailability, further work needs to be completed to gain a full understanding of the pathways and mechanisms involved in such a delivery system.

### **1.2.2 Mucus**

Mucus is a non-Newtonian, thixotropic gel which behaves like an elastic solid when under low magnitudes of shear (Lai *et al.*, 2009). The nasal mucus possesses a number of physiological functions including the enzymatic and physical protection of the mucosa and the transportation of particulate matter due to its adhesive nature.

The mucus also permits efficient heat transfer, exhibits surface electrical activity and is the fundamental factor in mucoadhesion.

Mucus is primarily made up of approximately 95% water, 1% salts, 1% of other proteins (immunoglobulins and albumins, lysosymes and lactoferrins) and < 1% lipids (phospholipids, fatty acids and cholesterol) (Baraniuk and Merck, 2009, Ozsoy *et al.*, 2009). Although the main component of mucus is water, the key constituent responsible for the gel like properties of mucus is mucin. Mucin is a high molecular weight glycoprotein ranging from 0.5 to 40 MDa in size (Cone, 2009) and is responsible for the rheological properties of the mucus. The concentration of the glycoprotein determines how cohesive the mucus is (Serra *et al.*, 2009b).

Mucin is highly glycosylated and approximately 80% of the total weight of mucin is composed of carbohydrates, namely N-acetyl-D-galactosamine, N-acetyl-D-glucosamine, L-fucose, D-galactose, and sialic acid (Serra *et al.*, 2009b). Mucin consists of many subunits which are connected by disulfide bridges. A typical mucin monomer is shown in Figure 1.4. The amino (N<sub>2</sub>H-) and carboxy (-COOH) terminal groups are rich in cysteines and are involved in the establishment of intermolecular and intramolecular disulfide bridges of mucin monomers (Figure 1.4 and 1.5).

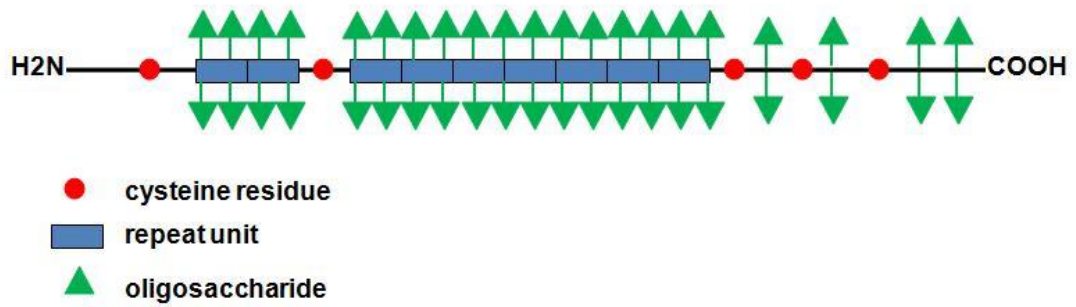


**Figure 1.4** Schematic drawing of a general mucin monomer showing the amino and carboxy terminals, the cysteine rich residues, repeating units and oligosaccharides.

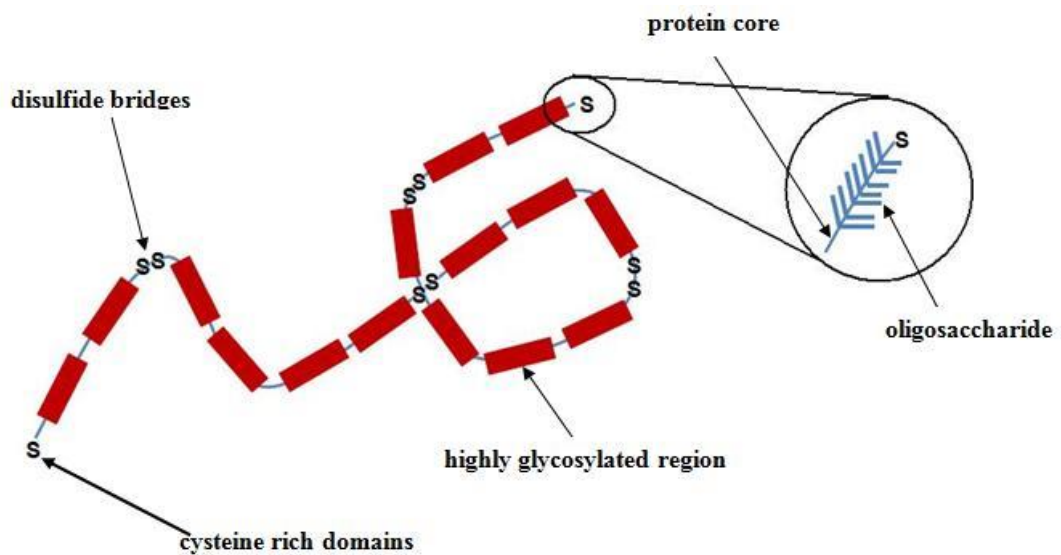


**Figure 1.5** Schematic diagram of a general mucin molecule showing the cysteine rich terminals, the highly glycosylated regions, disulfide bridges and oligosaccharides.

The protein core is surrounded by attached oligosaccharide chains providing a 'bottle brush' configuration. The oligosaccharides are attached to the hydroxyl side chains of serine and threonine, which make up the protein core, by O-glycosidic bonding. Sialic acid, which has an axial carboxyl group, makes up a large portion of the terminal residues in the oligosaccharide side chains. At neutral pH, mucus is negatively charged but it is uncharged when at an acidic pH. Mucin molecules contain a large number of hydroxyl and carboxyl groups which provide the opportunity for hydrogen bonding with nasal drug formulations.

A 5  $\mu\text{m}$  thick mucus layer covers the respiratory epithelium. This viscoelastic fluid is split into two very characteristic layers, a low viscous fluid known as the sol layer and an upper, more gellous layer. The sol layer has a thickness that is slightly less than the length of a fully extended cilium and enables the upper gel layer to be transported by the ciliary beating of the ciliated cells towards the nasopharynx (Livraghi and Randell, 2007). The rheology of either the sol layer or upper gel layer is important in ciliary beating and thus affects mucociliary clearance.

### **1.3 Factors influencing nasal absorption**

There are several factors that influence the nasal absorption efficacy of a drug. These include physiological conditions of the nose, physicochemical characteristics of the drug and formulation approaches, including the drug administration device. Absorption and transport of the drug are affected by the physiology of the nasal

cavity including, first and foremost, the mucociliary clearance, the circulatory system and enzyme activity. Drug physicochemical properties that influence absorption include such factors as molecular weight, viscosity, lipophilicity, and pH. These factors need to be considered by any formulator in order to optimise the drug formulation and thus allow for maximum efficacy.

### **1.3.1 Physiological factors affecting drug absorption**

#### **1.3.1.1 Mucociliary clearance**

Mucociliary clearance (MC) is a non-specific defence mechanism of the nasal cavity which helps protect the nose and lower airways from damage by inhaled harmful materials. Foreign particles are trapped in the upper, more viscous gel layer of the mucus, while the lower, less viscous sol layer acts as a lubricant and eases the action of the cilia. Due to the watery nature of the lower mucus layer, the cilia are free to beat with little or no resistance. This improves functionality and allows them to beat and fully extend. Once fully extended, the tip of the cilia will protrude through the gel layer which will aid the removal of foreign particles. The cilia work by engaging the upper layer of the mucus and propelling it towards the nasopharynx before disengaging and returning to its original position, ready for the next ciliary beat. The normal mucus clearance half life is variously reported as being approximately 12 to 15 minutes but this can vary between individuals (Marttin et al., 1998). However, a transport time of more than 30 minutes is deemed as being abnormal (Marttin et al., 1998). The rate of mucociliary clearance will influence the length of time a

formulation is in contact with the absorbing mucosa which in turn affects the amount of drug that crosses the membrane. Impairment of the MC system can result in a complete deceleration of the speed that the mucus moves (Privalova *et al.*, 2012). Factors that affect MC include the viscoelastic properties of the mucus layers along with the physiological features of the cilia, i.e. the cilia length, density and beat frequency (Privalova *et al.*, 2012). Drug formulations can also have a profound impact on the process.

### **1.3.1.2 Vasculature in the nasal cavity**

The nasal cavity is highly vascularised which allows for rapid absorption of drugs and gives this delivery route a distinct advantage over other non-parenteral routes. There are a variety of different blood vessels within the nose including resistance vessels, which control the overall blood flow, exchange vessels, which are responsible for the filtration and absorption of fluids, capacitance vessels, which deal with blood volume, and arteriovenous anastomoses, which regulate nasal blood flow. The presence of this vast blood vessel system makes the nasal mucosa a highly permeable site. However, drug absorption will depend dramatically on the rate of blood flow. Congestion, caused by an increase in blood flow, and relaxation, caused by a decrease in blood flow, can both have an effect of the amount of drug absorbed.

### **1.3.1.3 Enzymatic degradation**

One major advantage of drug delivery through the nasal cavity is the avoidance of the first pass metabolism but the enzymatic degradation with the nose itself cannot be ignored. The presence of enzymes, such as Cytochrome P450 and carboxyl esterase may affect the stability of the delivered drugs (Pires *et al.*, 2009, Dhakar *et al.*, 2011, Privalova *et al.*, 2012). Proteases and aminopeptidases, which are found at the mucosal membrane, are responsible for the degradation of proteins and peptides, although the level of aminopeptidases is still significantly lower than that present in the gastrointestinal tract (Dhakar *et al.*, 2011). Immunoglobulins within the mucus may also form complexes with peptides and this can cause an increase in the molecular weight and a subsequent decrease in permeability (Dhakar *et al.*, 2011). It can be seen that the pharmacodynamics and pharmacokinetics of a nasally delivered drug is subject to influences from the enzymes present within the nasal cavity.

### **1.3.2 Drug and formulation factors affecting absorption**

#### **1.3.2.1 Molecular weight**

Molecular weight (MW) as an influential factor on drug absorption has been investigated using a wide range of drugs with varying molecular weights of between 160 and 34,000 Da, such as vasopressin (MW of 1084 Da) and human growth hormone (MW of 22 kDa) (Ozsoy *et al.*, 2009). A study by McMartin and colleagues (1987) demonstrated that nasal absorption, through paracellular transport, decreases

exponentially as the molecular weight of the drug increases (Mcmartin *et al.*, 1987). A rate limiting molecular weight of 1000 Da was recorded in nasal absorption compared with 300 Da in oral absorption (Fisher *et al.*, 1987, Mcmartin *et al.*, 1987). This theory has been tested in both humans and rats and the trend was witnessed in both subjects. Hydrophilic substances with a range of molecular weights were studied (Fisher *et al.*, 1987) and it was found that a linear correlation existed between the log of percent absorbed and the log of the molecular weight. These results allowed the authors to infer that the absorption of hydrophilic compounds over the nasal mucosa is by way of aqueous channels.

### **1.3.2.2 Lipophilicity**

Lipophilic drugs are generally well absorbed by the nasal cavity and can present pharmacokinetic profiles comparable to those obtained by intravenous administration and a bioavailability close to 100% (Illum, 2003). An example of this was reported in a study by Borland and colleagues (2007) who looked at the efficacy of IN administration of fentanyl as a pain relief for children compared with IV administration of morphine. It was found that IN fentanyl provided effective pain relief and bioavailabilities were comparable with the IV administration (Borland *et al.*, 2007). It is thought that the absorption of lipophilic drugs occurs in a different manner to that of hydrophilic compounds, namely by the transcellular route. Although they are quickly and effectively absorbed across the nasal membrane, it must be stated that this is only true for lipophilic compounds with a molecular weight

less than 1 kDa. Nasal absorption of lipophilic drugs larger than 1 kDa is significantly reduced. The degree of absorption is associated with the drug's lipophilic characteristics and its partition coefficient between any buffer solution which may be used and the nasal mucosa (Behl et al., 1998), which will allow the drug to cross the lipid cell membrane (Hinchcliffe and Illum, 1999).

### **1.3.2.3 pH of drug formulation**

The pH of the formulation as well as the pH of the membrane surface can affect the drug's absorption ability. The effects of pH on absorption are variable but it is evident that it affects the solubility, partition behaviour and stability of many drugs, particularly proteins and peptides. It has been found that absorption of secretin in rats was higher at a pH below 4.79 and was optimal at pH 3 (Ohwaki *et al.*, 1987). The absorption was found to be minimal at pH >7. It was confirmed that changes in pH led to alterations in the extent of dissociation of functional groups as well as the actual polymer.

An appropriate formulation pH must be prepared in order to avoid irritation and damage to the nasal membrane which will result in altered drug absorption (Dondeti et al., 1996). It was reported that solutions with a pH between 4 and 8 caused minimal mucosal damage where formulations with a pH greater than 10 caused considerable intracellular damage (Pujara *et al.*, 1995, Kim, 2008).

## 1.4 Mucoadhesion

Mucoadhesion is defined as the attachment, by interfacial forces, of at least two materials, one of which being a mucous membrane, for an extended period of time (Peppas and Buri, 1985). Mucoadhesive delivery systems (Figure 1.6) are employed in an attempt to overcome the rapid MC which is ultimately responsible for the clearance of the formulation from the nasal cavity. This can be achieved with the use of mucoadhesive polymers which work by binding with the mucosal layer of the nose and thus reducing the formulation's rate of clearance from the nasal cavity. The consequential increased contact time between the drug delivery system and the nasal mucosa allows for an opportunity for increased absorption of the drug (Amboon *et al.*, 2012).

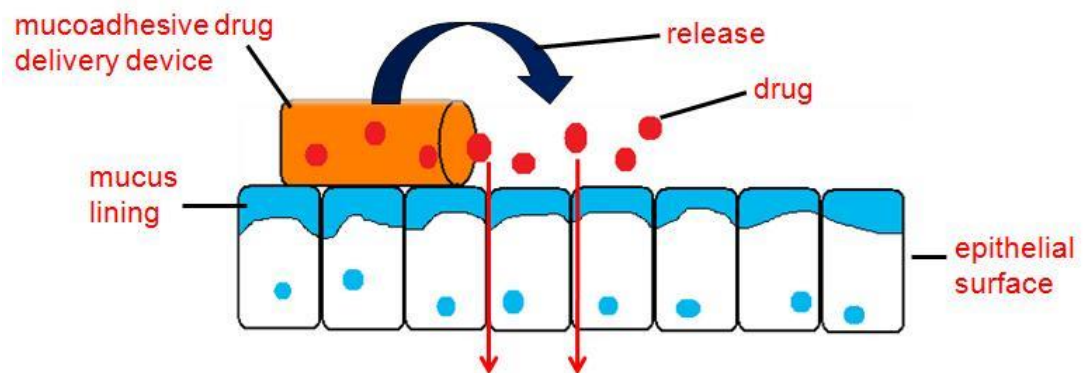


**Figure 1.6 Mucoadhesive drug delivery device action**

The mechanism of mucoadhesion was proposed by Duchene and colleagues in 1988 (Duchene *et al.*, 1988). This proposal involves a three stage process and is generally

accepted for solid delivery systems. The first stage involves an intimate contact between the mucoadhesive polymer and the mucus surface due to wetting and swelling of the mucoadhesive (wetting theory). The delivery system is able to adhere to the mucus layer with the help of the surface forces and tension that exist at the contact site (electronic and adsorption theories). The swelling of the polymers arise due to its hydrophilic components. The second stage takes place after the contact is established and involves the penetration of the mucoadhesive polymer chain into the mucus surface. Weak, chemical bonds then form between the entangled polymer chains in the final stage (electronic and adsorption theories). The wetting and swelling stage is unlikely to occur when the mucoadhesive delivery system is a polymer gel, due to the polymer already being in equilibrium with the aqueous medium it was formulated in.

#### **1.4.1 Theories of mucoadhesion**

Over the years of mucoadhesion investigation, six general adhesion theories have been developed (Huang *et al.*, 2000, Smart, 2005, Renner *et al.*, 2012b). These include adsorption, diffusion, electronic, fracture, wetting and mechanical theories. None of the theories give a complete description of the mechanisms of mucoadhesion and it is thought that ,in fact, a combination of all six theories exist (Amboon *et al.*, 2012). The thermodynamic and interpenetration/diffusion theories are by far the most widely accepted (Andrews *et al.*, 2009).

### 1.4.1.1 The wettability theory

The wetting theory is mainly concerned with liquid preparations and uses the interfacial and surface tensions to predict spontaneous spreading onto a surface and the resultant adhesion. Liquid has an affinity for a surface and this affinity can be investigated using techniques such as contact angle measurements. This technique measures the contact angle of the liquid in relation to the surface. The lower the contact angle, the greater affinity the liquid will have for the solid.

The work of adhesion ( $W_A$ ) can be used to find the energy required to separate the liquid from the solid. Work of adhesion is given by the following equation:

$$W_A = \gamma_B + \gamma_A - \gamma_{AB}$$

where  $\gamma_A$  is the surface tension of liquid A,  $\gamma_B$  is the surface energy of solid B and  $\gamma_{AB}$  is the interfacial energy between the liquid and the solid. The work of adhesion will be greater with the increased individual surface energies of the two phases relative to the interfacial energy. It is thought that a mucoadhesive system that has a better ability to spread will possess greater mucoadhesive properties (Amboon *et al.*, 2012).

### **1.4.1.2 The electronic theory**

The electronic theory relates to the assumption that electron transfer arises upon contact of the adhesive polymer and mucosal surfaces due to their differing electronic structure. The transfer is thought to lead to the formation of an interfacial electronic double layer (Edsman and Hagerstrom, 2005). The attractive forces which occur over the double layer are responsible for the adhesive effect. A charged system occurs when the mucoadhesive layer and the substrate are in contact and a separation of the two layers will result in a discharged system. A zeta potential meter can measure the surface charge properties of a polymer which can then be used to study its electrical structure.

### **1.4.1.3 The fracture theory**

The fracture theory is the most applicable theory for studying mucoadhesion through mechanical measurements. The theory relates to the severance of the polymer and mucus surface after adhesion and this fracture strength is considered to be equal to the adhesive strength. It has mainly been used to calculate adhesive bonds for formulations that are rigid (Edsman and Hagerstrom, 2005). Although the fracture theory is useful for analysing the force required for separation, it does not take into account entanglement, diffusion or interpenetration of the polymer chains. Tensile strength or shear stress tests are methods used to study the separation force.

#### **1.4.1.4 The adsorption theory**

The adsorption theory is concerned with the attaching of the adhesive polymer to the mucus because of surface forces between the molecules of both surfaces. These surface forces cause the formation of two types of chemical bonding. Primary chemical bonds of covalent nature are formed which are undesirable in mucoadhesion due to the permanency of the bonds. Secondary chemical bonds have many different forces of attractions including electrostatic forces, Van der Waals forces, hydrogen bonding and hydrophobic interactions. These hydrophobic interactions may explain the fact that a mucoadhesive polymer binds to a hydrophobic substrate more tightly than to a hydrophilic surface. The strong adhesive bond is due to the large number of individually weak hydrophobic interactions (Andrews *et al.*, 2009).

#### **1.4.1.5 The diffusion theory**

The diffusion theory relates to the interdiffusion of polymer chains of the formulation and mucus network. Concentration gradients drive the process which is also affected by the availability and mobility of molecular chain lengths (Amboon *et al.*, 2012). Rheological synergism can be used to determine the interdiffusion of mucoadhesive polymeric formulations and mucin formulations (Hassan and Gallo, 1990).

### **1.4.1.6 The mechanical theory**

The mechanical theory describes the notion that adhesion occurs from a liquid adhesive interlocking into the irregularities on an uneven surface. It must be noted, however, that an irregular surface will present an increased surface area available for further interactions and enhanced viscoelasticity which are deemed more important than a mechanical effect (Peppas and Sahlin, 1996, Smart, 2005).

### **1.4.2 Factors affecting mucoadhesion**

There are many influencing factors affecting mucoadhesion which must be considered when formulating a mucoadhesive drug delivery system. The knowledge of such factors, which includes functional groups, cross linking density, polymer molecular mass and polymer concentration, can allow the specific tailoring and modification in order to achieve the highest level of mucoadhesion.

#### **1.4.2.1 Molecular weight and chain length**

Mucoadhesive polymers can differ immensely in their molecular weight. It has been reported that increasing molecular weight (up to 100,000 Da) will increase the mucoadhesive strength of a polymer (Shaikh *et al.*, 2011). Smart and colleagues (1984) performed an investigation into the mucoadhesive properties of sodium carboxymethylcellulose (NaCMC) and found that the molecular weight of NaCMC should be greater than 78,600 Da in order to provide desirable mucoadhesive effects

(Smart *et al.*, 1984). It is apparent that a critical molecular weight exists for significant mucoadhesion to be achieved. An increase in molecular weight will also result in an increase in the chain length of a polymer. This increase in polymer length will influence mucoadhesion due to the increase in interpenetration and entanglement between the polymer and the substrate.

#### **1.4.2.2 Crosslinking and swelling**

An increased crosslinking density will cause a reduction in the degree of swelling of the polymer. This is due to a highly crosslinked polymer having a tighter structure which will impede the mobility of the polymer chain. This in turn will lower the level of swelling capabilities of the polymer. Conversely, a reduced crosslink density will allow the polymer chains a higher rate of flexibility, faster hydration rate and a larger surface area, all factors in favour of better mucoadhesion (Shaikh *et al.*, 2011). However, a polymer may hydrate and swell too much and cause a slippery mucilage to form. This can result in the premature removal of the mucoadhesive delivery device from the nasal mucosal surface.

#### **1.4.2.3 pH and charge**

The pH of the environment will have a significant effect on mucoadhesion due to the influence pH has on the charge characteristics of both the mucus and polymer. The functional groups of the mucus glycoproteins dissociate and cause different charge

distributions depending on the pH (Ugwoke *et al.*, 2001). This was seen in an early study by Park and Robinson (1985) involving the ionisable polymer polycarbophil. At pH 3 and below, the polymer was unionised and the adhesion capacity was deemed to be at its maximum. This environment favoured hydrogen bonding between the mucin glycoproteins and the carboxyl groups of the polymer. Increasing the pH to pH 6 and 7 caused the polymer to neutralise and thus no adhesion was seen (Park and Robinson, 1985).

#### **1.4.2.4 Concentration**

It has been shown that polymer concentration has a considerable influence on mucoadhesion; however, an optimum polymer concentration exists, beyond which the adhesive strength of some polymers is significantly reduced. High concentrations may result in the coiling of polymer molecules leading to a reduced flexibility of the polymer chains and thus the penetration of the polymer at the interface is decreased (Duchene *et al.*, 1988).

#### **1.4.2.5 Viscosity**

Another major factor which can affect the magnitude of mucoadhesive strength is the viscosity of the formulation. It has been previously shown that an increase in viscosity will increase the residence time of the mucoadhesive polymer within the nasal cavity (Dondeti *et al.*, 1995). However, this study contradicts the theory of

others which state that improved mucoadhesion results from the intimate contact between the polymer and mucus glycoprotein chains and thus a more viscous formulation would prevent this close contact (Livraghi and Randell, 2007, Serra *et al.*, 2009b). Increasing the polymer concentration will eventually have a negative effect on mucoadhesion. This is as a result of a decrease in polymer chain mobility and thus the occurrence of interactions between the polymer and glycoprotein chains will be reduced (Lee et al., 2000).

### **1.4.3. Mucoadhesive polymers**

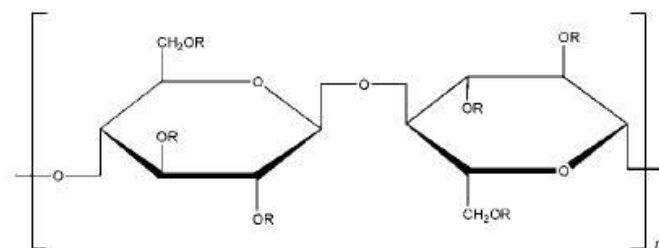
Hydrophilic macromolecules containing hydrogen bond forming groups are a group of mucoadhesives which have been widely investigated (Smart, 2005). These ‘first generation’ mucoadhesives present hydroxyl, carboxyl and/or amine groups which favours adhesion. Activation of the macromolecules is by moistening, resulting in the non-specific adherence to many differing surfaces. However, once they are activated they show stronger adhesion to dry static surfaces rather than those covered with mucus. The mucoadhesives can become over hydrated therefore it is imperative that the water uptake is restricted. Over-hydration may result in slippery mucilage and thus a reduced adhesion. Table 1.1 summarises the characteristics required by polymers to ensure good mucoadhesion.

**Table 1.1 Characteristics of mucoadhesive polymers.**

Characteristic	Details
Flexibility	Flexibility controls the extent of interpenetration between the polymers and the mucosal surface.
Hydrophilicity	Polymers that have a hydrophilic nature are able to form strong adhesive bonds with the mucosa due to the large quantities of water in the mucus layer.
Hydrogen bonding	Hydrogen bonding between the entangled polymer chains forms strong adhesive bonds. The presence of hydrogen bond-forming groups, i.e. hydroxyl and carboxyl groups, are vital.
High molecular weight	A high molecular weight provides a greater number of bonding sites.
Surface tensions	Surface tensions aide with the spreading of the mucoadhesive polymer into the mucosal surface.

### **1.4.3.1 Cellulose derivatives**

Hydroxypropyl methylcellulose (HPMC) is a non-ionic, water soluble polymer which is derived from cellulose. It is generally recognised as safe (GRAS) listed and is widely used as an excipient in many pharmaceutical formulations and dietary supplements. HPMC has a polymeric backbone of cellulose with a number of hydroxyl groups introduced throughout the molecule (Figure 1.7). It is these hydroxyl groups which promote its water solubility.



where R is H, CH<sub>3</sub>, or CH<sub>3</sub>CH(OH)CH<sub>2</sub>

**Figure 1.7** Typical chemical structure of hydroxypropyl methylcellulose. Reproduced from Handbook of Pharmaceutical Excipients (5<sup>th</sup> Edition).

HPMC is useful in mucoadhesive drug delivery systems as it is inexpensive and very stable, although it does become hygroscopic after drying. It is also available in a number of different grades which allow for the commercial availability of a wide range of viscosity types (Table 1.2).

**Table 1.2** Typical viscosity values for 2% (w/v) aqueous solutions of Methocel. Viscosities measured at 20°C. Reproduced from Handbook of Pharmaceutical Excipients (5th Edition)\*.

Methocel Product	USP 28 designation	Nominal viscosity (mPa.s)
Methocel K100P	2208	100
Methocel K4MP	2208	4000
Methocel K15MP	2208	15000
Methocel E4MP	2910	4000

\* The initial lettering within the Methocel name signifies the degree of substitution of the HPMC products, with K identifying the degree of substitution of methoxyl and hydroxypropyl as 22% and 8.1%, respectively. The preceding number denotes the viscosity in millipascal-seconds (mPa.s) of the Methocel product at 2% concentration in water at a temperature of 20 °C. The suffix "LV" stands for low viscosity, "P" signifies that the products are of premium grade and "M" represents 1000.

Microcrystalline cellulose (MCC) is a dispersible cellulose excipient that is used in a wide array of pharmaceutical suspensions, creams and nasal sprays. The polymer possesses a vast range of viscosities, thixotropies, dispersion characteristics and gel strengths giving them absolute suspension stability and functional versatility. MCC (Figure 1.8) is comprised of glucose units which are linked by a 1-4 glycosidic bond. The linear cellulose chains are packed together as microfibrils coiled together in the plant cell. Each single microfibril displays a high level of three dimensional internal bonding which results in a water insoluble crystalline structure which is resistant to reagents.

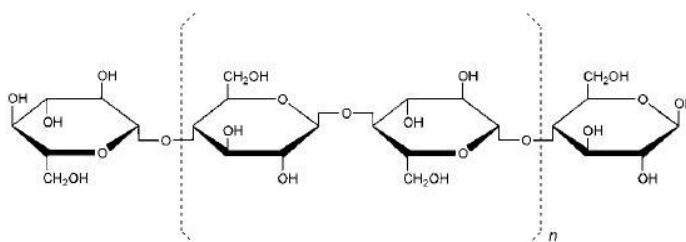


**Figure 1.8** Typical chemical structure of microcrystalline cellulose. Reproduced from Handbook of Pharmaceutical Excipients (5<sup>th</sup> Edition).

The advantages of using MCC as a mucoadhesive drug delivery system include its high thixotropic rheological behaviour. This means the formulation will possess non-drip characteristics, will be highly stable and most importantly, it can be sprayed. The excipient is also compatible with other ingredients due to it being largely insoluble and non reactive. Avicel<sup>®</sup> RC/CL (Figure 1.9) are grades of MCC

that are combined with sodium carboxymethylcellulose (NaCMC) to produce a dispersion aid which also acts as a protective colloid.

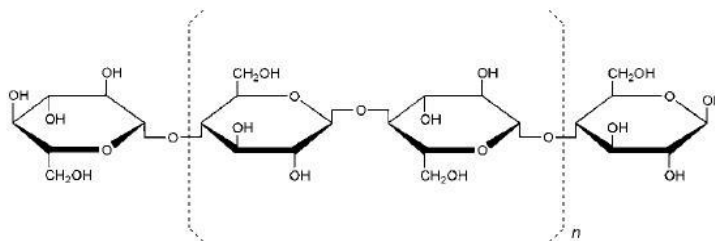


**Figure 1.9** Typical chemical structure of Avicel. Reproduced from *Handbook of Pharmaceutical Excipients* (5<sup>th</sup> Edition).

Sodium carboxymethylcellulose (NaCMC) (Figure 1.10) is the sodium salt of the cellulose polycarboxymethyl ether and is used as a viscosity enhancer in many formulations including corticoid nasal sprays (Sharpe *et al.*, 2003). NaCMC has been explored as an aid to mucoadhesion since the early 1980's (Roy *et al.*, 2009) and continues to be studied alongside other mucoadhesives as a means of increasing the residence time of the dosage form within the nasal cavity.

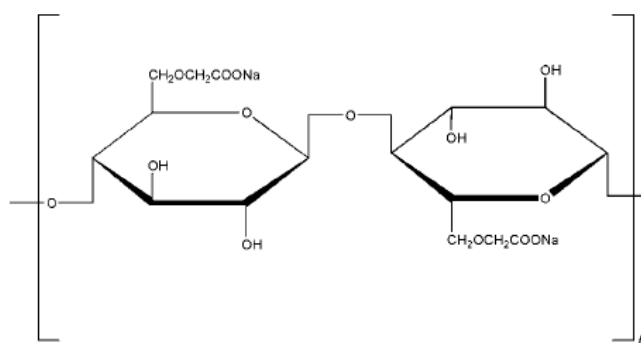


**Figure 1.10** Typical chemical structure of NaCMC. Reproduced from *Handbook of Pharmaceutical Excipients (5<sup>th</sup> Edition)*.

### 1.4.3.2 Carbomers

Carbomers are synthetic, high MW polymers of acrylic acid (Figure 1.11) copolymerised with allyl sucrose or allyl pentaerythriol. They are chemically crosslinked with polyalkenyl alcohols or divinyl glycol and are successfully used in a variety of commercial formulations (Lubrizol, 2011).

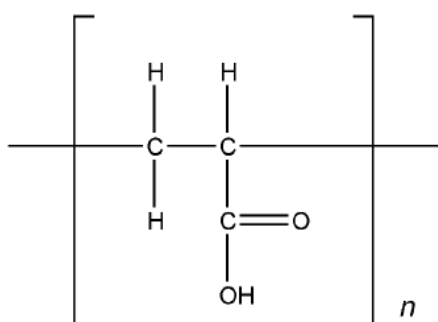


**Figure 1.11** Typical chemical structure of poly (acrylic acid). Reproduced from *Handbook of Pharmaceutical Excipients (5<sup>th</sup> Edition)*.

Carbomer polymers are utilised in a vast range of pharmaceutical applications due to advantages including high viscosity at low shear rates and compatibility with many active pharmaceutical ingredients (API) (Islam *et al.*, 2004). Although numerous grades of carbomer exist, only three of them (934P, 971P and 974P) are intended for internal use. Carbopol 934P is crosslinked with allyl ethers of sucrose and is polymerised in benzene (Lubrizol, 2011). Carbopol 971P and 974P are both crosslinked with allyl pentaerythritol and polymerised in ethyl acetate. The difference with Carbopol 971P and 974P is the level of crosslinking with Carbopol 971P having a lower crosslinking density than Carbopol 974P.

### **1.4.3.3 Chitosan**

Chitosan is a linear, cationic, natural polymer which is the N-deacetylated product of chitin. It has many desirable features which makes it an ideal candidate for use in various drug delivery applications. These features include strong mucoadhesivity, antimicrobial properties and low toxicity. Glutamate or hydrochloride salts are the most widely reported forms of chitosan and have molecular weights of approximately 150 – 250 kDa (Illum, 2012). The cationic nature of chitosan is of extreme importance in drug delivery across a mucosal layer. This is due to the ability of the positively charged amino groups of the chitosan to ionically interact with the negatively charged glycosylated regions of the mucus (George and Abraham, 2006). This will ultimately enable an increased residence time of the formulations at the site of deposition, i.e. the nasal cavity (Illum, 2003, Kumar *et al.*, 2004). It is well documented that the use of chitosan within a nasal formulation will

increase the bioavailability of some drugs, including insulin (Yu *et al.*, 2004) and morphine (Illum, 2003, Stoker *et al.*, 2008).

## **1.5 Mucoadhesive testing**

There have been many test methods proposed for the analysis and measurement of the mucoadhesive strength of formulations. The primary aim of mucoadhesion is to encourage drug absorption by increasing the residence time of the drug within the nose and assessment of this clearance rate using various *in-vitro* and *in-vivo* relevant techniques is an important aspect to consider. This section deals with a few of the direct and indirect methods used to measure the ability of a formulation to improve the residence time at the site of deposition.

### **1.5.1 Texture analyser**

The texture analyser (TA) (Figure 1.12) is a technique which is used to measure the tensile strength of a formulation. The results are presented as the maximum force of detachment ( $F_{\max}$ ), which is the maximum force required to completely detach the polymeric formulation from the surface of the substrate. The work of adhesion is also achieved through this method and is presented as the area under the force-time curve (AUC). It can be defined as the total work done to separate the formulation from the substrate. Other mechanical properties can be determined using the TA.

These include hardness, compressibility, and cohesiveness (Jones *et al.*, 1997) and are derived from the resultant force – time plot (Figure 1.13).

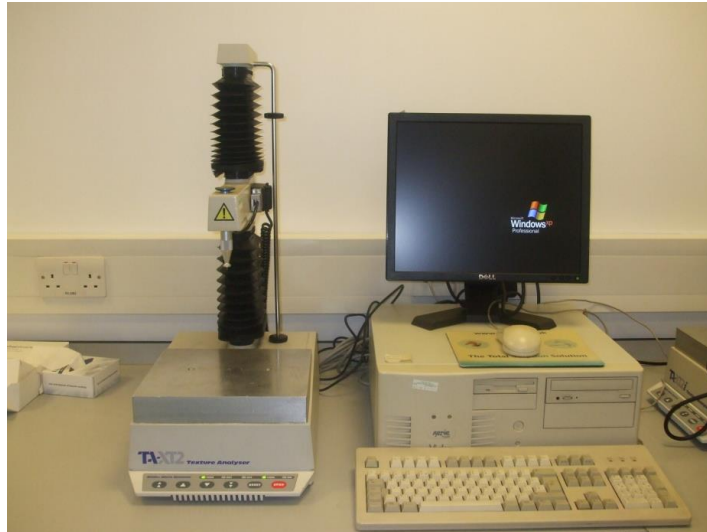
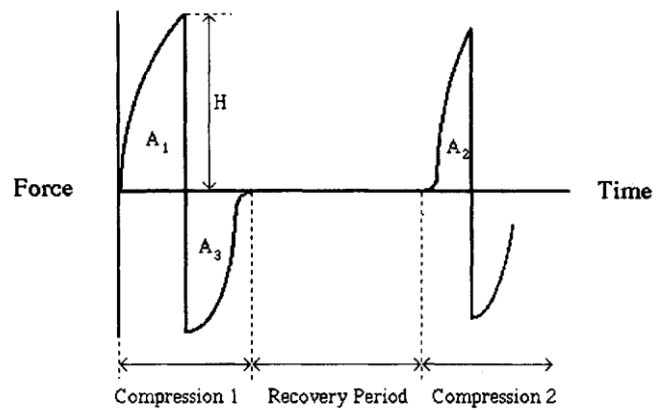


**Figure 1.12** Texture analyser apparatus.



H = Hardness  
A<sub>1</sub> = Compressibility  
A<sub>3</sub> = Adhesiveness  
A<sub>2</sub> / A<sub>1</sub> = Cohesiveness

**Figure 1.13** Graphical output from Texture Analyser. Reproduced from (Jones *et al.*, 1997).

In general, the method used to assess the mucoadhesive strength involves attaching the test polymer to the end of a TA probe, which is then lowered at a predetermined rate and force until the test polymer and mucosal substrate are in contact. The probe is held in position for a defined time and at a defined force before it is withdrawn at a programmed rate. Researchers have utilised a variety of model substrates to measure mucoadhesion including bovine sublingual mucosa (Eouani *et al.*, 2001, Accili *et al.*, 2004), bovine duodenal mucosa (Accili *et al.*, 2004), mucin discs (Jones *et al.*, 1997) and chicken pouch tissue (Wong *et al.*, 1999). It is without doubt that the most desirable substrate would be fresh mucosa from an animal model which would provide an environment close to the *in-vivo* situation. Although this is desirable, animal tissue is highly variable and the results obtained from an experimental method using this substrate would need to factor into account these differences. In order to clarify the test conditions and instrumental parameters that influence mucoadhesive strength measurements, the validation of the test method using the TA has been undertaken under simulated gastric conditions utilising porcine gastric tissue (Tobyn *et al.*, 1995). Tobyn and colleagues (1995) discovered that the TA results were significantly affected by the instrumental parameters set by the researcher, these included the contact time and force between the tissue and the sample, the speed at which the probe was withdrawn and the time the polymer samples were hydrated prior to testing. As of yet, there have been no defined parameters set for the analysis of mucoadhesive polymers and the test parameters and environments vary among published literature, making the correlation of any results very difficult and complicated. Another disadvantage of the TA is that the vast amounts of useable parameters have no direct rheological relevance such as

shear stress, viscosity and rate of shear. However, the use of the texture analyser to assess the mechanical characteristics of mucoadhesive polymers has many advantages including short analysis times, the applicability of multiple sample types, and the direct significance to topical formulations and so can be used in conjunction with other techniques, such as rheology, to gain a better understanding of the mucoadhesive properties of polymers.

### **1.5.2 Rheology**

Rheology is the study of the deformation and flow of matter experiencing an applied force and is measured using a rheometer (Figures 1.14 and 1.15). An optical encoder device measures angular displacement and can measure movements as small as 2.5  $\mu$ rad. The encoder is made up of a non-conducting light source with a photocell, which is arranged either side of a transparent disc attached to the drive shaft. Fine and accurate radial lines are photographically etched onto the edge of the disc providing the system with a diffraction grating. A second, stationary diffraction grating is located between the light source and the encoder disk. Interactions between the two disks causes an interference of the light and thus results in diffraction patterns which are detected by the photocell. The encoder disc moves as the sample strains under stress causing the diffraction patterns to change and the associated circuitry digitalises the resulting signal to produce data. This digital data directly relates to the angular deflection of the disc and thus the strain of the sample.



**Figure 1.14 Rheometer apparatus.**

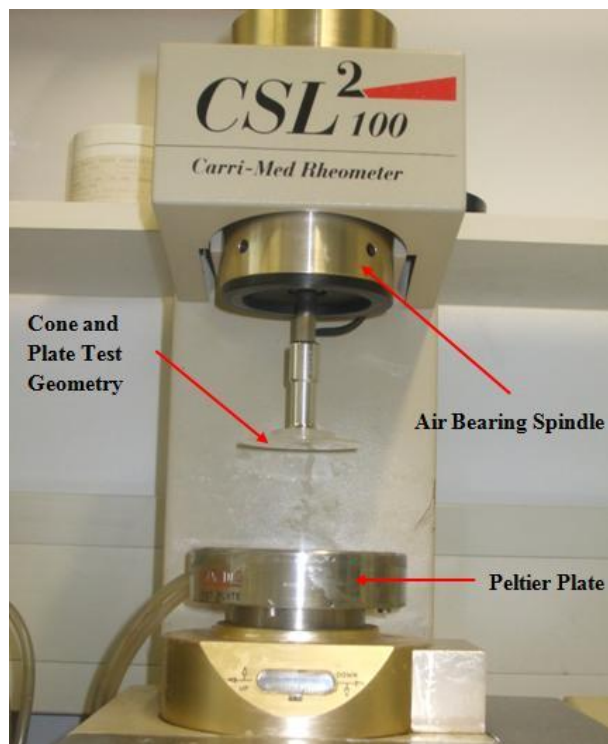


**Figure 1.15 Labelled rheology apparatus.**

The rheological properties of a mucoadhesive polymer are dominant features that can be quantified to characterise its behaviour and also the response of the polymer to a shearing flow. This is the basis for determining the specific rheological properties which are termed viscoelastic (the term given to a material which exhibits both elastic and viscous properties), Newtonian, nonNewtonian (shear thinning and shear thickening), thixotropic and rheopectic. Figure 1.16 shows the rheograms indicative of Newtonian and non-Newtonian behaviour.

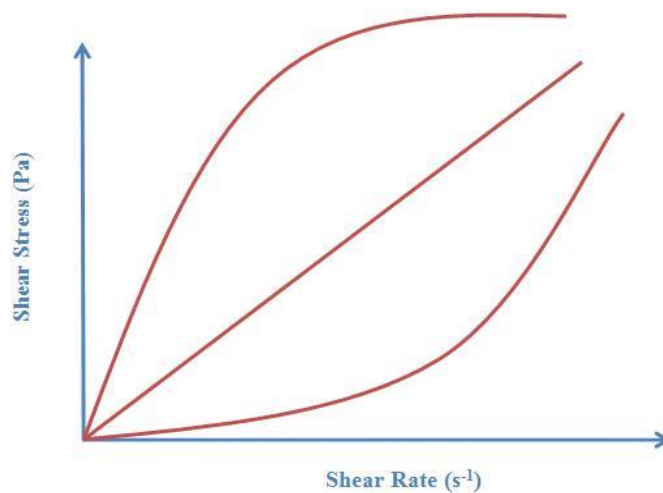


**Figure 1.16** Effect of shear rate on the viscosity of (A) shear-thinning systems, (B) Newtonian formulations and (C) shear thickening systems.

Newtonian fluids are fluids which exhibit a viscosity that is independent of the current shear conditions and as such their viscosity will not be altered by such shearing actions as spray actuation or shaking. Most fluids are nonNewtonian and their viscosity will be dependent on shear conditions. Shear thinning, also known as pseudoplasticity, is a behaviour which causes a reduction in viscosity as the rate of

shear increases. This is due to a shear dependent, temporary break down of the structure of the materials which will rebuild on removal of the shear. Shear thickening, also known as dilatancy, is the opposite to shear thinning and the system will experience an increase in viscosity with increasing shear. Again this behaviour is dependent on shear and removal of the shear will result in a reduction in the systems viscosity. This shear thickening behaviour is common in dispersions that contain a large quantity of small, deflocculated particles, such as clays and slurries (Lee *et al.*, 2009). Some shear thinning systems also show a degree of thixotropy. Thixotropic materials possess a time dependent reduction in viscosity at constant shear rates with the rebuilding of the structure, which occurs due to Brownian motion, taking place after the shear has been removed. Rheopectic samples, or anti thixotropic, show a time dependent increase in viscosity at constant shear rates and are seen in shear thickening materials.

Viscosity, elasticity, shear rate, shear strain and shear stress are quantitative parameters that are used in the study of rheology. Oscillatory flow at a selected frequency can obtain the broadest view of the polymer because both viscous and elastic properties are revealed. Steady flow rheology will only reveal viscosity. Many studies have been carried out to determine the rheological behaviours of mucus/mucoadhesive interactions (Carvalho *et al.*, 2010, Shahnaz *et al.*, 2010). Madsen and colleagues (1998) reported that rheological synergism was only found to occur at a certain concentration range and that the range of concentrations was dependent upon the mucoadhesive polymer used (Madsen *et al.*, 1998b). Rheology

can give some invaluable information regarding the properties of the polymer however the limitations of rheology has been studied (Hagerstrom and Edsman, 2003) and it has been reported that rheology should be used in conjunction with other tests to verify experimental results.

### **1.5.3 Atomic force microscopy**

Atomic force microscopy (AFM) is a high resolution type of scanning probe microscopy and is used to analyse, measure and manipulate matter at the nanoscale. It has recently been employed in the pharmaceutical industry as a non-invasive technique to study aggregates of mucoadhesive polymers and mucin and polymer adsorptions to the mucosal cell surface (Deacon *et al.*, 2000, Patel *et al.*, 2000, Edsman and Hagerstrom, 2005). The AFM is one of several scanning probe microscopy techniques which can be used to find topographical information about the surfaces of both the mucoadhesive polymer and the mucosal surface. The AFM (Figure 1.17) has two operational modes; contact mode and tapping mode. In contact mode, the miniscule pyramidal tip, which is commonly made of silicon nitride, is brought into contact with the mucosal surface where Van der Waals repulsive forces cause the flexible cantilever to deflect. The tip and sample are kept at a constant distance from each other with the use of a piezo-electric feedback scanner as it is scanned across the sample surface in a raster movement. The movement of the probe can be examined and translated into a digital image detailing the topographical information of the sample surface.

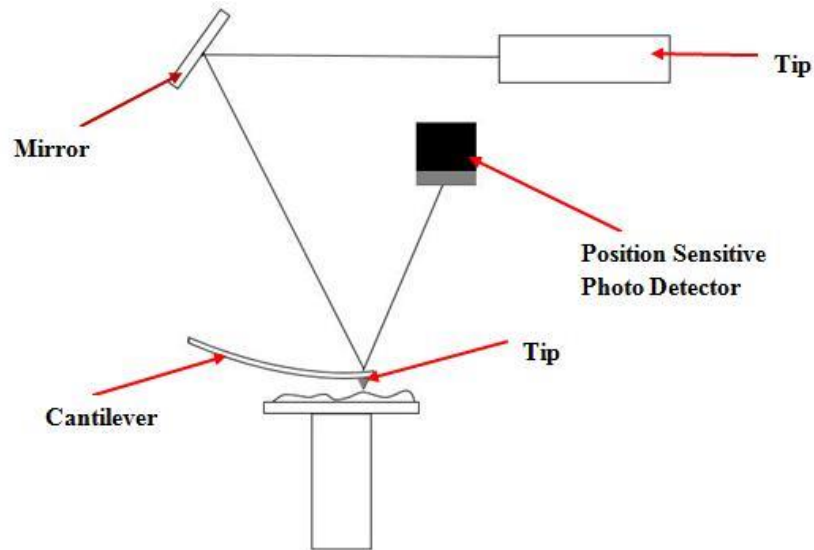


**Figure 1.17 Schematic Diagram of AFM Setup.**

Tapping mode AFM allows high resolution topographic images of delicate sample surfaces that are easily destroyed. In tapping mode, the cantilever is oscillated at or near the cantilever's resonant frequency using a piezoelectric system, with the cantilever oscillation reduced when intermittently coming into contact with the sample surface. The reduction in the amplitude of the oscillations identifies and measures the surface features of the sample.

### **1.5.3 Other techniques**

A wide range of techniques have been developed to study the efficacy of nasal formulations. Other techniques that have been utilised to measure the mucoadhesive properties of polymeric formulations include the use of gamma scintigraphy to

visually study the residence time of an insulin nasal insert (McInnes *et al.*, 2007) and a modified Franz cell to study the washability of mucoadhesive gels (Bonferoni *et al.*, 1999). Although each of the methods employed provide valuable information on the efficacy of mucoadhesive preparations it is imperative that the results are verified using other methods.

## **1.7 Project aim and objectives**

The aim of the project is to identify nasal mucoadhesive technologies applicable to current intranasal delivery strategies and investigate their potential to increase retention in the nasal cavity using *in vitro* techniques to clarify the key mechanisms in product performance.

The key objectives of the project are as follows:

1. Characterise and correlate the nature of the mucoadhesive performance and processes using a variety of physical testing.
2. Identify the critical components of the system that are relevant for its mucoadhesive properties.

## **Chapter 2 Rheological analysis of mucoadhesive polymeric nasal formulations**

### **2.1 Introduction**

It is known that rheological properties of nasal drug delivery systems, for example nasal spray suspensions, will have a dramatic effect on their overall performance (Lee *et al.*, 2009). Such delivery systems should have a sufficiently low apparent viscosity in order for adequate delivery through a spray device nozzle, but they must also show sufficient viscosities and formulation stability in order for optimum residence within the nasal cavity. It is for these reasons that many nasal spray formulations (e.g. Beconase®, Nasacort®, Flixonase® and Nasonex®) are thixotropic. Thixotropy, which is described in more detail later, describes a formulation that thins on shear but has a high apparent viscosity on relaxation. For systems which contain small suspended solids, this prevents particle sedimentation when the formulation is at rest. Research suggests that the thixotropic characteristics of a nasal spray is related to the efficacy of the delivery system and the increased viscosity after the formulation has recovered fully is considered an important factor in increasing adhesion to the nasal mucosa (Lee *et al.*, 2009).

The diffusion theory of mucoadhesion states that penetration of the polymer chains and polymer entanglement is reported to be responsible for mucoadhesion, which has been supported by studies using rheological measurements (Hassan and Gallo, 1990,

Mortazavi *et al.*, 1992). Chain diffusion, chain interlocking and the chemical interaction between the mucoadhesive polymer and the mucus are all factors which influence the rheological behaviour by increasing the strength of the weakest element of the adhesive bond (Sriamornsak *et al.*, 2008). Rheological measurements, which characterise the flow and deformation of a sample, can offer a simple means to measure the interaction between the two macromolecular species and thus predict the mucoadhesive ability of the formulation. In this chapter, flow and dynamic rheological methods were used to enable the assessment of rheological flow behaviour of low and high viscosity polymeric gels.

## **2.2 Materials**

### **2.2.1 Apparatus**

Rheological analysis was performed using a controlled stress Carrimed CSL<sup>2</sup> 100 rheometer (TA Instruments, Surrey, UK) with a 6cm stainless steel cone and plate geometry. The CSL V1.2a software package (TA Instruments, Surrey, UK) was used for system control along with data gathering and analysis.

### **2.2.2 Chemicals**

NaCMC low, medium and high MW (average molecular weight ~90, 250 and 700 kDa respectively) along with type III bound sialic acid mucin from porcine stomach were purchased from Sigma Aldrich Co (St Louis, MO, USA). Avicel RC591 and

CL611 were obtained from FMC Biopolymer (Philadelphia, PA, USA). Carbopol 971P and 974P were obtained from Lubrizol Advanced Materials Europe BVBA (Brussels, Belgium) and HPMC powder (Methocel grades E4MP, K4MP, K100P and K15MP) was received as a gift from Colorcon (Dartford, Kent, UK). Three placebo nasal spray formulations (ee521730, ee521950 and ee522260) were received from GlaxoSmithKline R & D (Ware, UK).

## **2.3 Methods**

### **2.3.1 Preparation of mucoadhesive polymeric nasal formulations**

The mucoadhesive polymeric nasal formulations were prepared by dissolving the required weight of each polymer in approximately one third of the final mass of distilled water with constant agitation by a magnetic stirrer. Stirring was continued by hand and the remaining water was subsequently added. The solution was further mixed on the magnetic stirrer and left to stand at room temperature overnight to remove air and to allow for complete hydration and structural build up of the polymer. The concentrations of each polymer solution used were 0.2, 0.5 and 1% w/w.

### 2.3.2 Preparation of placebo nasal formulation

Placebo nasal spray formulations (ee521730, ee521950 and ee522260) were received from GlaxoSmithKline R&D (Ware, UK) and their composition is shown in Tables 2.1 to 2.3. The placebo nasal formulations were used as received and no modification of their formulation was required.

**Table 2.1 Composition details of placebo nasal formulation ee521730 (Information supplied by GlaxoSmithKline R&D, Ware, UK).**

Material	% w/w	Required Quantity (g)	Actual Quantity (g)
HPMC E4MP	1	20	20.0002
Dextrose	5	100	100
EDTA*	0.015	0.3	0.3
BKC*	0.03	0.6	0.6001
Polysorbate 80	0.025	0.5	0.5001
Water	to 100	to 2000	1878.6

\*EDTA (Edetate Disodium), BKC (Benzalkonium Chloride).

**Table 2.2 Composition details of placebo nasal formulation ee521950 (Information supplied by GlaxoSmithKline R&D, Ware, UK).**

Material	% w/w	Required Quantity (g)	Actual Quantity (g)
Avicel RC591	1.5	30	30.0085
Dextrose	5	100	100
EDTA*	0.015	0.3	0.3002
BKC*	0.03	0.6	0.6003
Polysorbate 80	0.025	0.5	0.5009
Water	to 100	to 2000	2000

\*EDTA (Edetate Disodium), BKC (Benzalkonium Chloride).

**Table 2.3 Composition details of placebo nasal formulation ee522260  
(Information supplied by GlaxoSmithKline R&D, Ware, UK).**

Material	% w/w	Required Quantity (g)	Actual Quantity (g)
Avicel CL611	2.4	48	48.003
EDTA*	0.015	0.3	0.3098
Sodium Citrate	1.48	29.6	29.608
Citric Acid	0.96	19.2	19.2069
Polysorbate 80	0.0025	0.5	0.5068
Potassium Sorbate	0.3	6	6.0035
Propylene Glycol	1.5	30	30.0865
Water	to 100	to 2000	2000

\*EDTA (Edetate Disodium).

### **2.3.3 Preparation of mucin solution**

The mucin solution was prepared by dissolution of type III porcine gastric mucin in distilled water to yield a dispersion of 2% w/w. The mixture was gently stirred by hand until a uniform solution was obtained and then stored overnight at 4°C to allow for the removal of air bubbles. Prior to use, the mucin solution was allowed to equilibrate to room temperature and further mixed by hand. All mucin solutions were used within 48 hours of preparation to prevent microbial growth affecting results and stored at 4 °C when not in use.

### **2.3.4 Rheological flow behaviour of mucoadhesive polymeric nasal formulations**

The rheological behaviour and flow properties of the mucoadhesive polymeric nasal formulations and the placebo nasal formulations were measured using a Carrimed

CSL<sup>2</sup> 100 controlled stress rheometer (TA Instruments, Surrey, UK), equipped with a 6 cm steel cone and plate test geometry with a fixed gap of 57 microns and set at a temperature of 25±0.1 °C. The polymer samples were spooned onto the peltier plate to minimise further shearing of the polymer during transfer and the cone lowered to the fixed gap of 57 microns. Excess sample was carefully trimmed from the edge of the cone by a flat edged spatula to ensure sample overloading did not occur. The samples were allowed to condition and equilibrate for 180 s and flow data was generated with maximum shear rates of 100 s<sup>-1</sup> and 1200s<sup>-1</sup>, with a sweep time of 240 s. The flow behaviour index ( $n$ ) and consistency index ( $K$ ) were derived from the power law equation (Equation 2.1) described by Jones and colleagues (2002):

$$\tau = K\gamma^n \quad \text{[Equation 2.1]}$$

where  $\tau$  is the shear stress (Pa),  $K$  is the consistency index (Pa.s <sup>$n$</sup> ),  $\gamma$  is the shear rate (s<sup>-1</sup>), and  $n$  is the flow behaviour index (dimensionless) (Jones *et al.*, 2002). This model provides an approximation of the shearing behavior of the polymer formulations, with  $n = 1$  and  $k = 1$  for Newtonian systems,  $n < 1$  for shear thinning samples and  $n > 1$  for shear thickening samples (Bonacucina *et al.*, 2004). The apparent viscosity, taken at the apex of the flow curve, was also evaluated for each of the polymeric samples. The cone and plate were cleaned thoroughly with distilled water and dried between samples. All measurements were conducted in triplicate.

### **2.3.5 Analysis of viscoelasticity of mucoadhesive polymeric nasal formulations**

The viscoelasticity of the mucoadhesive polymeric nasal formulations was measured by an oscillatory shear technique conducted on a Carrimed CSL<sup>2</sup> 100 controlled stress rheometer (TA Instruments, Surrey, UK), equipped with a 6 cm steel cone and plate test geometry as described in section 2.3.4. An initial strain sweep measurement was conducted at a constant frequency of 1 Hz to determine the linear viscoelastic region (LVR) of each sample. This region shows the independent plateau of the sample where it can be measured without being destroyed. Frequency sweeps were carried out at strain values within the LVR over a frequency range of 40-0.01 Hz. The samples were individually loaded onto the rheometer as detailed in 2.3.4 and allowed to condition and equilibrate prior to testing. The viscoelastic behaviour of each mucoadhesive polymeric nasal formulation and mucin solution was determined using the storage or elastic modulus ( $G'$ ) and loss or viscous modulus ( $G''$ ). The loss tangent ( $\tan \delta$ ), a secondary indicator of overall viscoelasticity, was also determined from the data and was taken as a measure of the ratio of energy loss to the energy stored per cycle ( $G''/G'$ ). A solid-like response is reflected by a  $\tan \delta < 1$ , while  $\tan \delta > 1$  indicates a liquid-like response. Therefore, as the value of  $\tan \delta$  decreases the elasticity of the sample increases whilst the viscous behaviour becomes reduced.

## **2.4 Statistical analysis**

Statistical analysis was performed using Minitab 16 (Minitab LTD., Coventry, UK). Statistical significance was analysed by a one way analysis of variance (ANOVA) with Tukey's post hoc test. For all measurements,  $P < 0.05$  represented statistical significance.

## **2.5 Results and discussion**

### **2.5.1 Rheological flow behaviour of mucoadhesive polymeric nasal formulations and mucin formulations**

The rheological flow profile and viscosity of a pharmaceutical formulation, especially in intranasal drug delivery, is of paramount importance when considering their overall performance and efficacy (Eccleston *et al.*, 2000, Lee *et al.*, 2009). A desirable nasal spray formulation has an initial high viscosity which prevents the sedimentation of the drug particles and facilitates retention of the drug within the nose. Upon shaking, the formulation should thin to a viscosity which supports drug redispersion and ease of spraying. After application, the original higher viscosity will be restored allowing for improved residence and subsequent drug delivery within the nasal cavity (Eccleston *et al.*, 2000, Seiler *et al.*, 2002, Sharpe *et al.*, 2003, Lee *et al.*, 2009). This phenomenon is known as thixotropy and is due to the scaffold structure attained by the formulation during the dispersal phase. Thixotropy is a reversible gel-sol-gel conversion which results from time dependent changes in the structure. These changes can be induced by factors such as pH or temperature

(Mewis and Wagner, 2009). In short, thixotropy can be used to define the events of an isothermal system where the apparent viscosity reduces due to the application of a stress and then gradually recovers once this stress is removed (Lee *et al.*, 2009). This occurs as a result of the attractive forces between the particles and makes the structure labile and subject to destruction by mechanical forces. The viscosity would decrease as a result of the destruction of this structure but would increase as the scaffold starts to rebuild itself (Luond-Valeskeviciute I and Gruenwald, 2010).

Figures 2.1 to 2.3 show the mean apparent viscosity of the mucoadhesive polymeric nasal formulations at concentrations of 0.2, 0.5 and 1 % w/w measured at shear rates of 100 and 1200 s<sup>-1</sup>. The placebo nasal formulations were used as received and also measured at both low and high shear rates (100 and 1200 s<sup>-1</sup>).

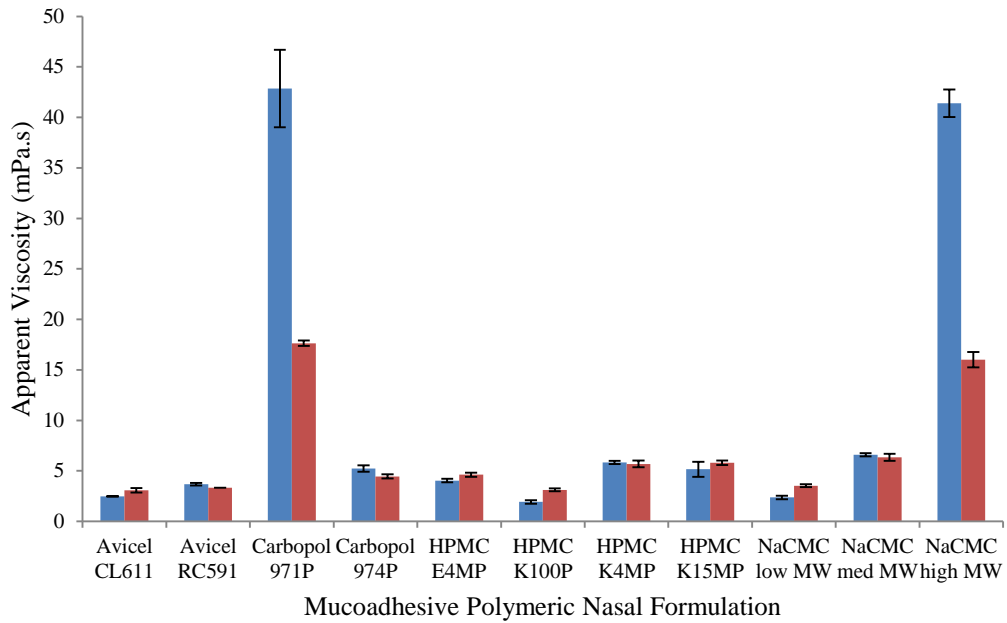


**Figure 2.1** Apparent viscosity of mucoadhesive polymeric nasal formulations measured at 25°C ± S.D. (0.2% w/w measured at a shear rate of 100 s<sup>-1</sup> (red) and 1200 s<sup>-1</sup> (blue)) (n=3).

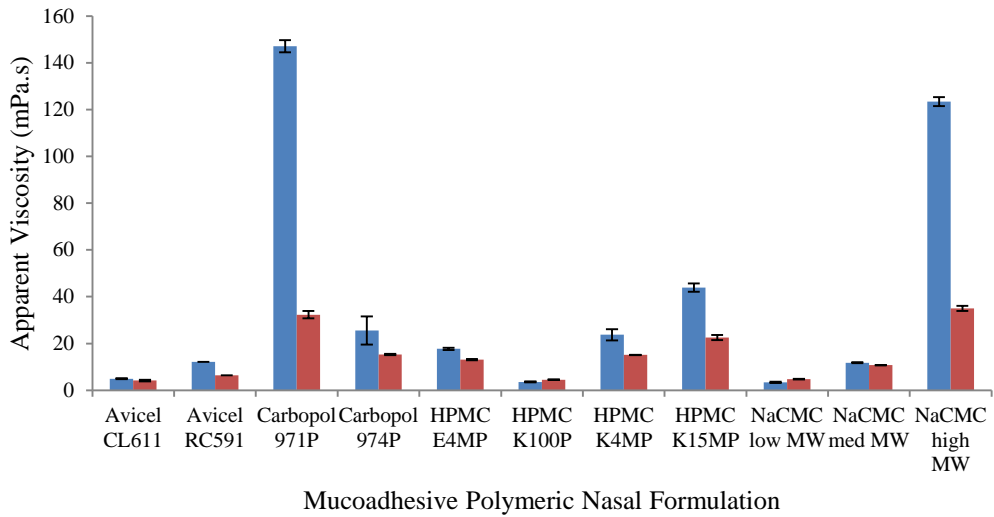


**Figure 2.2** Apparent viscosity of mucoadhesive polymeric nasal formulations measured at 25°C ± S.D. (0.5% w/w measured at a shear rate of 100 s<sup>-1</sup> (red) and 1200 s<sup>-1</sup> (blue)) (n=3).

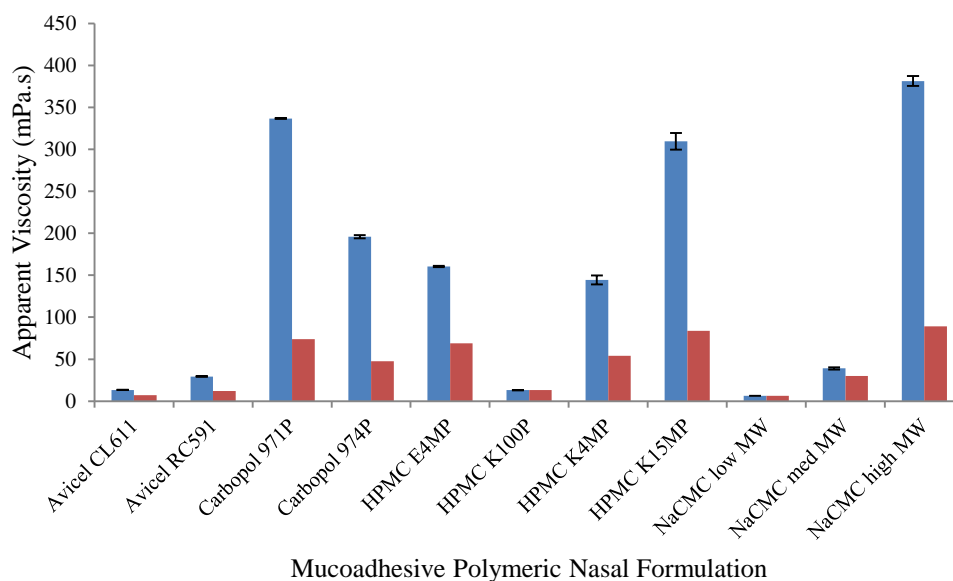


**Figure 2.3** Apparent viscosity of mucoadhesive polymeric nasal formulations measured at 25°C ± S.D. (1% w/w measured at a shear rate of 100 s<sup>-1</sup> (red) and 1200 s<sup>-1</sup> (blue)) (n=3).

It can be seen from the results that Carbopol 971P and NaCMC high MW exhibited considerably higher apparent viscosities compared to the other polymer formulations, regardless of concentration and shear rate. The polymers with the lowest recorded apparent viscosity at all concentrations were HPMC K100P, measured at 100 s<sup>-1</sup>, and Avicel CL611, measured at 1200 s<sup>-1</sup>. The majority of the apparent viscosity results of the polymeric formulations closely resembled the rank order of their molecular weights. This can be seen at the extremes of the results. Carbopol 971P has a molecular weight in the range of billions of daltons and NaCMC high MW has a high molecular weight of 700 kDa, compared with the least viscous polymeric formulations of HPMC K100P which has a molecular weight of only 26 kDa. The exception to this trend is Carbopol 974P and both Avicel grades. Carbopol 974P is a highly crosslinked polymer which has a molecular weight similar to Carbopol 971P.

However, due to the increased instance of crosslinking, Carbopol 974P has a lower viscosity than the lightly crosslinked variant of the polyacrylic acid. The increased molecular weight of Carbopol 974P results in the formation of intermolecular and intramolecular bonds, which subsequently increases the crosslinking density. This increased density causes the polymer molecule to internally link with itself resulting in shortened polymer chains, volume contraction of the polymer coil and thus a reduction in the viscosity (Gebben *et al.*, 1985). Avicel CL611 and RC591 both produce colloidal dispersions and their molecular weights are in the order of billions of daltons. The low apparent viscosity recorded for both grades of Avicel may have resulted from the instance of inter and intramolecular bond formation, as was seen with Carbopol 974P. Molecular weight and chain flexibility are generally recognised to be the two fundamental determinants of the magnitude of polymer viscosity (Morris *et al.*, 1981). Although not significantly different throughout the results, it can be seen from the data that the anionic polymers have an increased apparent viscosity over the uncharged polymers. Intramolecular repulsions between the charged groups, located along the polymer chains, cause the charged polymers to expand and a viscosity greater than their uncharged counterpart results (Williams, 2011). This theory is also evident with the Carbopol polymers. The Carbopol polymers achieve their optimum viscosity upon neutralisation with a base. The neutralisation causes the molecules within the polymer to ionise and expand due to the charge repulsions of the negatively charged carboxylate. This provides the aqueous systems, in which the polymer resides, with the suspending and thickening properties that is required in many pharmaceutical applications (Lubrizol, 2011). It was also seen that increasing the maximum shear rate from 100 to 1200 s<sup>-1</sup> had the

opposite effect and reduced the apparent viscosity of the polymer solutions. This behaviour is due to the shear thinning nature of the polymers and will be discussed further below. Another point to note is that the apparent viscosities of all the mucoadhesive polymeric nasal formulations increase steadily with increasing concentration. This is independent of shear rate. As the concentration of the system is increased, the number of chains within the system also increased. As a result, the degree of entanglement is also increased and the polymer cannot flow as freely as in a polymer with less intermolecular entanglements (Narkis and Rebhun, 1966).

Figure 2.4 illustrates the apparent viscosity of the placebo nasal formulations when measured at both the low and high shear rates.

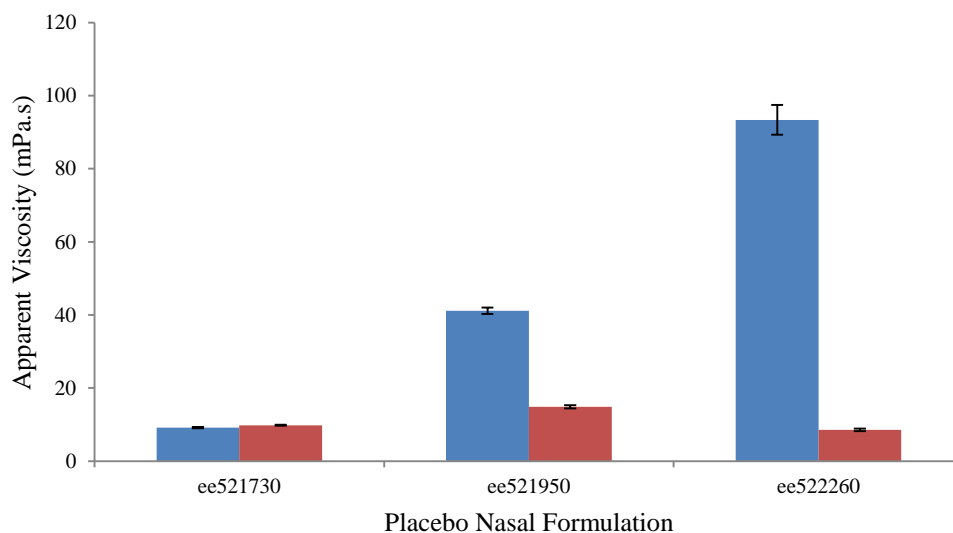


**Figure 2.4** Apparent viscosity of placebo nasal formulations measured at 25°C (blue represents 100 s<sup>-1</sup> and red represents 1200 s<sup>-1</sup>) (n=3).

The results obtained from the lower shear rate ( $100 \text{ s}^{-1}$ ) measurements for the placebo nasal formulations exhibited an overall trend in viscosity of ee521730 ( $9.157 \pm 0.166 \text{ mPa.s}$ ) < ee521950 ( $41.137 \pm 0.838 \text{ mPa.s}$ ) < ee522260 ( $93.373 \pm 4.076 \text{ mPa.s}$ ). Measured at a shear rate of  $1200 \text{ s}^{-1}$ , the placebo nasal formulations provided a different overall trend in viscosity: ee522260 ( $8.547 \pm 0.373 \text{ mPa.s}$ ) < ee521730 ( $9.810 \pm 0.144 \text{ mPa.s}$ ) < ee521950 ( $14.847 \pm 0.455 \text{ mPa.s}$ ). Formulation ee521730 exhibited no change when measured at both the low and high shear rates but ee521950 and ee522260 saw a statistically significant reduction in apparent viscosity between  $100$  and  $1200 \text{ s}^{-1}$ . When the polymeric formulations are subject to an increase in shear, the polymer chains will gradually untangle causing the magnitude of the polymer to reduce and any trapped solvent to be released and thus a reduced viscosity (Chen *et al.*, 2006). It can clearly be seen that ee522260 had a great shear thinning behaviour than ee521950 and so will reduce in viscosity at a greater magnitude with an increase in the application of shear. It can be seen from the data that the apparent viscosity values for the placebo nasal formulations contradict the previous results for the bulk mucoadhesive polymers used in the formulations. The mucoadhesive polymer content for each of the polymeric nasal formulations is summarised in Table 2.4.

**Table 2.4 Mucoadhesive polymer content of placebo nasal formulations (Data supplied from GlaxoSmithKline R&D, Ware, UK).**

Placebo Nasal Formulation	Mucoadhesive Polymer	Concentration of Mucoadhesive Polymer in Placebo Nasal Formulation (% w/w)
ee521730	HPMC E4MP	1
ee521950	Avicel RC591	1.5
ee522260	Avicel CL611	2.4

Concentrating on the concentration that most closely resembles the concentration of the polymer within the placebo nasal formulations, the order for apparent viscosity for 1% w/w HPMC E4MP, Avicel RC591 and Avicel CL611, regardless of the shear rate used, was Avicel CL611 < Avicel RC591 < HPMC E4MP. It is likely that the observed difference between the recorded apparent viscosity of the bulk mucoadhesive polymeric nasal formulations and that of the placebo nasal formulations is as a result of dilution by the added excipients to the latter. These excipients include solvents, buffers and preservatives (Tables 2.1 to 2.3). Another reason for the variations between the results may be due to the effect of these excipients on the mucoadhesive polymers. Further work would need to be completed in order to establish whether this explanation is valid.

The viscosity of the 2% w/w mucin formulation was obtained as a reference and is illustrated in Figure 2.5.

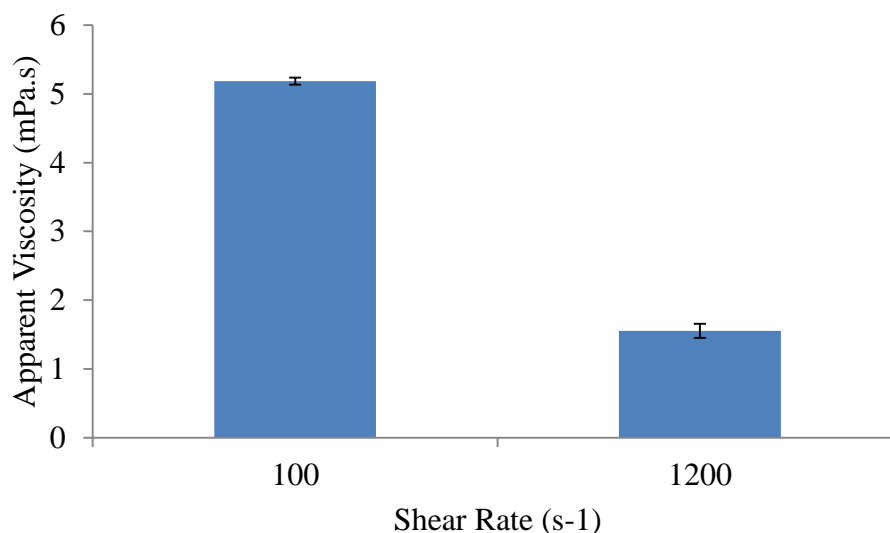


**Figure 2.5** Mean apparent viscosity of 2% w/w mucin formulation  $\pm$  S.D measured at 25°C (n=3).

It can be seen from the results that the apparent viscosity of 2% w/w crude gastric mucin was particularly low when measured at 100 s<sup>-1</sup> (5.186  $\pm$  0.051 mPa.s). The apparent viscosity decreased to 1.554  $\pm$  0.101 mPa.s when the higher shear rate was applied. This is synonymous with shear thinning behaviour, which has been reported in previous studies (Celli *et al.*, 2007, Boegh *et al.*, 2013).

Rheograms (shear stress v. shear rate curves) can be used to visually interpret the flow behaviour of the mucoadhesive formulations. Thixotropy can be quantified by measuring the area of the hysteresis loop of a rheogram. Figures 2.6 to 2.17 represent the rheograms obtained for the mucoadhesive polymeric formulations and placebo formulations. It can be seen from the rheograms that only some of the formulations investigated showed thixotropic behaviour. Thixotropy was not seen

for any of the 0.2% w/w formulations. It is known that concentration imparts on the polymeric chain structure and the dynamic behaviour of the formulation (Stoltz *et al.*, 2006). At low concentrations, the formulations experienced reduced structural interactions due to the lower availability of polymeric chains. This would lead to a less dense polymer structure which would see varied results when shear is applied. Thixotropy is a time dependent phenomenon which is seen in systems where the recovery of the polymeric structure is slower than the original structural breakdown caused by the application of a force. In lower concentration polymer formulations, the structure is simple enough to allow for a quick recovery when the force (shear) is removed. An increase in thixotropic behaviour, due to an increase in polymer concentration, has been seen in a study by Ghannam (2009) who investigated the rheological behaviour of crude oil polyacrylamide emulsions (Ghannam, 2009). The dependence of polymer structure on the thixotropic behaviour will also be affected by the molecular weight and cross linking density of the polymer. Signs of this dependency were seen in the results obtained from this study, although varying degrees of dependency were recorded for each polymeric formulation, which implied that factors other than those mentioned affect the rheological behaviour.

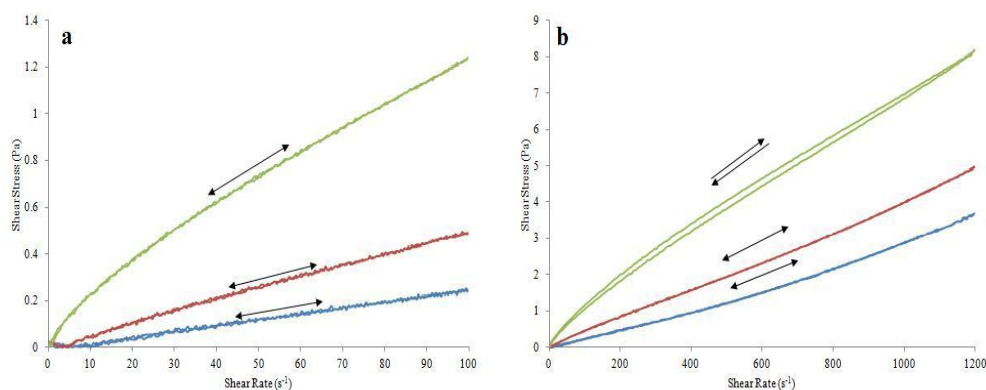


**Figure 2.6** Typical rheological flow profiles of 0.2% w/w (blue), 0.5% w/w (red) and 1% w/w (green) Avicel CL611 measured at  $100 \text{ s}^{-1}$  (a) and  $1200 \text{ s}^{-1}$  (b).

Avicel CL611 (Figure 2.6) showed no thixotropy for any concentration measured at  $100 \text{ s}^{-1}$  and only slight thixotropy was seen for the 1% w/w concentration at  $1200 \text{ s}^{-1}$ . Avicel CL611 is a large molecular weight polymer and is known to impart thixotropic behaviour at low concentrations (Hägerström and Edsman, 2003). However, the recommended concentration for use within a formulation is stated as 2-3% w/w (Hägerström and Edsman, 2003), which would suggest that concentrations lower than 2% do not yield the thixotropic behaviour that Avicel CL611 is known for. Other studies have shown thixotropic behaviour for Avicel CL611 in concentrations of 1% w/w to 6% w/w (Khutoryanskiy, 2011) and 2.5 % w/w (Dolzplanas *et al.*, 1988). It would appear that Avicel CL611 concentrations below 1% w/w do not possess a chain structure that requires time to rebuild following shear.

The same behaviour was recorded for NaCMC med MW with slight thixotropy seen at 1% w/w ( $1200 \text{ s}^{-1}$ ) (Figure 2.7).

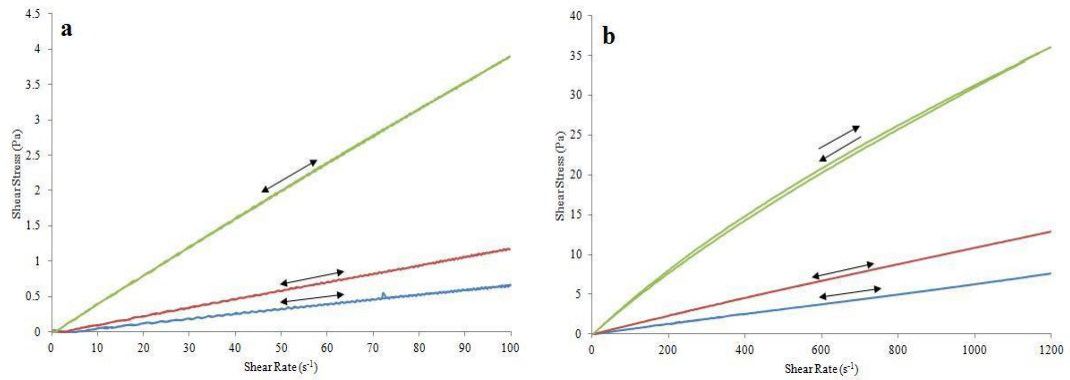


**Figure 2.7** Typical rheological flow profiles of 0.2% w/w (blue), 0.5% w/w (red) and 1% w/w (green) NaCMC med MW measured at  $100 \text{ s}^{-1}$  (a) and  $1200 \text{ s}^{-1}$  (b).

This is in line with previous studies carried out on NaCMC. It was found that NaCMC presented negligible thixotropic properties at low concentrations but an increase in polymeric concentration resulted in an increased value in thixotropy (Ghannam and Esmail, 1997, Edali *et al.*, 2001). These findings by Ghannam and Edali do not correlate with the results obtained for all grades of NaCMC investigated in this study.

NaCMC low MW (Figure 2.8) did not show any thixotropic behaviour, regardless of the concentration or shear rate applied. As was the case with the lower concentration of Avicel CL611, the polymeric network will be less defined and structured and the removal of the shear will result in an instantaneous recovery of the chains.

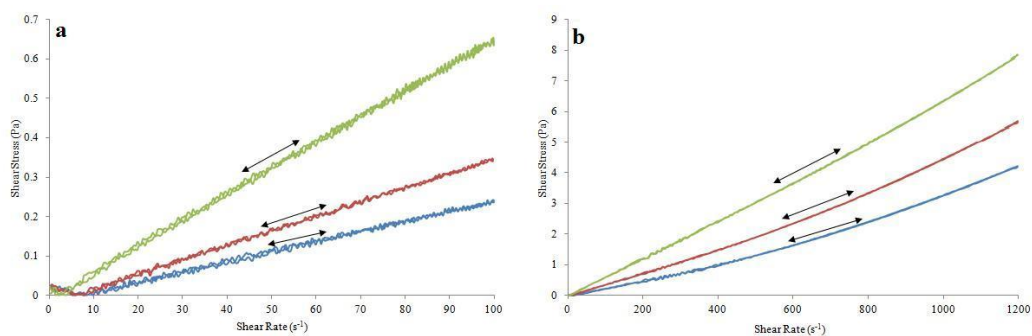


**Figure 2.8** Typical rheological flow profiles of 0.2% w/w (blue), 0.5% w/w (red) and 1% w/w (green) NaCMC low MW measured at  $100\text{ s}^{-1}$  (a) and  $1200\text{ s}^{-1}$  (b).

NaCMC high MW exhibited very different behaviour (Figure 2.9).

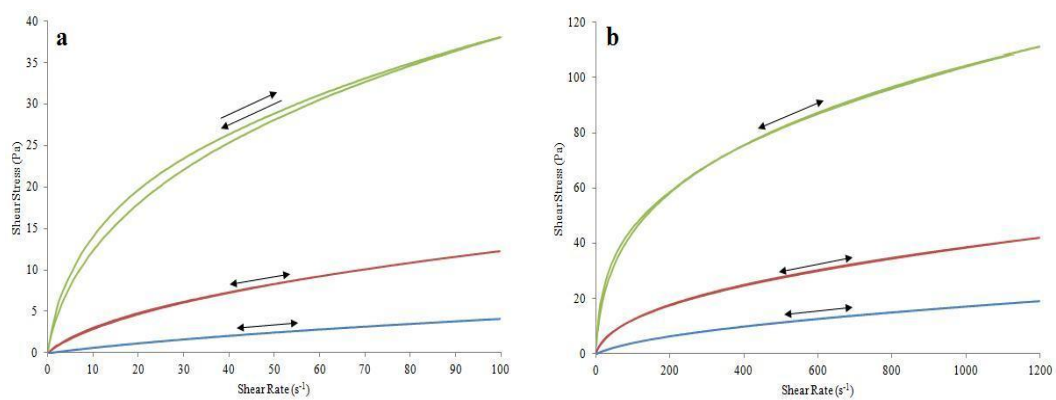


**Figure 2.9** Typical rheological flow profiles of 0.2% w/w (blue), 0.5% w/w (red) and 1% w/w (green) NaCMC high MW measured at  $100\text{ s}^{-1}$  (a) and  $1200\text{ s}^{-1}$  (b).

At  $100\text{ s}^{-1}$ , the polymeric formulation expressed thixotropy at 1% w/w but did not show any thixotropic behaviour at  $1200\text{ s}^{-1}$ . This can be described by orthokinetic

flocculation (Mewis and Wagner, 2009). A more detailed description of thixotropy describes the phenomenon as a result of weakly attractive inter-particulate forces. These forces will cause a network of flocs to form. Shear forces break down the flocs and an increase in shear will result in a decrease in floc aggregates (Mewis and Wagner, 2009). However, a low shear rate can induce flocculation, which will have an effect on the level of thixotropy expressed. It would seem that in the case of NaCMC high MW, the low shear rate has caused a build up of structure, which was not evident at the highest shear rate.

Thixotropy was not seen in any of the HPMC formulations (Figures 2.10 to 2.13). Reviews of the literature found many reports that agree with these findings but on many occasions the formulations contained an API as well as the HPMC. Quinones and Ghaly (2008) investigated the use of HPMC K4 and Carbopol 934 as a gel base for the delivery of the antifungal medicine nystatin (Quinones and Ghaly, 2008). The up and down curve of the rheograms for the nystatin/HPMC formulation were superimposed and thus the formulations were not found to be thixotropic. Hino and Ford (2001) studied the effect of nicotinamide on the rheological behaviour of 1-3% w/w HPMC E5 (Hino and Ford, 2001). Again it was found that the formulations containing both nicotinamide and HPMC were not thixotropic in nature. Although both of these studies confirm the non-thixotropic behaviour of HPMC, they are concerned with formulations that also contain drug. It should be noted that interaction between the drug and HPMC could directly impact on the rheological behaviour of the mucoadhesive polymer. The rheological behaviour of HPMC was

measured within another mixed formulation in a study conducted by Amboon and colleagues (2010). In this work, the effect of the addition of 0.2% w/w and 0.5% w/w HPMC K4 and E4 on various properties of rice flour batter (Amboon et al., 2012). It was found that the addition of both grades of HPMC increased the thixotropic nature of the batter. This work contradicts both the work done in this section and also the work carried out by the authors mentioned. It can be seen that additional excipients and active ingredients can have an impact on the rheological behaviour of the polymeric formulation. Although the occurrence of intermolecular hydrogen bonding between the hydroxyl groups of the HPMC chains and the water molecules is well known (Joshi, 2011), Sanz and colleagues (2005) reported that only small amounts of chain-chain interactions are present in fully hydrated HPMC systems and that simple entanglements prevail (Sanz *et al.*, 2005). The introduction of shear to such a simple structure would result in deformation of the ordered structure; however, the structure would rebuild and realign almost instantaneously upon the removal of the force. This would result in a non-thixotropic profile.

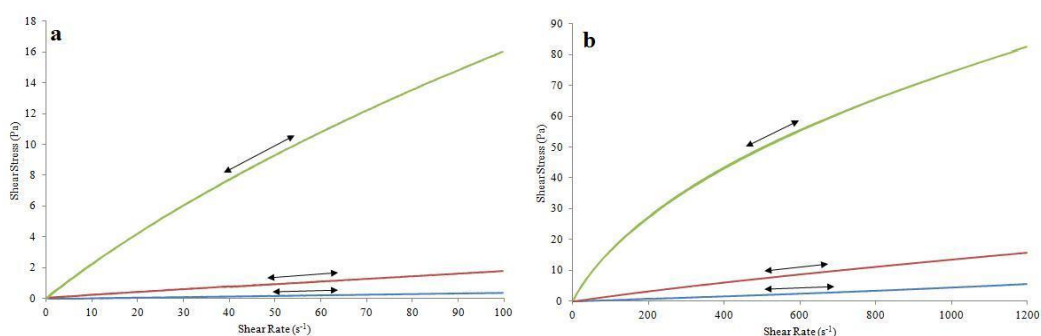


**Figure 2.10** Typical rheological flow profiles of 0.2% w/w (blue), 0.5% w/w (red) and 1% w/w (green) HPMC E4MP measured at 100 s<sup>-1</sup> (a) and 1200 s<sup>-1</sup> (b).

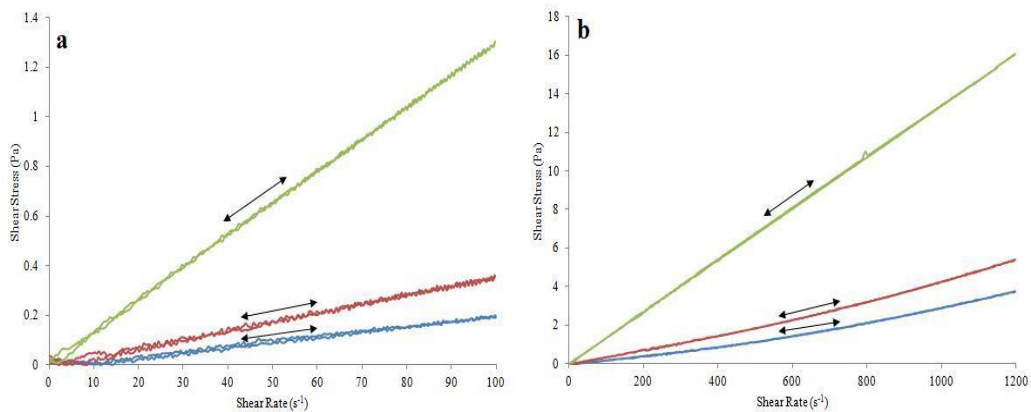


**Figure 2.11** Typical rheological flow profiles of 0.2% w/w (blue), 0.5% w/w (red) and 1% w/w (green) HPMC K100P measured at  $100 \text{ s}^{-1}$  (a) and  $1200 \text{ s}^{-1}$  (b).

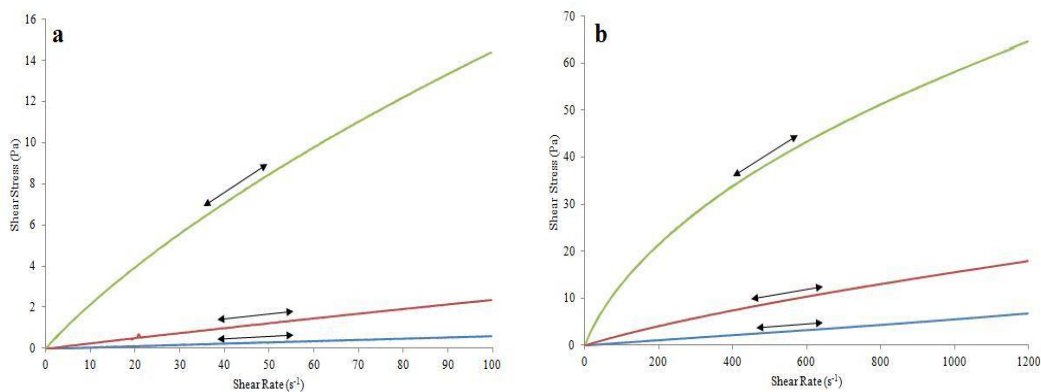


**Figure 2.12** Typical rheological flow profiles of 0.2% w/w (blue), 0.5% w/w (red) and 1% w/w (green) HPMC K4MP measured at  $100 \text{ s}^{-1}$  (a) and  $1200 \text{ s}^{-1}$  (b).

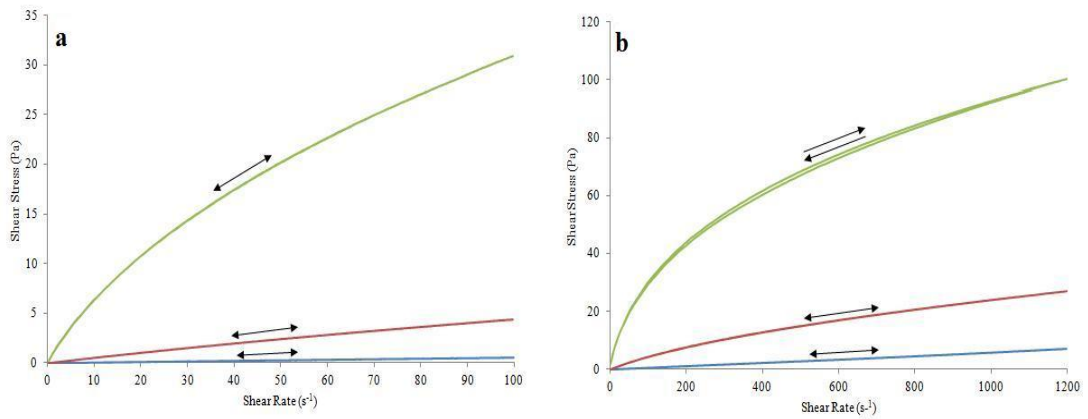


**Figure 2.13** Typical rheological flow profiles of 0.2% w/w (blue), 0.5% w/w (red) and 1% w/w (green) HPMC K15MP measured at 100 s<sup>-1</sup> (a) and 1200 s<sup>-1</sup> (b).

Avicel RC591, Carbopol 971P and Carbopol 974P produced the most prominent thixotropic profiles (Figures 2.14 to 2.16).

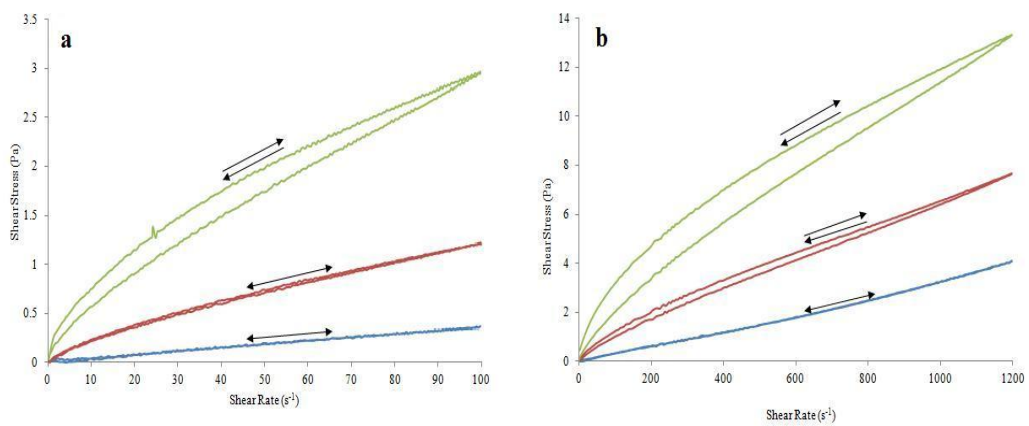


**Figure 2.14** Typical rheological flow profiles of 0.2% w/w (blue), 0.5% w/w (red) and 1% w/w (green) Avicel RC591 measured at 100 s<sup>-1</sup> (a) and 1200 s<sup>-1</sup> (b).

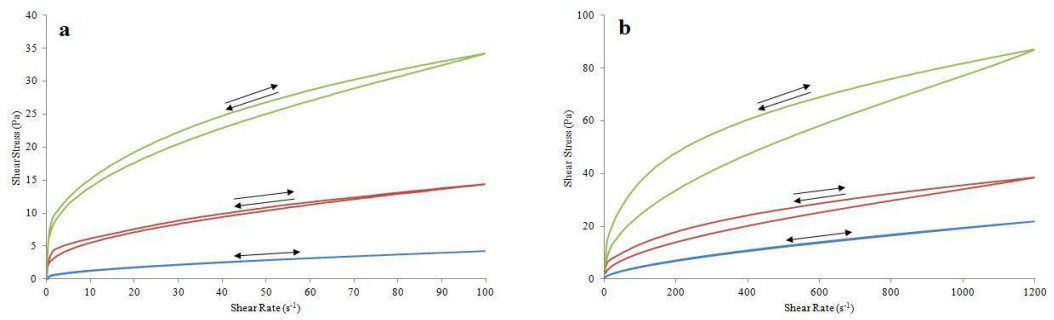


**Figure 2.15** Typical rheological flow profiles of 0.2% w/w (blue), 0.5% w/w (red) and 1% w/w (green) Carbopol 971P measured at  $100 \text{ s}^{-1}$  (a) and  $1200 \text{ s}^{-1}$  (b).

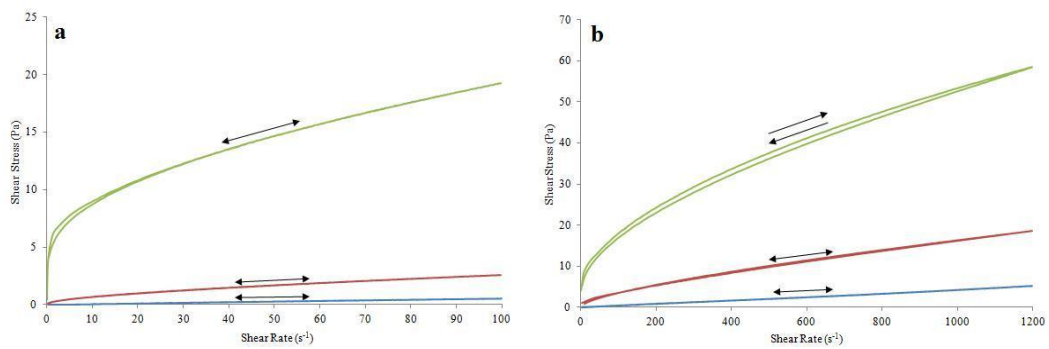


**Figure 2.16** Typical rheological flow profiles of 0.2% w/w (blue), 0.5% w/w (red) and 1% w/w (green) Carbopol 974P measured at  $100 \text{ s}^{-1}$  (a) and  $1200 \text{ s}^{-1}$  (b).

Avicel RC591 showed thixotropy at  $100 \text{ s}^{-1}$  for the 1% w/w concentration and at  $1200 \text{ s}^{-1}$  for both 0.5% w/w and 1% w/w formulations. This is in agreement with the information provided by the manufacturer and also Avicel CL611 discussed earlier (Hägerström and Edsman, 2003). Increased thixotropy was seen for Avicel RC591 compared with Avicel CL611, which may be as a result of the decreased NaCMC

content (0.8% in RC591 compared with 1.2% in CL611). The reduced concentration of NaCMC in Avicel RC591 may have allowed for the deformation of the structure with a lower magnitude of applied shear, resulting in thixotropy being seen for the lower shear rate. A greater level of thixotropy was evident for the 1% w/w formulation at  $1200\text{ s}^{-1}$ , which corresponds with the published literature stating that Avicel CL611 demonstrates thixotropic behaviour at a concentration of 1.2% (Hägerström and Edsman, 2003). The increased level of thixotropy seen for 1% w/w Avicel RC591 compared to the 0.5% w/w was due to the extensively structured network produced as a result of greater entanglement. The strengthened structure has resulted in the polymer requiring more time to return to its original state after the removal of the shear force. This increased recovery time with increasing viscosity was also found in a study by Zhao and colleagues (2011). The authors used increasing concentrations of Avicel RC591 to determine the properties of the hydrogel structure and found that the increase in hydrogel concentration caused an increase in the time of structural recovery after the application of shear (Zhao *et al.*, 2011). This linear relationship was also present in the results obtained for Carbopol 971P. Both the low and high shear rates produced rheograms that showed thixotropic behaviour for 0.5% w/w and 1% w/w. Carbopol 971P produced the greatest thixotropic behaviour of all the polymers investigated suggesting that this polymeric formulation has a strong polymeric structure and thus will take a greater length of time to recover following the exposure of shear. This thixotropic behaviour is contradictory to the information provided by the manufacturers who state that little or no thixotropy is exhibited by most Carbopol gels (Lubrizol, 2008). Other studies also confirmed this statement. Jiminez and colleagues (2007) studied the rheological

behaviours of binary gels including Carbopol Ultrez™ 10 and stated that in general, the thixotropic properties of Carbopol gels are severely limited (Jimenez *et al.*, 2007). Benmouffok-Benbelkacem and colleagues investigated the yield stress behaviour of Carbopol 940, Xanthan gum and ketchup and concluded that the Carbopol did not express thixotropy (Benmouffok-Benbelkacem *et al.*, 2010). Conversely, Ortan and colleagues (2011) found that Carbopol 940 (0.5% w/w and 1% w/w) was thixotropic (Ortan *et al.*, 2011). The study looked into the rheological properties of a Carbopol vehicle that contained oil filled liposomes. It could be inferred that the presence of these liposomes may have had an effect on the rheological properties of the Carbopol formulation. Another study that reported Carbopol as a thixotropic polymer was conducted by Labanda and colleagues (2004) who proposed a rheological model that could be used to define the rheological behaviour of a colloidal dispersion (Labanda *et al.*, 2004). The author commented that Carbopol gels express complex thixotropy in non steady state conditions, which is caused by the break down and subsequent recovery of the micro-gel structure. The investigation showed Carbopol 941 to exhibit a typical thixotropic profile with Carbopol 940 showing a level of negative thixotropy. All cited papers relating to Carbopol used a variety of solvents to make up the polymeric gels. These included demineralised water (Benmouffok-Benbelkacem *et al.*, 2010), an ethanol/Milli-Q water mixture (Jimenez *et al.*, 2007), deionised water (Labanda *et al.*, 2004) and a water/glycerin mix (Ortan *et al.*, 2011). The pH of these quoted Carbopol formulations was also altered with sodium hydroxide (NaOH) (Labanda *et al.*, 2004, Benmouffok-Benbelkacem *et al.*, 2010) or triethanolamide (TEA) (Islam *et al.*, 2004, Jimenez *et al.*, 2007, Ortan *et al.*, 2011). It is known that thixotropy is affected by

several formulation factors including pH, temperature and the addition of excipients (Lee *et al.*, 2009) and this is likely to be the reason behind the differing thixotropic behaviours seen between studies. However, a slight contradiction comes from the study conducted by Islam and colleagues (2004) who found no significant difference in rheological behaviour with a change in pH (Islam *et al.*, 2004). The Carbopol formulations used in this study composed of deionised water, glycerol and propylene glycol and therefore the overall formulation may have impacted on the thixotropy observed. Another factor that can affect the polymeric structure and thus the level of thixotropy is the crosslinking density. This was seen in Carbopol 974P. Carbopol 974P has a higher crosslinking density than Carbopol 971P and as such the polymer undergoes intermolecular and intramolecular bonding. The bonding increases the already high density of crosslinks and the strength of the polymer structure increases as a result. In this study, Carbopol 974P showed minimal thixotropy at 1% w/w for both low and high shear rates. This lack of thixotropic behaviour will be due to the increased strength of the structure and thus the applied shear rates have not been high enough for deformation to occur.

An effect of the addition of excipients was also seen with the rheological profiles of the three placebo nasal formulation (ee521730, ee521950 and ee522260) (Figure 2.17).

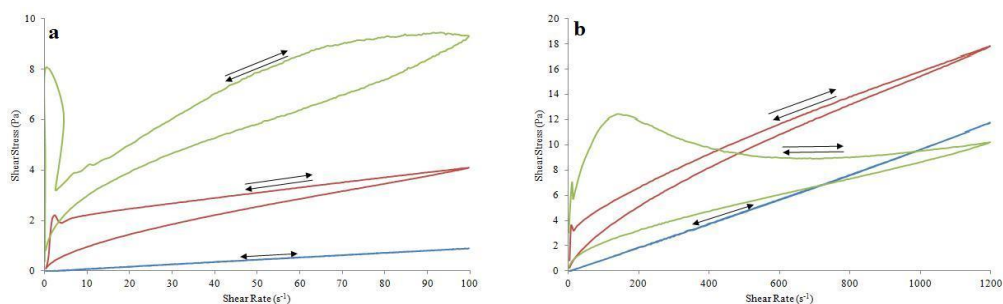


**Figure 2.17** Typical rheological flow profiles of placebo nasal formulations, ee521730 (blue), ee521950 (red) and ee522260 (green) NaCMC low MW measured at  $100 \text{ s}^{-1}$  (a) and  $1200 \text{ s}^{-1}$  (b).

Formulation ee521730 did not show any thixotropic behaviour at either the low or high shear rate, which suggests that the structure of the formulation is weak enough to recover after deformation. This is in line with the rheology results obtained for the formulation's polymeric component HPMC E4MP. The remaining formulations, ee521950 and ee522260 both showed classic thixotropic behaviour, with ee522260 exhibiting a more pronounced hysteresis loop over both shear rates. The polymeric constituent of ee521950 and ee522260, Avicel RC591 and Avicel CL611 respectively, also exhibited thixotropy at 1% w/w, although Avicel CL611 did not exhibit thixotropy at  $100 \text{ s}^{-1}$ . This rheological behaviour suggests that ee521950 and ee522260 consisted of a strengthened, three dimensional polymeric structure which has been broken down due to the application of a shear force. The removal of the shear does not result in an instantaneous recovery which is visualised by the hysteresis loop on the rheogram. Characterising the thixotropic behaviour of a sample is a complex task and is affected by a variety of different formulation factors. It is therefore imperative that a full analysis of the formulation's properties are

known in order to determine if any thixotropic behaviour is due to factors such as pH or temperature.

The power law, shown in Equation 2.1, is another description used to characterise the resultant rheograms of the mucoadhesive polymeric nasal formulations and the placebo nasal formulations. Plots of shear stress versus shear rate were used to calculate the flow behaviour index ( $n$ ) and consistency index ( $K_c$ ). The flow behaviour index can indicate a deviance from Newtonian behaviour. For shear thinning systems,  $0 < n < 1$ , and for shear thickening systems,  $n > 1$ . The flow of a system will become less dependent on shear as “ $n$ ” approaches 1 and thus the system is deemed Newtonian when  $n = 1$ . Tables 2.5 to Table 2.7 show the flow behaviour index ( $n$ ) and consistency index ( $K_c$ ) for the mucoadhesive polymeric nasal formulations and placebo nasal formulations. Due to instrumental error, a 2% deviation is applied to the results and therefore a Newtonian system will show a value from between 0.98 to 1.02, shear thinning will be less than 0.98 and shear thickening will be more than 1.02.

**Table 2.5 Flow behaviour index ( $n$ ) and consistency index ( $K_c$ ) derived from the power law model of mucoadhesive polymeric nasal formulations measured at  $100 \text{ s}^{-1}$  ( $n=3$ ).**

Mucoadhesive Polymeric Nasal Formulations	Flow Behaviour Index, $\eta$			Consistency Index, $K_c$ (Pa.s <sup>c</sup> )		
	0.2%	0.5%	1%	0.2%	0.5%	1%
Avicel CL611	0.991	0.938	0.721	0.005	0.015	0.046
Avicel RC591	0.947	0.757	0.729	0.005	0.038	0.102
Carbopol 971P	0.527	0.424	0.384	0.352	1.676	5.285
Carbopol 974P	0.959	0.601	0.344	0.007	0.147	3.679
HPMC E4MP	0.995	0.989	0.823	0.003	0.019	0.364
HPMC K100P	0.994	0.992	0.990	0.001	0.002	0.013
HPMC K4MP	0.996	0.959	0.803	0.004	0.029	0.369
HPMC K15MP	0.906	0.893	0.660	0.005	0.073	1.502
NaCMC low MW	0.998	0.992	0.985	0.002	0.003	0.006
NaCMC med MW	0.965	0.956	0.945	0.005	0.015	0.044
NaCMC high MW	0.774	0.593	0.432	0.118	0.813	5.889

**Table 2.6 Flow behaviour index ( $n$ ) and consistency index ( $K_c$ ) derived from the power law model of mucoadhesive polymeric nasal formulations measured at  $1200 \text{ s}^{-1}$  ( $n=3$ ).**

Mucoadhesive Polymeric Nasal Formulation	Flow Behaviour Index, $\eta$			Consistency Index, $K_c$ ( $\text{Pa}\cdot\text{s}^c$ )		
	0.2%	0.5%	1%	0.2%	0.5%	1%
Avicel CL611	0.918	0.902	0.837	0.006	0.014	0.083
Avicel RC591	0.908	0.840	0.769	0.004	0.020	0.062
Carbopol 971P	0.613	0.557	0.518	0.268	0.728	2.149
Carbopol 974P	0.903	0.700	0.513	0.004	0.104	1.345
HPMC E4MP	0.924	0.865	0.618	0.002	0.035	1.040
HPMC K100P	0.994	0.992	0.986	0.000	0.001	0.015
HPMC K4MP	0.905	0.807	0.612	0.005	0.406	0.920
HPMC K15MP	0.930	0.693	0.472	0.004	0.200	3.968
NaCMC low MW	0.931	0.922	0.915	0.004	0.001	0.005
NaCMC med MW	0.993	0.991	0.819	0.005	0.011	0.103
NaCMC high MW	0.607	0.489	0.355	0.261	1.313	9.153

**Table 2.7 Flow behaviour index ( $n$ ) and consistency index ( $K_c$ ) derived from the power law model of placebo nasal formulations measured at  $100 \text{ s}^{-1}$  ( $n=3$ ).**

Placebo Nasal Formulations	Flow Behaviour Index, $\eta$	Consistency Index, $K_c$ ( $\text{Pa}\cdot\text{s}^c$ )
ee521730	0.997	0.008
ee521950	0.640	0.210
ee522260	0.497	0.867

**Table 2.8 Flow behaviour index ( $n$ ) and consistency index ( $K_c$ ) derived from the power law model of placebo nasal formulations measured at  $1200 \text{ s}^{-1}$  ( $n=3$ ).**

Placebo Nasal Formulations	Flow Behaviour Index, $\eta$	Consistency Index, $K_c$ (Pa.s <sup>c</sup> )
ee521730	0.995	0.008
ee521950	0.694	0.128
ee522260	0.641	0.104

It can be seen from the results that the flow behaviour index of the majority of the mucoadhesive polymeric formulations and placebo formulations were less than one, indicating that each polymeric formulation was shear thinning ( $n = 1$ ); however, there were many that showed shear thickening behaviour. An instrumental error of 2% was taken into account and therefore not all flow behaviour index values correlated with the apparent rheological behaviour seen in the Rheograms. One explanation of this behaviour could be due to the noisy rheograms produced due to the low viscosity of the formulations. The Flow Behaviour Index is calculated using a best fit model rather than a calculation of the actual recorded data and the best fit has produced a shear thinning Flow Behaviour Index.

It was observed that the flow behaviour of the mucoadhesive polymeric nasal formulations departed further from Newtonian behaviour as the polymeric concentration of the formulations increased. This can be explained in terms of polymer chain entanglement. When shear stress was applied to the formulations the polymer chain disentangled, this rate of disentanglement was greater than the speed at which the chains were able to re-establish new chain entanglements. This

ultimately resulted in a reduction of viscosity. As the concentration of the polymeric formulations increased, so too did the instance of chain entanglement. An increased magnitude of chain entanglement resulted in an increased rate of chain disentanglement due to shear, with the rate of deformation far exceeding that of the reformation of the entangled chains. Thus, the shear thinning behaviour became more pronounced. The consistency index ( $K_c$ ) is an indicator of the viscosity of the system at low shear rates. The results showed that an increase in concentration resulted in an increased value for  $K_c$ . This is consistent with the previous apparent viscosity results obtained in this study. The highest  $K_c$  value obtained at both shear rates was for NaCMC high MW and the lowest  $K_c$  value at both low and high shear rates was HPMC K100P. Again this mimics the previously results achieved for the apparent viscosities of the mucoadhesive polymeric nasal formulations. The placebo nasal formulations also provided  $K_c$  values which mirrored the apparent viscosity results shown in Figure 2.4.

### **2.5.2 Analysis of viscoelasticity of mucoadhesive polymeric nasal formulations**

The spreadability and retention time of topical nasal treatments will be affected by the rheological properties of the formulation. After application of the formulation within the nasal cavity, the rheological properties of the formulation will overrule the physicochemical properties (Baloglu *et al.*, 2011). It is therefore imperative that formulators of nasally delivered drugs should look towards the development of mucoadhesive drug formulations that not only allow for optimum interaction

between the polymer and mucus, but also offer optimum elasticity in order to increase the resistance against detachment from the nasal cavity (Jones *et al.*, 2009). Analysis of the viscoelastic properties of the mucoadhesive polymeric nasal formulations and placebo nasal formulations was carried out using oscillatory rheology. Oscillation is designed to probe the structure of the material and can record a fingerprint spectrum of the characteristics of the material's structure in a non-destructive manner. The technique is different to that of flow rheology as the upper geometry plate is driven sinusoidally as opposed to continuously. Oscillation can classify materials into three behaviours; elastic, viscous or viscoelastic. In practice, purely elastic or viscous materials are rare and in the majority of instances the materials exhibit both viscous and elastic behaviours and are thus termed viscoelastic. In this study, the elastic or storage modulus ( $G'$ ), viscous or loss modulus ( $G''$ ) and the loss tangent ( $\tan \delta$ ) were analysed in order to validate the viscoelastic behaviour of the formulations. The elastic modulus is indicative of the extent of the structure of the materials and how the material stores elastic energy. The viscous modulus relates to the dissipation of viscous energy and a large value of  $G''$  represents a prevalent viscous material. The loss tangent represents the amount of energy in the cyclic deformation and is calculated as the ratio of the loss modulus to the storage modulus. A loss tangent less than 1 shows a predominantly elastic material (Jones *et al.*, 2003, Sriamornsak and Wattanakorn, 2008). The shape and magnitude of the  $G'$  and  $G''$  profiles can indicate the strength of a material (Madsen *et al.*, 1998a, Ikeda and Nishinari, 2001). In polymeric systems, entanglements among the polymeric chains are present at high concentrations, however, at low frequencies, there is sufficient time to allow for the polymeric chains to disentangle

and flow during one oscillation. In this instance,  $G'' > G'$ . As the elastic properties of the polymeric system increases, the time for chain entanglements to come apart is reduced and therefore the elastic modulus becomes larger than the storage modulus (Jones *et al.*, 2003). Gel formulations should exhibit a larger magnitude for  $G'$  than  $G''$  i.e. solid-like behaviour, over the entire frequency range of the experiment with insignificant frequency dependence from any of the moduli (Ikeda and Nishinari, 2001). A typical viscoelastic rheogram is shown in Figure 2.18.

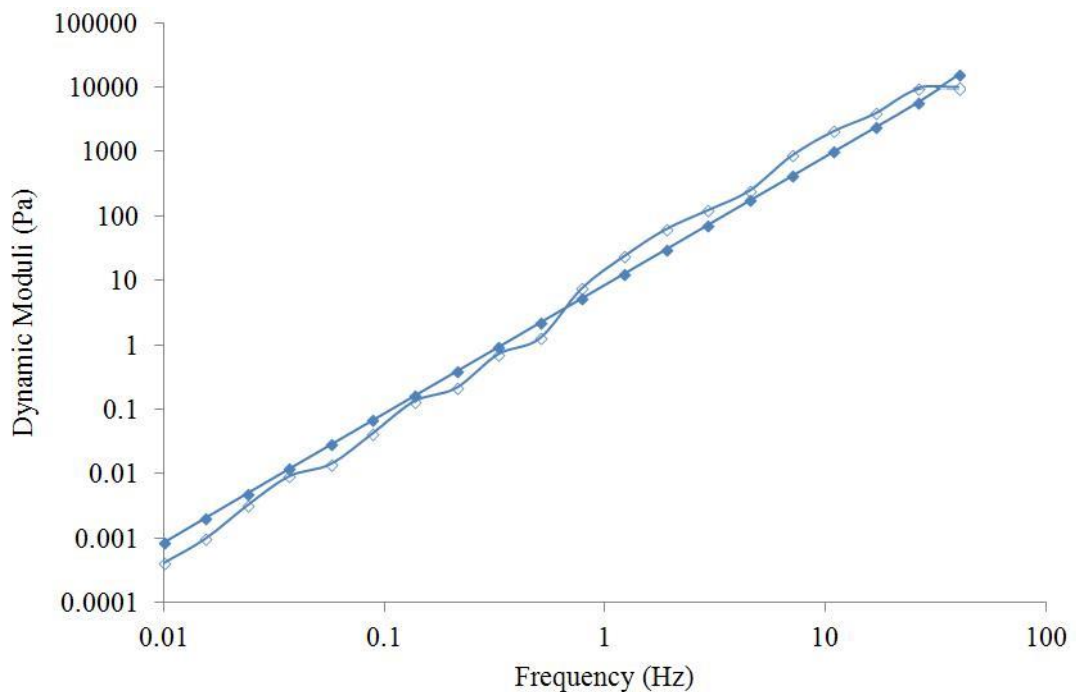


**Figure 2.18** Dynamic oscillation spectra of 2% w/w mucin at 25 °C. Open markers represent  $G''$  and closed markers represent  $G'$ .

This spectra indicated that mucin is a predominantly elastic gel, with  $G' > G''$ . However, this behaviour is only evident up until ~1 Hz where a crossover was seen.

At this point, the gel structure has relaxed and a largely viscous behaviour prevails. It is well known that mucin is a highly viscoelastic gel due to it possessing both elastic and viscous behaviours (Lai *et al.*, 2009) but changes in rheological behaviour may be found depending on the source of the mucin and whether it has been freshly excised or has been freeze-dried.

The  $\tan \delta$  results for the polymeric nasal formulations and the placebo nasal formulations were taken from five representative frequency points and are summarised in Tables 2.6 and 2.7 and oscillation rheograms for the mucoadhesive polymeric nasal formulations and placebo nasal formulations are shown in Figures 2.19 to 2.30.

**Table 2.9 Mean loss tangent ( $\tan \delta$ ) values  $\pm$  S.D. for mucoadhesive polymeric nasal formulations at five representative frequencies (n=3).**

Polymeric Nasal Formulation	Concentration (% w/w)	$\tan \delta$				
		0.01 Hz	0.14 Hz	0.79 Hz	7.02 Hz	40.02 Hz
Avicel CL611	0.2	25.882 (0.012)	0.297 (0.002)	0.134 (0.001)	0.380 (0.000)	0.141 (0.000)
	0.5	109.175 (0.009)	0.235 (0.002)	0.249 (0.000)	0.963 (0.000)	0.139 (0.002)
	1	3.409 (0.005)	0.105 (0.002)	0.008 (0.000)	0.001 (0.000)	0.050 (0.001)
Avicel RC591	0.2	0.225 (0.001)	0.016 (0.001)	0.003 (0.000)	0.002 (0.000)	0.026 (0.000)
	0.5	0.511 (0.001)	0.036 (0.000)	0.005 (0.000)	0.001 (0.000)	0.040 (0.001)
	1	0.613 (0.004)	0.105 (0.000)	0.018 (0.001)	0.003 (0.000)	0.019 (0.000)
Carbopol 971P	0.2	0.585 (0.001)	0.323 (0.005)	0.373 (0.002)	0.438 (0.005)	0.504 (0.002)
	0.5	0.142 (0.000)	0.109 (0.001)	0.098 (0.000)	0.202 (0.001)	0.290 (0.001)
	1	0.118 (0.000)	0.108 (0.000)	0.095 (0.000)	0.230 (0.002)	0.037 (0.000)
Carbopol 974P	0.2	0.052 (0.000)	0.093 (0.001)	0.186 (0.002)	0.275 (0.002)	0.482 (0.001)
	0.5	0.157 (0.000)	0.125 (0.002)	0.301 (0.001)	0.583 (0.005)	0.047 (0.000)
	1	0.114 (0.001)	0.061 (0.000)	0.046 (0.000)	0.151 (0.000)	0.170 (0.001)
HPMC E4MP	0.2	0.260 (0.002)	0.019 (0.001)	0.003 (0.000)	0.001 (0.000)	0.118 (0.001)
	0.5	0.449 (0.000)	0.086 (0.003)	0.015 (0.000)	0.003 (0.000)	0.030 (0.001)
	1	26.836 (0.045)	1.384 (0.001)	0.234 (0.000)	0.020 (0.000)	0.006 (0.000)
HPMC K100P	0.2	0.185 (0.001)	0.014 (0.001)	0.003 (0.001)	0.002 (0.000)	0.064 (0.000)
	0.5	0.296 (0.002)	0.022 (0.006)	0.004 (0.000)	0.003 (0.000)	0.089 (0.000)
	1	1.068 (0.001)	0.077 (0.004)	0.013 (0.001)	0.002 (0.000)	0.072 (0.001)

**Table 2.10 Mean loss tangent ( $\tan \delta$ ) values  $\pm$  S.D. for mucoadhesive polymeric nasal formulations at five representative frequencies (n=3).**

Polymeric Nasal Formulation	Concentration (% w/w)	$\tan \delta$				
		0.01 Hz	0.14 Hz	0.79 Hz	7.02 Hz	40.02 Hz
HPMC K4MP	0.2	0.184 (0.005)	0.014 (0.001)	0.002 (0.000)	0.001 (0.000)	0.026 (0.004)
	0.5	0.647 (0.005)	0.082 (0.002)	0.015 (0.000)	0.008 (0.000)	0.052 (0.002)
	1	18.580 (0.010)	1.217 (0.004)	0.206 (0.000)	0.017 (0.000)	0.003 (0.000)
HPMC K15MP	0.2	0.589 (0.005)	0.043 (0.002)	0.006 (0.001)	0.002 (0.000)	0.036 (0.001)
	0.5	0.956 (0.008)	0.019 (0.002)	0.003 (0.001)	0.002 (0.000)	0.032 (0.001)
	1	69.798 (1.598)	4.091 (0.015)	0.719 (0.001)	0.047 (0.000)	0.007 (0.000)
NaCMC low MW	0.2	0.204 (0.001)	0.015 (0.001)	0.003 (0.001)	0.001 (0.000)	0.108 (0.001)
	0.5	0.236 (0.001)	0.017 (0.000)	0.003 (0.000)	0.002 (0.000)	0.086 (0.003)
	1	11.638 (0.000)	0.960 (0.000)	2.784 (0.001)	0.651 (0.000)	0.045 (0.001)
NaCMC med MW	0.2	0.450 (0.002)	0.033 (0.003)	0.006 (0.000)	0.002 (0.000)	0.027 (0.001)
	0.5	0.975 (0.005)	0.071 (0.001)	0.013 (0.001)	0.002 (0.000)	0.067 (0.001)
	1	2.827 (0.001)	0.202 (0.000)	0.035 (0.000)	0.005 (0.000)	0.013 (0.001)
NaCMC high MW	0.2	4.641 (0.003)	0.243 (0.002)	0.044 (0.000)	0.004 (0.000)	0.011 (0.000)
	0.5	20.709 (0.010)	1.440 (0.004)	0.220 (0.001)	0.012 (0.000)	0.036 (0.001)
	1	7.459 (0.001)	1.862 (0.000)	0.698 (0.001)	0.046 (0.000)	0.004 (0.000)

**Table 2.11 Mean loss tangent ( $\tan \delta$ ) values  $\pm$  S.D. for placebo nasal formulations at five representative frequencies (n=3).**

Placebo Nasal Formulation	Tan $\delta$				
	0.01 Hz	0.14 Hz	0.79 Hz	7.02 Hz	40.02 Hz
ee521730	0.641 (0.001)	0.047 (0.002)	0.008 (0.000)	0.001 (0.000)	0.040 (0.000)
ee521950	203.795 (2.125)	1.025 (0.001)	0.200 (0.001)	0.006 (0.000)	0.095 (0.000)
ee522260	0.163 (0.001)	0.124 (0.000)	0.086 (0.000)	0.010 (0.000)	0.001 (0.000)

The dynamic rheological profiles showed that there were variations in the viscoelastic behaviour of the polymeric nasal formulations and the placebo nasal formulations. All three concentrations of Avicel CL611 behaved in a similar manner but with differing magnitudes of  $G'$  and  $G''$  (Figure 2.19).

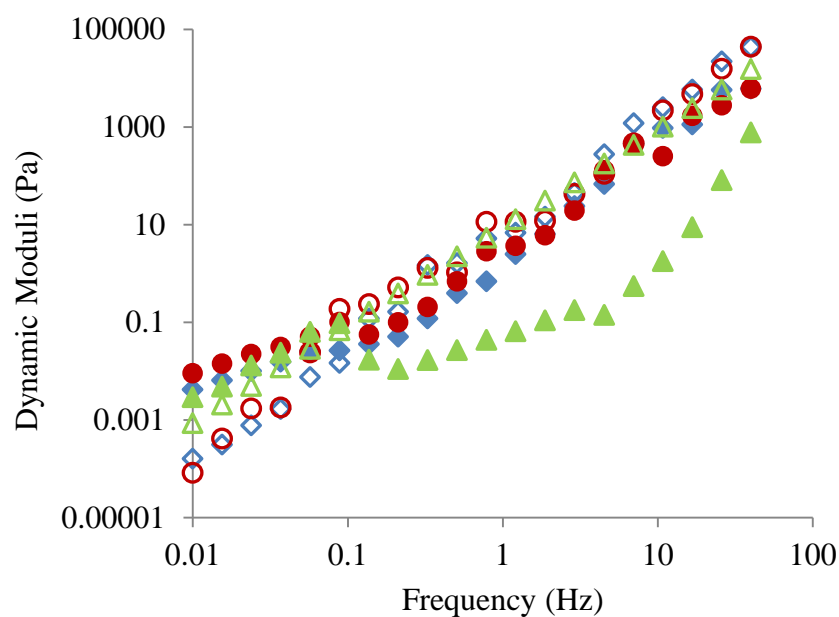


**Figure 2.19 Dynamic oscillation spectra of Avicel CL611 at 25 °C. 0.2% w/w  $G'$  ( $\diamond$ ) and  $G''$  ( $\blacklozenge$ ); 0.5% w/w  $G'$  ( $\circ$ ) and  $G''$  ( $\bullet$ ); 1% w/w  $G'$  ( $\triangle$ ) and  $G''$  ( $\blacktriangle$ ).**

The behaviour was frequency dependent with the dynamic moduli increasing with increasing oscillatory frequency. Initially, the profiles showed that Avicel CL611 was viscous in nature, with  $G'' > G'$  but a crossover of the moduli occurred at approximately 0.1 Hz, after which the formulation expressed a more solid like behaviour. These results contradicted those obtained by Adeyeye and colleagues (2002) who found that Avicel CL611 showed an initial greater magnitude of  $G'$  over  $G''$  before a crossover occurred and the polymeric structure started to breakdown ( $G'' > G'$ ) (Khutoryanskiy, 2011). It would appear from the results obtained that the polymeric structure of the Avicel formulation is building and gaining strength. This could be due to intermolecular changes that have occurred within the system during the experiment. The swelling behaviour of the NaCMC and MCC within the aqueous media will influence this change within the formulation and will cause it to build structure (Zhao *et al.*, 2011). This behaviour will be beneficial for a nasal spray, as the increased structural strength will prevent the formulation from breaking down within the nasal cavity when faced with oscillatory shearing forces associated with air flow within the airways. The profile shows that the 0.2% and 0.5% w/w concentrations have similar magnitudes for both the elastic and viscous modulus. The higher concentration (1% w/w) has a similar  $G'$  to the lower concentrations but has a significantly reduced  $G''$  suggesting that this formulation is stronger at lower concentrations. The results for  $\tan \delta$  are summarised in Table 2.6. There was some frequency dependency with an overall decrease in  $\tan \delta$  with increasing oscillation frequency. This is due to the elastic nature of the formulation becoming more pronounced as the material proceeds through a liquid-solid transition (Jiao *et al.*, 2012). With the exception of the results obtained at 0.01 Hz, all polymeric

concentrations showed values for  $\tan \delta$  that were less than one throughout the experiment, which has previously been reported as a highly desirable attribute for mucoadhesive performance (Tamburic and Craig, 1995). A  $\tan \delta$  value less than one suggested that Avicel CL611 contains particles that are highly associated and more densely packed (Herh *et al.*, 2002, Khutoryanskiy, 2011). These results showed no marked differences of the  $\tan \delta$  values for each of the different polymeric concentrations. This is in agreement with the study conducted by Adeyeye and colleagues who found no significant differences between 1 and 2 % Avicel CL611 (Adeyeye *et al.*, 2002). The frequency dependency of the dynamic moduli and the loss tangent indicated that Avicel CL611 is a weak, viscoelastic system.

Avicel RC591 showed the same viscoelastic profile for all three polymeric concentrations, with no significant variations in the magnitude of  $G'$  (Figure 2.20).

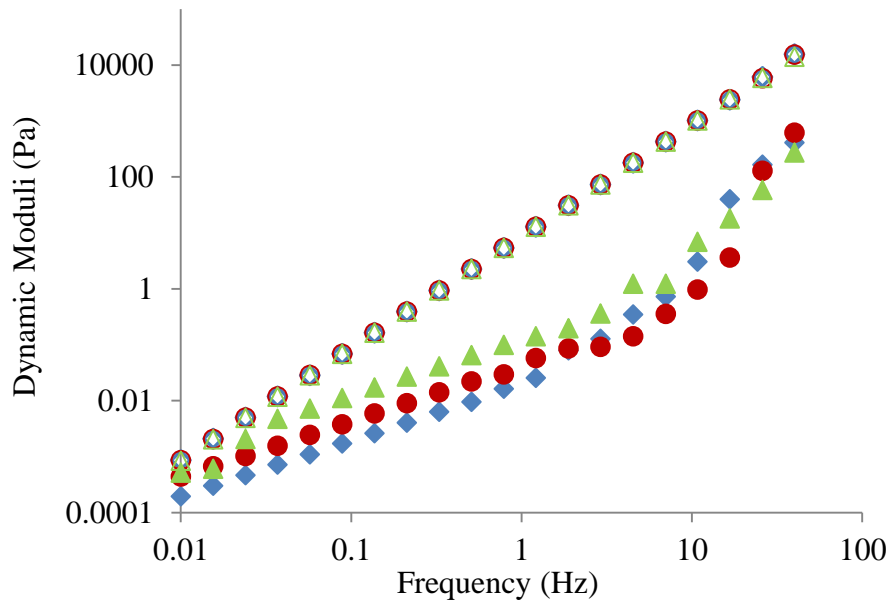


**Figure 2.20** Dynamic oscillation spectra of Avicel RC591 at 25 °C. 0.2% w/w G' (◇) and G'' (◆); 0.5% w/w G' (○) and G'' (●); 1% w/w G' (△) and G'' (▲).

There was an increase in  $G''$  that was proportional to the concentration of Avicel RC591 but this was only evident at lower frequencies.  $G'$  was significantly larger than  $G''$  throughout the experiment which implied that the formulation was exhibiting elastic behaviour. All moduli were frequency dependent with an increase in magnitude that corresponds with increasing oscillation frequency. This behaviour is related to the time available to enable polymeric chain elongation and contractions to occur. In this instance, at higher frequencies, there was insufficient time to allow for this chain movement but as the frequency decreased, the time available for network rearrangement was increased and thus the dynamic moduli increased as a result. At ~10 Hz, a deviation was seen in the results obtained for the viscous modulus. At high frequencies, inertia can impact on the normal rheological

behaviour and erratic results can be obtained (Clare, 2011). This would explain the deviations obtained for the polymeric formulation above 10 Hz. Previous rheological studies have shown an increase in both dynamic moduli that is in proportion to the increase in concentration but saw the same frequency dependency modelled in this experiment (Brownsey and Ridout, 1985, Rudraraju and Wyandt, 2005, Zhao *et al.*, 2011). Mihranyan and colleagues reported that Avicel RC591 showed a frequency independent profile at concentrations above 1% but the formulation was dependent on frequency at lower concentrations (Mihranyan *et al.*, 2007). The same study also suggested that a frequency dependent  $G'$  and/or a high magnitude of  $G''$  is characteristic for fluid dispersions. This is in agreement with information received from the manufacturer (FMC Biopolymer) who state that Avicel RC591 concentrations of less than 1% create fluid dispersions. The loss tangent data for Avicel RC591 showed an overall decrease in magnitude with increasing frequency. The value obtained at 40.02 Hz did not follow this rule. All values were less than one which suggested an elastic material with highly associated particles.

Carbopol 971P exhibited a similar rheological profile for all three investigated concentrations (Figure 2.21).

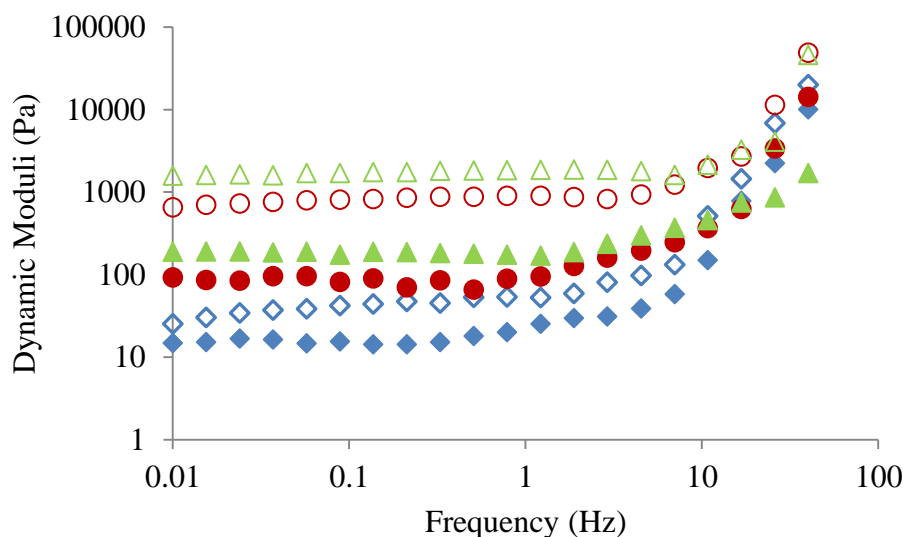


**Figure 2.21** Dynamic oscillation spectra of Carbopol 971P at 25 °C. 0.2% w/w G' (◇) and G'' (◆); 0.5% w/w G' (○) and G'' (●); 1% w/w G' (△) and G'' (▲).

G' was significantly larger than G'' for all the formulations with a corresponding increase for each moduli with increasing concentration. This is in agreement with previous studies which have looked at the rheological behaviour of Carbopol 971P (Chu *et al.*, 1991, Bonacucina *et al.*, 2004, Bonacucina *et al.*, 2008). It can be seen from the rheological spectra (Figure 2.10) that the dynamic moduli were independent of frequency until approximately 10 Hz when both G' and G'' increased with increasing concentration, due to the increased entanglements between the polymeric chains (Jones *et al.*, 2001). These results would suggest that the Carbopol formulation was a predominantly strongly gelled network until it was subjected to high frequencies. After 10 Hz, the strength of the structure reduced and a weak viscoelastic system prevailed. In part, these results correspond with the previous work of other investigators (Chu *et al.*, 1991, Bonacucina *et al.*, 2004, Bonacucina *et*

*al.*, 2008) however, these experiments report complete spectra that are typical of weak gels (Rosalina and Bhattacharya, 2002). Bonacucina and colleagues (2008) stated that a weak gel expresses rheological behaviour that is midway between the behaviour of a strong gel and a solution and that a weak gel is taken from the continued breakdown of the 3D network caused by increasing deformation (Bonacucina *et al.*, 2008). A weak gel will also lack strong bonds between the polymeric chains and a prevalence of polymer to solvent interactions will be evident (Chu *et al.*, 1991). The spectra obtained for Carbopol 971P showed no signs of crossover between  $G'$  and  $G''$ , unlike that observed in the Bonacucina study (Bonacucina *et al.*, 2006). A crossover between the dynamic moduli is an indication of the relaxation point of the entangled polymeric network within the solution. Table 2.6 shows that the  $\tan \delta$  values for Carbopol 971P were unpredictable and varied with changing concentration and frequency. This inconsistency in  $\tan \delta$  is characteristic of an untrue gel structure (Bonacucina *et al.*, 2004). All values for  $\tan \delta < 1$  which corresponds to elastic behaviour within the system and follows the results provided by the other investigators.

Carbopol 974P showed very similar rheological behaviour to Carbopol 971P but with higher magnitudes for both dynamic moduli compared (Figure 2.22).

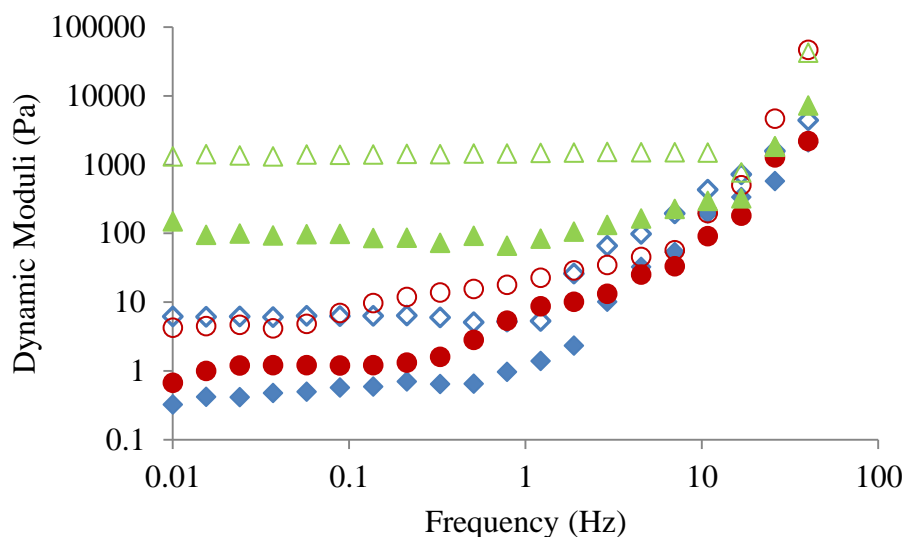


**Figure 2.22** Dynamic oscillation spectra of Carbopol 974P at 25 °C. 0.2% w/w  $G'$  ( $\diamond$ ) and  $G''$  ( $\blacklozenge$ ); 0.5% w/w  $G'$  ( $\circ$ ) and  $G''$  ( $\bullet$ ); 1% w/w  $G'$  ( $\triangle$ ) and  $G''$  ( $\blacktriangle$ ).

This is due to the higher occurrence of crosslinks found in Carbopol 974P (Bonacucina *et al.*, 2008). Compared with Carbopol 971P, the higher crosslinked polyacrylic acid variant has a decreased molecular weight between neighbouring crosslinks. It has been suggested that the elastic modulus,  $G'$ , is inversely proportional to this inter-crosslinking molecular weight (Hoshmani, 2006). This theory was confirmed in our results. As with Carbopol 971P,  $G' > G''$  over the entire frequency range with a distinct frequency independence until  $\sim 1$  Hz, after which both moduli showed an increase in magnitude with increasing frequency. This behaviour is typical of a weak gel which is elastic in nature. The same behaviour was echoed by all three concentrations but a corresponding increase in the value for  $G'$  and  $G''$  occurred with increasing concentration. This increase in storage moduli with increasing polymeric concentrations was found by Bonacucina and colleagues (2004)

who compared the properties of Carbopol 971P and 974P in different pure cosolvents (Bonacucina *et al.*, 2004). It was also stated by the author that an increase in polymeric concentration will improve the rheological characteristics of the system. The values obtained for  $\tan \delta$  largely contradict those obtained in the Bonacucina study (Bonacucina *et al.*, 2004). In this investigation, the majority of the results indicated that  $\tan \delta$  was variable and no connection between  $\tan \delta$  and oscillation frequency existed. This would suggest a non-real gel structure. The results for the lowest concentration (0.2% w/w) did correspond with the results recorded by Bonacucina and colleagues and showed frequency dependence for  $\tan \delta$ , with an increase in frequency resulting in a proportional increase in  $\tan \delta$ . An increase in the tangent of the phase angle is indicative of loss of elasticity of the material and the viscous nature will prevail. However, all  $\tan \delta$  results were less than one suggesting the Carbopol 974P was exhibiting solid like, elastic behaviour. These conflicting results between the three concentrations could be as a result of sample degradation of the lower concentration formulation. Although the test is non-destructive, water loss from the aqueous medium could have resulted in the variations. This could have been prevented by employing a solvent trap to control the sample environment.

The oscillation results for all four grades of HPMC (Figures 2.23 to 2.26) showed a largely prevalent elastic behaviour ( $\tan \delta < 1$ ), the exception to this was seen in the results for the higher concentration which showed signs of a viscous nature ( $\tan \delta > 1$ ).

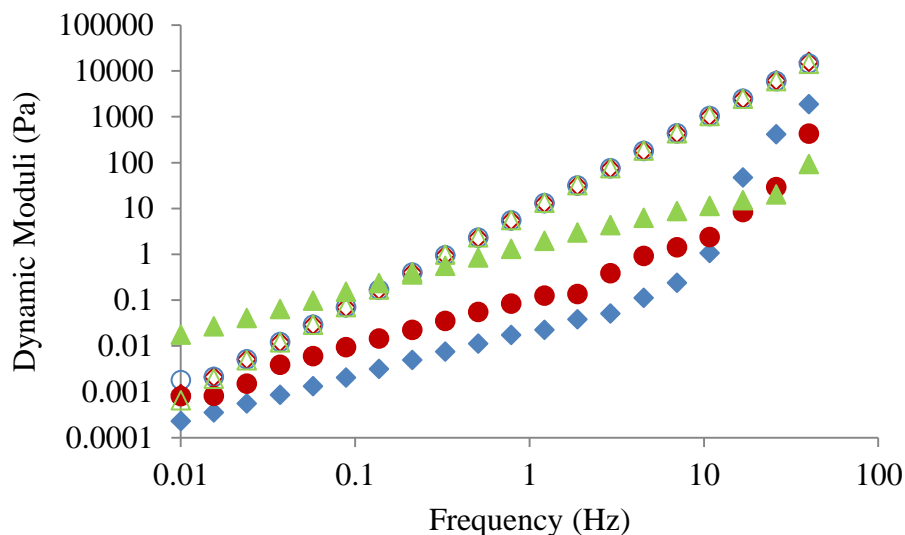


**Figure 2.23** Dynamic oscillation spectra of HPMC E4MP at 25 °C. 0.2% w/w G' (◇) and G'' (◆); 0.5% w/w G' (○) and G'' (●); 1% w/w G' (△) and G'' (▲).

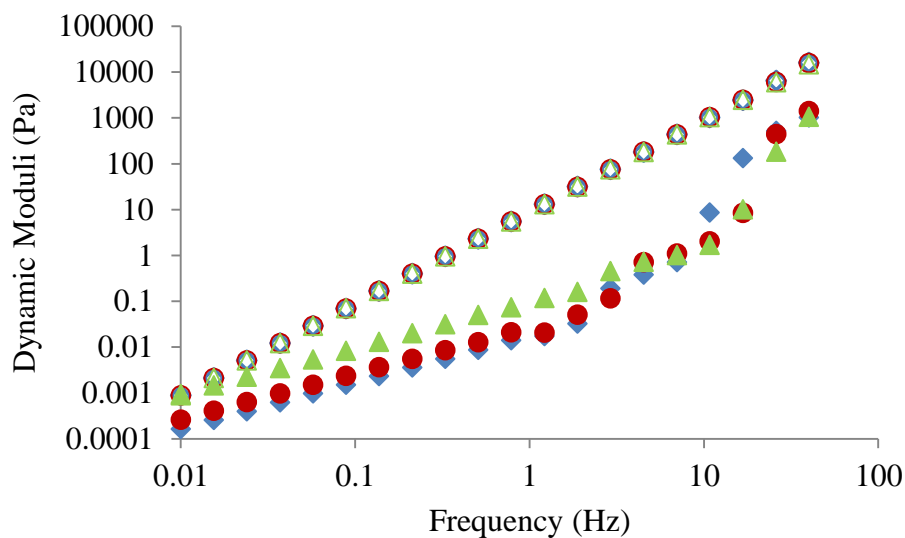


**Figure 2.24** Dynamic oscillation spectra of HPMC K100P at 25 °C. 0.2% w/w G' (◇) and G'' (◆); 0.5% w/w G' (○) and G'' (●); 1% w/w G' (△) and G'' (▲).

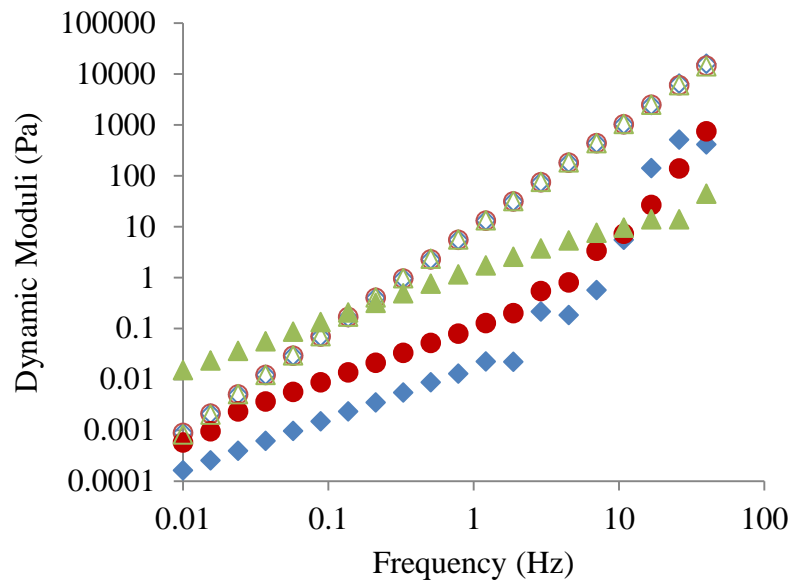


**Figure 2.25** Dynamic oscillation spectra of HPMC K4MP at 25 °C. 0.2% w/w  $G'$  ( $\diamond$ ) and  $G''$  ( $\blacklozenge$ ); 0.5% w/w  $G'$  ( $\circ$ ) and  $G''$  ( $\bullet$ ); 1% w/w  $G'$  ( $\triangle$ ) and  $G''$  ( $\blacktriangle$ ).

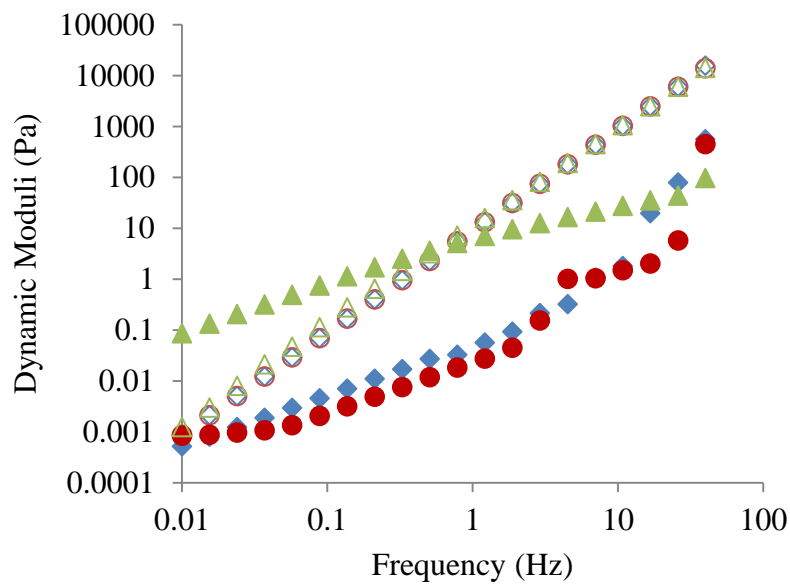


**Figure 2.26** Dynamic oscillation spectra of HPMC K15MP at 25 °C. 0.2% w/w  $G'$  ( $\diamond$ ) and  $G''$  ( $\blacklozenge$ ); 0.5% w/w  $G'$  ( $\circ$ ) and  $G''$  ( $\bullet$ ); 1% w/w  $G'$  ( $\triangle$ ) and  $G''$  ( $\blacktriangle$ ).

All four HPMC formulations exhibited an increase in the dynamic moduli ( $G'$  and  $G''$ ) with increasing oscillation frequency. This solid like behaviour is in line with results obtained by Demirkesen and colleagues (2010), who studied the rheological properties of gluten free bread products including the addition of HPMC (Demirkesen *et al.*, 2010). However, other authors have reported contradictory rheological properties for HPMC. Maltese and colleagues (2006) studied the potential use of bioadhesive polymers, including HPMC, for use as ophthalmic viscosurgical devices (OVD) during cataract surgery (Maltese *et al.*, 2006). It was found that the viscoelastic nature of HPMC tended towards a viscous like behaviour with  $G'' > G'$ . The value of  $\tan \delta$  was always greater than one. This phenomenon was echoed by Fatimi and colleagues (2008) who investigated the rheological properties of sialated HPMC used in biomaterial domains as 3-D synthetic matrices for tissue engineering (Fatimi *et al.*, 2008). In this study the 3% HPMC formulation was also found to be viscous in nature with the loss modulus prevailing over the storage modulus over the entire frequency range. This variation in results could be as a result of differing formulation procedures or grades of HPMC employed during the other investigations cited. With the exception of HPMC K15MP, all four grades showed an increase in  $G''$  with increasing polymeric concentration up until  $\sim 10$  Hz, when the results become varied for each formulation.  $G'$  remained largely unaffected by the change in concentration. As mentioned previously, this increase in dynamic moduli is as a result of increased entanglement amongst the polymeric chains. The presence of crossovers was seen for each 1% w/w formulation, with the exception of K100P. HPMC E4MP and K4MP presented a crossover at  $\sim 0.1$  Hz but the crossover for K15MP was found later at 1 Hz. The crossover point, where the

dynamic moduli are equal, is regarded as the point of relaxation of the entangled network of the polymer. The relaxation is a sign that the chains of the polymer are twisted with each other and the likelihood of disentanglement and flow, or relaxation of the polymer, depends primarily on the frequency of the applied stress (Maltese et al., 2006). K15MP presented a relaxation time at a higher frequency compared with E4MP and K4MP. This suggested that K15MP possessed longer lasting elastic properties and the polymeric structure is stronger and more resilient. The observed behaviour for 1% w/w E4MP, K4MP and K15MP is typical of an entangled polymer with no real gel like characteristics present (Chesham Chemicals Ltd, 2003, Maltese et al., 2006). This is confirmed with the  $\tan \delta$  results. At lower frequencies  $\tan \delta > 1$  and  $\tan \delta < 1$  at higher frequencies. The remainder of the HPMC polymers showed elastic behaviour with  $\tan \delta < 1$ . In general, the  $\tan \delta$  values decreased with increasing frequency which indicates more elastic behaviour initially at the lower frequencies which decreased in strength as the frequency increased. The values obtained at 40 Hz opposed this trend and showed a slight increase for all polymeric formulations. It is well known that at high frequencies, inertial problems can occur and erroneous results can be produced (Clare, 2011).

The frequency sweep for NaCMC showed varied results between the grades and concentrations. There was no correlation between the dynamic moduli and polymer concentration for NaCMC low MW (Figure 2.27).

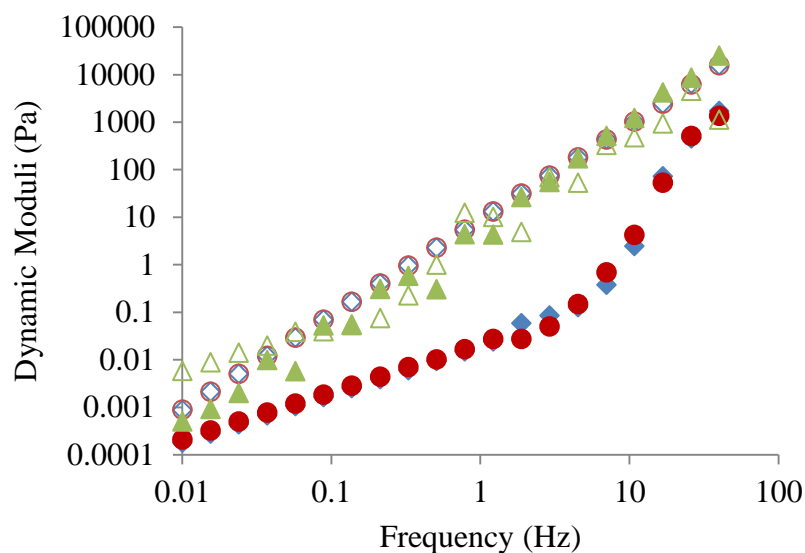


**Figure 2.27** Dynamic oscillation spectra of NaCMC low MW at 25 °C. 0.2% w/w G' (◇) and G'' (●); 0.5% w/w G' (○) and G'' (●); 1% w/w G' (△) and G'' (▲).

A degree of frequency dependence was seen for 0.2 and 0.5% w/w with the elastic modulus greater than the viscous modulus over the entire frequency range. This is a classic example of a weak gel where elastic behaviour prevails of the viscous nature of the polymeric system. The results obtained for 1% w/w NaCMC low MW were inconsistent and the values for G' and G'' were almost equal. There was a linear increase in both dynamic moduli with increasing frequency. This signified a behaviour that is between that of a concentrated polymeric system and a weak gel and was also found in an earlier study conducted by Bayarri (Bayarri *et al.*, 2009). Bayarri and colleagues were investigating the use of NaCMC in milk systems and found that G' and G'' equalled one another at a concentration of 0.75% w/w. The magnitude of the elastic and viscous moduli did not differ between the lower concentrations but a considerable increase was observed for the higher concentration.

NaCMC medium MW provided a less unpredictable rheological behaviour profile (Figure 2.28).

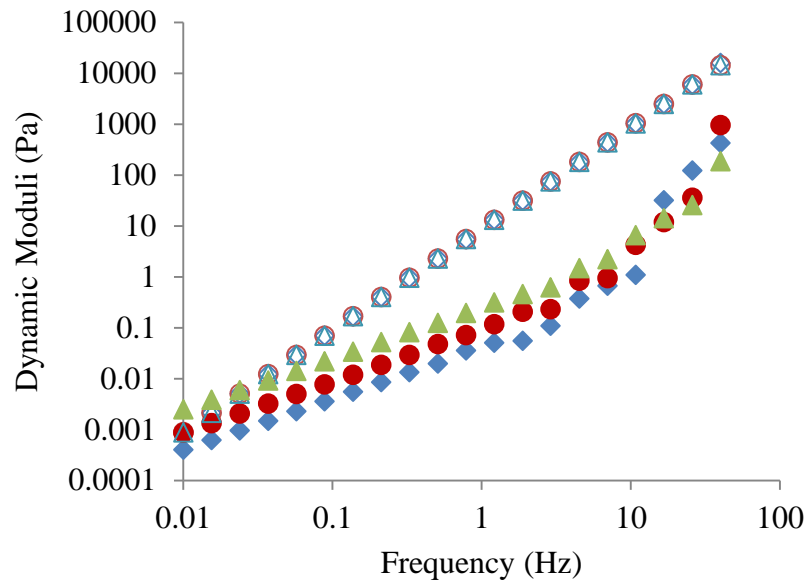


**Figure 2.28** Dynamic oscillation spectra of NaCMC med MW at 25 °C. 0.2% w/w G' (◇) and G'' (◆); 0.5% w/w G' (○) and G'' (●); 1% w/w G' (△) and G'' (▲).

All three concentrations displayed similar viscoelastic behaviour with  $G' > G''$ , again suggesting that the cellulose derived polymer is a weak gel. Both moduli were dependent on frequency and increased correspondingly. This behaviour remained until  $\sim 10$  Hz, after which the values for  $G''$  showed less frequency dependence. An increase in concentration affected all three rheological profiles with the values of  $G'$  and  $G''$  increasing with increasing concentrations. This was as a result of increased chain entanglement brought about by the increasing concentration and was confirmed in the Bayarri (2009) study among others (Kulicke *et al.*, 1996, Bayarri *et*

*al.*, 2009, Bonacucina *et al.*, 2009). The rheological properties of NaCMC high MW are shown in Figure 2.18. It can be seen from the Frequency vs. Dynamic Moduli graph that all three concentrations are almost identical.

Each concentration of NaCMC high MW showed an initial viscous behaviour with  $G'' > G'$  (Figure 2.29).

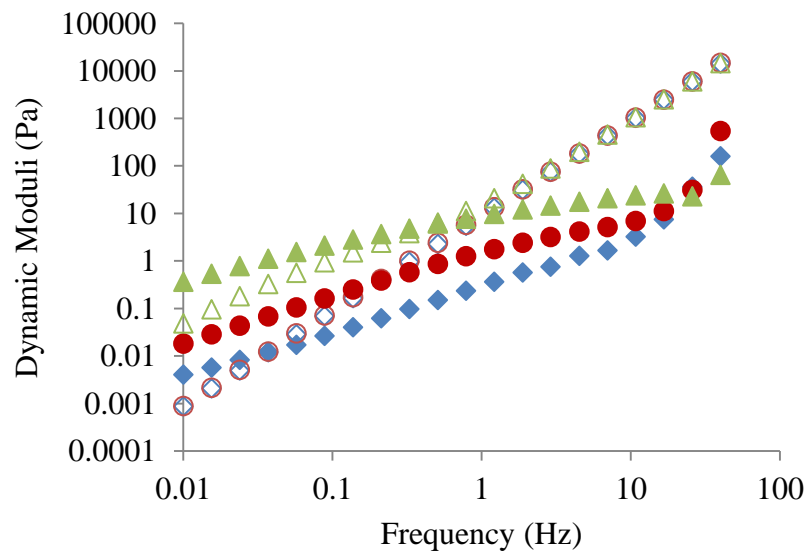


**Figure 2.29** Dynamic oscillation spectra of NaCMC high MW at 25 °C. 0.2% w/w  $G'$  ( $\diamond$ ) and  $G''$  ( $\blacklozenge$ ); 0.5% w/w  $G'$  ( $\circ$ ) and  $G''$  ( $\bullet$ ); 1% w/w  $G'$  ( $\triangle$ ) and  $G''$  ( $\blacktriangle$ ).

A crossover point then occurred with  $G' = G''$  before an elastic system was shown ( $G' > G''$ ). As with the other grades of NaCMC investigated in this study, increasing the concentration caused an increase in the magnitude of both  $G'$  and  $G''$ . An increase in concentration also resulted in the crossover frequency to increase from  $<0.01$  Hz for 0.2% w/w to 0.1 Hz and 1 Hz for 0.5 and 1% w/w respectively. This crossover point is thought to be the point at which the polymer structure relaxes and mechanical breakdown ensues (Janssen *et al.*, 2007). The increase in crossover frequency is a sign that the polymer network of NaCMC increases with concentration and a higher level of frequency is required to break the structure of the 1% w/w formulation (Bayarri *et al.*, 2009). Overall, the  $\tan \delta$  values for all three grades of NaCMC at three concentrations were less than one, indicating elastic behaviour. This was confirmed by the frequency sweep curves. NaCMC high MW provided early signs of viscous behaviour ( $\tan \delta > 1$ ) but this reverted back to elastic behaviour upon reaching the crossover frequency. The rheological profiles of different grades and concentrations of NaCMC have been characterised before by many authors (Bayarri *et al.*, 2009). It is known that the mucoadhesive polymer presents a somewhat complicated rheological behaviour due to its ability to form aggregates and associations whilst in aqueous solutions (Kulicke *et al.*, 1999). One other major characteristic of NaCMC is that modifications can manifest in the magnitude of both dynamic moduli as a consequence of its polymeric concentration and/or molecular weight (Bonacucina *et al.*, 2009).

The viscoelastic behaviour of three placebo nasal formulations (ee521730, ee521950 and ee522260) was also investigated and the results are shown in Figure 2.30.

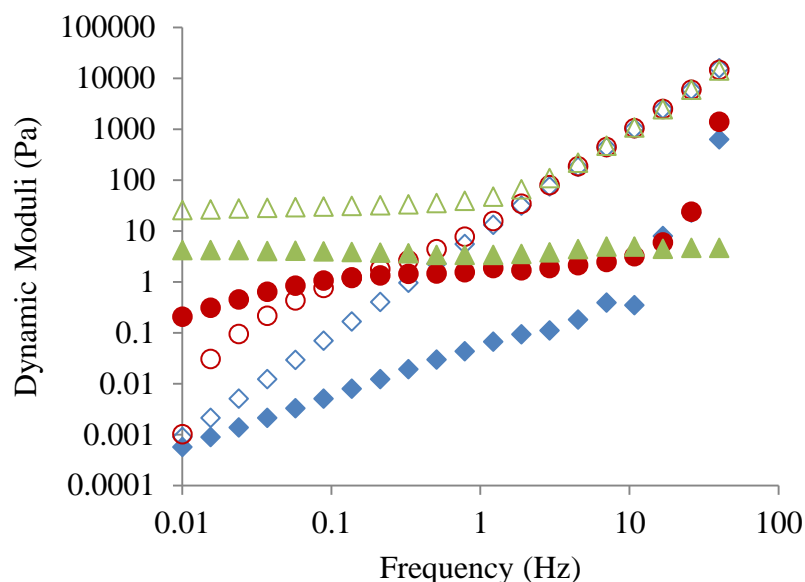


**Figure 2.30** Dynamic oscillation spectra of placebo nasal formulations at 25 °C. ee521730 w/w  $G'$  ( $\diamond$ ) and  $G''$  ( $\blacklozenge$ ); ee521950 w/w  $G'$  ( $\circ$ ) and  $G''$  ( $\bullet$ ); ee522260 w/w  $G'$  ( $\triangle$ ) and  $G''$  ( $\blacktriangle$ ).

It can be clearly seen that all three formulations produced profoundly different spectra and thus different rheological behaviour. Formulation ee521730 exhibited behaviour that can be attributed to a weak gel. The elastic modulus is greater than the viscous modulus over the full frequency range with a degree of frequency dependency evident, suggesting the ee521730 is solid in nature. This corresponds with the  $\tan \delta$  results obtained. All reported loss angles results reported for ee521730 were less than one, again indicating a solid like behaviour. The data for ee521950 showed an initial prevalence of viscous behaviour over elastic behaviour. At  $\sim 0.1$

Hz the dynamic moduli were equal and a crossover occurred, after which the placebo formulation expressed elastic behaviour. From the results it can be deduced that ee521950 is an entangled system.  $\tan \delta$  results showed values higher than one at low frequencies but these became less than one, synonymous with solid behaviour, after the crossover frequency was reached. A weak gel behaviour was expressed by ee522260. The elastic modulus ( $G'$ ) was greater than the viscous modulus ( $G''$ ) for all results obtained. An element of frequency dependency was also observed.  $\tan \delta$  values were all less than one, which supported the elastic behaviour seen in the dynamic rheology spectra (Figure 2.19). Although all three placebo nasal formulation consisted of different excipients, namely the mucoadhesive polymer, their viscosity values correlated with the magnitude of the dynamic moduli. Figure 2.4 showed the order of viscosity values for the placebo nasal formulations as ee521730 < ee521950 < ee522260, which was the same as the trend found for the dynamic moduli magnitude. It can therefore be concluded that the viscosity and thus the entanglement density of the placebo nasal formulations has affected the rheological behaviour.

The recorded rheological behaviour for the placebo nasal formulations can be compared to those obtained for the individual mucoadhesive polymer components. HPMC E4MP is the mucoadhesive polymer used in the ee521730 formulation. The rheological behaviour obtained for the 1% w/w polymer compared with the placebo nasal formulation presented vast differences. In comparison, the HPMC E4MP formulation initially expressed viscous behaviour ( $G'' > G'$ ) before a crossover

occurred at  $\sim 0.1$  Hz resulting in a final solid like behaviour ( $G' > G''$ ). The entangled system observed for ee521950 was not echoed by the mucoadhesive polymer (Avicel RC591), which showed solid behaviour throughout the experiment. Again the data obtained for the mucoadhesive polymer (Avicel CL611) and that obtained for the placebo nasal formulation (ee522260) did not corroborate. The data presented for the polymer alone showed an entangled system with a crossover of dynamic moduli occurring at  $\sim 0.1$  Hz. It can clearly be seen that the rheological profiles obtained for the three placebo nasal formulations did not match that obtained for the mucoadhesive polymer constituent that was measured earlier in the experiment. These differences in observed rheological behaviour could be as a result of the interactions occurring between the mucoadhesive polymer and the other excipients. This theory should be studied in greater detail to eliminate any negative effects that excipients may have on the rheological behaviour of mucoadhesive polymeric systems.

## **2.6 Conclusion**

In this work a quick and easy method was utilised to quantify the flow and viscoelastic nature of mucoadhesive polymeric formulations and placebo nasal formulations. The results reported here indicated that Carbopol 971P and NaCMC high MW exhibited the most promising rheological behaviour for use within a nasal spray formulation. Carbopol 971P displayed the highest apparent viscosity at both low and high shear rates which would enable the formulation to remain within the

nasal cavity once administered. The viscoelastic properties of Carbopol 971P also confirmed its suitability for use within a nasal formulation. The dynamic moduli showed a highly elastic system and a tan value of less than one, characteristics that would allow for the stresses within the nasal cavity to be exerted onto the formulation without negative effect. Another major rheological characteristic of Carbopol 971P is its thixotropic behaviour. A thixotropic formulation is beneficial in nasal formulation as it will allow for the polymer to be thinned upon shaking and will then thicken towards the original viscosity on removal of the shear force experienced during spraying. NaCMC high molecular weight had a comparatively high apparent viscosity and thixotropy. Its viscoelastic properties were slightly different and a crossover point was evident. This crossover point between the dynamic moduli was a sign that the polymeric structure was undergoing mechanical breakdown. This in itself is not beneficial for nasal drug delivery but the frequency at which the crossover occurred increased with increasing polymeric concentration which suggested that the polymer gains structure as the concentration is increased. It can also be seen that different factors affect the rheological properties of the formulation and it is therefore imperative that a full analysis is conducted on a nasal product to optimise its performance. Rheology plays an important part in determining the efficacy of a nasal spray itself; however, the properties of the formulation will be crucial whilst at the site of deposition and further work should be done to clarify the rheological properties of the formulation when it is in contact with the mucosal layer of the nasal cavity.

## **Chapter 3 Investigation into mucus/polymer interfacial interactions using rheology and microrheology**

### **3.1 Introduction**

Mucoadhesion can be defined as the adherence of two materials, one of which is a mucous membrane, secured by interfacial forces (Smart, 2005). The most common mucoadhesive materials, known as the first generation mucoadhesives, are hydrophilic macromolecules with a high number of functional groups that are capable of hydrogen bonding. Groups such as hydroxyl, carboxyl and amine groups increase adhesion with mucosal membranes. The main disadvantages of using first generation mucoadhesive polymers, such as NaCMC and chitosan, is their non-specific nature (Andrews *et al.*, 2009). This means that the mucoadhesive formulations may bind to sites not intended by the application. Second generation mucoadhesives have the ability to bind directly to their intended sites and thus a more targeted and specific attachment may be accomplished. One example of a second generation polymer is thiomers. These mucoadhesives are derived from hydrophilic polymers that have undergone thiolation. The thiol groups present on the polymer interact with the mucin glycoprotein chains and covalently bond with the cysteine rich sub domains of the mucus. This leads to an increased residence time and thus a greater bioavailability (Albrecht *et al.*, 2006).

The exact nature of the mucoadhesive process has yet to be fully defined; however, numerous theories have been proposed by many researchers (Andrews *et al.*, 2009).

The theories that are frequently cited include chain interpenetration and surface energy thermodynamics (Madsen *et al.*, 1998b). These hypotheses hint at the establishment of an intimate contact between the mucoadhesive polymer and the mucosal surface due to wetting and absorption of the two surfaces. Chain interlocking and interdiffusion between the polymeric and mucin glycoprotein chains is then followed by the formation of secondary bonds, usually hydrogen bonds, that further develop and strengthen the polymer/mucus interface (Duchene *et al.*, 1988). The developments of bonds between the two surfaces will result in a change in the rheology of the polymer and mucin and an analysis of the interface is considered a reflection of the strength of the mucoadhesive bond (Madsen *et al.*, 1998b). Hassan and Gallo (1990) reported a rheological method that looked at quantifying the bond strength between the polymer and mucin (Hassan and Gallo, 1990). The authors reported a synergistic effect on the recorded viscosity when mucin was added to a mucoadhesive polymer. More recently, Sriamornsak and colleagues (2008) studied the interactions of pectin and mucin using dynamic rheology and also found a synergistic increase in the viscoelastic properties of the polymer and mucin interface (Sriamornsak *et al.*, 2008). It was concluded that a greater magnitude of synergy was indicative of a stronger bond between the polymer and mucin chains. A similar rheological method suggested by Hallan and Gasso (1990) was employed in this study to quantify the mucoadhesive bond between a range of mucoadhesive formulations and gastric porcine mucin (Hassan and Gallo, 1990).

This study involved a standard bulk rheological technique which measured the viscoelastic properties of the polymeric formulations, the mucin formulations and a formulation containing both the polymer and mucin.

A second study was carried out using a passive microrheological technique known as optical tweezers. The technique involved the monitoring of a polystyrene microsphere which was embedded into the formulation (Brau *et al.*, 2007). The optical tweezers were used to trap and manipulate the trapped microsphere using a highly focussed laser beam and determined the viscosity and viscoelastic properties of small volumes of sample by detailed analysis of the microsphere position as a function of time (Yao *et al.*, 2009, Tassieri *et al.*, 2010, Preece *et al.*, 2011). The motion of the microsphere due to thermal fluctuations (Brownian motion) was investigated to find the high frequency viscoelastic properties of the material. To maximise the frequency range of this measurement the lowest trap strength where the microsphere remains stably trapped was used. Initially the time dependence of the mean square displacement was calculated. The Fourier transform of the mean square displacement was directly related to the complex modulus of the material. Low frequency responses were also calculated using a different approach. The microsphere was tracked as the trap was rapidly switched from one position to another using a special light modulator (SLM) (Tassieri *et al.*, 2010). This approach was limited to materials with a low viscosity due to the microspheres escaping from the trap. A high trap strength was used here to maximise the viscosity range that can be studied. The switching was repeated several times and the microsphere trajectory

averaged. The Fourier transform of this trajectory was related to the complex modulus of the material in the low frequency regime. Again the analysis was done using a custom LabView program. Advantages, along with some disadvantages of microrheology are presented in Table 3.1.

**Table 3.1 Summary of the advantages and disadvantages of the optical trap system to measure microrheology\*.**

Advantages	Disadvantages
Cost of equipment	Samples must be transparent to light
Can be used to analyse small volumes	High viscosity samples are a challenge
Low viscosity samples can be easily analysed	Difficult to study the non-linear rheological properties of a sample
Wide frequency range of analysis	Computationally extensive

\* Adapted from (Cicuta and Donald, 2007)

It can be seen that the optical trapping technique offers advantages to the study of interactions between the polymer and mucin chains. These main advantages of this method over the bulk rheological method include the ability to measure low viscosity samples and also the requirement for small volume sample sizes. Bulk rheology also has some advantages over microrheology including the facility to measure high viscosity samples.

The aim of this study was to utilise the rheological and micro-rheological techniques to quantify this synergy and to classify polymeric formulations in terms of their efficacy for use as a mucoadhesive in nasal sprays.

## 3.2 Materials

### 3.2.1 Apparatus

The bulk rheological synergy analysis was performed using a controlled stress Carrimed CSL<sup>2</sup> 100 rheometer (TA Instruments, Surrey, UK) with a 6 cm stainless steel cone and plate geometry. The CSL V1.2a software package (TA Instruments, Surrey, UK) was used for system control along with data gathering and analysis. Microrheological synergy measurements were performed using a home built optical trapping system (Figure 3.1). All microrheological analysis was done using a custom written LabView program.

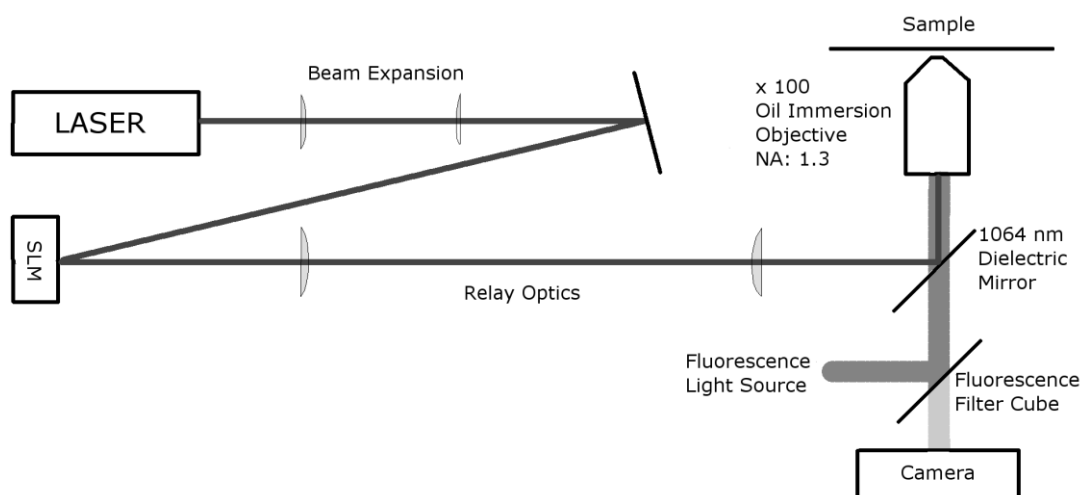


**Figure 3.1** The optical trapping setup used for microrheology measurements

### **3.2.2 Chemicals**

NaCMC low, medium and high MW (average molecular weight ~90, 250 and 700 kDa respectively) along with type III bound sialic acid mucin from porcine stomach were purchased from Sigma Aldrich Co (St Louis, MO, USA). Avicel RC591 and CL611 were obtained from FMC Biopolymer (Philadelphia, PA, USA). Carbopol 971P and 974P were obtained from Lubrizol Advanced Materials Europe BVBA (Brussels, Belgium) and HPMC powder (Methocel grades E4MP, K4MP, K100P and K15MP) was received as a gift from Colorcon (Dartford, Kent, UK). Three placebo nasal spray formulations (ee521730, ee521950 and ee522260) were received from GlaxoSmithKline R & D (Ware, UK). Polybead<sup>®</sup> polystyrene microspheres (3.0 µm) were purchased from Polysciences Inc. (Warrington, PA, USA). Single depression cavity microslides were purchased from Agar Scientific (Essex, UK). Glass coverslips (22 x 22 mm) were purchased from VWR (Leicestershire, UK).

## **3.3 Methods**

### **3.3.1 Preparation of mucoadhesive polymeric nasal formulations**

The mucoadhesive polymers were prepared as described in Section 2.3.1.

### **3.3.2 Preparation of placebo nasal formulation**

The placebo nasal formulations were used as received.

### **3.3.3 Preparation of mucin solution**

The mucin solution was prepared as described in Section 2.3.3.

### **3.3.4 Preparation of samples for rheological analysis**

Mucoadhesive polymeric nasal formulations, placebo nasal formulations and mucin solutions were prepared as described in 2.3.1, 2.3.2 and 3.3.3 respectively. Fifteen-gram aliquots of each polymeric formulation were mixed with 15 g of mucin solution to give a polymer to mucin ration of 1:1. The polymer/mucin formulations were allowed to mix on a magnetic stirrer at room temperature for four hours and were stored overnight at 4 °C to enable complete interactions between the polymer and mucin chains. All polymer/mucin systems were equilibrated at room temperature and stirred by hand prior to analysis.

### **3.3.5 Preparation of samples for microrheological analysis**

The Polybead<sup>®</sup> polystyrene microbeads (3.0  $\mu\text{m}$ ) formulation was prepared by pipetting 200  $\mu\text{L}$  of the concentrated microbead solution to a 10 mL volumetric flask and making up to volume with distilled water. The diluted microsphere formulation was kept at 4  $^{\circ}\text{C}$  when not in use and used within seven days. Mucoadhesive polymeric formulations, placebo nasal formulations and mucin formulations were prepared as described in the previous section. The samples were prepared for microrheological analysis by adding 40  $\mu\text{L}$  of microsphere formulation to 400  $\mu\text{L}$  of both polymeric and mucin formulations into a 1 mL centrifuge tube. The polymer/mucin/microsphere solution was thoroughly shaken by hand and kept at 4  $^{\circ}\text{C}$  until required. Fresh samples were prepared daily. Immediately prior to analysis, the samples were allowed to equilibrate to room temperature before 200  $\mu\text{L}$  was carefully added to the cavity of a single depression cavity microscope. The cavity was then covered by a 22 x 22 mm glass cover slip ensuring no air bubbles were present in the sample. A calibration sample was prepared using the same method with 800  $\mu\text{L}$  of water replacing the 400  $\mu\text{L}$  of polymer and mucin formulations.

### **3.3.6 Assessment of interfacial interactions of mucoadhesive polymeric nasal formulations using rheology**

The interfacial interactions, or rheological synergism, between the mucoadhesive polymeric nasal formulations and the mucin were measured by carrying out oscillatory shear runs, as described in Section 2.3.4, on the polymer/mucin

formulations. The synergism was calculated as the difference between the actual viscoelastic component values obtained from the polymer/mucin tests and the sum of the dynamic moduli values of the mucoadhesive polymeric nasal formulations and the mucin solutions found in section 2.3.4, calculated as follows:

$$\Delta G' = G'_{(\text{mix})} - (G'_{(\text{polymer})} + G'_{(\text{mucin})}) \quad \text{[Equation 3.1]}$$

$$\Delta G'' = G''_{(\text{mix})} - (G''_{(\text{polymer})} + G''_{(\text{mucin})}) \quad \text{[Equation 3.2]}$$

### **3.3.7 Assessment of interfacial interactions of mucoadhesive polymeric nasal formulations using microrheology**

The microrheological synergism was investigated using a home built optical trapping system as shown in Figure 3.1. The system consisted of a 3 W diode laser which worked at 1064 nm (Laser Quantum, Ventus IR). The laser was expanded and relayed to a conventional inverted microscope (Nikon, TE2000U) and focused using a high numerical aperture oil immersion objective. Holographic optical traps are created using a spatial light modulator (SLM) (Boulder Nonlinear Systems, XY Series) placed in a fourier plane of the focal plane of the objective. Polystyrene microspheres were used as a trapping material as they can be optically trapped by the tightly focused laser (Figure 3.2). This is due to the high gradient of light intensity created by the high numerical aperture objective (Ashkin et al., 1986).

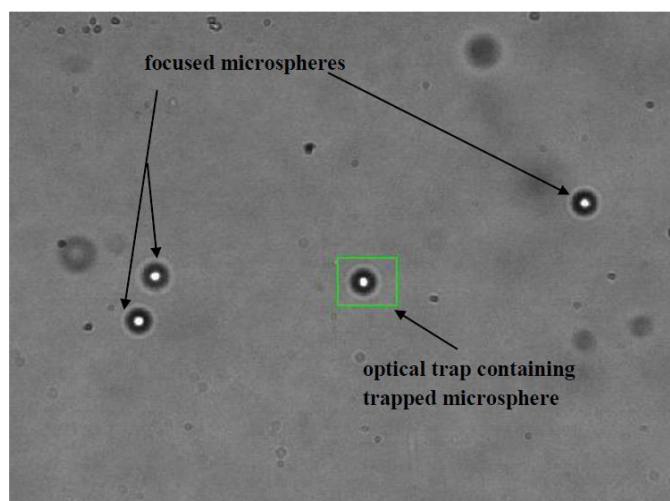


**Figure 3.2** Image taken using the microrheology set up showing a microsphere trapped by the laser and focussed, untrapped microspheres.

Water was tested prior to the analysis and also routinely throughout the course of the experiment to ensure the accuracy of the test parameters. Thermal fluctuation of the polystyrene microspheres was visualised in the bright field using the microscope objective. Digital images were then recorded using a Dalsa Genie Camera (Stemmer Imaging LTD, Surrey, UK), which had the ability of recording images at up to 4 kHz within a limited region of interest. The laser, SLM, and camera were all controlled using a LabView program written specifically for the system. The LabView program was also able to track the microspheres, which were tracked for either 5 s or 20,000 data points. By detailed analysis of the bead positions as a function of time, the microrheological storage and loss moduli can be extracted (Yao *et al.*, 2009, Tassieri *et al.*, 2010, Preece *et al.*, 2011). The microrheological synergism of the polymeric nasal formulations and placebo nasal formulations was calculated as described in Section 3.3.6 using Equations 3.1 and 3.2.

### **3.4 Statistical analysis**

Statistical analysis was performed using Minitab 16 (Minitab LTD., Coventry, UK). Statistical significance was analysed by a one way analysis of variance (ANOVA) with Tukey's post hoc test. For all measurements,  $P < 0.05$  represented statistical significance.

### **3.5 Results and discussion**

#### **3.5.1 Assessment of interfacial interactions of polymeric nasal formulations and mucin using rheology**

The rheological synergism between the polymeric nasal formulations and mucin are shown in Figures 3.3 to 3.5. The results were taken at a midrange frequency of 1.22 Hz.

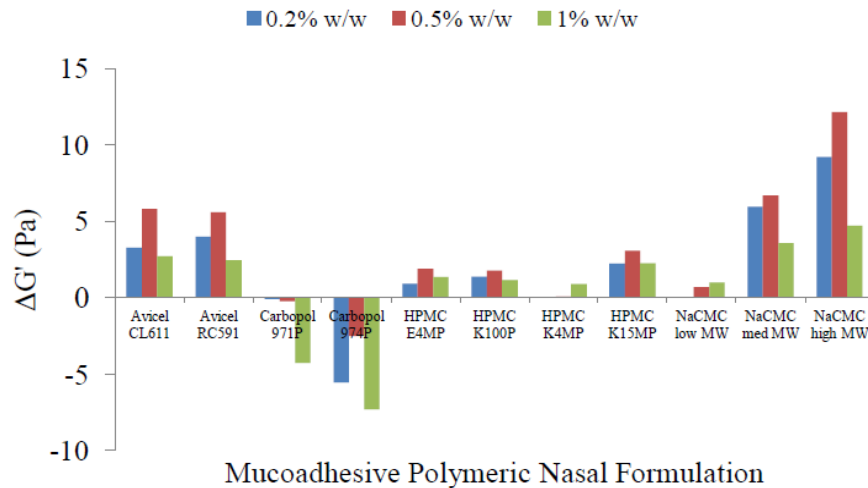


**Figure 3.3** Rheological synergism of mucoadhesive polymeric nasal formulations at a frequency of 1.22 Hz. Data represents the average  $\Delta G'$  value of three replicates. The standard error bars were omitted due to their minimal size.

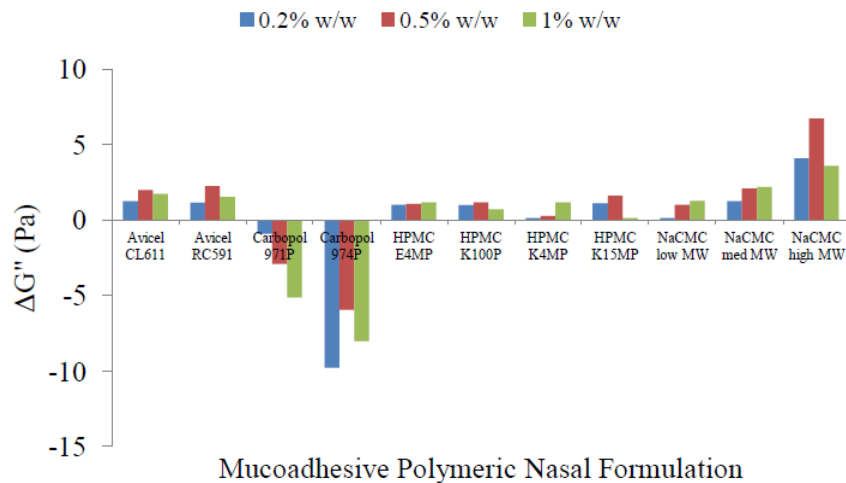


**Figure 3.4** Rheological synergism of mucoadhesive polymeric nasal formulations at a frequency of 1.22 Hz. Data represents the average  $\Delta G''$  value of three replicates. The standard error bars were omitted due to their minimal size.

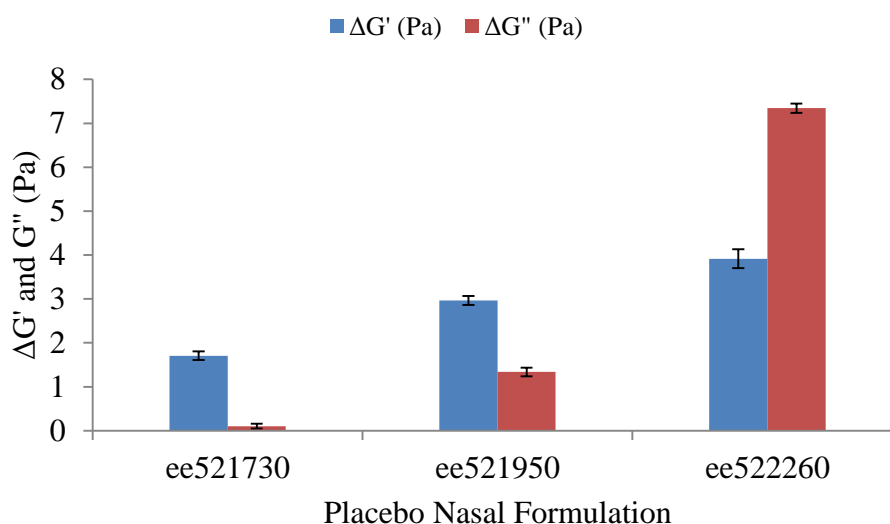


**Figure 3.5 Rheological synergism of placebo nasal formulations at a frequency of 1.22 Hz. Data represents the average  $\Delta G'$  and  $\Delta G''$  value of three replicates.**

It can be seen that all the investigated polymeric formulations exhibited a form of synergism with Carbopol 971P and 974P showing negative synergy. Negative synergism was seen in other studies involving the interaction between various Carbopol formulations and commercially available homogenised mucin (Rossi *et al.*, 1995, Tamburic and Craig, 1997). The occurrence of negative synergism signified that little or no rheological interaction took place between either of the Carbopol formulations and the mucin. Compared with Carbopol 974P, Carbopol 971P showed a smaller magnitude of negative synergism at all the concentrations investigated. A significant increase ( $P < 0.05$ ) in negative synergy for both  $G'$  and  $G''$  was seen with increasing polymeric concentration. Carbopol 974P showed a slightly different trend for both the storage and loss moduli synergy results. It can be seen for both moduli that at a concentration of 0.5% w/w, Carbopol 974P gave the lowest negative

magnitude. This suggested that the addition of mucin at this concentration had less of a detrimental impact on the interactions between the polymeric chains and the mucin glycoprotein chains. It has been reported that the crosslinking density of the system will impact on any gel strengthening that may occur between the Carbopol and mucin (Mortazavi and Smart, 1994). It will be for this reason that the variations in results between the two grades of Carbopol were observed. Carbopol 971P has a lesser degree of crosslinking and will thus have greater chain flexibility – a parameter that is important for entanglement with the mucin chains. This theory was supported by the work of Hagerstrom and Edsman (2003) who considered the limitations of this rheological method in the study of polymer/mucin interaction (Hagerstrom and Edsman, 2003). In this paper, the authors stated that the addition of mucin to the formulation may ‘dilute’ the polymer by filling the interstitial spaces and thus causing a weaker polymeric system. There are differing theories of why Carbopol exhibits negative rheological synergism. One thought is that the macromolecules of the acidic hydrogel are only slightly uncoiled which will result in the inability to form an elastic network (Tamburic and Craig, 1997). It has also been suggested that the rheological synergism can be strongly influenced by the type of mucin used in the experiment (Rossi *et al.*, 1995). It was thought that the ions present in some forms of mucin caused the polymeric gel network to weaken but this theory was dismissed by Hagerstrom and colleagues (2000) (Hagerstrom *et al.*, 2000). The authors found that using a mucin with a greater number of ions actually gave larger positive synergy values compared with the use of mucin with lower ion content. Carbopol contains a high degree of carboxyl groups and should adopt a macromolecular conformation that will allow for more favourable access to these

hydrogen bonding groups. This means that, in theory, Carbopol should provide a system that favours the interactions between the polymeric and glycoprotein chains. For this reason it can be assumed that the effect of crosslinking density has resulted in the inter- and intramolecular bonding of the polymer chains thus shielding the hydrogen bonding groups of the polymer. The other ionic polymeric formulations investigated in this study (Avicel and NaCMC) exhibited the highest synergy values. The overall rank order for synergy was found to be NaCMC high MW > NaCMC med MW > Avicel CL611 > Avicel RC591 > HPMC K15MP > HPMC E4MP > HPMC K4MP > NaCMC low MW > HPMC K100P > Carbopol 971P > Carbopol 974P. When the ionic polymeric formulations were introduced to mucin, more network links were created and a strengthened gel network was obtained. These additional network links are contributed to by the physical entanglements between the polymeric and mucin chains and the resulting hydrogen bonds (Madsen *et al.*, 1998b). The average pH of the posterior part of the human nasal cavity is pH 6.27 (Washington *et al.*, 2000). At this pH the anionic formulations will be in an uncoiled state which will allow for a greater instance of physical entanglement and secondary interactions with the glycoprotein chains (Madsen *et al.*, 1998b). The non-ionic HPMC polymers tended to exhibit smaller values of  $G'$ , which in turn related to the formation of weak gels. This weaker structure will result in a conformation that is unfavourable, the available hydrogen bonding sites are then shielded and thus the opportunity for entanglement is reduced (Madsen *et al.*, 1998b). NaCMC high MW showed the highest rheological synergism for both the elastic and viscous moduli at all three concentrations. The polymer has a high molecular weight and long, linear polymeric chains which has allowed for optimal interactions with the mucin chains.

Avicel CL611 and RC591 exhibited a comparably high level of synergy and have a significantly higher molecular weight than the NaCMC polymers. The reduction in synergy that was seen with the higher molecular weight polymer was due to some coiling of the long polymeric chains which resulted in a reduction in the available hydrogen bonding sites. With the exception of the Avicel and Carbopol polymeric formulations, the overall trend inferred that the magnitude of synergy increased with increasing molecular weight. It is clear from the results that an increase in polymeric concentration did not result in an increase in rheological synergism, although there was an effect with changing concentration (Madsen *et al.*, 1998b). For each polymer investigated, the 0.5% w/w concentration exhibited the greatest synergism for both  $G'$  and  $G''$ . This phenomenon was seen in previous work (Madsen *et al.*, 1998b) and it was confirmed that a maximum polymeric concentration was required to show sufficient synergy. A polymeric concentration that is too high might result in any synergistic behaviour being concealed by the rheological properties of the polymer alone. Conversely, a polymeric concentration that is too low will not provide enough entanglement points to allow for optimum interaction with the mucin glycoprotein chains. HPMC K100P and NaCMC low MW exhibited the lowest magnitude of positive synergy. Both polymers are low molecular weight polymers (26 and 90 kDa respectively) which do not offer as much hydrogen bonding sites as polymers of greater molecular weight. This will result in a reduced opportunity for the mucin glycoproteins to entangle with the polymeric chains. The rheological synergism results for the placebo nasal formulations are shown in Figure 3.4. It can clearly be seen that ee522260 is significantly larger ( $P < 0.05$ ) than both ee521950 and ee521730. This was comparable to the rheological synergism rank order obtained for

the formulations' mucoadhesive polymeric component (Avicel CL611 > Avicel RC591 > HPMC E4MP). The flow and oscillation rheological behaviour of the placebo nasal formulations investigated in Chapter 2 showed that the addition of excipients within the three placebo formulations affected the rheology of the polymeric components. This was not seen in this study and therefore it is imperative that the effect of excipients on the rheological and mucoadhesive behaviour is investigated further.

### **3.5.2 Assessment of interfacial interactions of mucoadhesive polymeric nasal formulations and mucin using microrheology**

Characterisation of the microrheological synergism was evaluated using a purpose built optical tweezer set up. The interactions between the polymeric and mucin chains is summarised in Figures 3.6 to 3.8.

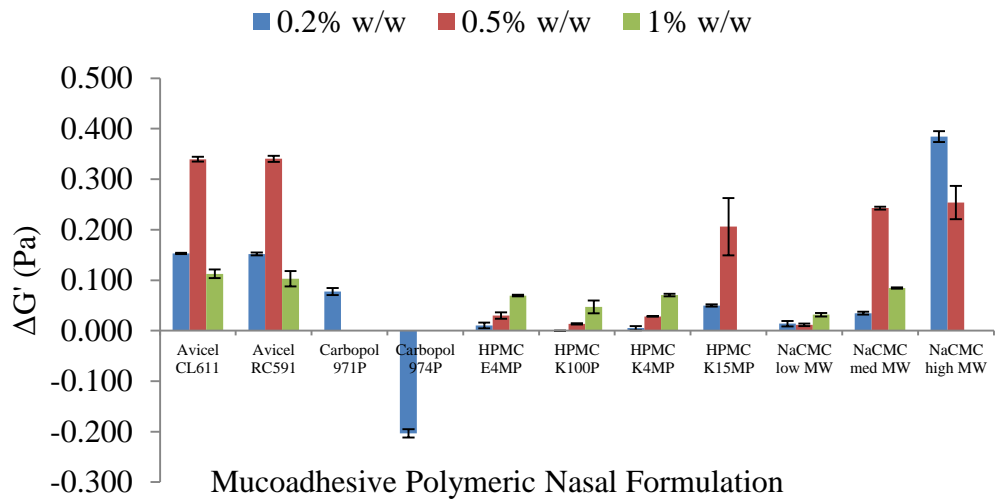


**Figure 3.6** Microrheological synergism of mucoadhesive polymeric nasal formulations at a frequency of 1.22 Hz. Data represents the average  $\Delta G'$  value of three replicates  $\pm$  S.D.

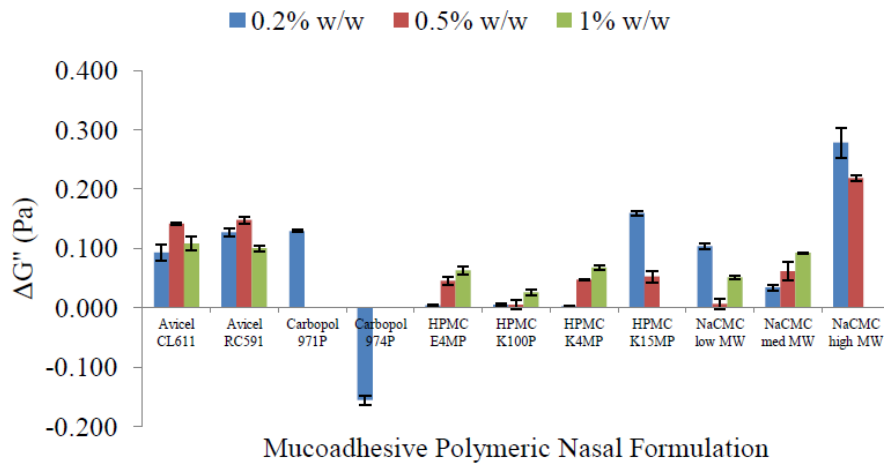


**Figure 3.7** Microrheological synergism of mucoadhesive polymeric nasal formulations at a frequency of 1.22 Hz. Data represents the average  $\Delta G''$  value of three replicates  $\pm$  S.D.

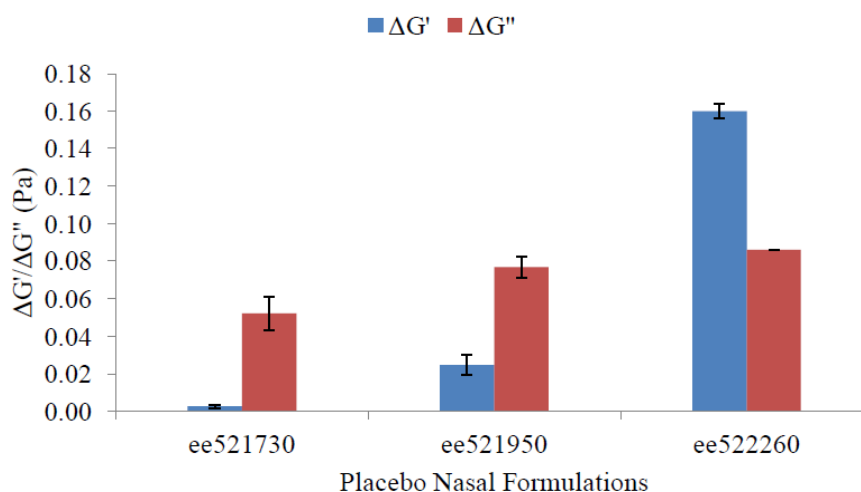


**Figure 3.8** Microrheological synergism of placebo nasal formulations at a frequency of 1.22 Hz. Data represents the average  $\Delta G''$  value of three replicates  $\pm$  S.D.

It can be seen from the results that microrheology was a useful technique to evaluate the level of interactions that occurred between the polymeric and mucin formulations. Although the magnitude of synergism recorded at the microscopic level is smaller than those obtained from the macrorheological experiment, the rank order is comparable and only one major difference was evident. In the previous synergism experiments (Section 3.5.1) both Carbopol 971P and 974P exhibited antagonism (negative synergism). It was hypothesised that the reason for this apparent reduction in gel strength was due to the unfavourable conformation of the polymeric chains, due to the cross linking density, which resulted in reduced chain flexibility and thus the opportunity for entanglement with the mucin glycoprotein chains was adversely affected. The results obtained through the use of optical tweezers suggest that in fact a level of interaction was achieved by the weakly crosslinked Carbopol polymer (971P) at 0.2% w/w. This is in line with the theory

that the Carbopol polymer should provide the optimum opportunity for entanglement due to the high abundance of hydrogen bonding groups present. The difference in results between the macro and microrheology could be due to the latter technique's ability to probe the polymeric structure at a microscopic level and provide a more detailed analysis of the network (Lai *et al.*, 2009). It can therefore be deduced that interactions between the polymeric chains and the mucin glycoprotein chains have occurred but at a microscopic level, a level at which bulk rheology cannot probe. The high molecular weight, high viscosity polymeric formulations (Carbopol 971P (0.5 and 1% w/w), Carbopol 974P (0.5 and 1% w/w), HPMC K15MP (1% w/w) and NaCMC high MW (1% w/w)) could not be tested using the microrheology method due to the inability of the microspheres to fluctuate within the thick formulation. The thermal motion of the trapped microspheres is used to calculate the viscoelastic properties of the sample and if this movement is impeded the measurements cannot be recorded. This is the reason that results were unavailable for the mentioned polymers and is a major disadvantage to microrheology (Cicuta and Donald, 2007). The results that were obtained for Carbopol 974P showed a negative thixotropy that confirmed the bulk rheological results obtained. It would seem that even at the microscopic level, the crosslinking density of the polymer is hindering the chain flexibility and further shielding the available hydrogen bonding sites that would enable interaction between the chains. Again it can be seen that the greatest synergistic effect was found with a polymeric concentration of 0.5% w/w, with the exception of NaCMC medium and high MW which both exhibited reduced synergy at this concentration. These results confirmed those obtained in the earlier rheology work and also those achieved by Madsen and colleagues (1998) (Madsen *et al.*,

1998b). The microrheological assessment of the mucoadhesive polymeric formulations has established that the greatest synergy occurred with the ionic polymers, in particular Avicel CL611 and RC591 and NaCMC medium and high molecular weight. Even at the microscopic level, these ionic polymers allow for greater interaction with the mucin chains by offering a favourable chain conformation. HPMC K100P continued to show the lowest positive synergy due to the reduced molecular weight. The results obtained for the placebo nasal formulations during the microrheology method were somewhat varied to those obtained using standard bulk rheology. The bulk rheology results showed a predominantly elastic behaviour ( $\Delta G' > \Delta G''$ ) for both ee521730 and ee521950 when mixed with the mucin formulations. The third formulation, ee522260, was more viscous with the viscous modulus exceeding the elastic moduli. When examined using optical tweezer, it was found that this behaviour was inverted with a viscous behaviour exhibited by ee521730 and ee521950 and a more solid like behaviour exhibited by ee522260. This change in behaviour observed is due to the ability of microrheology to measure heterogeneity in the physical properties of a sample as opposed to bulk rheology which produces an average measurements of these same properties (Lai *et al.*, 2009). The overall trend of synergy exhibited by the placebo nasal formulations follows that of the bulk rheology results; ee522260 > ee521950 > ee521730. In this instance, the results do not mimic those obtained for the polymeric component of the formulations alone. It would seem that any effects of the excipients on the polymers ability to interact with the mucin were not evident at a bulk scale. This strengthens the idea that bulk rheology and microrheology should be used in conjunction to assess the full rheological properties of a formulation.

### 3.6 Conclusion

This study investigated the rheological synergism between mucoadhesive polymeric formulations and mucin using a standard bulk rheological method and a microrheological technique. Both methods produced very similar results. Polymeric formulations which offer the greatest opportunity for interaction include such properties as long, flexible chains and an abundance of available hydrogen bonding sites. The formulations which exhibited the greatest synergy included the ionic polymers Avicel CL611, Avicel RC591 and high molecular weight NaCMC. When combined with mucin, each of these polymers showed an increased gel strength which would hint to a stronger adhesivity when applied in the nasal cavity. Carbopol 971P and 974P showed antagonism when mixed with mucin and measured using bulk rheology. This would suggest that these formulations would form a weakened gel when applied at the application site in the nose and thus residence time would be reduced. Microrheological analysis suggested that Carbopol 971P showed a positive synergy when mixed with the mucin formulation which implies that any rheological interactions are of a magnitude too small for detection by a bulk rheology method. Overall, the results provided useful information on the properties of the polymeric formulations when combined with mucin and demonstrated the structural changes that occurred when the two systems came into contact. The results confirmed that the entanglement and interpenetration of the polymeric chains and the mucin glycoprotein chains are a vital factor in the mucoadhesive process by increasing the strength of the polymer/mucus interfacial layer. This work also showed that microrheology is a useful tool in elucidating the rheological properties of systems at

the microscopic level; however, some differences in results between the macro and microrheology results were obtained which suggested that further work should be carried out using both methods.

## **Chapter 4 Adhesion studies of mucoadhesive polymeric nasal formulations**

### **4.1 Introduction**

Many techniques for the *in-vitro* determination of mucoadhesion have been reported in the literature with methods based on tensile testing (Carvalho *et al.*, 2010, Ivarsson and Wahlgren, 2012) and texture analysis (Shahnaz *et al.*, 2010). The latter test is regarded as the industry standard and is currently the most widely employed. The mucoadhesive tests, employing either the tensile tester or texture analyser, measure the maximum force required to detach the polymer from the surface of the substrate after contact at a specified force and contact time (Costantino *et al.*, 2007), which in turn allows for the total work of adhesion to be calculated. Substrates such as mucin gel (Varum *et al.*, 2010), mucin discs (Curran *et al.*, 2009, Carvalho *et al.*, 2010) and *ex-vivo* mucosal substrates such as porcine gastric tissue (Shahnaz *et al.*, 2010) have been employed as model substrates using the texture analyser method. Test parameters for the texture analyser, e.g. applied force, contact time, pre and post test speed and the test environment, vary amongst the published literature allowing for the impact of these altered variables on adhesion to be assessed.

Assessing the mechanical properties of mucoadhesive polymers employed in formulations is vital in the development of any drug delivery system in order to optimise desirable features, such as optimal drug release and absorption, adequate

viscosity and effective mucoadhesion, resulting in retention of the formulation at the application site.

In this work, the texture analyser was assessed for its capabilities in measuring the mucoadhesive strength of polymeric gels of both low and high viscosities. The mucoadhesive strength of a number of polymeric nasal formulations and placebo nasal formulations was also investigated using the texture analysis method. It was envisaged that the effect of the polymeric characteristics, such as molecular weight and viscosity, could be distinguished using this method.

## **4.2 Materials**

### **4.2.1 Apparatus**

Mucoadhesive measurements of the polymer gels were made using a TA-XT2 texture analyser (Stable Micro Systems, Godalming, UK) equipped with a 5 Kg load cell. The texture analyser was fitted with a 10 mm delrin cylindrical probe (P/10) (Stable Micro Systems, Godalming, UK) and used together with a mucoadhesion test rig (A/Muc) (Stable Micro Systems, Godalming, UK). All data was gathered and analysed using Texture Exponent 32 software (Stable Micro Systems, Godalming, UK).

Nitrocellulose membrane filters with a pore size of 0.45  $\mu\text{m}$  and a diameter of 45 mm (Whatman GmbH, Dassel, Germany) were used in conjunction with the

mucoadhesion test rig and a 10 mm Acu-punch biopsy punch (Acuderm Inc. Fort Lauderdale, FL, USA) was used to precisely cut the excised nasal tissue to size. Double sided adhesive tape was used to stick the excised tissue to the probe during testing.

#### **4.2.2 Chemicals**

NaCMC low, medium and high MW (average molecular weight ~90, 250 and 700 kDa respectively), calcium chloride dihydrate ( $\text{CaCl}_2 \cdot 2\text{H}_2\text{O}$ ), potassium chloride (KCl), sodium bicarbonate ( $\text{NaHCO}_3$ ), sodium chloride (NaCl), magnesium sulphate heptahydrate ( $\text{MgSO}_4 \cdot 7\text{H}_2\text{O}$ ), sodium phosphate ( $\text{NaH}_2\text{PO}_4$ ), dextrose and type III bound sialic acid mucin from porcine stomach were purchased from Sigma Aldrich Co (St Louis, MO, USA). Avicel RC591 and CL611 were obtained from FMC Biopolymer (Philadelphia, PA, USA). Carbopol 971P and 974P were obtained from Lubrizol Advanced Materials Europe BVBA (Brussels, Belgium) and HPMC powder (Methocel grades E4MP, K4MP, K100P and K15MP) was received as a gift from Colorcon (Dartford, Kent, UK). Three placebo nasal spray formulations (batch numbers ee521730, ee521950 and ee522260) were received from GlaxoSmithKline R & D (Ware, UK).

## **4.3 Methods**

### **4.3.1 Preparation of mucoadhesive polymeric nasal formulations**

The mucoadhesive polymeric nasal formulations were prepared as described in Section 2.3.1.

### **4.3.2 Preparation of placebo nasal formulations**

The placebo nasal formulations were used as received.

### **4.3.3 Preparation of Krebs Bicarbonate Ringer solution**

The Krebs Bicarbonate Ringer solution (KBR) was prepared as described by Hall (Hall *et al.*, 2002). 133 mM NaCl, 4.7 mM KCl, 16.3 mM NaHCO<sub>3</sub>, 1.35 mM NaH<sub>2</sub>PO<sub>4</sub>, 0.6 mM MgSO<sub>4</sub>·7H<sub>2</sub>O and 7.8 mM dextrose were added to a Duran flask along with the required volume of deionised water (Table 4.1). The mixture was stirred and gassed (95% O<sub>2</sub>, 5% CO<sub>2</sub>) until all excipients were dissolved. 2.5 mM of CaCl<sub>2</sub>·H<sub>2</sub>O was then added and the solution gassed for a further ten minutes. The KBR solution was stored refrigerated and used within 24 hours to avoid microbial growth.

**Table 4.1 KBR buffer solution composition (Hall *et al.*, 2002)**

Chemicals	[mM]	g/1L	g/2L	g/3L
Water	-	1L	2L	3L
NaCl	133	7.773	15.545	23.319
KCl	4.7	0.35	0.701	1.051
NaHCO <sub>3</sub>	16.3	1.369	2.739	4.107
NaH <sub>2</sub> PO <sub>4</sub>	1.35	0.162	0.324	0.486
MgSO <sub>4</sub> .7H <sub>2</sub> O	0.6	0.148	0.296	0.444
Dextrose	7.8	1.406	2.811	4.218
CaCl <sub>2</sub> .2H <sub>2</sub> O	2.5	0.368	0.736	1.104

#### 4.3.4 Preparation of porcine nasal tissue

Porcine heads were received as halves from six month old male and female pigs from the local abattoir (Ramsays of Carluke, Carluke, UK). A scalpel was used to remove the cartilaginous septum from the nasal cavity which allowed access to the turbinates (Figure 4.1). The time from slaughter to the removal of the nasal tissue was approximately two hours.

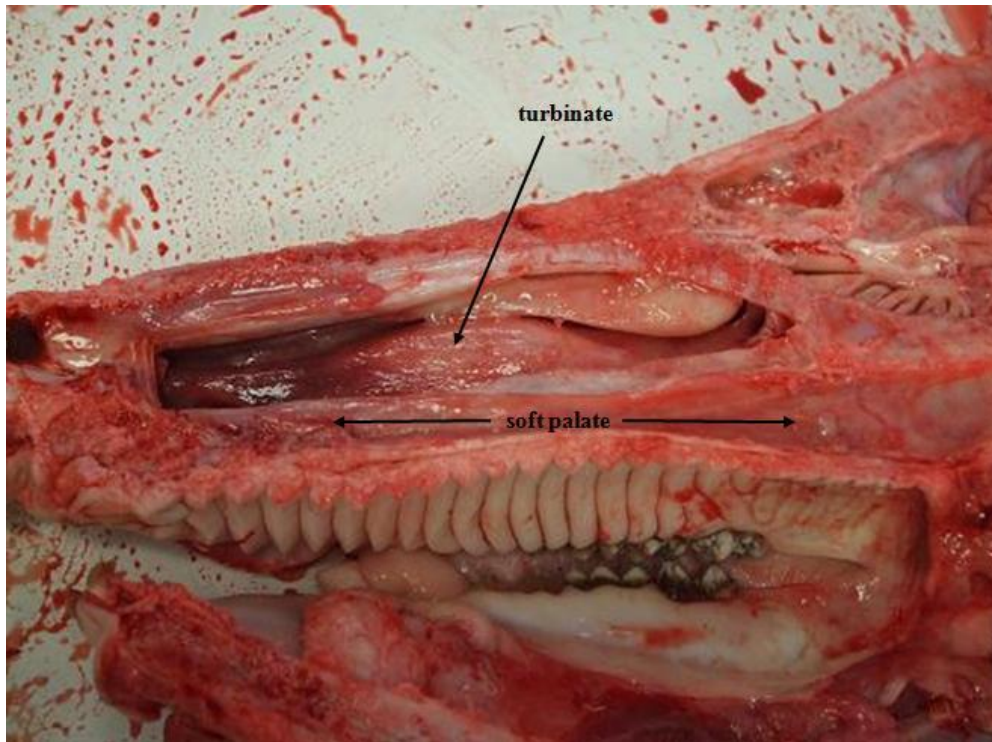


**Figure 4.1** Sagittal cross section of a porcine nasal cavity

The turbinate was carefully removed by using forceps and dissecting scissors and cutting the cartilage free from the nasal cavity before gently peeling the nasal mucosa from the cartilage scroll (Figure 4.2). The mucosa was washed with cold KBR solution before being put into individual vials filled with ice cold KBR solution until required. Each piece of tissue was used once and discarded after analysis. The tissue was used on the day of excision and was not frozen.

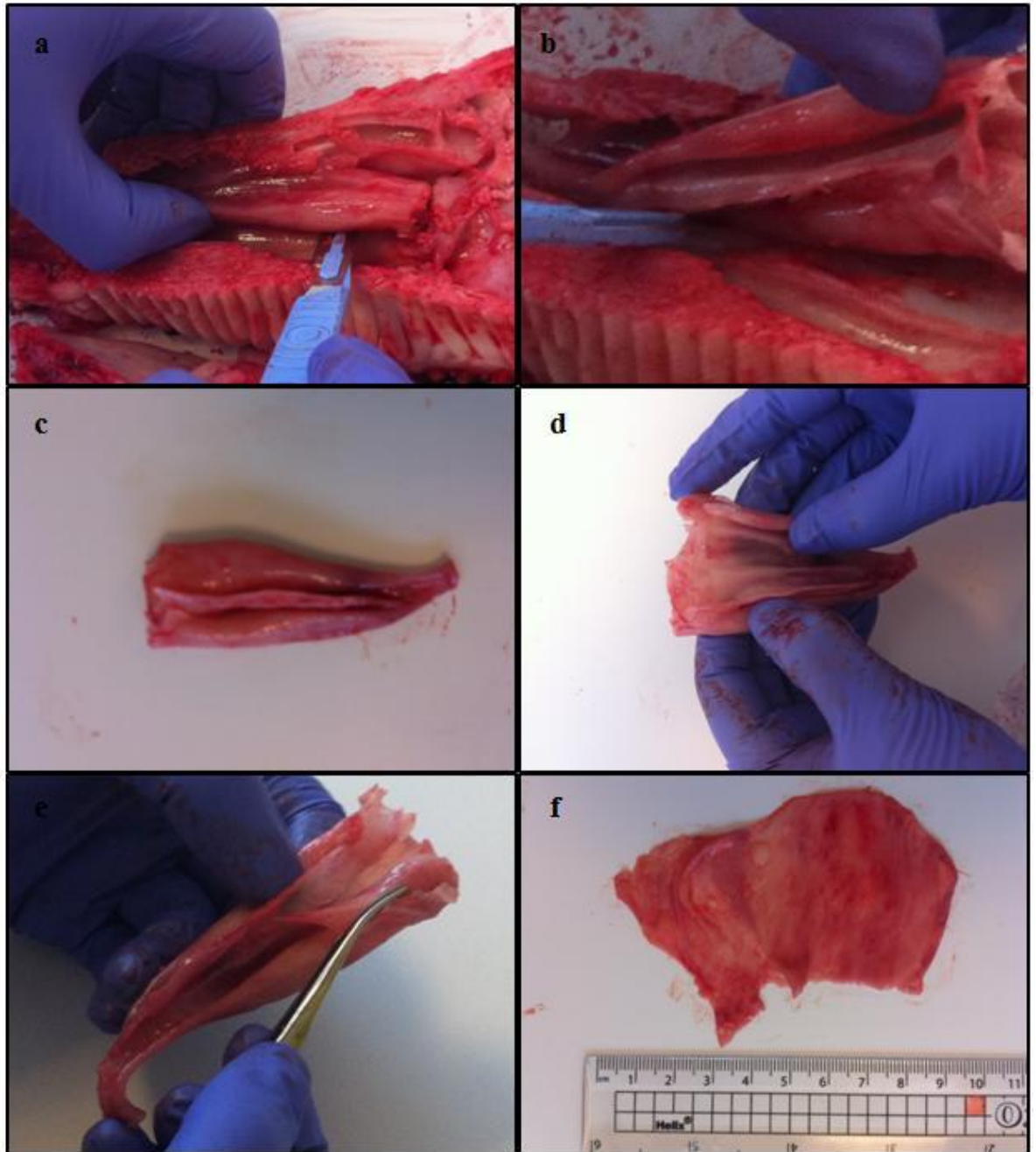


**Figure 4.2** Diagrammatical method showing excision of respiratory mucosa from a porcine nasal cavity. (a) shows the incisions made in order to free the turbinate from the nasal cavity, (b) shows further removal of the turbinate, (c) the excised turbinate, (d) unravelling the turbinate scroll, (e) the respiratory mucosa is gently peeled away from the cartilaginous scroll, (f) the fully excised respiratory mucosa.

### 4.3.7 Measurement of mucoadhesive strength of polymeric nasal formulations and placebo nasal formulations

The TA-XT2 texture analyser was used in adhesion mode to measure the mucoadhesive strength between the mucoadhesive polymeric nasal formulations and the placebo nasal formulations to porcine nasal mucosa. Figure 4.3 shows the set up of the texture analyser and mucoadhesion test rig. The tissue holder of the mucoadhesive test rig was lined with a 45 mm diameter nitrocellulose membrane filter and filled with approximately 2 mL of the polymeric formulation to be tested. The cellulose membrane was used to provide an extra barrier against leakage of the polymeric formulations during analysis.

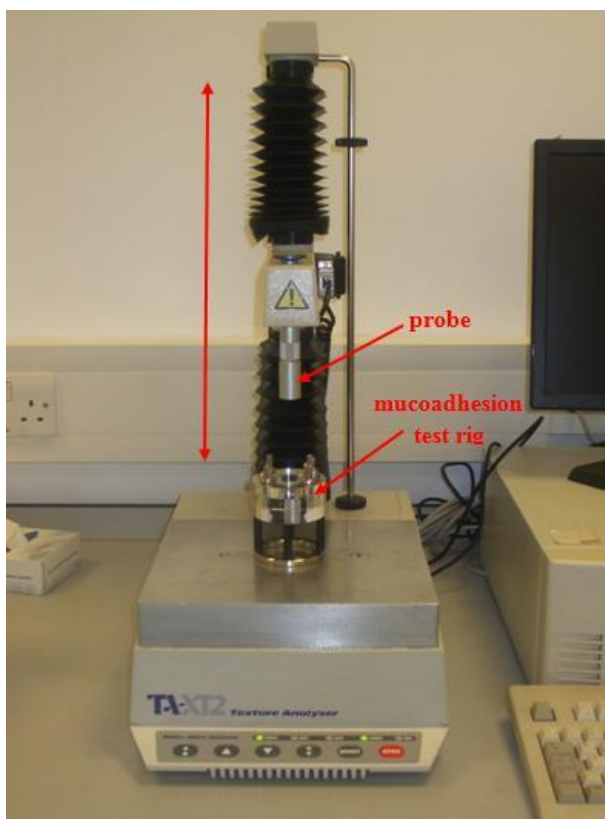


**Figure 4.3** Texture analysis set up showing probe and mucoadhesive test rig.

The nasal tissue was cut into 10 mm diameter discs using an Acu-punch biopsy punch and placed mucus side up in a piece of paper towel. This allowed the non-mucus side to be dried of excess KBR solution and ease the adherence to the probe. The tissue disc was secured to the delrin probe using double sided adhesive tape and rehydrated with KBR. Rehydration was achieved by immersing the mucosal surface in KBR for 10 s. The probe was lowered onto the polymer at a speed of 1.00 mm/s until a trigger force of 1.0 mN was detected which initiated the data collection. The probe applied a force of 5 mN for 30 s before withdrawing at a speed of 1.00 mm/s to a distance of 15 mm (Figure 4.4). This ensured a break occurred between the porcine nasal tissue and the polymeric formulation. The maximum force of detachment and the work done by the texture analyser to detach the polymeric formulations from the mucosal surface was measured.

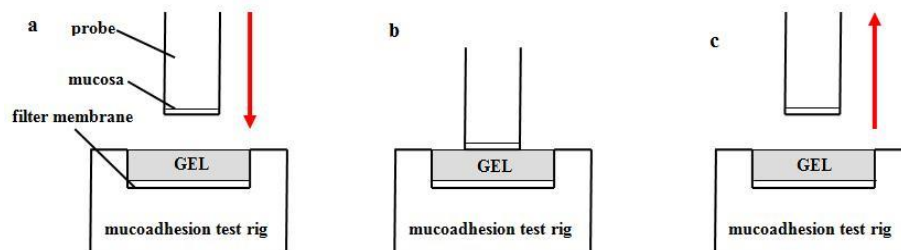


**Figure 4.4** Experimental procedure used in mucoadhesive strength measurements. a. the probe is lowered at a speed of 1.00 mm/s. b. the probe applies a force of 5 N ensures a contact time of 30 s between the mucosa and gel formulation. c. the probe is withdrawn at a speed of 1.00 mm/s to a distance of 15 mm.

## 4.4 Results and discussion

### 4.4.1 Measurement of mucoadhesive strength of polymeric nasal formulations

A typical force/time plot obtained from the texture analyser for adhesion between a polymeric nasal formulation and excised porcine nasal mucosa is shown in Figure 4.5.

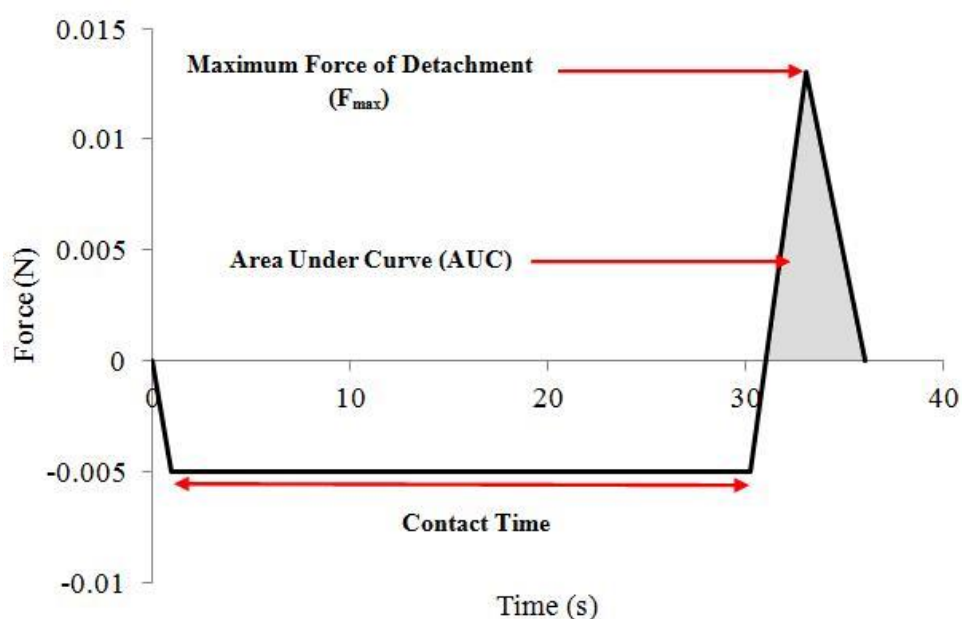


**Figure 4.5** Representation of a typical texture analyser force/time plot showing  $F_{\max}$  and AUC.

The maximum detachment force ( $F_{\max}$ ), which is defined as the maximum force required to detach the polymeric nasal formulation from the nasal mucosa, and the area under the force/time curve (AUC), which is a measure of the actual work done

by the texture analyser whilst withdrawing the mucosa from the mucoadhesive formulation, were measured and evaluated. In general, the experimental parameters previously set by others for the mucoadhesive strength measurements, would be different to those utilised in this investigation. There are no standardised test parameters set out for texture analysis and thus the experimental parameters used are rationalised by the investigator to suit the sample being tested. It is thought a contact time of approximately 300 s is a suitable timeframe within which to gain valuable results (Tobyn *et al.*, 1997) but a shorter contact time of 30 s was chosen to minimise the risk of sample dehydration when analysing the low viscosity formulations. Another parameter that was considered during the experiment was the use of fresh or frozen excised porcine tissue. One study (Madsen *et al.*, 1999) stated that no differences could be detected between frozen and fresh tissue when looking at the optical properties of porcine nasal cartilage. Freezing did not affect the fentanyl permeability of porcine buccal tissue when wrapped in aluminium foil and stored at -20 °C (Kulkarni *et al.*, 2010, Zhao *et al.*, 2011). Another study (Mattes and Mattes, 1992) reported that enzyme activity in rat nasal tissue was not affected by the freezing and thawing of the tissue but conversely, the enzyme activity in human nasal tissue was somewhat labile with the repeated freeze/thaw process and it was advised that the tissue be stored in individual aliquots. With the uncertainty surrounding the effects of freezing on the mucus coating, it was decided that all tissue be used on the day of excision.

The results for the maximum detachment force ( $F_{\max}$ ) required to detach the mucoadhesive polymeric nasal formulations from the excised porcine mucosa and

the work done (AUC) to achieve the removal of the two substrates are shown in Figures 4.6 and 4.7. The results for the three placebo nasal formulations are shown in Figures 4.8 and 4.9.

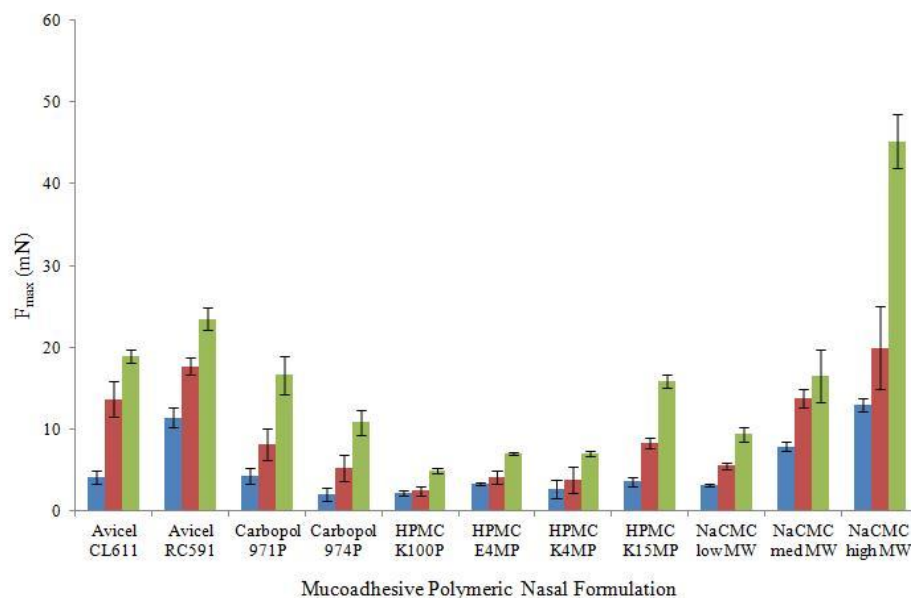


**Figure 4.6** Mean  $F_{\max}$  ( $\pm$  S.D.) results for 0.2% (blue), 0.5% (red) and 1% w/w (green) mucoadhesive polymeric nasal formulations. (n=3).

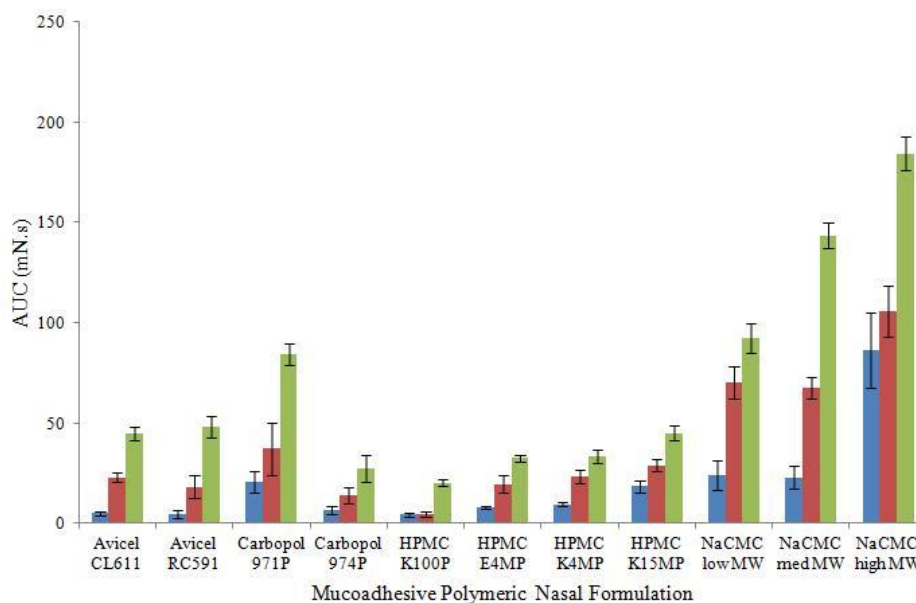


**Figure 4.7 Mean AUC( $\pm$  S.D.) results for 0.2% (blue), 0.5% (red) and 1% w/w (green) mucoadhesive polymeric nasal formulations. (n=3).**

Increasing the concentration and thus the viscosity of the mucoadhesive polymeric nasal formulations resulted in an increase in both the maximum detachment force (Figure 4.4) and the AUC (Figure 4.5). The observed increase in both variables appeared to be an exponential increase which could suggest that an increase in concentration/viscosity of the mucoadhesive polymer within the formulation will result in an increased mucoadhesive strength. NaCMC high MW at all three concentrations showed the highest values for both the maximum detachment force and also the area under the curve. This suggests that of all the polymers tested, NaCMC high MW provided the greatest mucoadhesive strength and should prolong residence of the formulation within the nasal cavity. Avicel RC591 also exhibited a high affinity for the excised mucosa and produced consistently high values for both variables. From the results, it can be seen that HPMC K100P proved the weakest mucoadhesive polymer and the maximum force to break the bond between the

polymer and the mucosal layer, along with the work done to achieve this result, were the lowest values obtained. It is already well known that viscosity plays a vital role in extending the residence time of formulations within the nasal cavity (Dolzplanas *et al.*, 1988, Majithiya *et al.*, 2006, Privalova *et al.*, 2012) but this theory challenges the ideas put forth by others which argue that a higher viscosity formulation will prevent the close contact required between the polymer chains and the mucus glycoproteins to achieve mucoadhesion (Livraghi and Randell, 2007, Serra *et al.*, 2009b). It has also been argued that an increase in polymer concentration would result in a mobility decrease of the polymeric chain which would result in reduced interaction opportunities with the glycoproteins of the mucus and thus a loss of mucoadhesive efficacy (Lee *et al.*, 2000). However, it can be clearly seen that the results in this study consistently opposed the latter theories and that in fact an increased concentration has resulted in an increased mucoadhesive strength. Another theory related to a reduction in chain mobility is the theory that crosslinking can have a detrimental effect on mucoadhesion. It has been suggested that an increased cross linking density will also reduce the mobility of the polymer chains and therefore affect the interdiffusion and interactions between the mucus glycoproteins chains and the polymer chains (Lee *et al.*, 2000, Zhu *et al.*, 2011). This is evident in the result obtained for Carbopol 971P and 974P. Rheological measurements (Chapter 2) determined that both variations of Carbopol were significantly different in terms of viscosity. Carbopol 974P presented a significantly lower viscosity than the lesser crosslinked variable, Carbopol 971P. It was suggested that this was due to the highly crosslinked polymer internally interacting with itself resulting in the chains coiling and contracting the size of the polymer (Gebben *et al.*, 1985). With this in mind it

would seem that in the case of crosslinked polymers, the lack of available polymer chains with which to interact with the mucus glycoproteins has had a detrimental effect on the mucoadhesive strength of Carbopol 974P and thus the mucoadhesive strength was reduced.

Another factor important for mucoadhesion is the molecular weight of the mucoadhesive polymer. It is generally accepted that an increase in molecular weight will result in an increase in mucoadhesion (Serra *et al.*, 2009a). However, it has been found that there is a desirable molecular weight above which increased mucoadhesion does not exist. A study looked at the mucoadhesive strength of dextran and found that the mucoadhesive efficacy of the polymer with a molecular weight of 19,500,000 Da was no more adhesive than the polymer with a molecular weight of 200,000 Da (Ugwoke *et al.*, 2001). The author suggested that the high molecular weight of the non-linear polymer caused the binding sites to be hidden by the coiling of the large polymer chain resulting in them being unavailable for interaction with the mucus layer. Dondeti and colleagues (1996) proposed that linearly structured polymers increased the opportunity for entanglement with the mucus glycoproteins and will inevitably result in an increase in adhesion (Dondeti *et al.*, 1996). It would seem that the theory suggested by Dondeti explains the results achieved through the texture analysis method utilised in this study. HPMC K100P has the lowest molecular weight of the linear polymers (26 kDa) and showed the lowest mucoadhesive strength at all concentrations. NaCMC high MW has the highest molecular weight (700 kDa) and at all concentrations exhibited the highest level of mucoadhesive strength. It has been suggested that successful mucoadhesion

requires a linear mucoadhesive polymer to have an average molecular weight of 100 kDa. This would explain the poor mucoadhesive properties of the low molecular weight HPMC K100P due to the reduced availability of sites for interaction between the polymeric chains and the mucus glycoprotein chains.

Polymer gels are already hydrated when they meet the mucosal surface and therefore do not undergo swelling in the same way that dry dosage forms will. However, polymer gels can still become over hydrated and as such will result in a loss of mucoadhesive strength (Renner *et al.*, 2012a). Accili and colleagues (2004) found that the mucoadhesive capabilities of Carbopol were reduced when over-hydrated (Accili *et al.*, 2004). This was as a result of two factors. Firstly, the excess water reduced the concentration and therefore the viscosity of the polymer and secondly, the water causes a reduction in the number of functional groups which will enable adhesion. The latter stems from the competition from the water against the hydroxyl groups of the mucus glycoproteins for the establishment of hydrogen bonds with the Carbopol's carboxylic groups (Renner *et al.*, 2012a).

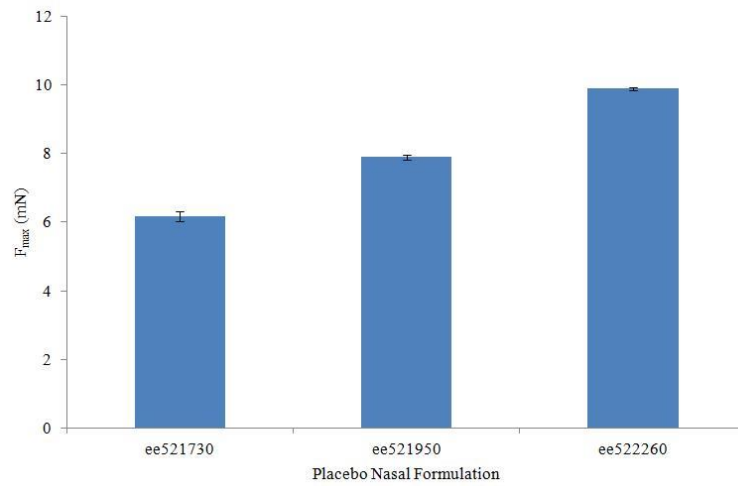


**Figure 4.8 Mean  $F_{max}$  ( $\pm$  S.D.) results for placebo nasal formulations. (n=3).**

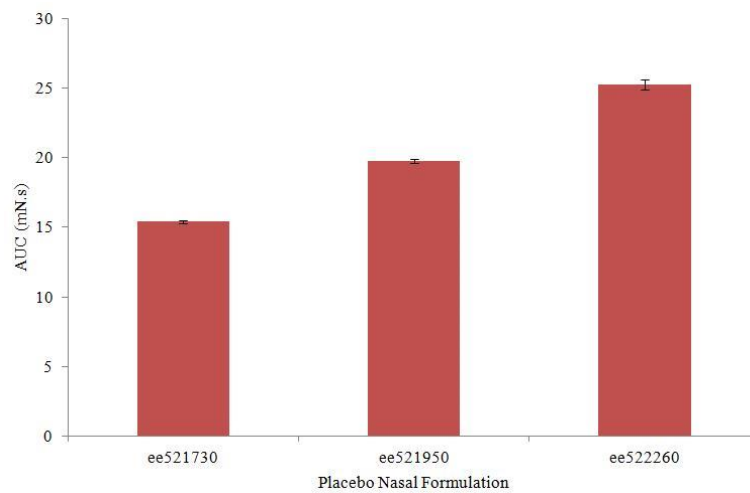


**Figure 4.9 Mean AUC ( $\pm$  S.D.) results for placebo nasal formulations. (n=3).**

The results obtained for the placebo nasal formulations (Figures 4.8 and 4.9) showed a mucoadhesive trend of ee521730 < ee521950 < ee522260. This is consistent with the rheology results obtained at  $100 \text{ s}^{-1}$  (Section 2.5.1). It can be seen that the mucoadhesive strength results for the three mucoadhesive polymers alone provide

very different results to the results achieved for the placebo nasal formulation containing the polymers and other excipients. The results, for both the  $F_{\max}$  and AUC, for the polymeric formulations were significantly larger than the same results obtained for the placebo nasal formulations. It would seem that yet again the presence of other excipients within the placebo nasal formulations had a major impact on the mucoadhesive results obtained (Section 2.5.1). This could be due to the excipients competing for interaction sites within the formulation/mucus interface. A reduction in interaction opportunities will prove detrimental to the overall mucoadhesive capabilities of the system.

Although the methodology provided reliable results, it is worth noting that other factors may have come in to play during the analysis. One major implication for the experimental design is the use of excised porcine tissue. Excised tissue is a much more desirable substrate to use than an artificial substrate but it does not come without its limitations. One such limitation is the variability within the animals and also mucosal thickness (Zhu *et al.*, 2011). Varum (2010) looked at the results obtained for mucoadhesive strength at different mucosal points along the intestinal tract and found that the thickness of the mucosa did in fact impact significantly on the measurements obtained (Varum *et al.*, 2010). It is there essential that repeats are conducted using the same piece of excised tissue and so major thickness variabilities are avoided. Another major consideration in texture analysis is in the definition of the fracture point at which the maximum detachment force is measured. During this study, it was assumed that the maximum detachment force occurred between the polymer and mucosal substrate and no thought was placed on the fracture point in

fact occurring within the mucin or polymer itself. It is for this reason that authors have relied more on the data obtained from the area under the curve rather than the maximum detachment force (Hagerstrom and Edsman, 2001). Hagesaether and colleagues (2009) tested a method which could distinguish between an adhesive and cohesive bond failure (Hagesaether *et al.*, 2009). They added indigo to chitosan films, which they then tested against mucin or buffer using a texture analyser. They found that the coloured method was adequate to distinguish between an adhesive failure between the polymer and mucin and a cohesive failure within either the mucin or the polymer. This method can be adapted to suit this experiment by adding a dye, such as indigo, to the polymeric gel formulations and measuring the mucoadhesive strength in the same manner. Due to the variables involved with the texture analysis method and the range of experimental parameters that can be used, it would be advisable to accompany this test method with another, such as rheology, in order to gain a more accurate representation of the mucoadhesive powers of the polymers.

#### **4.5 Conclusion**

It can be concluded that using the texture analyser in adhesion mode is a quick and convenient way of measuring and comparing the mucoadhesive properties of low and high viscosity polymer gels. The information derived from texture analysis can prove to be important in the development of mucoadhesive formulations (Jones *et al.*, 1996) as it can describe the mechanical properties in terms of adhesiveness and cohesiveness, which relates to the extent of structural recovery following the application of shear stress – an occurrence in nasal spray formulations. It must be noted however that there are many instrumental parameters and test conditions,

including contact time, contact force, test medium and test speed, which may ultimately influence the measurement of mucoadhesion. A further consideration is that the measurement of maximum detachment force of the polymer gel formulations may not represent actual adhesion to the mucin but instead may represent only the cohesive break of the gel itself. This may explain any variation in results between  $F_{\max}$  and AUC. These results can be compared to the results of a study which found that the assessment of mucoadhesion is best carried out using tensile testing than measuring the fracture strength of the polymer gel (Hagerstrom and Edsman, 2001). It is therefore imperative that any test system is adequately assessed to optimise the conditions used in conducting the experiment. Researchers often couple texture analysis with other experimental techniques in order to gain the whole picture of the process of mucoadhesion (Haque and Khan, 2008, Ivarsson and Wahlgren, 2012). Previous investigations have centred on the use of a variety of forms of mucoadhesive polymer. These have included lyophilised wafers and compressed tablets of polymer (Stasiak *et al.*, 2011).

The results reported here have clearly shown that concentration, viscosity and molecular weight, which are closely related factors, are fundamental in improving the mucoadhesive strength of a polymeric nasal formulation. The polymers with increased magnitudes of these three factors exhibited increased mucoadhesive strength which was as a result of the increased occurrence of entanglements between the polymeric chains and the mucus glycoprotein chains. This increased mucoadhesive strength will inevitably result in an increased residence time of the formulation within the nasal cavity and this should, in theory, improve the absorption

of drug into the systemic circulation. However, there has been very little traceable work carried out using low viscosity polymer gels, as in this study, and therefore it is imperative that further work be carried out in order to assess the validity of texture analysis as a method to determine the mucoadhesive strength of low viscosity formulations.

## **Chapter 5 The impact of spray device actuation on the rheological behaviour of mucoadhesive polymeric nasal formulations**

### **5.1 Introduction**

Nasal sprays, which utilise mucoadhesive polymers, may be beneficial in overcoming the major limiting factor for the delivery of drugs to the nasal mucosa. Seiler and colleagues (2002) reported that the clearance rate and bioavailability of a virally-mediated gene transfer system was improved when delivered intranasally using a thixotropic nasal solution containing methylcellulose derivatives (Seiler *et al.*, 2002). Thixotropic formulations are desirable in nasal drug delivery as these materials will have an initial high viscosity at rest; however, they will undergo reversible shear thinning on the application of stress (e.g. stirring or spraying). It is also a desirable characteristic when preparing suspensions. Such formulations allow for a uniform distribution of the drug and thus may prolong its action on the site of application (Lee *et al.*, 2009). Thixotropy is generally accepted to be a reversible gel-sol-gel conversion initiated as a result of time-dependent viscosity changes and can be generated by temperature or pH changes (Lee *et al.*, 2009). Thixotropic formulations become less viscous when shear is applied; however, on the removal of the shear the formulation enables a gradual recovery of the viscosity, demonstrating a hysteresis. The delay in recovery is due to the time required to anneal the polymeric interactions within the formulation, following the application of shear (Mohamed, 2004). The level of thixotropy can be evaluated from the area of the hysteresis loop between the up and down curves of the shear stress vs. shear rate plot (rheograms).

A rapid recovery to the original higher viscosity indicating restoration of the original structure would yield a final, more desirable viscosity and thus the chance of the formulation draining from the nasal cavity would be reduced. In previous work, the previous processing (sometimes referred to as sample shear history) has been shown to play a role in the rheograms produced (Sharpe *et al.*, 2003). Vigorous and heavy stirring of the polymer during preparation may begin to break the structure prior to sample analysis and cause structural displacement within the polymer chains. This in turn could lead to erroneous estimations of polymer rheology.

A wide range of therapeutic agents are applied in nasal sprays. These include drugs for indications such as migraine, hormone replacement therapy and endometriosis (Grassin-Delyle *et al.*, 2012). The impact of polymer viscosity on clearance of nasal spray formulations from the nose has been demonstrated using gamma scintigraphy (Pennington *et al.*, 1988). Using different concentrations of hydroxypropylmethylcellulose (HPMC) in the spray formulations, the clearance half life of the formulation was increased from 1 hour at 0.6% w/w HPMC to 2.2 hours at 1.25% w/w HPMC, demonstrating that viscosity will impact on the residence time of the formulation in the nasal cavity. Different corticosteroid nasal sprays have been shown to demonstrate thixotropy at different rheometer induced shear rates including  $10\text{ s}^{-1}$ ,  $100\text{ s}^{-1}$  and  $1200\text{ s}^{-1}$  (Eccleston *et al.*, 2000, Eccleston and Hudson, 2000, Sharpe *et al.*, 2002, Sharpe *et al.*, 2003). Sharpe and colleagues (2003) simulated patient shaking and spraying on the thixotropic behaviour of six nasal drug formulations. All spray formulations tested were shown to exhibit thixotropy in varying degrees, with the commercial formulation Nasonex<sup>®</sup> determined to have the

highest apparent thixotropy (Sharpe et al., 2003). In the studies mentioned, the thixotropic behaviour of the formulation as a whole was studied. In addition each formulation was sprayed in its original spray bottle, whose design differed, which potentially altered the initial shear rate applied to each formulation. Commercially, the application of pesticides and biocides in agricultural practice involves the use of pressurised sprays systems of low viscosity emulsions and solutions. In the field of agricultural science there is a body of work describing the interaction of formulation effects and nozzle design (Miller and Butler Ellis, 2000). The study found that different formulations had differing effects on the spray formation process but that it was not only related to the formulation but to the nozzle design also. This may also relate to the delivery of intranasal spray formulations and work should be carried out to deduce such effects. The rheological behaviour of a nasal spray formulation is also of great importance to a nasal spray formulation. As a result, the development and final design of nasal spray formulations represents several challenges to the formulator. A desirable formulation should include such attributes as sufficient spreading qualities over the nasal mucosa, prolonged adhesion and also a viscosity low enough to be easily actuated from a spray device (Charlton *et al.*, 2007). Following from this, the formulation should also allow quick structural reformation and a re-establishment of viscosity after the effects of shear, caused by the action of spraying, have been applied in order to prevent the formulation from running out of the nasal cavity and into the nasopharynx (Luond-Valeskeviciute I and Gruenwald, 2010).

Inevitably, side projects stepped away from the main direction of research. It was thought that it would be relevant to examine the effects of spray device actuation on the polymeric formulations, the rationale being that the hysteresis curves might be reflected in the recovery of rheological properties post-delivery. To our knowledge, this had not been previously reported. The work involved in this chapter centres around the assessment of rheological flow behaviour before and after spraying. The formulations will experience a high level of shear when actuated from a spray nozzle and could undergo a variety of structural changes. Such behaviour may or may not be time dependant and could have an overall impact on the formulations ability as a mucoadhesive delivery device. It is therefore imperative that the properties of the formulation, post-spray, are fully understood in order to evaluate their performance within the nasal cavity after application. It is assumed that the effects of spray device actuation on the flow properties of the formulations can be easily assessed using the same rheology method as described in Chapter 2. Additionally, the extent of the effects within different mucoadhesive polymers will be illustrated.

## **5.2 Materials**

### **5.2.1 Apparatus**

Rheological analysis was performed using a controlled stress Carrimed CSL<sup>2</sup> 100 rheometer (TA Instruments, Surrey, UK) with a 6cm stainless steel cone and plate geometry. The CSL V1.2a software package (TA Instruments, Surrey, UK) was used for system control along with data gathering and analysis.

VP7 spray pump actuators (batch number 091211694) and 10 mL amber glass spray bottles (batch number N152948) were supplied by GlaxoSmithKline R&D, Ware, UK and used to conduct the spray actuation.

## **5.2.2 Chemicals**

NaCMC low, medium and high MW (average molecular weight ~90, 250 and 700 kDa respectively) were purchased from Sigma Aldrich Co (St Louis, MO, USA). Avicel RC591 and CL611 were obtained from FMC Biopolymer (Philadelphia, PA, USA). Carbopol 971P and 974P were obtained from Lubrizol Advanced Materials Europe BVBA (Brussels, Belgium) and HPMC powder (Methocel grades E4MP, K4MP, K100P and K15MP) was received as a gift from Colorcon (Dartford, Kent, UK).

## **5.3 Methods**

### **5.3.1 Preparation of mucoadhesive polymeric nasal formulations**

The mucoadhesive polymeric nasal formulations were prepared as described in Section 2.3.1.

### **5.3.2 Rheological investigation into the effect of spray device actuation on the flow behaviour of mucoadhesive polymeric nasal formulations**

The effect of spray device actuation on the apparent viscosities and rheological flow behaviour of eleven mucoadhesive polymers was performed using a Carrimed CSL<sup>2</sup> 100 controlled stress rheometer (TA Instruments, Dorking, UK), equipped with a 6 cm steel cone and plate test geometry with a fixed gap of 57 microns and set at a temperature of  $25 \pm 0.1$  °C. The polymer samples were poured into separate, labelled pump actuated spray bottles before being lightly shaken by hand for fifteen seconds. The formulations were then individually sprayed into clearly labelled sample containers until ~ 6 mL of sample was actuated. The samples were spooned onto the peltier plate to minimise further shearing of the polymer during transfer and the cone lowered to the fixed gap of 57 microns. Excess sample was carefully trimmed from the edge of the cone by a flat edged spatula to ensure sample overloading did not occur. The samples were allowed to condition and equilibrate for 180 s and flow data was generated with maximum shear rates of  $100 \text{ s}^{-1}$  and  $1200 \text{ s}^{-1}$ , with a sweep time of 240 s. The remaining sample was kept in the container until 15 minutes had elapsed and loaded onto the peltier plate in the same manner. The apparent viscosity, taken at the apex of the rheogram, was evaluated for the polymeric formulations and also the same formulation following the process of spray device actuation. The cone and plate were cleaned thoroughly with distilled water and dried between samples. All measurements were conducted in triplicate.

## **5.4 Statistical Analysis**

The effects of spray device actuation on the rheological behaviour of the mucoadhesive polymeric nasal spray formulations were statistically analysed by a one way analysis of variance (ANOVA) with Tukey's post hoc test, using Minitab 16 (Minitab LTD., Coventry, UK). For all measurements,  $P < 0.05$  represented statistical significance.

## **5.5 Results and discussion**

### **5.5.1 The effect of spray device actuation on the rheological flow behaviour of mucoadhesive polymeric nasal formulations**

The apparent viscosity and rheological flow behaviour of each polymeric nasal formulations was affected by the exposure of shear and extensional flow due to spray actuation. The results are shown in Figures 5.1 to 5.6.

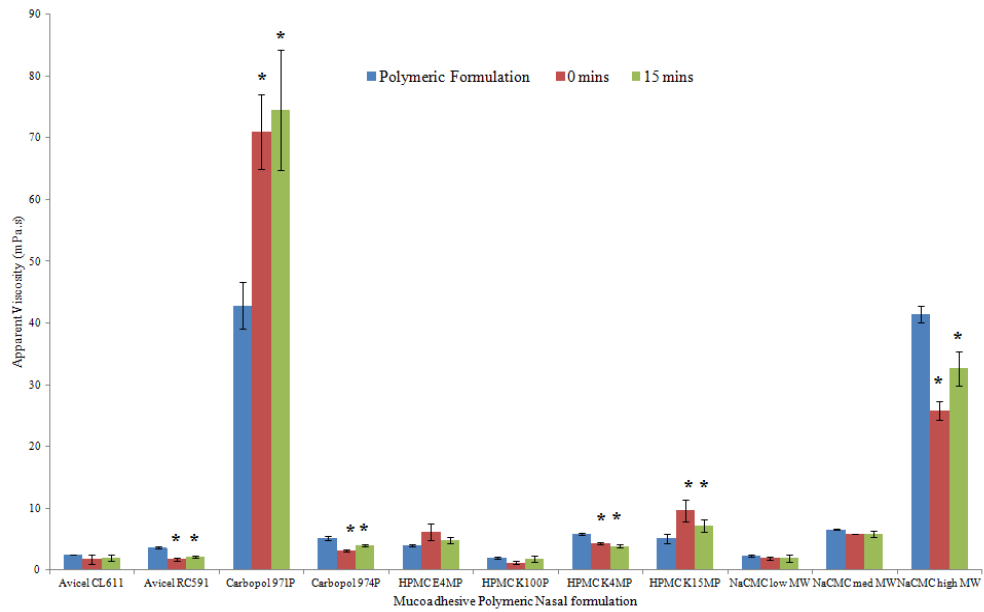


**Figure 5.1** Effect of spray actuation on mean apparent viscosity ( $\pm$  S.D) of 0.2% w/w mucoadhesive polymeric nasal formulations measured at  $100 \text{ s}^{-1}$ . \*denotes statistical significance to polymeric formulations ( $P < 0.05$ ) ( $n=3$ ).

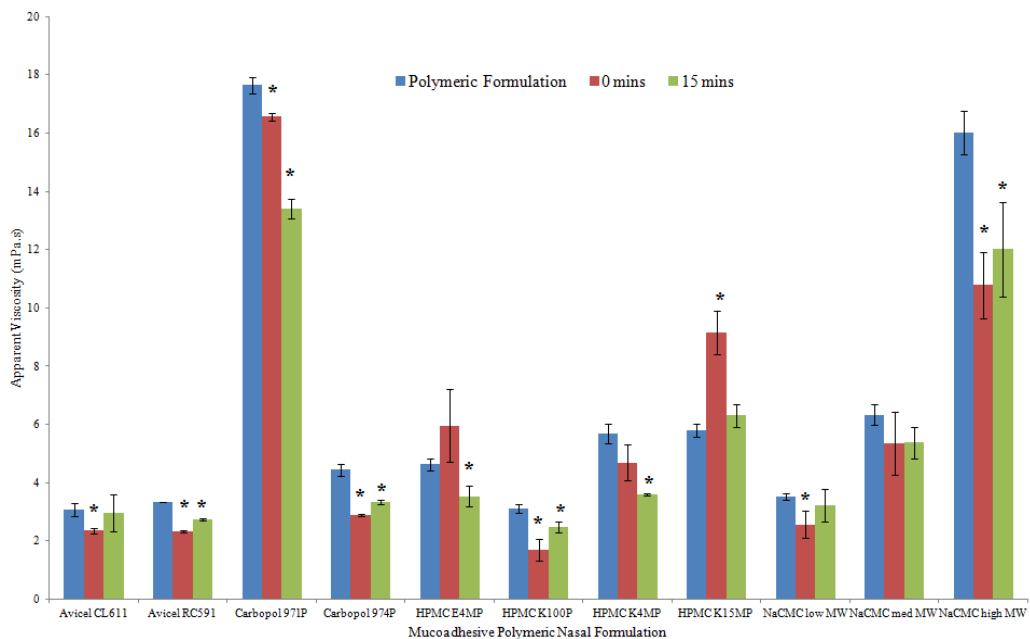


**Figure 5.2** Effect of spray actuation on mean apparent viscosity ( $\pm$  S.D) of 0.2% w/w mucoadhesive polymeric nasal formulations measured at  $1200 \text{ s}^{-1}$ . \*denotes statistical significance to polymeric formulations ( $P < 0.05$ ) ( $n=3$ ).

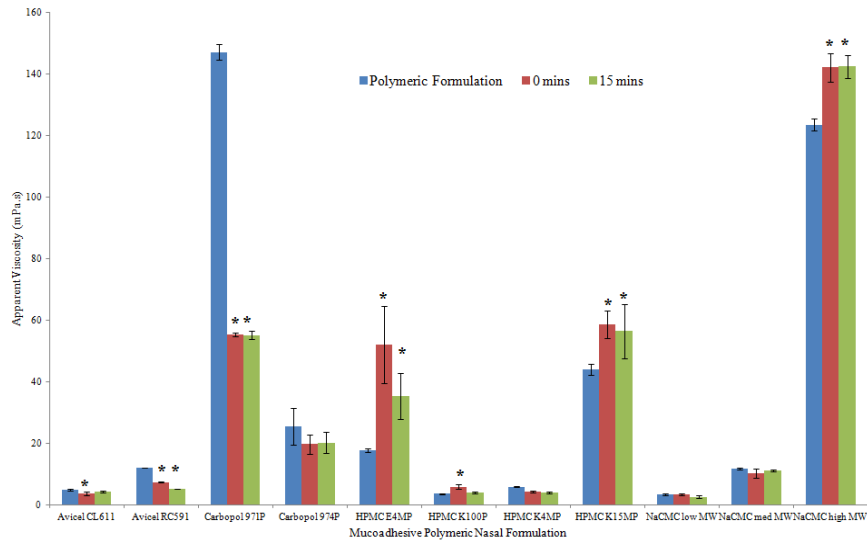


**Figure 5.3** Effect of spray actuation on mean apparent viscosity ( $\pm$  S.D) of 0.5% w/w mucoadhesive polymeric nasal formulations measured at  $100\text{ s}^{-1}$ . \*denotes statistical significance to polymeric formulations ( $P < 0.05$ ) ( $n=3$ ).

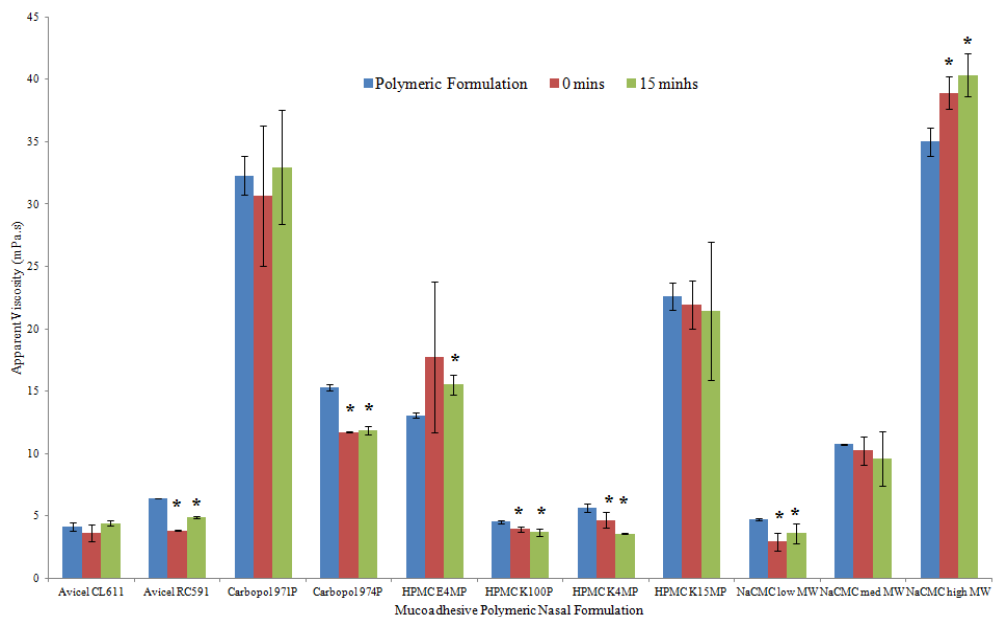


**Figure 5.4** Effect of spray actuation on mean apparent viscosity ( $\pm$  S.D) of 0.5% w/w mucoadhesive polymeric nasal formulations measured at  $1200\text{ s}^{-1}$ . \* denotes statistical significance to polymeric formulations ( $P < 0.05$ ) ( $n=3$ ).

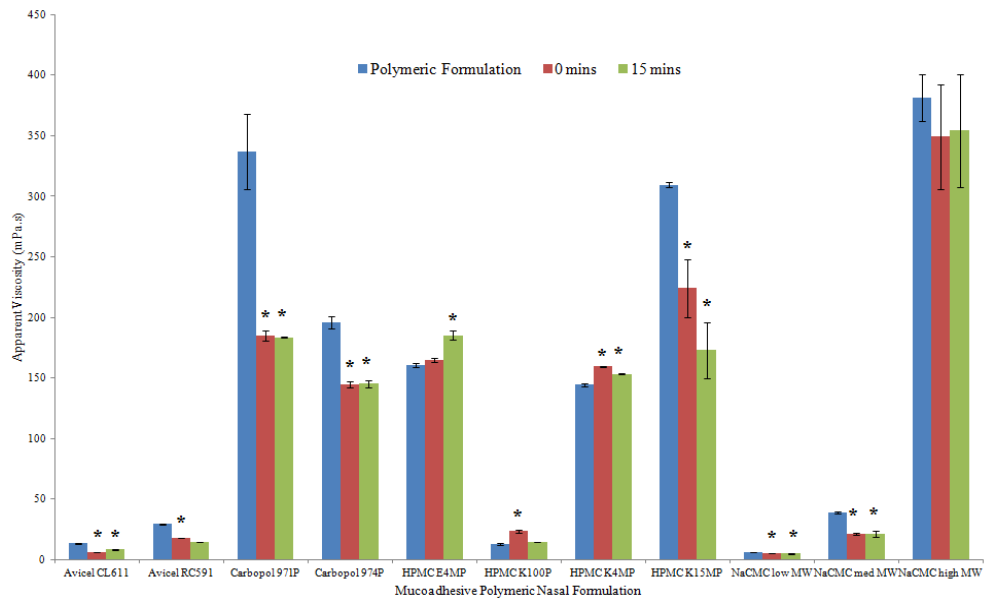


**Figure 5.5** Effect of spray actuation on mean apparent viscosity ( $\pm$  S.D) of 1% w/w mucoadhesive polymeric nasal formulations measured at  $100 \text{ s}^{-1}$ . \*denotes statistical significance to polymeric formulations ( $P < 0.05$ ) (n=3).

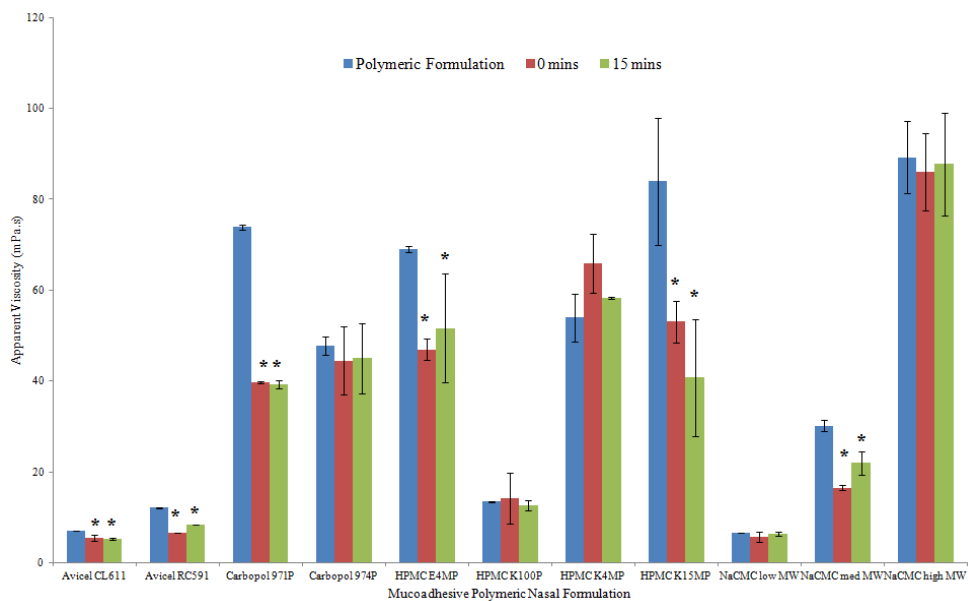


**Figure 5.6** Effect of spray actuation on mean apparent viscosity ( $\pm$  S.D) of 1% w/w mucoadhesive polymeric nasal formulations measured at  $1200 \text{ s}^{-1}$ . \*denotes statistical significance to polymeric formulations ( $P < 0.05$ ) (n=3).

It is evident from the results that the effect of spraying on the apparent viscosities varied amongst the polymers. However, it can be seen that the greatest effects were noticed immediately after spraying.

Avicel CL611 and RC591 are processed blends of MCC and NaCMC and are common excipients used in aqueous suspensions of corticosteroid nasal sprays as a viscosity enhancer (Sharpe et al., 2003). In aqueous colloidal formulations of Avicel, the MCC microcrystals are weakly crosslinked with the NaCMC and the two components of the system work together to bring about a higher viscosity. Avicel CL611 is combined with a higher level of NaCMC than RC591. This makes liberation of the colloidal MCC easier on aqueous dispersions, even at low levels of shear. With the exception of 1% w/w Avicel CL611 measured at  $1200\text{ s}^{-1}$ , the polymer exhibited the same behaviour when exposed to shear. Immediately after spraying the polymer lost magnitude in apparent viscosity and after a period of recovery of 15 minutes the polymer structure began to rebuild and the apparent viscosity increased. The exception to this trend is seen with 1% w/w measured at the high shear rate. In this instance the apparent viscosity of the polymer did not change. Although changes in the apparent viscosity were seen with Avicel CL611, the only significant changes were seen with 0.2% w/w ( $1200\text{ s}^{-1}$ ) immediately after spraying and both measurements of 1% w/w at both recovery time points after spraying. The insignificant changes may be as a result of environmental factors rather than the effects of spray actuation. Like Avicel CL611, RC591 showed similar behaviours throughout the study. Immediately after spraying the recorded apparent viscosity

significantly decreased. This was independent of the concentration of the polymer or the shear rate at which the results were measured. There was some structural rebuild which caused the viscosity to increase slightly but even at 15 minutes after spraying, the apparent viscosity remained significantly reduced compared to the recorded apparent viscosity of the polymeric formulation. This behaviour is as a result of the polymer's shear thinning behaviour. This rheological phenomenon sees the viscosity of a formulation decrease as the magnitude of shear increases. It is shear dependant and a normalised viscosity will return upon the removal of the shear. In the case of both Avicel CL611 and RC591, this shear thinning behaviour occurred when the weak network of MCC and NaCMC is exposed to shear, such as that induced by spray actuation. During the application of shear, the polymer chains are able to unravel and slip past each other and it is this free movement that results in the reduced viscosity. After the shear is removed, the weak, temporary crosslinks reform between the MCC and NaCMC, thus increasing the apparent viscosity (Sharpe *et al.*, 2003).

Carbopol 971P is a high molecular weight, anionic polymer. It is lightly crosslinked and has recently been investigated for its mucoadhesive characteristics (Celli *et al.*, 2007, Boegh *et al.*, 2013). Carbopol polymers are utilised in a vast range of pharmaceutical applications due to advantages including high viscosity at low shear rates and compatibility with many active pharmaceutical ingredients (API) (Khandare and Haag, 2010). Carbopol 971P displayed the same behaviour throughout the study regardless of the shear rate, with the exception of 0.2%

measured at  $100 \text{ s}^{-1}$ . Immediately after spraying, the apparent viscosity of each polymer formulation decreased. Significant reductions in the apparent viscosity were witnessed in the all experimental setups except 0.5% w/w measured at  $1200 \text{ s}^{-1}$ . Fifteen minutes after spraying the polymer's viscosity remained unchanged; however, the apparent viscosity of the four significantly decreased samples remained significantly less than the polymeric formulation's viscosity. 0.2% of the polymer, measured at the low shear rate, exhibited a significant increase in apparent viscosity immediately after spraying. The viscosity remained unchanged after 15 minutes of recovery but it was still significantly larger than the original polymeric formulation apparent viscosity. This increase in the apparent viscosity can be attributed to water loss from the low concentration formulation. The water loss would inevitably increase the polymeric concentration of the system and thus demonstrated the properties of a higher concentrated polymeric formulation. Overall, the polymer displayed an initial large viscosity, owing to the high molecular weight of the polymer, which decreased with spraying. This decrease was significant in all the formulations with the exception of 0.5% w/w measured at  $1200 \text{ s}^{-1}$ . At 15 minutes after spraying insignificant variations were observed. Background noise and structural degradation of the polymer structure may be accountable for these deviations. The apparent viscosity results for Carbopol 971P implied a shear thinning rheological behaviour. This shear thinning was also seen in the study conducted by Bonacucina (Bonacucina *et al.*, 2004).

Carbopol 974P closely resembled the behaviour of Carbopol 971P. All six variations of the polymeric formulation reduced in viscosity immediately after spray actuation.

The apparent viscosity of 0.2% w/w, measured at both 100 and 1200 s<sup>-1</sup>, 0.5% w/w measured at 1200 s<sup>-1</sup> and 1% w/w measured at 100 s<sup>-1</sup> decreased significantly and continued to show a significantly reduced apparent viscosity at 15 minutes post-spray compared with the viscosity of the polymeric formulation. As with Carbopol 971P, the apparent viscosity 15 minutes after the initial spray action remained unchanged. The high molecular weight and increased crosslinks of Carbopol 974P should, in theory, give a viscosity that is greater than the lower crosslinked variant Carbopol 971P. It can be seen from the results that this is not the case and Carbopol 971P has a notably larger viscosity as a polymeric solution and also after spraying. The theory of an increasing viscosity with increasing crosslink density is as a result of intermolecular crosslinking, where a matrix occurs between different polymer molecules. A decrease in viscosity with increasing levels of the number of crosslinks, as is the case with Carbopol 974P, was due to intramolecular crosslinking. This occurs when a single polymer molecule internally interlinks with itself, resulting in a volume contraction of the polymer coil and thus a reduction in the viscosity (Gebben *et al.*, 1985). In this study, it was found that the apparent viscosity of Carbopol 974P decreased after spraying for all concentrations measured at both low and high shear rates (100 and 1200 s<sup>-1</sup>). After 15 minutes of recovery time the viscosity of the polymer remained unchanged for all concentrations at both shear rates. The shear thinning nature can be seen in all polymer concentrations, measured at both 100 s<sup>-1</sup> and 1200 s<sup>-1</sup>. This is in line with the product information data sheet from Lubrizol which stated that the application of shear causes the microgel structure of Carbopol 974P to displace and flow (Lubrizol, 2012).

HPMC is a linear, non-ionic polymer, which has been shown to exhibit a level of mucoadhesivity (Kundu *et al.*, 2008). It is utilised in pharmaceutical applications due to its marked viscoelasticity and its structure building properties. It is added as a suspending and thickening agent or as a stabiliser (Dixit and Puthli, 2009). It has been used in previous studies to manufacture lyophilised nasal inserts for the improved nasal delivery of nicotine (McInnes *et al.*, 2005) and insulin (McInnes *et al.*, 2007). The latter study showed that 2% HPMC did not greatly increase the absorption of insulin but it did enhance the residence time of the nasal insert by 4-5 h. All four HPMC grades used throughout the study elicited different effects of the shear induced by spray actuation.

HPMC E4MP exhibited varying results depending on the concentration that was measured and the shear rate used. There was no significant difference in the apparent viscosity of 0.2% w/w HPMC E4MP. At this concentration the polymer is subject to many environmental effects such as temperature and background noise. These effects can be seen clearly in the large errors present in the results (Figures 6.1 and 6.2). 0.5% and 1% w/w HPMC E4MP provided very interesting apparent viscosity results. At both shear rates the apparent viscosity of 0.5% increased after spraying with a significant increase observed at the lower shear rate for 0.5%. The apparent viscosity of the polymer then decreased towards the original apparent viscosity of the polymeric formulation but the results were still significantly higher. Similar behaviour can be seen for 1% w/w. At  $100\text{ s}^{-1}$ , the polymer increased immediately after spraying and a further significant increase was observed at 15 minutes after spraying. The apparent viscosity of the polymer, measured at  $1200\text{ s}^{-1}$ ,

exhibited a significant reduction immediately after spraying with an increase observed at the 15 minute recovery time. This behaviour is indicative of a shear thickening rheology but it is well established that HPMC is a shear thinning polymer (Lai *et al.*, 2009). The shear thickening anomaly may be attributable to the theory that intramolecular bonding offsets intermolecular bonding (Shaikh *et al.*, 2011). The spray action exposed the polymer to shear and caused the polymer coils to stretch (Tsuneji *et al.*, 1984). This stretching promotes the occurrence of intermolecular interactions and as such the polymeric network is distorted in an uneven manner. The polymer will attempt to correct this and a form of structuring, which is induced by shear, will occur and intramolecular forces will be destroyed in favour of the formations of intermolecular forces. This results in an increase in apparent viscosity (George and Abraham, 2006).

HPMC K100P is the polymer within the investigation with the lowest viscosity and produced a variety of trends when exposed to shear. At 0.2% w/w the polymer exhibited classic shear thinning behaviour. The apparent viscosity of the polymer, measured at both 100 and 1200 s<sup>-1</sup>, reduced immediately after spraying – although this reduction was only statistically significant at the higher shear rate. Fifteen minutes post-spray, the polymer measured at 100 s<sup>-1</sup> did not change and remained at the lower apparent viscosity. The polymer measured at the higher shear rate increased significantly after 15 minutes rest, although the viscosity was still significantly lower than that of the bulk formulation. The results for 0.5% w/w K100P varied depending on the shear rate used to measure the polymer's apparent viscosity. At the lower shear rate, the polymer exhibited a statistically significant

increase in apparent viscosity immediately after spraying. The measured apparent viscosity at 15 minutes after spraying showed a decrease but the viscosity of the formulation was still significantly more viscous at this time point than before spraying. At  $1200\text{ s}^{-1}$  the polymer showed different behaviour. Immediately after spraying, the apparent viscosity decreased significantly before decreasing further after a recovery time of 15 minutes. A further variation in behaviour was observed with the higher concentration of HPMC K100P. At the lower shear rate the apparent viscosity significantly increased immediately after spray actuation. This was followed by a significant decrease in apparent viscosity at 15 minutes post spray. At  $1200\text{ s}^{-1}$ , the polymer showed no change in viscosity due to the action of shearing brought on by spraying. The results for the low viscosity polymer K100P were varied and no trend can be identified. This difference in results may be as a result of solvent dehydration or background noise.

HPMC K4MP is a variant of HPMC E4MP with the difference between the two HPMC grades being the degree of substituent groups on the anhydroglucose units of the cellulose (Yu *et al.*, 2004). At 0.2% w/w, the polymer behaved in the same manner regardless of the shear rate. Immediately after spraying the apparent viscosity of the formulation decreased. This decrease was significant for the apparent viscosity measurement at  $100\text{ s}^{-1}$ . The sprayed formulation was allowed to rest for 15 minutes after which the apparent viscosity was measured again. It was found that after this recovery time, the apparent viscosity decreased further. This final apparent viscosity was significantly lower than the apparent viscosity of the polymeric formulation before spraying, at both  $100$  and  $1200\text{ s}^{-1}$ . Both 0.5 and 1%

w/w concentrations of HPMC K4MP, measured at low and high shear rates, exhibited an increase in apparent viscosity immediately after spraying. The increase noted for the 0.5% w/w concentration, measured at  $1200\text{ s}^{-1}$  and 1% w/w measured at  $100\text{ s}^{-1}$  were statistically significant. After a recovery time of 15 minutes the trend of apparent viscosity altered for each concentration at both 100 and  $1200\text{ s}^{-1}$ . At lower shear rates, the viscosity decreased, but not significantly, for all the polymers with the exception of 0.5% w/w HPMC K4MP measured at  $100\text{ s}^{-1}$ , which showed a slight, insignificant increase in viscosity. As well as the reasons discussed earlier, another reason for the difference in results may be down to the actuation technique. Guo and Doub (2006) found that the forces applied during manual actuation are dependent on the operator and could lead to lower reproducibility of results (Guo and Doub, 2006). These researchers employed techniques to elucidate any errors by eliminating manual actuations. The HPMC polymer formulation, measured at a high shear rate of  $1200\text{ s}^{-1}$ , exhibited an initial shear thinning behaviour before spraying. This behaviour was as a result of strong hydrogen bonding between HPMC and water molecules, which resulted in the formation of aggregates of the molecules at microscopic level (Ferdous, 1992). The subsequent decrease in apparent viscosity owes to the breakdown of these aggregates and a decrease in the extent of molecular gathering (Ferdous, 1992).

HPMC K15MP is another grade of HPMC which boasts a high apparent viscosity. The apparent viscosity of the 2% w/w formulation of HPMC K15MP exhibited the same rheological behaviours at both 100 and  $1200\text{ s}^{-1}$ . Immediately after spraying, the apparent viscosity of the polymer significantly reduced, which is indicative of the

shear thinning nature of HPMC K15MP where the viscosity reduced with the application of shear. At 15 minutes after spraying, the apparent viscosity decreased further to a level that was significantly lower than the original viscosity prior to spraying. The results obtained for 0.5% w/w were varied with the shear rate. The lower shear rate saw the apparent viscosity of the polymer significantly increase after undergoing spray actuation. This increased viscosity then begins to reduce after the shear is removed and at 15 minutes post spray the polymer structure has started to recover and the apparent viscosity has reduced back towards the initial polymeric formulation. However, at 15 minutes after spraying the polymer has not recovered fully and the apparent viscosity is still significantly higher than the formulation prior to spray actuation. The apparent viscosity of the 0.5% w/w polymer, when measured at  $1200 \text{ s}^{-1}$ , was not affected by the action of spraying. 1% w/w HPMC K15MP provided the same results at both shear rates and the shear thinning behaviour can be seen in the apparent viscosity results before and after spraying. A significant reduction in viscosity was observed immediately after spraying with a further reduction recorded at the 15 minute recovery time. Shear thinning behaviour is regarded as a general loss of consistency, or viscosity, as the magnitude of shear increases (Jones *et al.*, 1997) and is independent of time. This means that the removal of shear should, in theory, have ceased the further reduction in apparent viscosity exhibited by the polymer at the higher shear rate. As such, it would seem that some form of time dependant rheological behaviour has occurred. In order to verify this, the rheological profile will have to be examined further.

NaCMC has been explored as an aid to mucoadhesion since the early 1980's (Roy *et al.*, 2009) and continues to be studied alongside other mucoadhesives as a means of increasing the residence time of the dosage form within the nasal cavity. It can be seen from the apparent viscosity data that there were notable differences in the effect of shearing on the three molecular weight variants and all three concentrations of the NaCMC polymers. NaCMC low MW behaved in a similar way when measured at both low and high shear rates. The apparent viscosity immediately after spraying for all three concentrations, measured at  $100\text{ s}^{-1}$ , decreased and no further change was observed after 15 minutes. Although an initial change in viscosity was noted, the only significant difference was with the 1% w/w concentration. Concentrating on the results achieved at the higher shear rate, the apparent viscosity recorded immediately after spraying decreased, with this decrease significant for 0.2 and 0.5% w/w. The apparent viscosity for all three concentrations then proceeded to recover and an increase was observed at 15 minutes after spray actuation.

The three concentrations of NaCMC medium MW reacted the same regardless of the shear rate used for analysis. The only exception to this was 1% w/w measured at  $1200\text{ s}^{-1}$ . All polymers exhibited loss in apparent viscosity when measured immediately after spraying with no further change in viscosity recorded after recovery. 1% NaCMC medium MW, measured at a high shear rate, diverged from this trend and although it showed an initial decrease in apparent viscosity after spraying, the recovery time encouraged the structure to rebuild and a significant increase in the viscosity was seen at 15 minutes post spray.

NaCMC high MW provided varied results within the three concentrations. At 0.2% and 1% w/w the apparent viscosity of the polymer formulation decreased immediately after spraying before a structural recovery occurred and a significant increased viscosity resulted. This was the same for measurements taken at both shear rates. At both 100 and 1200 s<sup>-1</sup>, the apparent viscosity of 0.5% w/w significantly increased after spraying but no further change was detected after the polymer was allowed to recover for 15 minutes, although the viscosity at this timepoint continued to be significantly larger than the viscosity of the polymeric formulation prior to spraying. The increase in viscosity of NaCMC high MW immediately after spraying, which is linked with shear thickening behaviour, could be as a result of intramolecular crosslinking as seen in Carbopol 974P. It may also be due to the recoiling of the polymer macromolecular crystallites, which are formed due to NaCMC molecular chain scission (Jayabalan, 1989). This recoiling of the polymer crystallites results in an increased viscosity.

Another method of assessing the effect of spray on the polymeric formulations is to study their corresponding rheological flow profiles obtained from the rheometer. Figures 6.7 to 6.17 show the rheological flow profiles obtained for all 11 polymers at both 100 and 1200 s<sup>-1</sup>. The rheological profiles can indicate whether the polymer is shear thinning or shear thickening and if it is thixotropic. The gradient of the line is also an indicator of the viscosity of the polymer with the gradient increasing with increasing viscosity.

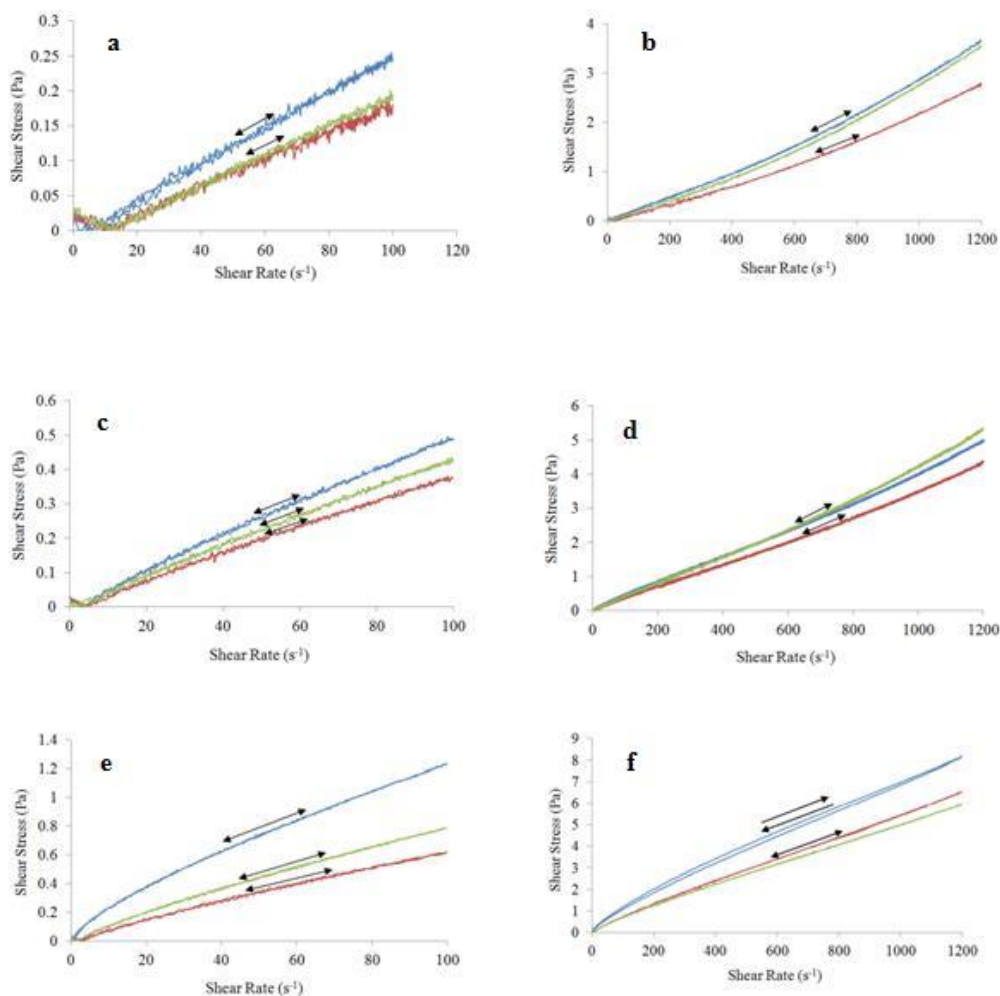


**Figure 5.7** Rheological flow profiles of Avicel CL611 before spraying (blue), immediately after spraying (red) and 15 minutes after spraying (green). Profiles are representative of 0.2% w/w measured at  $100 \text{ s}^{-1}$  (a) and  $1200 \text{ s}^{-1}$  (b), 0.5% w/w measured at  $100 \text{ s}^{-1}$  (c) and  $1200 \text{ s}^{-1}$  (d) and 1% w/w measured at  $100 \text{ s}^{-1}$  (e) and  $1200 \text{ s}^{-1}$  (f).

All six rheological profiles for Avicel CL611 indicated that the polymer was shear thinning before and after spraying, with the exception of 0.2% and 0.5% w/w measured at the high shear rate that indicated a slight shear thickening behaviour. There was a small level of thixotropy evident in the profile displayed for the polymeric formulation of 1% w/w measured at  $1200 \text{ s}^{-1}$ . The flow profile for Avicel

CL611 immediately after spraying reverted back to a simple shear thinning profile and therefore the short instance of thixotropy may be as a result of shear history. It is widely known that thixotropic nature is dependent on shear history (Lee *et al.*, 2009) and as the hysteresis loop, synonymous with thixotropy, is only apparent in one profile it would lead to the conclusion that the sample had a different shear history to the other samples of Avicel CL611 tested.

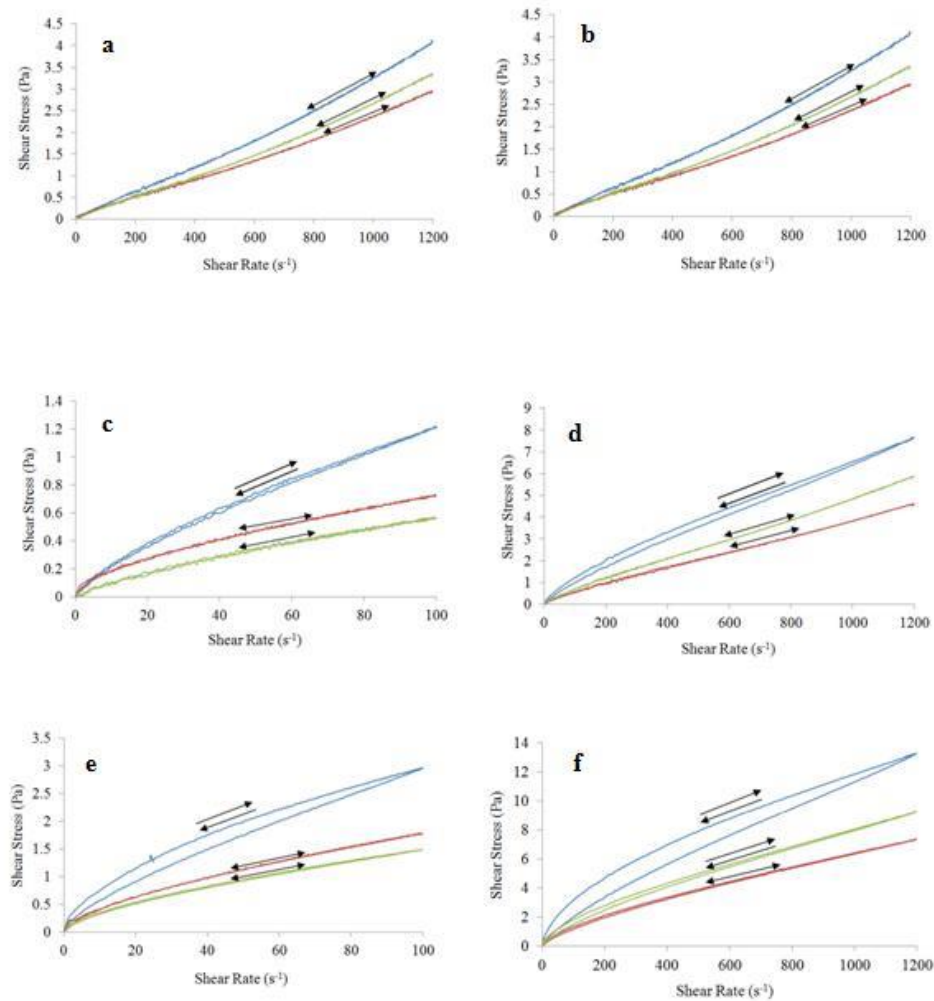


**Figure 5.8** Rheological flow profiles of Avicel RC591 before spraying (blue), immediately after spraying (red) and 15 minutes after spraying (green). Profiles are representative of 0.2% w/w measured at 100 s<sup>-1</sup> (a) and 1200 s<sup>-1</sup> (b), 0.5% w/w measured at 100 s<sup>-1</sup> (c) and 1200 s<sup>-1</sup> (d) and 1% w/w measured at 100 s<sup>-1</sup> (e) and 1200 s<sup>-1</sup> (f).

Figure 6.8 illustrates the flow profiles of Avicel RC591. It can be seen from the rheograms that Avicel RC591 showed a predominantly shear thinning behaviour. The 0.2% w/w formulation exhibited shear thickening behaviour but this can be attributed to inertial effects due to the low viscosity of the polymer. 0.2% w/w Avicel RC591 measured at both shear rates showed a small level of thixotropy in the

formulation prior to spraying but this was not evident after spraying. The same phenomenon was seen with the 1% w/w concentration of the polymer but in this instance the thixotropy is more pronounced. The lack of thixotropic evidence immediately after spraying from both 0.5 and 1% w/w Avicel RC591 could be as a result of the breaking of the weak crosslinks of MCC and NaCMC within the polymer. The action of spraying will have impacted on the structure causing the entangled structure to become loose and thus affecting the thixotropic properties of the formulation.

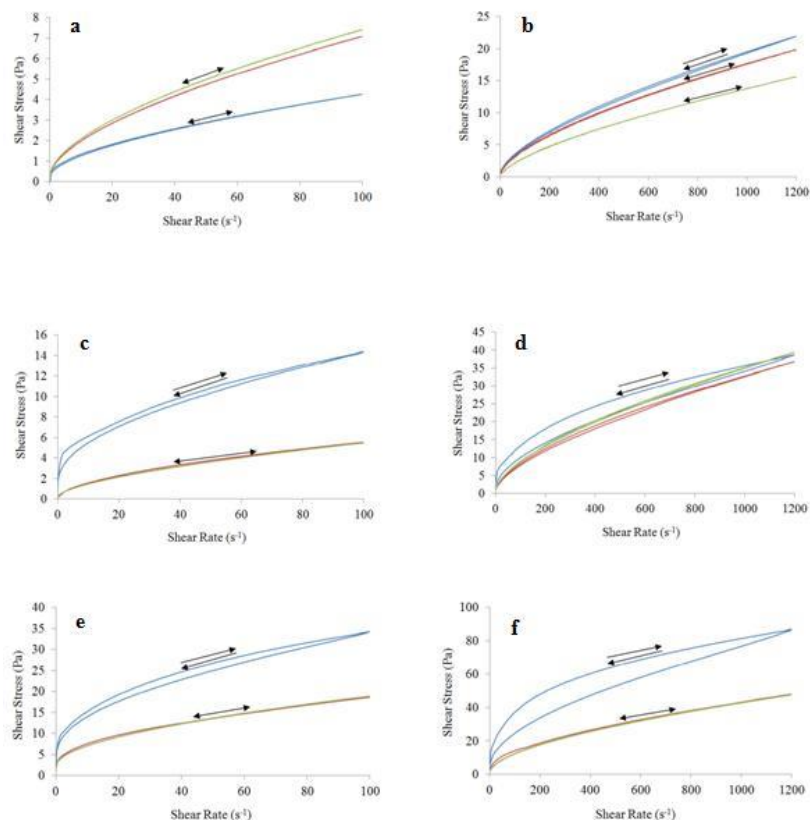


**Figure 5.9** Rheological flow profiles of Carbopol 971P before spraying (blue), immediately after spraying (red) and 15 minutes after spraying (green). Profiles are representative of 0.2% w/w measured at  $100 \text{ s}^{-1}$  (a) and  $1200 \text{ s}^{-1}$  (b), 0.5% w/w measured at  $100 \text{ s}^{-1}$  (c) and  $1200 \text{ s}^{-1}$  (d) and 1% w/w measured at  $100 \text{ s}^{-1}$  (e) and  $1200 \text{ s}^{-1}$  (f).

Like Avicel, Carbopol 971P exhibited features of a shear thinning polymer both before and after spraying. The lower concentration showed no thixotropy throughout the experiment but a varying degree of thixotropy can be seen for 0.5 and 1% w/w Carbopol 971P measured at both shear rates. After spraying, the thixotropic nature of the polymeric formulations was not evident and instead the polymer exhibited the behaviour of simple shear thinning polymer. This shift in rheological behaviour could be attributed to crosslinking of the Carbopol structure. The increased

entanglement caused by the crosslinking is changed by the imposed shear and the molecules will become separated. This will have a resulting effect on the rheological flow properties of the polymer.

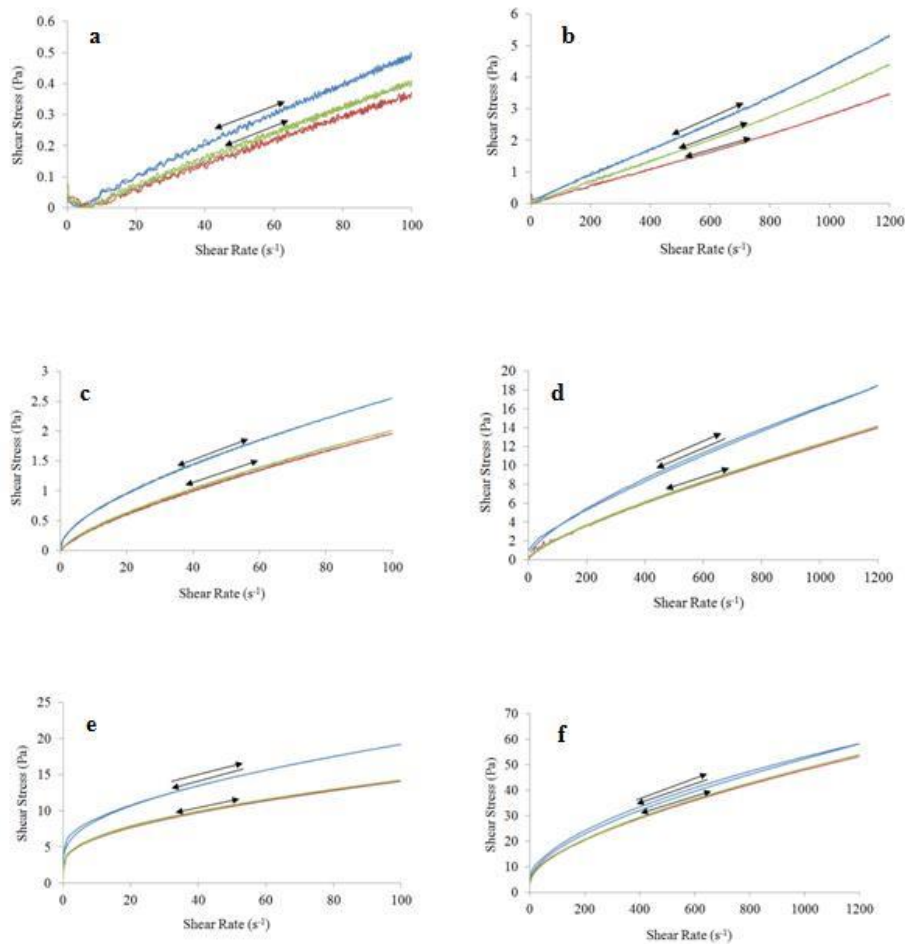


**Figure 5.10** Rheological flow profiles of Carbopol 974P before spraying (blue), immediately after spraying (red) and 15 minutes after spraying (green). Profiles are representative of 0.2% w/w measured at  $100 \text{ s}^{-1}$  (a) and  $1200 \text{ s}^{-1}$  (b), 0.5% w/w measured at  $100 \text{ s}^{-1}$  (c) and  $1200 \text{ s}^{-1}$  (d) and 1% w/w measured at  $100 \text{ s}^{-1}$  (e) and  $1200 \text{ s}^{-1}$  (f).

The rheograms for Carbopol 974P (Figure 6.10) showed a predominant shear thinning nature with no significant thixotropy. 0.2% w/w measured at  $1200 \text{ s}^{-1}$

exhibited a slight shear thickening behaviour, seen in the shape of the rheogram, but the apparent viscosity results are indicative of a shear thinning nature and this anomaly will be due to an error such as sample dehydration during analysis.

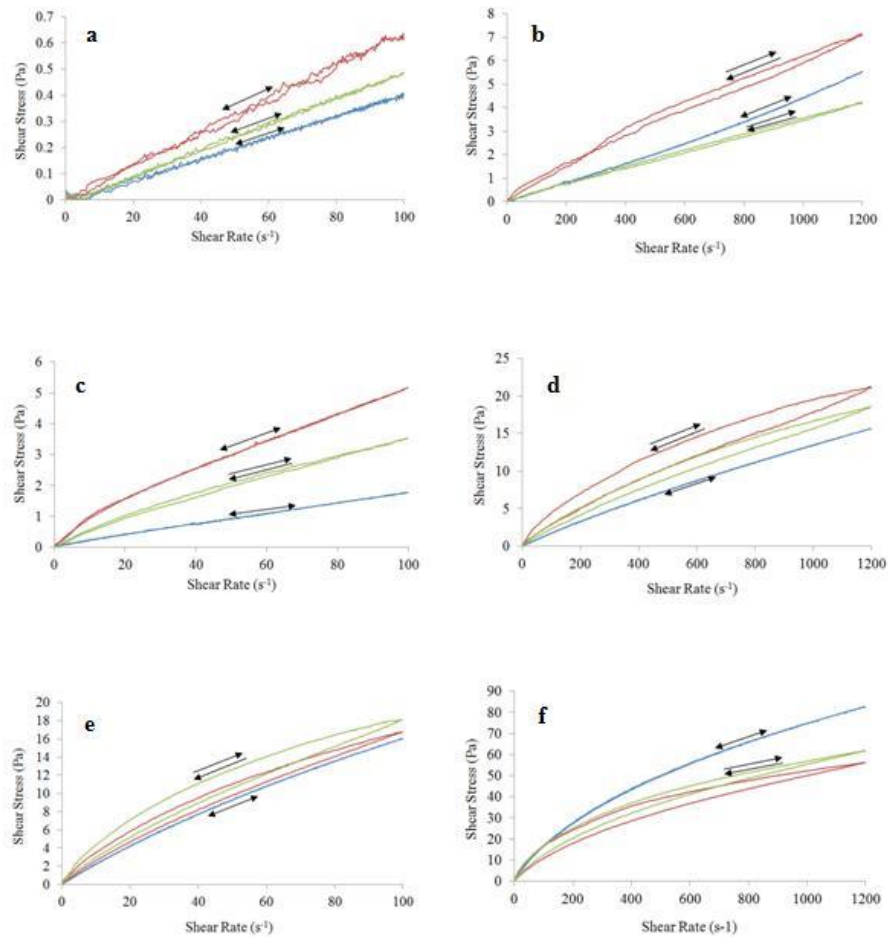


**Figure 5.11** Rheological flow profiles of HPMC E4MP before spraying (blue), immediately after spraying (red) and 15 minutes after spraying (green). Profiles are representative of 0.2% w/w measured at  $100 \text{ s}^{-1}$  (a) and  $1200 \text{ s}^{-1}$  (b), 0.5% w/w measured at  $100 \text{ s}^{-1}$  (c) and  $1200 \text{ s}^{-1}$  (d) and 1% w/w measured at  $100 \text{ s}^{-1}$  (e) and  $1200 \text{ s}^{-1}$  (f).

HPMC is classified as a shear thinning polymer but the apparent viscosity results signified that the polymer is shear thickening. This shear thickening indication may, again, be as a result of sample dehydration or degradation of the polymer structure as the rheograms themselves indicated the polymer is shear thinning. This was evident in the direction of the rheograms, represented by the arrows. The formulations before spraying, for all concentrations at both shear rates, showed a simple shear thinning behaviour. For all polymers, with the exception of 0.5% w/w measured at  $100 \text{ s}^{-1}$ , the rheogram exhibited a shear thinning, thixotropic nature immediately after spraying. The thixotropy was not witnessed again in the 0.2% w/w concentration and the rheological behaviour reverted back to a simple shear thinning polymer. 0.5% w/w, measured at  $100 \text{ s}^{-1}$ , continued to show simple shear thinning behaviour with any amount of thixotropy being as a result of back ground noise. 1% w/w, measured at both shear rates continued to exhibit shear thinning, thixotropic behaviour even at 15 minutes after spraying. The thixotropic behaviour was attributed to the polymeric molecular aggregates breaking down (Ferdous, 1992), as would be seen in shear thinning behaviour. However, the removal of the shear did not allow the relaxed polymer structure to reform within the time frame of the experiment. The main reason for this behaviour is the competition between the detachment of the entangled chains and the re-establishment of the chain interactions by Brownian motion.

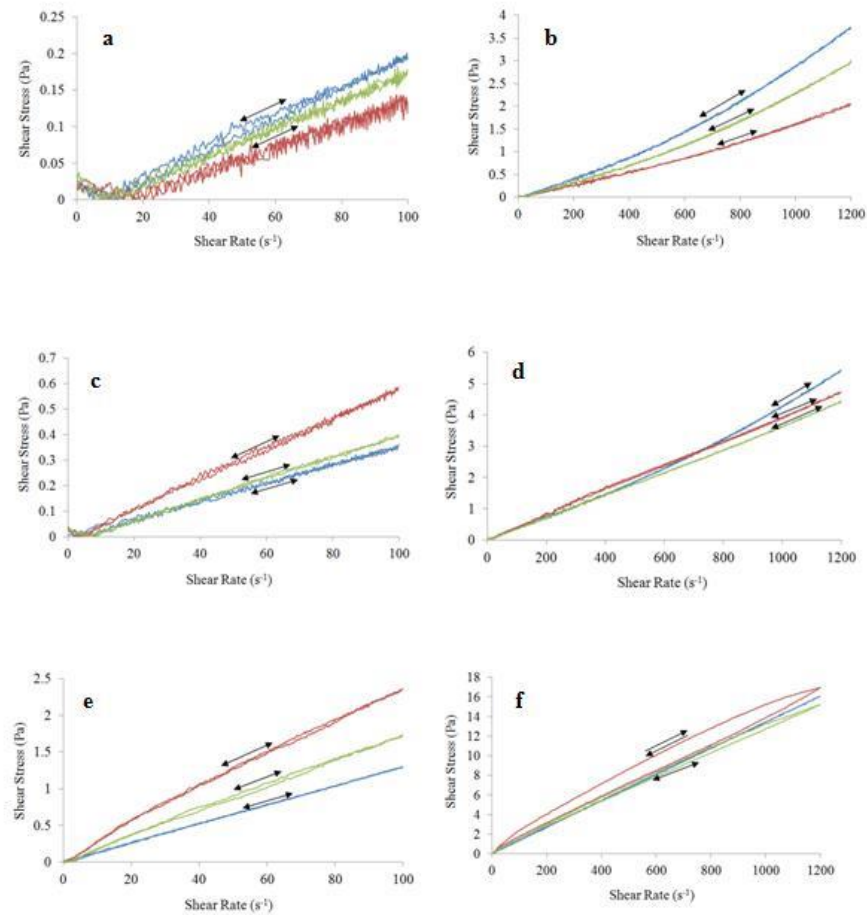


**Figure 5.12** Rheological flow profiles of HPMC K100P before spraying (blue), immediately after spraying (red) and 15 minutes after spraying (green). Profiles are representative of 0.2% w/w measured at 100  $s^{-1}$  (a) and 1200  $s^{-1}$  (b), 0.5% w/w measured at 100  $s^{-1}$  (c) and 1200  $s^{-1}$  (d) and 1% w/w measured at 100  $s^{-1}$  (e) and 1200  $s^{-1}$  (f).

The rheograms for HPMC K100P (Figure 6.12) provided rheograms as expected. Each rheogram produced flow behaviours indicative of simple shear thinning materials. There was evidence of thixotropy in the rheogram for 1% w/w measured at 1200  $s^{-1}$ , immediately after spraying, but due to the low viscosity of the polymer, this has been attributed to dehydration of the aqueous medium of the polymer during sample analysis.

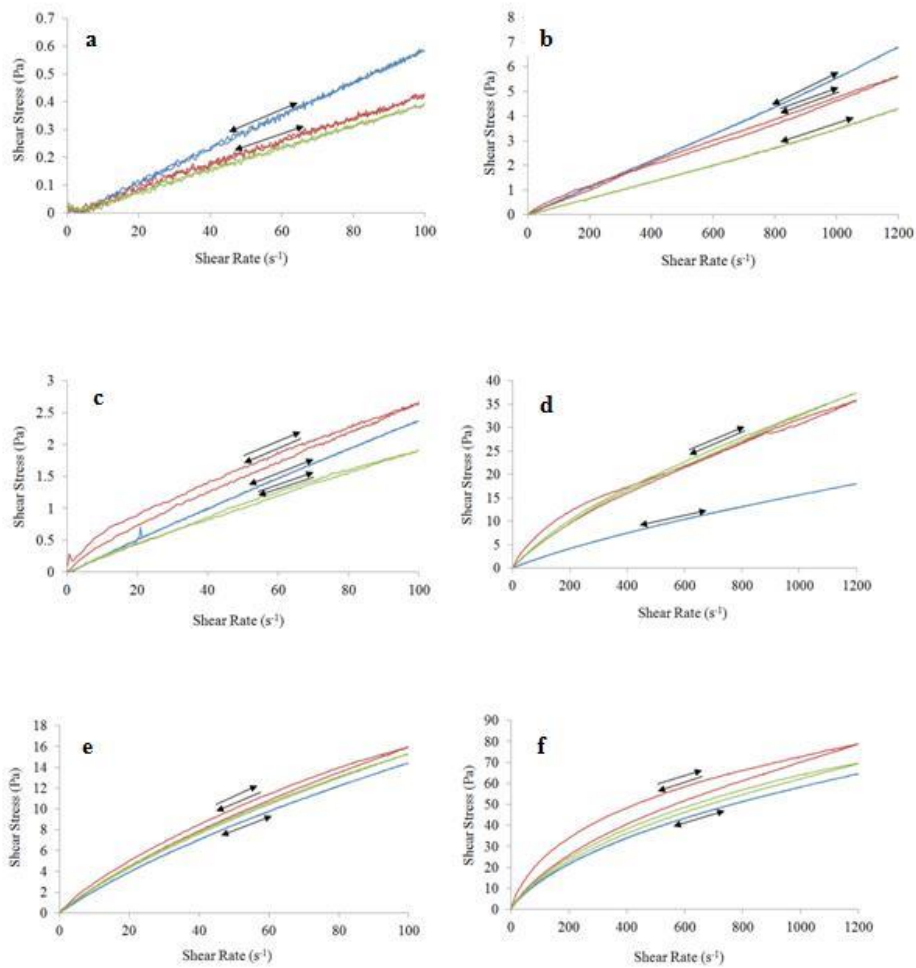


**Figure 5.13** Rheological flow profiles of HPMC K4MP before spraying (blue), immediately after spraying (red) and 15 minutes after spraying (green). Profiles are representative of 0.2% w/w measured at  $100 \text{ s}^{-1}$  (a) and  $1200 \text{ s}^{-1}$  (b), 0.5% w/w measured at  $100 \text{ s}^{-1}$  (c) and  $1200 \text{ s}^{-1}$  (d) and 1% w/w measured at  $100 \text{ s}^{-1}$  (e) and  $1200 \text{ s}^{-1}$  (f).

At the lowest concentration (0.2% w/w), HPMC K4MP showed shear thinning behaviour with no thixotropy. Both 0.5 and 1% w/w showed similar rheological behaviour regardless of the shear rate used. The rheological behaviour altered from a simple shear thinning polymer to a shear thinning and thixotropic polymer, immediately after spraying. The level of thixotropy is less pronounced for 0.5% w/w

polymers. At 15 minutes post-spray, the level of thixotropy decreased for both concentrations, with the 0.5% w/w concentration showing no thixotropy at this time point. Again shear thickening behaviour was recorded for the apparent viscosity results but the direction of the rheograms indicated that HPMC K4MP was a shear thinning polymer.

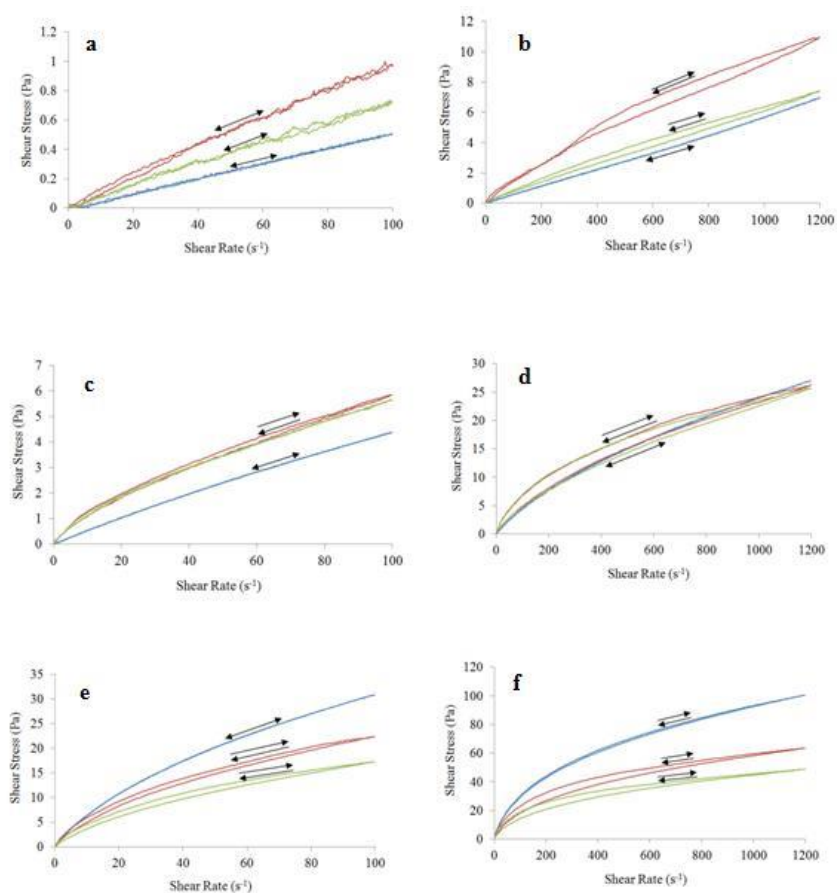


**Figure 5.14** Rheological flow profiles of HPMC K15MP before spraying (blue), immediately after spraying (red) and 15 minutes after spraying (green). Profiles are representative of 0.2% w/w measured at  $100\text{ s}^{-1}$  (a) and  $1200\text{ s}^{-1}$  (b), 0.5% w/w measured at  $100\text{ s}^{-1}$  (c) and  $1200\text{ s}^{-1}$  (d) and 1% w/w measured at  $100\text{ s}^{-1}$  (e) and  $1200\text{ s}^{-1}$  (f).

HPMC K15MP showed relatively simple flow curves for both shear rates used. The main rheological behaviour seen was that of a shear thinning polymer. The polymeric formulation prior to spraying did not show any thixotropic nature. Immediately after spraying, thixotropy could be seen in the flow curves for the higher concentrations at both shear rates. The level of thixotropy was more pronounced in the rheograms produced at a maximum shear rate of  $1200 \text{ s}^{-1}$ . This indicated that the higher shear rate has caused a greater degree of deformation within the structure of the polymer. At 15 minutes post-spray the level of thixotropy reduced completely in the 0.5% w/w concentration and the polymer retained the shear thinning behaviour of the polymeric formulation. The higher concentration remained to show thixotropic behaviour after a recovery time of 15 minutes implying that the structure within the high concentration polymer was taking longer to repair than the lower concentration polymers.

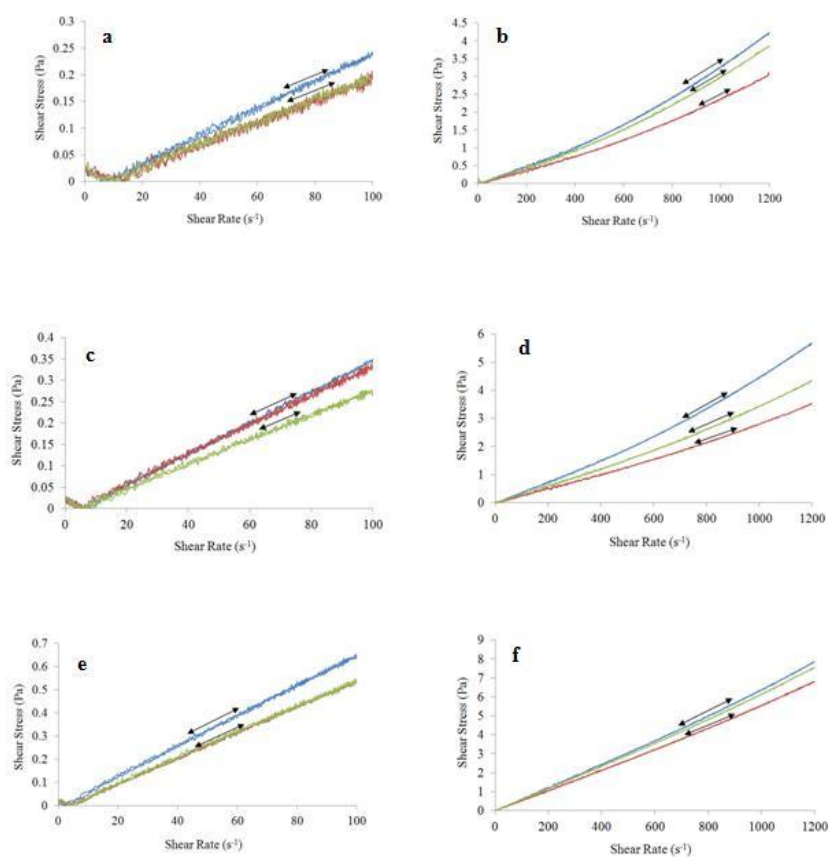


**Figure 5.15** Rheological flow profiles of NaCMC low MW before spraying (blue), immediately after spraying (red) and 15 minutes after spraying (green). Profiles are representative of 0.2% w/w measured at 100 s<sup>-1</sup> (a) and 1200 s<sup>-1</sup> (b), 0.5% w/w measured at 100 s<sup>-1</sup> (c) and 1200 s<sup>-1</sup> (d) and 1% w/w measured at 100 s<sup>-1</sup> (e) and 1200 s<sup>-1</sup> (f).

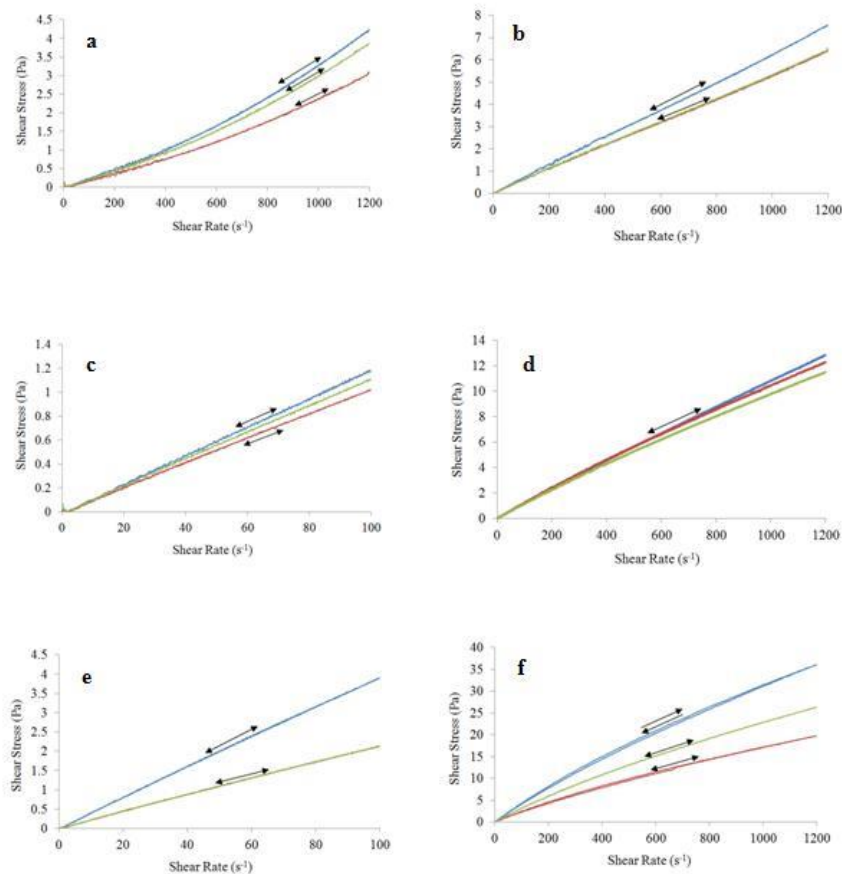


**Figure 5.16** Rheological flow profiles of NaCMC med MW before spraying (blue), immediately after spraying (red) and 15 minutes after spraying (green). Profiles are representative of 0.2% w/w measured at 100 s<sup>-1</sup> (a) and 1200 s<sup>-1</sup> (b), 0.5% w/w measured at 100 s<sup>-1</sup> (c) and 1200s<sup>-1</sup> (d) and 1% w/w measured at 100 s<sup>-1</sup> (e) and 1200 s<sup>-1</sup> (f).

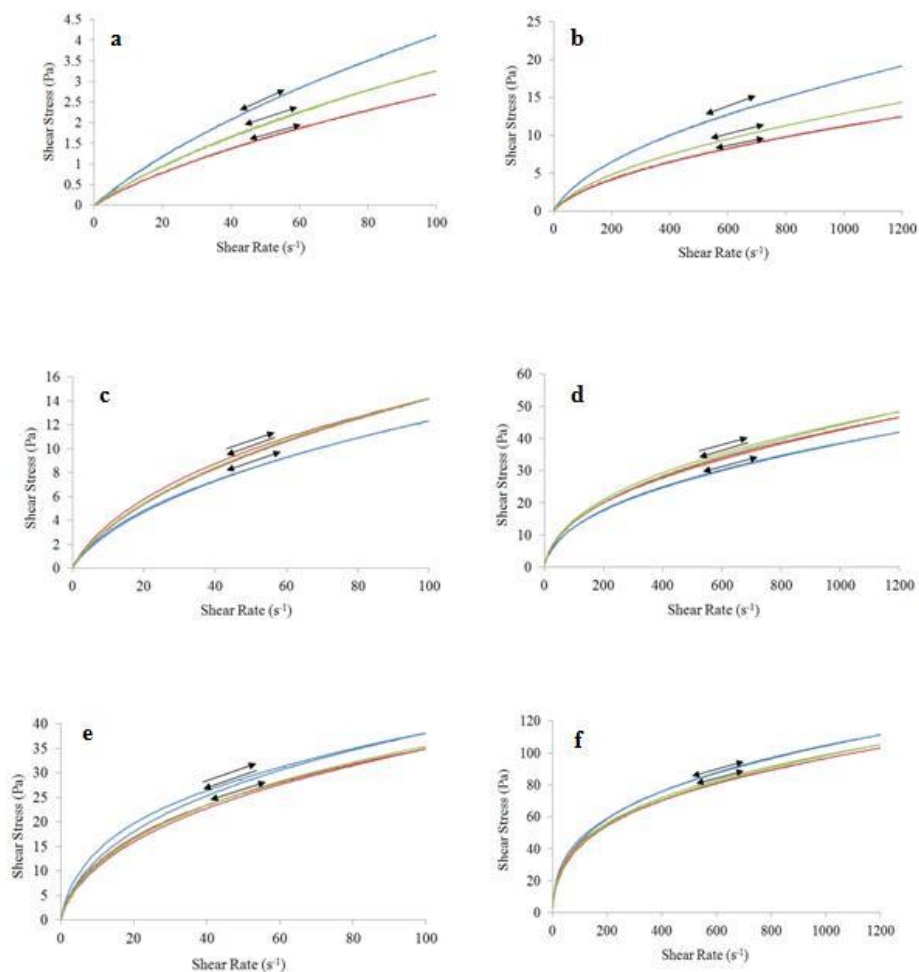


**Figure 5.17** Rheological flow profiles of NaCMC high MW before spraying (blue), immediately after spraying (red) and 15 minutes after spraying (green). Profiles are representative of 0.2% w/w measured at  $100\text{ s}^{-1}$  (a) and  $1200\text{ s}^{-1}$  (b), 0.5% w/w measured at  $100\text{ s}^{-1}$  (c) and  $1200\text{ s}^{-1}$  (d) and 1% w/w measured at  $100\text{ s}^{-1}$  (e) and  $1200\text{ s}^{-1}$  (f).

The rheological flow curves for NaCMC low MW, NaCMC med MW and NaCMC high MW are shown in Figures 5.15 to 5.17, respectively. There was no difference observed among the three molecular weight variants of NaCMC. The behaviour was also independent of concentration and applied shear rate. Each rheogram indicated that NaCMC was a simple shear thinning polymer with no thixotropy.

It was noted that at both low and high shear rates, the apparent viscosity of all polymers increased with increasing polymer concentration. This was due to the macromolecule entanglement phenomena (Talukdar *et al.*, 1996), which states that higher polymer concentrations increase the entanglement density and thus increase the viscosity as a consequence. It was also seen that increasing the maximum shear rate from  $100 \text{ s}^{-1}$  to  $1200 \text{ s}^{-1}$  had the opposite effect and reduced the apparent viscosity of the polymer solutions. This behaviour was due to the shear thinning nature of the polymers. From the overall viscosity data achieved at  $100 \text{ s}^{-1}$  and  $1200 \text{ s}^{-1}$ , it was evident that as a polymeric formulation and after spraying, NaCMC high MW and Carbopol 971P provided the highest apparent viscosities both before and after spraying. The lack of obvious thixotropy in these high viscosity samples would allude to the theory that thixotropy is not the deciding factor when dealing with nasal sprays and that viscosity is what is important to enhance the residence time of the formulation within the nasal cavity.

## **5.6 Conclusion**

In this study the effects of spraying on the rheological flow behaviour of eleven mucoadhesive polymer dispersions commonly used in intranasal formulations were examined. It has been hypothesised that increasing the residence time of the formulation on the nasal mucosa may have a desired effect on the rate of absorption of drugs across the epithelium (Illum, 2006, Meltzer, 2011). In this study the apparent viscosities and rheological flow behaviour before and after spraying were

determined for each of the polymeric formulations at varying concentrations and at low and high shear rates. The results have given an idea of the effects of spray device actuation on the polymeric properties of polymer formulations and any implication this may have for increased residence time within the nasal cavity.

It can be seen from this chapter that the rheometer is an accurate method to measure the effects of spray actuation of both low and high viscosity polymeric nasal formulation. The results show that all polymeric formulations are affected in some way by the enormous shear imposed on them by the action of spraying and that their rheological properties within the nasal cavity, after spraying, are very different to the properties recorded prior to spraying. The recovery time varied within the polymers measured but it can be seen that even at 15 minutes after spraying, some of the polymers did not fully recover back to their original viscosity. This could pose a problem for ensuring the formulation is maintained at the site of application long enough to allow for full absorption of the drug into the circulatory system. The method and results can be validated further by utilising the same experimental idea with other techniques such as texture analysis and atomic force microscopy (AFM).

## Chapter 6 Summary and future work

In this study the mucoadhesive properties of polymeric formulations were examined in order to assess their performance in nasal dosage forms. The study also sought to define the critical components of the system in order to achieve optimum mucoadhesive efficacy. There are many reports of work investigating the use of absorption or penetration enhancers to improve the performance of nasally delivered drugs (Bae and Lee, 2013, Na *et al.*, 2013) but due to the potential for mucosal disruption, this line of work was not considered. Instead, a number of polymeric formulations were chosen for their range of desirable characteristics, including viscosity, hydrogen bonding groups, crosslinking, and charge, and their potential as a component of a mucoadhesive drug delivery device was assessed using a variety of techniques.

In the early stages, the development of a texture analysis technique for the purpose of quantification of mucoadhesive strength, was achieved and enabled the assessment of the mucoadhesive bond that formed between the formulations and excised porcine tissue. The relative low viscosity of the formulations meant that a gel adhesive probe could not be utilised and the formulation could not be loaded onto the nasal tissue as would occur *in-vivo*. An inverted system was designed which saw the mucosal tissue attached to the probe and lowered onto the polymeric formulations. Overall, molecular weight, concentration, viscosity and charge all positively impacted on the adhesive strength of the formulation. High molecular weight NaCMC at 2% w/w, an

anionic, high molecular weight polymer, exhibited the highest force of detachment and work of adhesion compared with the other formulations. All formulations showed an increase in mucoadhesive strength with increasing concentration and thus viscosity which suggested that the opportunity for interaction between the polymeric chains and mucin chains is greater as the concentration is increased. An increased crosslinking density was found to have a detrimental effect on the mucoadhesive strength of high molecular weight Carbopol 974P which implied that the crosslinking may have shielded the hydrogen bonding groups of the polymer. Although the results were reproducible, errors were found due to the diversity of the excised tissue. Work has been carried out by a number of authors using a variety of different mucosal substrates including mucin discs (Carvalho *et al.*, 2013) and mucosal epithelium models (Jackson *et al.*, 2013). These substrates would reduce the variations on results caused by natural mucosal differences, including epithelial thickness, found in animal models. Future work could see the texture analysis technique modified. A nasal model, using EpiAirway tissue could be built which would incorporate a mucociliary clearance and an environment which mimics the nasal cavity. This would ensure a testing environment similar to that found *in-situ* resulting in more *in-vivo* relevant results. The texture analysis assessment concentrated on the adhesive nature of the polymeric formulations but future work should also look into how cohesive they are too. A cohesive formulation will result in large droplet sizes and this stringing of the formulation will occur, factors not desirable for effective delivery via a spray device. Formulators are currently looking at means of reducing the cohesiveness of their products in order to achieve an efficient delivery device (Boraey *et al.*, 2013) and future investigations using the

texture analyser should follow suit and determine the cohesive nature of the formulations. Another factor that would need to be analysed is the droplet size and spray pattern achieved by spraying the nasal formulations. The cohesiveness of the formulations will ultimately affect this and further work has already been done looking into the effects of patient use, which found a difference in droplet size depending on the method used to spray the formulation (Doughty *et al.*, 2013).

A large proportion of this thesis centred on the rheological analysis of the polymeric formulations. This work assessed the structural properties of the nasal sprays and provided vital information including viscosity, flow behaviour and viscoelasticity. In the initial development of this work, challenges arose due to the limitations of the instrument but valuable results were achieved nonetheless. It was decided that flow experiments would be carried out at a high ( $1200 \text{ s}^{-1}$ ) and low ( $100 \text{ s}^{-1}$ ) shear rates to study the effects of both levels of shear on the nasal formulations. In general, the apparent viscosity of all polymers increased with increasing polymeric concentration and decreased as a result of applied shear. The greatest apparent viscosity was seen with the negatively charged polymers; high molecular weight NaCMC (1% w/w) and Carbopol 971P (1% w/w), which was also lightly crosslinked. From the literature, thixotropy was identified as a desirable property in nasal spray formulations and as such, a decision was made to assess the thixotropic nature of the formulations. The most pronounced rheological behaviour was found with Avicel RC591 and Carbopol 971P. An increase in concentration, which resulted in a subsequent increase in viscosity, related to an increase in thixotropic behaviour for these polymeric

formulations. Again the charge of the formulation impacted on the thixotropy with anionic polymers producing favourable rheological behaviours over non-ionised formulations. Further rheological assessment was carried out through an oscillation technique in which the viscoelastic properties of the polymeric formulations were investigated. Previous work has shown that a strongly gelled network will ensure the polymeric formulation can withstand the forces associated with the nasal cavity and thus it will remain *in-situ* for an adequate time period. The most desirable viscoelastic properties were seen for Carbopol 971P at 2% w/w which exhibited a more solid, gel like behaviour with a tan delta value of less than one. These results showed that the Carbopol 971P formulation could withstand the stresses it would experience after administration to the nasal cavity.

In order to progress further with the characterisation of the polymeric formulations, the synergistic interactions between the polymers and mucin were investigated using two rheological techniques. These two techniques were employed as a means to study the chain interpenetration and interdiffusion that may have occurred between the mucoadhesive polymeric nasal formulations and the mucin glycoproteins. The mucoadhesive interactions between the polymer and mucin chains can be quantitatively evaluated by comparing the dynamic moduli ( $G'$  and  $G''$ ) of polymer-mucin combinations against the polymeric formulations. The initial bulk rheology test used the same oscillation technique used in Chapter 2. All polymeric formulations showed rheological synergism upon mixing with the mucin. The ionic, high molecular weight polymers all showed the greatest synergy leading to an

improved mucoadhesive attachment with the mucin than the low molecular weight, non-ionic polymers such as HPMC K100P. Carbopol 971P and 974P, at all three concentrations, showed a negative synergism which suggested that the crosslinking has impeded the interaction opportunities for both formulations. These levels of interaction are largely in agreement with the results obtained by the PAS/Schiff glycoprotein assay that was discussed earlier. The second rheological technique used to measure the interactions between the polymers and mucin was microrheology. This technique is a fairly novel technique in the nasal drug delivery research area and no other work has been published discussing this technique in this field. A method was developed which enabled the dynamic moduli to be analysed at the microscopic level. The results obtained for the investigated polymeric formulations were comparable to the results achieved through bulk rheology. The only exception to this was the results for Carbopol 971P which showed positive synergism as opposed to the negative values seen with the bulk rheology technique. This would suggest that at small, microscopic scales the crosslinked polymeric formulations present themselves to a more gel like structure when mixed with mucin rather than a thin viscous solution seen with the bulk rheometer. Limitations were found with the microrheology technique when more viscous formulations were tested. Due to the lack of Brownian motion within the sample, due to the thick nature of the formulations, trapping of the microparticle was not possible and results could not be obtained. However, this technique provided more valuable information than was established by bulk rheology and included the added advantage of fast sample analysis time and small sample volume requirements. Microrheology is a technique that is currently being used for a variety of methods (Bansil *et al.*, 2013) and should

be used for further analysis in the field of nasally delivered drugs. It would be of significant interest if the microrheological technique could be expanded to incorporate an analysis of the interfacial layer that occurs between the mucin and polymer. This would give vital information towards a better understanding of the mucoadhesive processes.

The work carried out in this thesis then led on to an opportunity to branch out and investigate the effects of spray actuation on the overall properties on the mucoadhesive polymeric formulations. This information is key to understanding the effects of spraying on the original properties of any formulation intended for use in a nasal spray device. The formulations were analysed before spraying, immediately after spraying and 15 minutes after spray actuation. Apparent viscosity and level of thixotropy were assessed. It was found that all the formulations investigated were affected by spraying with the greatest effect being noted immediately after spraying. The recovery time for each of the formulations varied and some of the samples analysed did not fully recover after the 15 minute time point. This recovery time is crucial for the intranasal delivery of drugs using a spray actuator. The formulation must recover sufficiently to ensure optimum residence time. A recovery time of greater than 30 minutes could result in the formulation being carried to the nasopharynx by the action of mucociliary clearance. There is scope to further enhance this work by studying the effects of spraying using other techniques including AFM and texture analysis. Recent work has been carried out that showed a difference in performance of formulations sprayed from different delivery devices

(Djupestrand, 2013). It would be of interest to study the effects of spraying on the polymeric formulations when delivered by different devices. This would give us further insight into whether or not the original polymeric formulation, or the formulation after spraying, holds the key to better mucoadhesive performance of the delivery device.

Throughout this thesis three placebo nasal formulations were assessed alongside polymeric formulations. In all experimental data recorded, there was a significant difference between the results obtained for the polymeric formulations and the results obtained for the polymer plus excipients. It is therefore imperative that further work is carried out to assess the effects of these excipients and to determine if the addition of such components has an effect on the overall mucoadhesive strength of the formulation.

The research presented in this thesis holds significant value in adding to the understanding of how the properties of a nasal polymeric formulation affect its mucoadhesive performance. The mucoadhesive performances of a variety of polymeric formulations were assessed using a variety of physical techniques, including rheology, microrheology, and texture analysis and yielded important results. Throughout the work, it was clear that Carbopol 971P and high molecular weight NaCMC provided the most desirable mucoadhesive characteristics. Lower molecular weight polymers, such as HPMC K100P and low molecular weight NaCMC did not yield results that would point to a successful mucoadhesive

performance *in-vitro*. It can be seen that not one critical component can be singled out as the most vital characteristic; instead, a combination of high molecular weight, viscosity, charge and a moderate level of crosslinking are all favourable properties for optimum mucoadhesion. This knowledge will impact on the mucoadhesive polymer candidate selection process for use in a nasal spray formulation where an increased residence time will result in an increased drug absorption and bioavailability.

## References

- Accili, D., Menghi, G., Bonacucina, G., Di Martino, P. & Palmieri, G. F. (2004) 'Mucoadhesion dependence of pharmaceutical polymers on mucosa characteristics', *European Journal of Pharmaceutical Sciences*, 22 (4), 225-234.
- Adeyeye, M. C., Jain, A. C., Ghorab, M. K. M. & Reilly, W. J., Jr. (2002) 'Viscoelastic evaluation of topical creams containing microcrystalline cellulose/sodium carboxymethyl cellulose as stabilizer', *Aaps Pharmscitech*, 3 (2), E8.
- Albrecht, K., Greindl, M., Kremser, C., Wolf, C., Debbage, P. & Bernkop-Schnürch, A. (2006) 'Comparative in vivo mucoadhesion studies of thiomers formulations using magnetic resonance imaging and fluorescence detection', *Journal of Controlled Release*, 115 (1), 78-84.
- Ali, J., Ali, M., Baboota, S., Sahni, J. K., Ramassamy, C., Dao, L. & Bhavna. (2010) 'Potential of Nanoparticulate Drug Delivery Systems by Intranasal Administration', *Current Pharmaceutical Design*, 16 (14), 1644-1653.
- Amboon, W., Tulyathan, V. & Tattiyakul, J. (2012) 'Effect of Hydroxypropyl Methylcellulose on Rheological Properties, Coating Pickup, and Oil Content of Rice Flour-Based Batters', *Food and Bioprocess Technology*, 5 (2), 601-608.
- Andrews, G. P., Laverty, T. P. & Jones, D. S. (2009) 'Mucoadhesive polymeric platforms for controlled drug delivery', *European Journal of Pharmaceutics and Biopharmaceutics*, 71 (3), 505-518.
- Ashkin, A., Dziedzic, J. M., Bjorkholm, J. E. & Chu, S. (1986) 'Observation of a single-beam gradient force optical trap for dielectric particles', *Optics Letters*, 11 (5), 288-290.
- Bae, H.-D. & Lee, K. (2013) 'On employing a translationally controlled tumor protein-derived protein transduction domain analog for transmucosal delivery of drugs', *Journal of Controlled Release*, 170 (3), 358-364.
- Baloglu, E., Karavana, S. Y., Senyigit, Z. A., Hilmioglu-Polat, S., Metin, D. Y., Zekioglu, O., Guneri, T. & Jones, D. S. (2011) 'In-situ gel formulations of econazole nitrate: preparation and in-vitro and in-vivo evaluation', *Journal of Pharmacy and Pharmacology*, 63 (10), 1274-1282.
- Bansil, R., Celli, J. P., Hardcastle, J. M. & Turner, B. S. (2013) 'The influence of mucus microstructure and rheology in *Helicobacter pylori* infection', *Frontiers in Immunology*, 4.
- Baraniuk, J. N. & Merck, S. J. (2009) 'New concepts of neural regulation in human nasal mucosa', *Acta Clinica Croatica*, 48 (1), 65-73.
- Bayarri, S., Gonzalez-Tomas, L. & Costell, E. (2009) 'Viscoelastic properties of aqueous and milk systems with carboxymethyl cellulose', *Food Hydrocolloids*, 23 (2), 441-450.
- Behl, C. R., Pimplaskar, H. K., Sileno, A. P., Demeireles, J. & Romeo, V. D. (1998) 'Effects of physicochemical properties and other factors on systemic nasal drug delivery', *Advanced Drug Delivery Reviews*, 29 (1-2), 89-116.

- Benmouffok-Benbelkacem, G., Caton, F., Baravian, C. & Skali-Lami, S. (2010) 'Non-linear viscoelasticity and temporal behavior of typical yield stress fluids: Carbopol, Xanthan and Ketchup', *Rheologica Acta*, 49 (3), 305-314.
- Boegh, M., Baldursdottir, S. G., Nielsen, M. H., Mullerts, A. & Nielsen, H. M. (2013) 'Development and Rheological Profiling of Biosimilar Mucus', *Annual Transactions of the Nordic Rheology society*, 21.
- Bonacucina, G., Cespi, M., Misici-Falzi, M. & Palmieri, G. F. (2006) 'Rheological, adhesive and release characterisation of semisolid Carbopol/tetraglycol systems', *International Journal of Pharmaceutics*, 307 (2), 129-140.
- Bonacucina, G., Cespi, M., Misici-Falzi, M. & Palmieri, G. F. (2008) 'Rheological evaluation of silicon/carbopol hydrophilic gel systems as a vehicle for delivery of water insoluble drugs', *Aaps Journal*, 10 (1), 84-91.
- Bonacucina, G., Cespi, M. & Palmieri, G. F. (2009) 'Characterization and Stability of Emulsion Gels Based on Acrylamide/Sodium Acryloyldimethyl Taurate Copolymer', *Aaps Pharmscitech*, 10 (2), 368-375.
- Bonacucina, G., Martelli, S. & Palmieri, G. F. (2004) 'Rheological, mucoadhesive and release properties of Carbopol gels in hydrophilic cosolvents', *International Journal of Pharmaceutics*, 282 (1-2), 115-130.
- Bonferoni, M. C., Rossi, S., Ferrari, F. & Caramella, C. (1999) 'A modified Franz diffusion cell for simultaneous assessment of drug release and washability of mucoadhesive gels', *Pharmaceutical Development and Technology*, 4 (1), 45-53.
- Boraey, M. A., Hoe, S., Sharif, H., Miller, D. P., Lechuga-Ballesteros, D. & Vehring, R. (2013) 'Improvement of the dispersibility of spray-dried budesonide powders using leucine in an ethanol-water cosolvent system', *Powder Technology*, 236 (0), 171-178.
- Borland, M., Jacobs, I., King, B. & O'brien, D. (2007) 'A Randomized Controlled Trial Comparing Intranasal Fentanyl to Intravenous Morphine for Managing Acute Pain in Children in the Emergency Department', *Annals of Emergency Medicine*, 49 (3), 335-340.
- Brau, R. R., Ferrer, J. M., Lee, H., Castro, C. E., Tam, B. K., Tarsa, P. B., Matsudaira, P., Boyce, M. C., Kamm, R. D. & Lang, M. J. (2007) 'Passive and active microrheology with optical tweezers', *Journal of Optics a-Pure and Applied Optics*, 9 (8), S103-S112.
- Brownsey, G. J. & Ridout, M. J. (1985) 'Rheological characterization of microcrystalline cellulose dispersion - Avicel RC591', *Journal of Food Technology*, 20 (2), 237-243.
- Carvalho, F. C., Barbi, M. S., Sarmiento, V. H. V., Chiavacci, L. A., Netto, F. M. & Gremiao, M. P. D. (2010) 'Surfactant systems for nasal zidovudine delivery: structural, rheological and mucoadhesive properties', *Journal of Pharmacy and Pharmacology*, 62 (4), 430-439.
- Carvalho, F. C., Campos, M. L., Peccinini, R. G. & Gremião, M. P. D. (2013) 'Nasal administration of liquid crystal precursor mucoadhesive vehicle as an alternative antiretroviral therapy', *European Journal of Pharmaceutics and Biopharmaceutics*, 84 (1), 219-227.
- Celli, J. P., Turner, B. S., Afdhal, N. H., Ewoldt, R. H., Mckinley, G. H., Bansil, R. & Erramilli, S. (2007) 'Rheology of gastric mucin exhibits a pH-dependent sol-gel transition', *Biomacromolecules*, 8 (5), 1580-1586.

- Charlton, S. T., Davis, S. S. & Illum, L. (2007) 'Evaluation of bioadhesive polymers as delivery systems for nose to brain delivery: In vitro characterisation studies', *Journal of Controlled Release*, 118 (2), 225-234.
- Chen, S. C., Eiting, K., Cui, K. Y., Leonard, A. K., Morris, D., Li, C. Y., Farber, K., Sileno, A. P., Houston, M. E., Johnson, P. H., Quay, S. C. & Costantino, H. R. (2006) 'Therapeutic utility of a novel tight junction modulating peptide for enhancing intranasal drug delivery', *Journal of Pharmaceutical Sciences*, 95 (6), 1364-1371.
- Chesham Chemicals Ltd. 2003. *Polysaccharide based gel*. EP20010940726. March 26, 2003.
- Chu, J. S., Chandrasekharan, R., Amidon, G. L., Weiner, N. D. & Goldberg, A. H. (1991) 'Viscometric study of polyacrylic-acid systems as mucoadhesive sustained-release gels', *Pharmaceutical Research*, 8 (11), 1408-1412.
- Cicuta, P. & Donald, A. M. (2007) 'Microrheology: a review of the method and applications', *Soft Matter*, 3 (12), 1449-1455.
- Clare, R. (2011). *Understanding Rheology* [ONLINE]. Available at: <http://www.uow.edu.au/content/groups/public/@web/@sci/@chem/document/s/doc/uow107427.pdf> [Accessed 19 August 2013].
- Cone, R. A. (2009) 'Barrier properties of mucus', *Advanced Drug Delivery Reviews*, 61 (2), 75-85.
- Costantino, H. R., Illum, L., Brandt, G., Johnson, P. H. & Quay, S. C. (2007) 'Intranasal delivery: Physicochemical and therapeutic aspects', *International Journal of Pharmaceutics*, 337 (1-2), 1-24.
- Csaba, N., Garcia-Fuentes, M. & Alonso, M. J. (2009) 'Nanoparticles for nasal vaccination', *Advanced Drug Delivery Reviews*, 61 (2), 140-157.
- Curran, R. M., Donnelly, L., Morrow, R. J., Fraser, C., Andrews, G., Cranage, M., Malcolm, R. K., Shattock, R. J. & Woolfson, A. D. (2009) 'Vaginal delivery of the recombinant HIV-1 clade-C trimeric gp140 envelope protein CN54gp140 within novel rheologically structured vehicles elicits specific immune responses', *Vaccine*, 27 (48), 6791-6798.
- Deacon, M. P., Mcgurk, S., Roberts, C. J., Williams, P. M., Tendler, S. J. B., Davies, M. C., Davis, S. S. & Harding, S. E. (2000) 'Atomic force microscopy of gastric mucin and chitosan mucoadhesive systems', *Biochemical Journal*, 348 557-563.
- Demirkesen, I., Mert, B., Sumnu, G. & Sahin, S. (2010) 'Rheological properties of gluten-free bread formulations', *Journal of Food Engineering*, 96 (2), 295-303.
- Dhakar, R. C., Maurya, S. D., Tilak, V. K. & Gupta, A. K. (2011) 'A review on factors affecting the design of nasal drug delivery system', *International Journal of Drug Delivery*, 4 (2), 194-208.
- Dixit, R. P. & Puthli, S. P. (2009) 'Oral strip technology: Overview and future potential', *Journal of Controlled Release*, 139 (2), 94-107.
- Djupesland, P. G. (2013) 'Nasal drug delivery devices: characteristics and performance in a clinical perspective—a review', *Drug delivery and translational research*, 3 (1), 42-62.
- Dolzplanas, M., Gonzalezrodriguez, F., Beldamaximino, R. & Herraedominguez, J. V. (1988) 'Thixotropic behavior of a microcrystalline cellulose sodium

- carboxymethylcellulose gel', *Journal of Pharmaceutical Sciences*, 77 (9), 799-801.
- Dondeti, P., Zia, H. & Needham, T. E. (1996) 'Bioadhesive and formulation parameters affecting nasal absorption', *International Journal of Pharmaceutics*, 127 (2), 115-133.
- Dondeti, P., Zia, H. S. & Needham, T. E. (1995) 'In-vivo evaluation of spray formulations of human insulin for nasal delivery', *International Journal of Pharmaceutics*, 122 (1-2), 91-105.
- Doughty, D. V., Hsu, W. & Dalby, R. N. (2013) 'Automated actuation of nasal spray products: effect of hand-related variability on the in vitro performance of Flonase nasal spray', *Drug Development and Industrial Pharmacy*, 0 (0), 1-8.
- Duchene, D., Touchard, F. & Peppas, N. A. (1988) 'Pharmaceutical and medical aspects of bioadhesive systems for drug administration', *Drug Development and Industrial Pharmacy*, 14 (2-3), 283-318.
- Eccleston, G. M., Bakhshae, M., Hudson, N. E. & Richards, D. H. (2000) 'Rheological behavior of nasal sprays in shear and extension', *Drug Development and Industrial Pharmacy*, 26 (9), 975-983.
- Eccleston, G. M. & Hudson, N. E. (2000) 'The use of a capillary rheometer to determine the shear and extensional flow behaviour of nasal spray suspensions', *Journal of Pharmacy and Pharmacology*, 52 (10), 1223-1232.
- Edali, M., Esmail, M. N. & Vatistas, G. H. (2001) 'Rheological properties of high concentrations of carboxymethyl cellulose solutions', *Journal of Applied Polymer Science*, 79 (10), 1787-1801.
- Edsman, K. & Hagerstrom, H. (2005) 'Pharmaceutical applications of mucoadhesion for the non-oral routes', *Journal of Pharmacy and Pharmacology*, 57 (1), 3-22.
- Eouani, C., Piccerelle, P., Prinderre, P., Bourret, E. & Joachim, J. (2001) 'In-vitro comparative study of buccal mucoadhesive performance of different polymeric films', *European Journal of Pharmaceutics and Biopharmaceutics*, 52 (1), 45-55.
- Fatimi, A., Tassin, J. F., Quillard, S., Axelos, M. a. V. & Weiss, P. (2008) 'The rheological properties of silylated hydroxypropylmethylcellulose tissue engineering matrices', *Biomaterials*, 29 (5), 533-543.
- Ferdous, A. J. (1992) 'Viscosity and stability studies of hydroxypropyl methylcellulose polymer solutions', *Pakistan Journal of Pharmaceutical Sciences*, 5 (2), 115-119.
- Fisher, A. N., Brown, K., Davis, S. S., Parr, G. D. & Smith, D. A. (1987) 'The effect of molecular-size on the nasal absorption of water-soluble compounds in the albino-rat', *Journal of Pharmacy and Pharmacology*, 39 (5), 357-362.
- Gebben, B., Vandenberg, H. W. A., Bargeman, D. & Smolders, C. A. (1985) 'Intramolecular crosslinking of polyvinyl-alcohol', *Polymer*, 26 (11), 1737-1740.
- George, M. & Abraham, T. E. (2006) 'Polyionic hydrocolloids for the intestinal delivery of protein drugs: Alginate and chitosan — a review', *Journal of Controlled Release*, 114 (1), 1-14.
- Ghannam, M. T. (2009) 'Investigation of thixotropy behavior of crude oil—Polyacrylamide emulsions', *Journal of Applied Polymer Science*, 112 (2), 867-875.

- Ghannam, M. T. & Esmail, M. N. (1997) 'Rheological properties of carboxymethyl cellulose', *Journal of Applied Polymer Science*, 64 (2), 289-301.
- Gizurarson, S. (2012) 'Anatomical and Histological Factors Affecting Intranasal Drug and Vaccine Delivery', *Current Drug Delivery*, 9 (6), 566-582.
- Grassin-Delye, S., Buenestado, A., Naline, E., Faisy, C., Blouquit-Laye, S., Couderc, L.-J., Le Guen, M., Fischler, M. & Devillier, P. (2012) 'Intranasal drug delivery: An efficient and non-invasive route for systemic administration Focus on opioids', *Pharmacology & Therapeutics*, 134 (3), 366-379.
- Guo, C. & Doub, W. H. (2006) 'The influence of actuation parameters on in vitro testing of nasal spray products', *Journal of Pharmaceutical Sciences*, 95 (9), 2029-2040.
- Hagerstrom, H. & Edsman, K. (2001) 'Interpretation of mucoadhesive properties of polymer gel preparations using a tensile strength method', *Journal of Pharmacy and Pharmacology*, 53 (12), 1589-1599.
- Hagerstrom, H. & Edsman, K. (2003) 'Limitations of the rheological mucoadhesion method: The effect of the choice of conditions and the rheological synergism parameter', *European Journal of Pharmaceutical Sciences*, 18 (5), 349-357.
- Hägerström, H. & Edsman, K. (2003) 'Limitations of the rheological mucoadhesion method: The effect of the choice of conditions and the rheological synergism parameter', *European Journal of Pharmaceutical Sciences*, 18 (5), 349-357.
- Hagerstrom, H., Paulsson, M. & Edsman, K. (2000) 'Evaluation of mucoadhesion for two polyelectrolyte gels in simulated physiological conditions using a rheological method', *European Journal of Pharmaceutical Sciences*, 9 (3), 301-309.
- Hagesaether, E., Hiorth, M. & Sande, S. A. (2009) 'Mucoadhesion and drug permeability of free mixed films of pectin and chitosan: An in vitro and ex vivo study', *European Journal of Pharmaceutics and Biopharmaceutics*, 71 (2), 325-331.
- Hall, R., Andrews, P. L. R. & Hoyle, C. H. V. (2002) 'Effects of testosterone on neuromuscular transmission in rat isolated urinary bladder', *European Journal of Pharmacology*, 449 (3), 301-309.
- Haque, M. M. & Khan, A. A. (2008) 'Investigation on structure and properties of brass casting', *Journal of Materials Science & Technology*, 24 (3), 299-301.
- Harkema, J. R., Carey, S. A. & Wagner, J. G. (2006) 'The nose revisited: A brief review of the comparative structure, function, and toxicologic pathology of the nasal epithelium', *Toxicologic Pathology*, 34 (3), 252-269.
- Hassan, E. E. & Gallo, J. M. (1990) 'A simple rheological method for the invitro assessment of mucin-polymer bioadhesive bond strength', *Pharmaceutical Research*, 7 (5), 491-495.
- Herh, P. K. W., Mei, B. C., Roye, N. & Hedman, K. (2002) 'Rheology of high-performance coatings', *American Laboratory*, 34 (13), 6-9.
- Hinchcliffe, M. & Illum, L. (1999) 'Intranasal insulin delivery and therapy', *Advanced Drug Delivery Reviews*, 35 (2-3), 199-234.
- Hino, T. & Ford, J. L. (2001) 'Effect of nicotinamide on the properties of aqueous HPMC solutions', *International Journal of Pharmaceutics*, 226 (1-2), 53-60.

- Hoshmani, H. A. (2006). *Carbopol and its pharmaceutical significance - a review* [ONLINE]. Available at: <http://www.pharmainfo.net/reviews/carbopol-and-its-pharmaceutical-significance-review> [Accessed 17 August 2013].
- Huang, Y. B., Leobandung, W., Foss, A. & Peppas, N. A. (2000) 'Molecular aspects of muco- and bioadhesion: Tethered structures and site-specific surfaces', *Journal of Controlled Release*, 65 (1-2), 63-71.
- Ikeda, S. & Nishinari, K. (2001) "'Weak gel"-type rheological properties of aqueous dispersions of nonaggregated kappa-carrageenan helices', *Journal of Agricultural and Food Chemistry*, 49 (9), 4436-4441.
- Illum, L. (2003) 'Nasal drug delivery - possibilities, problems and solutions', *Journal of Controlled Release*, 87 (1-3), 187-198.
- Illum, L. (2006) 'Nasal clearance in health and disease', *Journal of Aerosol Medicine-Deposition Clearance and Effects in the Lung*, 19 (1), 92-99.
- Illum, L. (2012) 'Nasal drug delivery — Recent developments and future prospects', *Journal of Controlled Release*, 161 (2), 254-263.
- Illum, L., Jorgensen, H., Bisgaard, H., Krogsgaard, O. & Rossing, N. (1987) 'Bioadhesive microspheres as a potential nasal drug delivery system', *International Journal of Pharmaceutics*, 39 (3), 189-199.
- Islam, M. T., Rodriguez-Hornedo, N., Ciotti, S. & Ackermann, C. (2004) 'Rheological characterization of topical carbomer gels neutralized to different pH', *Pharmaceutical Research*, 21 (7), 1192-1199.
- Ivarsson, D. & Wahlgren, M. (2012) 'Comparison of in vitro methods of measuring mucoadhesion: Ellipsometry, tensile strength and rheological measurements', *Colloids and Surfaces B-Biointerfaces*, 92 353-359.
- Jackson, G., Armento, A., Letasiova, S., Klausner, M. & Hayden, P. (2013) 'Rapid toxicity and drug delivery screening in an in vitro human airway model', *Toxicology Letters*, 221, Supplement (0), S95.
- Janssen, A. M., Terpstra, M. E. J., De Wijk, R. A. & Prinz, J. F. (2007) 'Relations between rheological properties, saliva-induced structure breakdown and sensory texture attributes of custards', *Journal of Texture Studies*, 38 (1), 42-69.
- Jayabalan, M. (1989) 'Newtonian behavior of sheared aqueous carboxymethylcellulose solution on aging', *British Polymer Journal*, 21 (3), 233-235.
- Jiao, Y., Gyawali, D., Stark, J. M., Akcora, P., Nair, P., Tran, R. T. & Yang, J. (2012) 'A rheological study of biodegradable injectable PEGMC/HA composite scaffolds', *Soft Matter*, 8 (5), 1499-1507.
- Jimenez, M. M., Fresno, M. J. & Ramirez, A. (2007) 'Rheological study of binary gels with Carbopol (R) Ultre (TM) 10 and hyaluronic acid', *Chemical & Pharmaceutical Bulletin*, 55 (8), 1157-1163.
- Jones, D. S., Brown, A. F. & Woolfson, A. D. (2001) 'Rheological characterization of bioadhesive, antimicrobial, semisolids designed for the treatment of periodontal diseases: Transient and dynamic viscoelastic and continuous shear analysis', *Journal of Pharmaceutical Sciences*, 90 (12), 1978-1990.
- Jones, D. S., Bruschi, M. L., De Freitas, O., Daflon Gremiao, M. P., Guimaraes Lara, E. H. & Andrews, G. P. (2009) 'Rheological, mechanical and mucoadhesive properties of thermoresponsive, bioadhesive binary mixtures composed of poloxamer 407 and carbopol 974P designed as platforms for implantable drug

- delivery systems for use in the oral cavity', *International Journal of Pharmaceutics*, 372 (1-2), 49-58.
- Jones, D. S., Lawlor, M. S. & Woolfson, A. D. (2002) 'Examination of the flow rheological and textural properties of polymer gels composed of poly(methylvinylether-co-maleic anhydride) and poly(vinylpyrrolidone): Rheological and mathematical interpretation of textural parameters', *Journal of Pharmaceutical Sciences*, 91 (9), 2090-2101.
- Jones, D. S., Lawlor, M. S. & Woolfson, A. D. (2003) 'Rheological and mucoadhesive characterization of polymeric systems composed of poly(methylvinylether-co-maleic anhydride) and poly(vinylpyrrolidone), designed as platforms for topical drug delivery', *Journal of Pharmaceutical Sciences*, 92 (5), 995-1007.
- Jones, D. S., Woolfson, A. D. & Brown, A. F. (1997) 'Textural analysis and flow rheometry of novel, bioadhesive antimicrobial oral gels', *Pharmaceutical Research*, 14 (4), 450-457.
- Jones, D. S., Woolfson, A. D. & Djokic, J. (1996) 'Texture profile analysis of bioadhesive polymeric semisolids: Mechanical characterization and investigation of interactions between formulation components', *Journal of Applied Polymer Science*, 61 (12), 2229-2234.
- Joshi, S. C. (2011) 'Sol-Gel Behavior of Hydroxypropyl Methylcellulose (HPMC) in Ionic Media Including Drug Release', *Materials*, 4 (10), 1861-1905.
- Kerr, D., Dietze, P. & Kelly, A.-M. (2008) 'Intranasal naloxone for the treatment of suspected heroin overdose', *Addiction*, 103 (3), 379-386.
- Khandare, J. & Haag, R. (2010) 'Pharmaceutically used polymers: principles, structures, and applications of pharmaceutical delivery systems', *Handbook of experimental pharmacology*, (197), 221-50.
- Khutoryanskiy, V. V. (2011) 'Advances in Mucoadhesion and Mucoadhesive Polymers', *Macromolecular Bioscience*, 11 (6), 748-764.
- Kim, D.-D. (2008) *In vitro cellular models for nasal drug absorption studies*. Springer.
- Kulicke, W. M., Kull, A. H., Kull, W., Thielking, H., Engelhardt, J. & Pannek, J. B. (1996) 'Characterization of aqueous carboxymethylcellulose solutions in terms of their molecular structure and its influence on rheological behaviour', *Polymer*, 37 (13), 2723-2731.
- Kulicke, W. M., Reinhardt, U., Fuller, G. G. & Arendt, O. (1999) 'Characterization of the flow properties of sodium carboxymethylcellulose via mechanical and optical techniques', *Rheologica Acta*, 38 (1), 26-33.
- Kulkarni, U., Mahalingam, R., Pather, I., Li, X. & Jasti, B. (2010) 'Porcine Buccal Mucosa as In Vitro Model: Effect of Biological and Experimental Variables', *Journal of Pharmaceutical Sciences*, 99 (3), 1265-1277.
- Kumar, M., Muzzarelli, R. a. A., Muzzarelli, C., Sashiwa, H. & Domb, A. J. (2004) 'Chitosan chemistry and pharmaceutical perspectives', *Chemical Reviews*, 104 (12), 6017-6084.
- Kundu, J., Patra, C. & Kundu, S. C. (2008) 'Design, fabrication and characterization of silk fibroin-HPMC-PEG blended films as vehicle for transmucosal delivery', *Materials Science & Engineering C-Biomimetic and Supramolecular Systems*, 28 (8), 1376-1380.

- Labanda, J., Marco, P. & Llorens, J. (2004) 'Rheological model to predict the thixotropic behaviour of colloidal dispersions', *Colloids and Surfaces a-Physicochemical and Engineering Aspects*, 249 (1-3), 123-126.
- Lai, S. K., Wang, Y.-Y., Wirtz, D. & Hanes, J. (2009) 'Micro- and macrorheology of mucus', *Advanced Drug Delivery Reviews*, 61 (2), 86-100.
- Lansley, A. B. (1993) 'Mucociliary clearance and drug delivery via the respiratory tract', *Advanced Drug Delivery Reviews*, 11 (3), 299-327.
- Lee, C. H., Moturi, V. & Lee, Y. Y. (2009) 'Thixotropic property in pharmaceutical formulations', *Journal of Controlled Release*, 136 (2), 88-98.
- Lee, J. W., Park, J. H. & Robinson, J. R. (2000) 'Bioadhesive-based dosage forms: The next generation', *Journal of Pharmaceutical Sciences*, 89 (7), 850-866.
- Liu, Y., Johnson, M. R., Matida, E. A., Kherani, S. & Marsan, J. (2009) 'Creation of a standardized geometry of the human nasal cavity', *Journal of Applied Physiology*, 106 (3), 784-795.
- Livraghi, A. & Randell, S. H. (2007) 'Cystic fibrosis and other respiratory diseases of impaired mucus clearance', *Toxicologic Pathology*, 35 (1), 116-129.
- Lochhead, J. J. & Thorne, R. G. (2012) 'Intranasal delivery of biologics to the central nervous system', *Advanced Drug Delivery Reviews*, 64 (7), 614-628.
- Lubrizol (2008). *Flow and Suspension Properties* [ONLINE]. Available at: <http://www.lubrizol.com/> [Accessed 25 September 2013].
- Lubrizol 2011. *Pharmaceutical Polymers for Liquid and Semisolid Dosage Forms*. In: Lubrizol (ed.).
- Lubrizol (2012). *Formulating toothpaste using Carbopol polymer* [ONLINE]. Lubrizol. [Accessed 14th May 2012].
- Luond-Valeskeviciute I, H. B. & Gruenwald, J. (2010) 'Efficacy of three thixotropic nasal spray preparations on seasonal allergic rhinitis', *Allergy*, 1 (10).
- Madsen, F., Eberth, K. & Smart, J. D. (1998a) 'A rheological assessment of the nature of interactions between mucoadhesive polymers and a homogenised mucus gel', *Biomaterials*, 19 (11-12), 1083-1092.
- Madsen, F., Eberth, K. & Smart, J. D. (1998b) 'A rheological examination of the mucoadhesive/mucus interaction: the effect of mucoadhesive type and concentration', *Journal of Controlled Release*, 50 (1-3), 167-178.
- Madsen, S. J., Chu, E. A. & Wong, B. J. F. (1999) 'The optical properties of porcine nasal cartilage', *Ieee Journal of Selected Topics in Quantum Electronics*, 5 (4), 1127-1133.
- Majithiya, R. J., Ghosh, P. K., Umrethia, M. L. & Murthy, R. S. R. (2006) 'Thermoreversible-mucoadhesive gel for nasal delivery of sumatriptan', *AAPS PharmSciTech*, 7 (3).
- Maltese, A., Borzacchiello, A., Mayol, L., Bucolo, C., Maugeri, F., Nicolais, L. & Ambrosio, L. (2006) 'Novel polysaccharides-based viscoelastic formulations for ophthalmic surgery: Rheological characterization', *Biomaterials*, 27 (29), 5134-5142.
- Martin, E., Schipper, N. G. M., Verhoef, J. C. & Merkus, F. (1998) 'Nasal mucociliary clearance as a factor in nasal drug delivery', *Advanced Drug Delivery Reviews*, 29 (1-2), 13-38.
- Mattes, P. M. & Mattes, W. B. (1992) 'Alpha-naphthyl butyrate carboxylesterase activity in human and rat nasal tissue', *Toxicology and Applied Pharmacology*, 114 (1), 71-76.

- McInnes, F. J., O'mahony, B., Lindsay, B., Band, J., Wilson, C. G., Hodges, L. A. & Stevens, H. N. E. (2007) 'Nasal residence of insulin containing lyophilised nasal insert formulations, using gamma scintigraphy', *European Journal of Pharmaceutical Sciences*, 31 (1), 25-31.
- McInnes, F. J., Thapa, P., Baillie, A. J., Welling, P. G., Watson, D. G., Gibson, I., Nolan, A. & Stevens, H. N. E. (2005) 'In vivo evaluation of nicotine lyophilised nasal insert in sheep', *International Journal of Pharmaceutics*, 304 (1-2), 72-82.
- McMartin, C., Hutchinson, L. E. F., Hyde, R. & Peters, G. E. (1987) 'Analysis of structural requirements for the absorption of drugs and macromolecules from the nasal cavity', *Journal of Pharmaceutical Sciences*, 76 (7), 535-540.
- Meltzer, E. O. (2011) 'The Role of Nasal Corticosteroids in the Treatment of Rhinitis', *Immunology and Allergy Clinics of North America*, 31 (3), 545-+.
- Merlin, M. A., Saybolt, M., Kapitanyan, R., Alter, S. M., Jeges, J., Liu, J., Calabrese, S., Rynn, K. O., Perritt, R. & Pryor, P. W., II. (2010) 'Intranasal naloxone delivery is an alternative to intravenous naloxone for opioid overdoses', *American Journal of Emergency Medicine*, 28 (3), 296-303.
- Mewis, J. & Wagner, N. J. (2009) 'Thixotropy', *Advances in Colloid and Interface Science*, 147-148 (0), 214-227.
- Mihranyan, A., Edsman, K. & Stromme, M. (2007) 'Rheological properties of cellulose hydrogels prepared from Cladophora cellulose powder', *Food Hydrocolloids*, 21 (2), 267-272.
- Miller, P. C. H. & Butler Ellis, M. C. (2000) 'Effects of formulation on spray nozzle performance for applications from ground-based boom sprayers', *Crop Protection*, 19 (8-10), 609-615.
- Mohamed, M. I. (2004) 'Optimization of chlorphenesin emulgel formulation', *Aaps Journal*, 6 (3).
- Morris, E. R., Cutler, A. N., Ross-Murphy, S. B., Rees, D. A. & Price, J. (1981) 'Concentration and shear rate dependence of viscosity in random coil polysaccharide solutions', *Carbohydrate Polymers*, 1 (1), 5-21.
- Mortazavi, S. A., Carpenter, B. G. & Smart, J. D. (1992) 'An investigation of the rheological behaviour of the mucoadhesive mucosal interface', *International Journal of Pharmaceutics*, 83 (1-3), 221-225.
- Mortazavi, S. A. & Smart, J. D. (1994) 'Factors influencing the gel strengthening at the mucoadhesive-mucus interface', *Journal of Pharmacy and Pharmacology*, 46 (2), 86-90.
- Mygind, N. & Dahl, R. (1998) 'Anatomy, physiology and function of the nasal cavities in health and disease', *Advanced Drug Delivery Reviews*, 29 (1-2), 3-12.
- Na, L., Wang, J., Wang, L. & Mao, S. (2013) 'A novel permeation enhancer: N-succinyl chitosan on the intranasal absorption of isosorbide dinitrate in rats', *European Journal of Pharmaceutical Sciences*, 48 (1-2), 301-306.
- Narkis, N. & Rebhun, M. (1966) 'Ageing effects in measurements of polyacrylamide solution viscosities', *Polymer*, 7 (10), 507-512.
- Ohwaki, T., Ando, H., Kakimoto, F., Uesugi, K., Watanabe, S., Miyake, Y. & Kayano, M. (1987) 'Effects of dose, pH and osmolarity on nasal absorption of secretin in rats. 2. Histological aspects of the nasal-mucosa in relation to the

- absorption variation due to the effects of pH and osmolarity', *Journal of Pharmaceutical Sciences*, 76 (9), 695-698.
- Ortan, A., Parvu, C. D., Ghica, M. V., Popescu, L. M. & Ionita, L. (2011) 'Rheological Study of a Liposomal Hydrogel Based On Carbopol', *Romanian Biotechnological Letters*, 16 (1), 47-54.
- Ozsoy, Y., Gungor, S. & Cevher, E. (2009) 'Nasal Delivery of High Molecular Weight Drugs', *Molecules*, 14 (9), 3754-3779.
- Park, H. & Robinson, J. R. (1985) 'Physicochemical properties of water insoluble polymers important to mucin-epithelial adhesion', *Journal of Controlled Release*, 2 47-58.
- Patel, D., Smith, J. R., Smith, A. W., Grist, N., Barnett, P. & Smart, J. D. (2000) 'An atomic force microscopy investigation of bioadhesive polymer adsorption onto human buccal cells', *International Journal of Pharmaceutics*, 200 (2), 271-277.
- Pennington, A. K., Ratcliffe, J. H., Wilson, C. G. & Hardy, J. G. (1988) 'The influence of solution viscosity on nasal spray deposition and clearance', *International Journal of Pharmaceutics*, 43 (3), 221-224.
- Peppas, N. A. & Buri, P. A. (1985) 'Surface, interfacial and molecular aspects of polymer bioadhesion on soft tissues', *Journal of Controlled Release*, 2 (0), 257-275.
- Peppas, N. A. & Sahlin, J. J. (1996) 'Hydrogels as mucoadhesive and bioadhesive materials: A review', *Biomaterials*, 17 (16), 1553-1561.
- Pires, A., Fortuna, A., Alves, G. & Falcao, A. (2009) 'Intranasal Drug Delivery: How, Why and What for?', *Journal of Pharmacy and Pharmaceutical Sciences*, 12 (3), 288-311.
- Preece, D., Warren, R., Evans, R. M. L., Gibson, G. M., Padgett, M. J., Cooper, J. M. & Tassieri, M. (2011) 'Optical tweezers: wideband microrheology', *Journal of Optics*, 13 (4), 044022.
- Privalova, A. M., Gulyaeva, N. V. & Bukreeva, T. V. (2012) 'Intranasal administration: a prospective drug delivery route to the brain', *Neurochemical Journal*, 6 (2), 77-88.
- Pujara, C. P., Shao, Z. Z., Duncan, M. R. & Mitra, A. K. (1995) 'Effects of formulation variables on nasal epithelial-cell integrity - biochemical evaluations', *International Journal of Pharmaceutics*, 114 (2), 197-203.
- Quinones, D. & Ghaly, E. S. (2008) 'Formulation and characterization of nystatin gel', *Puerto Rico Health Sciences Journal*, 27 (1), 61-67.
- Renner, D. B., Frey Ii, W. H. & Hanson, L. R. (2012a) 'Intranasal delivery of siRNA to the olfactory bulbs of mice via the olfactory nerve pathway', *Neuroscience Letters*, 513 (2), 193-197.
- Renner, D. B., Svitak, A. L., Gallus, N. J., Ericson, M. E., Frey, W. H., Ii & Hanson, L. R. (2012b) 'Intranasal delivery of insulin via the olfactory nerve pathway', *Journal of Pharmacy and Pharmacology*, 64 (12), 1709-1714.
- Rosalina, I. & Bhattacharya, M. (2002) 'Dynamic rheological measurements and analysis of starch gels', *Carbohydrate Polymers*, 48 (2), 191-202.
- Rossi, S., Bonferoni, M. C., Lippoli, G., Bertoni, M., Ferrari, F., Caramella, C. & Conte, U. (1995) 'Influence of mucin-type on polymer-mucin rheological interactions', *Biomaterials*, 16 (14), 1073-1079.

- Roy, S., Pal, K., Anis, A., Pramanik, K. & Prabhakar, B. (2009) 'Polymers in Mucoadhesive Drug-Delivery Systems: A Brief Note', *Designed Monomers and Polymers*, 12 (6), 483-495.
- Rudraraju, V. S. & Wyandt, C. M. (2005) 'Rheology of microcrystalline cellulose and sodiumcarboxymethyl cellulose hydrogels using a controlled stress rheometer: part II', *International Journal of Pharmaceutics*, 292 (1-2), 63-73.
- Sanz, T., Fernandez, M. A., Salvador, A., Munoz, J. & Fiszman, S. M. (2005) 'Thermogelation properties of methylcellulose (MC) and their effect on a batter formula', *Food Hydrocolloids*, 19 (1), 141-147.
- Seiler, M. P., Luner, P., Moninger, T. O., Karp, P. H., Keshavjee, S. & Zabner, J. (2002) 'Thixotropic solutions enhance viral-mediated gene transfer to airway epithelia', *American Journal of Respiratory Cell and Molecular Biology*, 27 (2), 133-140.
- Serra, L., Domenech, J. & Peppas, N. A. (2009a) 'Engineering design and molecular dynamics of mucoadhesive drug delivery systems as targeting agents', *European Journal of Pharmaceutics and Biopharmaceutics*, 71 (3), 519-528.
- Serra, L., Doménech, J. & Peppas, N. A. (2009b) 'Engineering design and molecular dynamics of mucoadhesive drug delivery systems as targeting agents', *European Journal of Pharmaceutics and Biopharmaceutics*, 71 (3), 519-528.
- Shahnaz, G., Perera, G., Sakloetsakun, D., Rahmat, D. & Bernkop-Schnürch, A. (2010) 'Synthesis, characterization, mucoadhesion and biocompatibility of thiolated carboxymethyl dextran–cysteine conjugate', *Journal of Controlled Release*, 144 (1), 32-38.
- Shaikh, R., Singh, T. R. R., Garland, M. J., Woolfson, A. D. & Donnelly, R. (2011) 'Mucoadhesive drug delivery systems', *Journal of Pharmacy and Bioallied Sciences*, 3 (1), 89-100.
- Sharpe, S. A., Sandweiss, V., Tuazon, J., Giordano, M., Witchey-Lakshmanan, L., Hart, J. & Sequeira, J. (2003) 'Comparison of the flow properties of aqueous suspension corticosteroid nasal sprays under differing sampling conditions', *Drug Development and Industrial Pharmacy*, 29 (9), 1005-1012.
- Sharpe, S. A., Sandweiss, V., Tuazon, J., Giordano, M., Witchey-Lakshmanan, L. & Sequeira, J. (2002) 'Comparison of the flow properties of mometasone furoate nasal spray with other nasal corticosteroid sprays', *Journal of Allergy and Clinical Immunology*, 109 (1), S106-S106.
- Sibley, T., Jacobsen, R. & Salomone, J. (2013) 'Successful administration of intranasal glucagon in the out of hospital environment', *Prehospital Emergency Care*, 17 (1), 98-102.
- Smart, J. D. (2005) 'The basics and underlying mechanisms of mucoadhesion', *Advanced Drug Delivery Reviews*, 57 (11), 1556-1568.
- Smart, J. D., Kellaway, I. W. & Worthington, H. E. C. (1984) 'An in-vitro investigation of mucosa-adhesive materials for use in controlled drug delivery', *Journal of Pharmacy and Pharmacology*, 36 (5), 295-299.
- Sriamornsak, P. & Wattanakorn, N. (2008) 'Rheological synergy in aqueous mixtures of pectin and mucin', *Carbohydrate Polymers*, 74 (3), 474-481.
- Sriamornsak, P., Wattanakorn, N., Nunthanid, J. & Puttipipatkachorn, S. (2008) 'Mucoadhesion of pectin as evidence by wettability and chain interpenetration', *Carbohydrate Polymers*, 74 (3), 458-467.

- Stasiak, P., Placzek, M., Lepek, P. & Sznitowska, M. (2011) 'Influence of Polymer Type, Active Substance, and Experimental Model on Mucoadhesive Properties of Selected Drug Formulations', *Journal of Dispersion Science and Technology*, 32 (12), 1780-1785.
- Stoker, D. G., Reber, K. R., Waltzman, L. S., Ernst, C., Hamilton, D., Gawarecki, D., Mermelstein, F., Mcnicol, E., Wright, C. & Carr, D. B. (2008) 'Analgesic efficacy and safety of morphine-chitosan nasal solution in patients with moderate to severe pain following orthopedic surgery', *Pain Medicine*, 9 (1), 3-12.
- Stoltz, C., De Pablo, J. J. & Graham, M. D. (2006) 'Concentration dependence of shear and extensional rheology of polymer solutions: Brownian dynamics simulations', *Journal of Rheology*, 50 (2), 137-167.
- Storms, W. & Farrar, J. R. (2009) 'Guaifenesin in rhinitis', *Current Allergy and Asthma Reports*, 9 (2), 101-106.
- Talukdar, M. M., Vinckier, I., Moldenaers, P. & Kinget, R. (1996) 'Rheological characterization of xanthan gum and hydroxypropylmethyl cellulose with respect to controlled-release drug delivery', *Journal of Pharmaceutical Sciences*, 85 (5), 537-540.
- Tamburic, S. & Craig, D. Q. M. (1995) 'An investigation into the rheological, dielectric and mucoadhesive properties of poly(acrylic acid) gel systems', *Journal of Controlled Release*, 37 (1-2), 59-68.
- Tamburic, S. & Craig, D. Q. M. (1997) 'A comparison of different in vitro methods for measuring mucoadhesive performance', *European Journal of Pharmaceutics and Biopharmaceutics*, 44 (2), 159-167.
- Tassieri, M., Gibson, G. M., Evans, R. M. L., Yao, A. M., Warren, R., Padgett, M. J. & Cooper, J. M. (2010) 'Measuring storage and loss moduli using optical tweezers: Broadband microrheology', *Physical Review E*, 81 (2), 026308.
- Tobyn, M. J., Johnson, J. R. & Dettmar, P. W. (1995) 'Factors affecting in-vitro gastric mucoadhesion. 1. Test conditions and instrumental parameters', *European Journal of Pharmaceutics and Biopharmaceutics*, 41 (4), 235-241.
- Tobyn, M. J., Johnson, J. R. & Dettmar, P. W. (1997) 'Factors affecting in vitro gastric mucoadhesion .4. Influence of tablet excipients, surfactants and salts on the observed mucoadhesion of polymers', *European Journal of Pharmaceutics and Biopharmaceutics*, 43 (1), 65-71.
- Tsuneji, N., Yuji, N., Naoki, N., Yoshiki, S. & Kunio, S. (1984) 'Powder dosage form of insulin for nasal administration', *Journal of Controlled Release*, 1 (1), 15-22.
- Turker, S., Onur, E. & Ozer, Y. (2004) 'Nasal route and drug delivery systems', *Pharmacy World & Science*, 26 (3), 137-142.
- Ugwoke, M. I., Verbeke, N. & Kinget, R. (2001) 'The biopharmaceutical aspects of nasal mucoadhesive drug delivery', *Journal of Pharmacy and Pharmacology*, 53 (1), 3-21.
- Varum, F. J. O., Veiga, F., Sousa, J. S. & Basit, A. W. (2010) 'An investigation into the role of mucus thickness on mucoadhesion in the gastrointestinal tract of pig', *European Journal of Pharmaceutical Sciences*, 40 (4), 335-341.
- Washington, N., Steele, R. J. C., Jackson, S. J., Bush, D., Mason, J., Gill, D. A., Pitt, K. & Rawlins, D. A. (2000) 'Determination of baseline human nasal pH and

- the effect of intranasally administered buffers', *International Journal of Pharmaceutics*, 198 (2), 139-146.
- Williams, P. A. (2011) *Renewable Resources for Functional Polymers and Biomaterials. Polysaccharides, Proteins and Polyesters*. RSC Publications.
- Wolf, D. A., Hanson, L. R., Aronovich, E. L., Nan, Z., Low, W. C., Frey Ii, W. H. & Mcivor, R. S. (2012) 'Lysosomal enzyme can bypass the blood–brain barrier and reach the CNS following intranasal administration', *Molecular Genetics and Metabolism*, 106 (1), 131-134.
- Wong, C. F., Yuen, K. H. & Peh, K. K. (1999) 'An in-vitro method for buccal adhesion studies: importance of instrument variables', *International Journal of Pharmaceutics*, 180 (1), 47-57.
- Yao, A., Tassieri, M., Padgett, M. & Cooper, J. (2009) 'Microrheology with optical tweezers', *Lab on a Chip*, 9 (17), 2568-2575.
- Yu, S. Y., Zhao, Y., Wu, F. L., Zhang, X., Lu, W. L., Zhang, H. & Zhang, Q. (2004) 'Nasal insulin delivery in the chitosan solution: in vitro and in vivo studies', *International Journal of Pharmaceutics*, 281 (1-2), 11-23.
- Zhao, G. H., Kapur, N., Carlin, B., Selinger, E. & Guthrie, J. T. (2011) 'Characterisation of the interactive properties of microcrystalline cellulose-carboxymethyl cellulose hydrogels', *International Journal of Pharmaceutics*, 415 (1-2), 95-101.
- Zhu, W., Cheng, S., Xu, G., Ma, M., Zhou, Z., Liu, D. & Liu, X. (2011) 'Intranasal nerve growth factor enhances striatal neurogenesis in adult rats with focal cerebral ischemia', *Drug Delivery*, 18 (5), 338-343.

## Abbreviations

AFM	Atomic Force Microscopy
ANOVA	Analysis of Variance
API	Active Pharmaceutical Ingredient
AUC	Area Under Curve (Work of Adhesion)
BKC	Benzalkonium Chloride
CaCl <sub>2</sub> .2H <sub>2</sub> O	Calcium Chloride Dihydrate
CNS	Central Nervous System
EDTA	Edetate Disodium
F <sub>max</sub>	Maximum Detachment Force
GRAS	Generally Regarded As Safe
HPMC	Hydroxypropyl Methylcellulose
<i>K</i>	Consistency Index
KBR	Krebs Bicarbonate Ringer Solution
KCl	Potassium Chloride
LV	Low Viscosity
LVR	Linear Viscoelastic Region
MC	Mucociliary Clearance
MCC	Microcrystalline Cellulose
MgSO <sub>4</sub> .7H <sub>2</sub> O	Magnesium Sulphate
MW	Molecular Weight
<i>n</i>	Flow Behaviour Index
NaCl	Sodium Chloride
NaCMC	Sodium Carboxymethylcellulose
NaHCO <sub>3</sub>	Sodium Bicarbonate
NaH <sub>2</sub> PO <sub>4</sub>	Sodium Phosphate
NaOH	Sodium Hydroxide

OH	Hydroxyl
P	Premium Grade
PAS	Period Acid/Schiff
SLM	Spatial Light Modulator
TA	Texture Analyser
TEA	triethanolamide
UV	Ultraviolet
W <sub>A</sub>	Work of Adhesion

## List of figures

Figure 1.1	Illustrating the difference in nasal deposition achieved with the use of different delivery devices.....	2
Figure 1.2	Sagittal section of the nasal cavity (Liu et al., 2009). .....	4
Figure 1.3	Frontal plane midway through the nasal cavity (Liu et al., 2009). .....	5
Figure 1.4	Schematic drawing of a general mucin monomer showing the amino and carboxy terminals, the cysteine rich residues, repeating units and oligosaccharides. ....	9
Figure 1.5	Schematic diagram of a general mucin molecule showing the cysteine rich terminals, the highly glycosylated regions, disulfide bridges and oligosaccharides.....	9
Figure 1.6	Mucoadhesive drug delivery device action.....	16
Figure 1.7	Typical chemical structure of hydroxypropyl methylcellulose. Reproduced from Handbook of Pharmaceutical Excipients (5 <sup>th</sup> Edition).....	26
Figure 1.8	Typical chemical structure of microcrystalline cellulose. Reproduced from Handbook of Pharmaceutical Excipients (5 <sup>th</sup> Edition).....	27
Figure 1.9	Typical chemical structure of Avicel. Reproduced from Handbook of Pharmaceutical Excipients (5 <sup>th</sup> Edition). .....	28
Figure 1.10	Typical chemical structure of NaCMC. Reproduced from Handbook of Pharmaceutical Excipients (5 <sup>th</sup> Edition). .....	29
Figure 1.11	Typical chemical structure of poly (acrylic acid). Reproduced from Handbook of Pharmaceutical Excipients (5 <sup>th</sup> Edition).....	29
Figure 1.12	Texture analyser apparatus.....	32
Figure 1.13	Graphical output from Texture Analyser. Reproduced from (Jones <i>et al.</i> , 1997). .....	32
Figure 1.14	Rheometer apparatus.....	35
Figure 1.15	Labelled rheology apparatus. ....	35
Figure 1.16	Effect of shear rate on the viscosity of (A) shear-thinning systems, (B) Newtonian formulations and (C) shear thickening systems. ....	36

Figure 1.17	Schematic Diagram of AFM Setup.....	39
Figure 2.1	Apparent viscosity of mucoadhesive polymeric nasal formulations measured at 25°C ± S.D. (0.2% w/w measured at a shear rate of 100 s <sup>-1</sup> (red) and 1200 s <sup>-1</sup> (blue)) (n=3). .....	51
Figure 2.2	Apparent viscosity of mucoadhesive polymeric nasal formulations measured at 25°C ± S.D. (0.5% w/w measured at a shear rate of 100 s <sup>-1</sup> (red) and 1200 s <sup>-1</sup> (blue)) (n=3). .....	51
Figure 2.3	Apparent viscosity of mucoadhesive polymeric nasal formulations measured at 25°C ± S.D. (1% w/w measured at a shear rate of 100 s <sup>-1</sup> (red) and 1200 s <sup>-1</sup> (blue)) (n=3). .....	52
Figure 2.4	Apparent viscosity of placebo nasal formulations measured at 25°C (blue represents 100 s <sup>-1</sup> and red represents 1200 s <sup>-1</sup> ) (n=3). .....	54
Figure 2.5	Mean apparent viscosity of 2% w/w mucin formulation ± S.D measured at 25°C (n=3). .....	57
Figure 2.6	Typical rheological flow profiles of 0.2% w/w (blue), 0.5% w/w (red) and 1% w/w (green) Avicel CL611 measured at 100 s <sup>-1</sup> (a) and 1200 s <sup>-1</sup> (b). .....	59
Figure 2.7	Typical rheological flow profiles of 0.2% w/w (blue), 0.5% w/w (red) and 1% w/w (green) NaCMC med MW measured at 100 s <sup>-1</sup> (a) and 1200 s <sup>-1</sup> (b).....	60
Figure 2.8	Typical rheological flow profiles of 0.2% w/w (blue), 0.5% w/w (red) and 1% w/w (green) NaCMC low MW measured at 100 s <sup>-1</sup> (a) and 1200 s <sup>-1</sup> (b).....	61
Figure 2.9	Typical rheological flow profiles of 0.2% w/w (blue), 0.5% w/w (red) and 1% w/w (green) NaCMC high MW measured at 100 s <sup>-1</sup> (a) and 1200 s <sup>-1</sup> (b).....	61
Figure 2.10	Typical rheological flow profiles of 0.2% w/w (blue), 0.5% w/w (red) and 1% w/w (green) HPMC E4MP measured at 100 s <sup>-1</sup> (a) and 1200 s <sup>-1</sup> (b). .....	63
Figure 2.11	Typical rheological flow profiles of 0.2% w/w (blue), 0.5% w/w (red) and 1% w/w (green) HPMC K100P measured at 100 s <sup>-1</sup> (a) and 1200 s <sup>-1</sup> (b). .....	64

Figure 2.12	Typical rheological flow profiles of 0.2% w/w (blue), 0.5% w/w (red) and 1% w/w (green) HPMC K4MP measured at 100 s <sup>-1</sup> (a) and 1200 s <sup>-1</sup> (b). .....	64
Figure 2.13	Typical rheological flow profiles of 0.2% w/w (blue), 0.5% w/w (red) and 1% w/w (green) HPMC K15MP measured at 100 s <sup>-1</sup> (a) and 1200 s <sup>-1</sup> (b). .....	65
Figure 2.14	Typical rheological flow profiles of 0.2% w/w (blue), 0.5% w/w (red) and 1% w/w (green) Avicel RC591 measured at 100 s <sup>-1</sup> (a) and 1200 s <sup>-1</sup> (b). .....	65
Figure 2.15	Typical rheological flow profiles of 0.2% w/w (blue), 0.5% w/w (red) and 1% w/w (green) Carbopol 971P measured at 100 s <sup>-1</sup> (a) and 1200 s <sup>-1</sup> (b). .....	66
Figure 2.16	Typical rheological flow profiles of 0.2% w/w (blue), 0.5% w/w (red) and 1% w/w (green) Carbopol 974P measured at 100 s <sup>-1</sup> (a) and 1200 s <sup>-1</sup> (b). .....	66
Figure 2.17	Typical rheological flow profiles of placebo nasal formulations, ee521730 (blue), ee521950 (red) and ee522260 (green) NaCMC low MW measured at 100 s <sup>-1</sup> (a) and 1200 s <sup>-1</sup> (b). .....	70
Figure 2.18	Dynamic oscillation spectra of 2% w/w mucin at 25 °C. Open markers represent G' and closed markers represent G'' .....	77
Figure 2.19	Dynamic oscillation spectra of Avicel CL611 at 25 °C. 0.2% w/w G' (◇) and G'' (◆); 0.5% w/w G' (○) and G'' (●); 1% w/w G' (△) and G'' (▲).....	81
Figure 2.20	Dynamic oscillation spectra of Avicel RC591 at 25 °C. 0.2% w/w G' (◇) and G'' (◆); 0.5% w/w G' (○) and G'' (●); 1% w/w G' (△) and G'' (▲).....	84
Figure 2.21	Dynamic oscillation spectra of Carbopol 971P at 25 °C. 0.2% w/w G' (◇) and G'' (◆); 0.5% w/w G' (○) and G'' (●); 1% w/w G' (△) and G'' (▲).....	86
Figure 2.22	Dynamic oscillation spectra of Carbopol 974P at 25 °C. 0.2% w/w G' (◇) and G'' (◆); 0.5% w/w G' (○) and G'' (●); 1% w/w G' (△) and G'' (▲).....	88

Figure 2.23	Dynamic oscillation spectra of HPMC E4MP at 25 °C. 0.2% w/w G' (◇) and G'' (◆); 0.5% w/w G' (○) and G'' (●); 1% w/w G' (△) and G'' (▲).....	90
Figure 2.24	Dynamic oscillation spectra of HPMC K100P at 25 °C. 0.2% w/w G' (◇) and G'' (◆); 0.5% w/w G' (○) and G'' (●); 1% w/w G' (△) and G'' (▲).....	90
Figure 2.25	Dynamic oscillation spectra of HPMC K4MP at 25 °C. 0.2% w/w G' (◇) and G'' (◆); 0.5% w/w G' (○) and G'' (●); 1% w/w G' (△) and G'' (▲).....	91
Figure 2.26	Dynamic oscillation spectra of HPMC K15MP at 25 °C. 0.2% w/w G' (◇) and G'' (◆); 0.5% w/w G' (○) and G'' (●); 1% w/w G' (△) and G'' (▲).....	91
Figure 2.27	Dynamic oscillation spectra of NaCMC low MW at 25 °C. 0.2% w/w G' (◇) and G'' (◆); 0.5% w/w G' (○) and G'' (●); 1% w/w G' (△) and G'' (▲).....	94
Figure 2.28	Dynamic oscillation spectra of NaCMC med MW at 25 °C. 0.2% w/w G' (◇) and G'' (◆); 0.5% w/w G' (○) and G'' (●); 1% w/w G' (△) and G'' (▲).....	95
Figure 2.29	Dynamic oscillation spectra of NaCMC high MW at 25 °C. 0.2% w/w G' (◇) and G'' (◆); 0.5% w/w G' (○) and G'' (●); 1% w/w G' (△) and G'' (▲).....	96
Figure 2.30	Dynamic oscillation spectra of placebo nasal formulations at 25 °C. ee521730 w/w G' (◇) and G'' (◆); ee521950 w/w G' (○) and G'' (●); ee522260 w/w G' (△) and G'' (▲).....	98
Figure 3.1	The optical trapping setup used for microrheology measurements .	106
Figure 3.2	Image taken using the microrheology set up showing a microsphere trapped by the laser and focussed, untrapped microspheres. ....	111
Figure 3.3	Rheological synergism of mucoadhesive polymeric nasal formulations at a frequency of 1.22 Hz. Data represents the average $\Delta G'$ value of three replicates. The standard error bars were omitted due to their minimal size.....	113

Figure 3.4	Rheological synergism of mucoadhesive polymeric nasal formulations at a frequency of 1.22 Hz. Data represents the average $\Delta G''$ value of three replicates. The standard error bars were omitted due to their minimal size. ....	113
Figure 3.5	Rheological synergism of placebo nasal formulations at a frequency of 1.22 Hz. Data represents the average $\Delta G'$ and $\Delta G''$ value of three replicates. ....	114
Figure 3.6	Microrheological synergism of mucoadhesive polymeric nasal formulations at a frequency of 1.22 Hz. Data represents the average $\Delta G'$ value of three replicates $\pm$ S.D. ....	119
Figure 3.7	Microrheological synergism of mucoadhesive polymeric nasal formulations at a frequency of 1.22 Hz. Data represents the average $\Delta G''$ value of three replicates $\pm$ S.D. ....	119
Figure 3.8	Microrheological synergism of placebo nasal formulations at a frequency of 1.22 Hz. Data represents the average $\Delta G''$ value of three replicates $\pm$ S.D. ....	120
Figure 4.1	Sagittal cross section of a porcine nasal cavity .....	130
Figure 4.2	Diagrammatical method showing excision of respiratory mucosa from a porcine nasal cavity. (a) shows the incisions made in order to free the turbinate from the nasal cavity, (b) shows further removal of the turbinate, (c) the excised turbinate, (d) unravelling the turbinate scroll, (e) the respiratory mucosa is gently peeled away from the cartilaginous scroll, (f) the fully excised respiratory mucosa. ....	131
Figure 4.3	Texture analysis set up showing probe and mucoadhesive test rig. ....	132
Figure 4.4	Experimental procedure used in mucoadhesive strength measurements. a. the probe is lowered at a speed of 1.00 mm/s. b. the probe applies a force of 5 N ensures a contact time of 30 s between the mucosa and gel formulation. c. the probe is withdrawn at a speed of 1.00 mm/s to a distance of 15 mm. ....	133
Figure 4.5	Representation of a typical texture analyser force/time plot showing $F_{max}$ and AUC. ....	134

Figure 4.6	Mean $F_{\max}$ ( $\pm$ S.D.) results for 0.2% (blue), 0.5% (red) and 1% w/w (green) mucoadhesive polymeric nasal formulations. (n=3). ....	136
Figure 4.7	Mean AUC( $\pm$ S.D.) results for 0.2% (blue), 0.5% (red) and 1% w/w (green) mucoadhesive polymeric nasal formulations. (n=3). ....	137
Figure 4.8	Mean $F_{\max}$ ( $\pm$ S.D.) results for placebo nasal formulations. (n=3)..	141
Figure 4.9	Mean AUC ( $\pm$ S.D.) results for placebo nasal formulations. (n=3).	141
Figure 5.1	Effect of spray actuation on mean apparent viscosity ( $\pm$ S.D) of 0.2% w/w mucoadhesive polymeric nasal formulations measured at $100\text{ s}^{-1}$ . *denotes statistical significance to polymeric formulations ( $P < 0.05$ ) (n=3).....	153
Figure 5.2	Effect of spray actuation on mean apparent viscosity ( $\pm$ S.D) of 0.2% w/w mucoadhesive polymeric nasal formulations measured at $1200\text{ s}^{-1}$ . *denotes statistical significance to polymeric formulations ( $P < 0.05$ ) (n=3).....	153
Figure 5.3	Effect of spray actuation on mean apparent viscosity ( $\pm$ S.D) of 0.5% w/w mucoadhesive polymeric nasal formulations measured at $100\text{ s}^{-1}$ . *denotes statistical significance to polymeric formulations ( $P < 0.05$ ) (n=3).....	154
Figure 5.4	Effect of spray actuation on mean apparent viscosity ( $\pm$ S.D) of 0.5% w/w mucoadhesive polymeric nasal formulations measured at $1200\text{ s}^{-1}$ . * denotes statistical significance to polymeric formulations ( $P < 0.05$ ) (n=3).....	154
Figure 5.5	Effect of spray actuation on mean apparent viscosity ( $\pm$ S.D) of 1% w/w mucoadhesive polymeric nasal formulations measured at $100\text{ s}^{-1}$ . *denotes statistical significance to polymeric formulations ( $P < 0.05$ ) (n=3). ....	155
Figure 5.6	Effect of spray actuation on mean apparent viscosity ( $\pm$ S.D) of 1% w/w mucoadhesive polymeric nasal formulations measured at $1200\text{ s}^{-1}$ . *denotes statistical significance to polymeric formulations ( $P < 0.05$ ) (n=3). ....	155
Figure 5.7	Rheological flow profiles of Avicel CL611 before spraying (blue), immediately after spraying (red) and 15 minutes after spraying	

	(green). Profiles are representative of 0.2% w/w measured at 100 s <sup>-1</sup> (a) and 1200 s <sup>-1</sup> (b), 0.5% w/w measured at 100 s <sup>-1</sup> (c) and 1200 s <sup>-1</sup> (d) and 1% w/w measured at 100 s <sup>-1</sup> (e) and 1200 s <sup>-1</sup> (f). .....	167
Figure 5.8	Rheological flow profiles of Avicel RC591 before spraying (blue), immediately after spraying (red) and 15 minutes after spraying (green). Profiles are representative of 0.2% w/w measured at 100 s <sup>-1</sup> (a) and 1200 s <sup>-1</sup> (b), 0.5% w/w measured at 100 s <sup>-1</sup> (c) and 1200 s <sup>-1</sup> (d) and 1% w/w measured at 100 s <sup>-1</sup> (e) and 1200 s <sup>-1</sup> (f). .....	169
Figure 5.9	Rheological flow profiles of Carbopol 971P before spraying (blue), immediately after spraying (red) and 15 minutes after spraying (green). Profiles are representative of 0.2% w/w measured at 100 s <sup>-1</sup> (a) and 1200 s <sup>-1</sup> (b), 0.5% w/w measured at 100 s <sup>-1</sup> (c) and 1200 s <sup>-1</sup> (d) and 1% w/w measured at 100 s <sup>-1</sup> (e) and 1200 s <sup>-1</sup> (f). .....	171
Figure 5.10	Rheological flow profiles of Carbopol 974P before spraying (blue), immediately after spraying (red) and 15 minutes after spraying (green). Profiles are representative of 0.2% w/w measured at 100 s <sup>-1</sup> (a) and 1200 s <sup>-1</sup> (b), 0.5% w/w measured at 100 s <sup>-1</sup> (c) and 1200 s <sup>-1</sup> (d) and 1% w/w measured at 100 s <sup>-1</sup> (e) and 1200 s <sup>-1</sup> (f). .....	172
Figure 5.11	Rheological flow profiles of HPMC E4MP before spraying (blue), immediately after spraying (red) and 15 minutes after spraying (green). Profiles are representative of 0.2% w/w measured at 100 s <sup>-1</sup> (a) and 1200 s <sup>-1</sup> (b), 0.5% w/w measured at 100 s <sup>-1</sup> (c) and 1200 s <sup>-1</sup> (d) and 1% w/w measured at 100 s <sup>-1</sup> (e) and 1200 s <sup>-1</sup> (f). .....	173
Figure 5.12	Rheological flow profiles of HPMC K100P before spraying (blue), immediately after spraying (red) and 15 minutes after spraying (green). Profiles are representative of 0.2% w/w measured at 100 s <sup>-1</sup> (a) and 1200 s <sup>-1</sup> (b), 0.5% w/w measured at 100 s <sup>-1</sup> (c) and 1200 s <sup>-1</sup> (d) and 1% w/w measured at 100 s <sup>-1</sup> (e) and 1200 s <sup>-1</sup> (f). .....	175
Figure 5.13	Rheological flow profiles of HPMC K4MP before spraying (blue), immediately after spraying (red) and 15 minutes after spraying (green). Profiles are representative of 0.2% w/w measured at 100 s <sup>-1</sup>	

	(a) and 1200 s <sup>-1</sup> (b), 0.5% w/w measured at 100 s <sup>-1</sup> (c) and 1200 s <sup>-1</sup> (d) and 1% w/w measured at 100 s <sup>-1</sup> (e) and 1200 s <sup>-1</sup> (f). .....	176
Figure 5.14	Rheological flow profiles of HPMC K15MP before spraying (blue), immediately after spraying (red) and 15 minutes after spraying (green). Profiles are representative of 0.2% w/w measured at 100 s <sup>-1</sup> (a) and 1200 s <sup>-1</sup> (b), 0.5% w/w measured at 100 s <sup>-1</sup> (c) and 1200s <sup>-1</sup> (d) and 1% w/w measured at 100 s <sup>-1</sup> (e) and 1200 s <sup>-1</sup> (f). .....	177
Figure 5.15	Rheological flow profiles of NaCMC low MW before spraying (blue), immediately after spraying (red) and 15 minutes after spraying (green). Profiles are representative of 0.2% w/w measured at 100 s <sup>-1</sup> (a) and 1200 s <sup>-1</sup> (b), 0.5% w/w measured at 100 s <sup>-1</sup> (c) and 1200s <sup>-1</sup> (d) and 1% w/w measured at 100 s <sup>-1</sup> (e) and 1200 s <sup>-1</sup> (f). .	179
Figure 5.16	Rheological flow profiles of NaCMC med MW before spraying (blue), immediately after spraying (red) and 15 minutes after spraying (green). Profiles are representative of 0.2% w/w measured at 100 s <sup>-1</sup> (a) and 1200 s <sup>-1</sup> (b), 0.5% w/w measured at 100 s <sup>-1</sup> (c) and 1200s <sup>-1</sup> (d) and 1% w/w measured at 100 s <sup>-1</sup> (e) and 1200 s <sup>-1</sup> (f). .	180
Figure 5.17	Rheological flow profiles of NaCMC high MW before spraying (blue), immediately after spraying (red) and 15 minutes after spraying (green). Profiles are representative of 0.2% w/w measured at 100 s <sup>-1</sup> (a) and 1200 s <sup>-1</sup> (b), 0.5% w/w measured at 100 s <sup>-1</sup> (c) and 1200s <sup>-1</sup> (d) and 1% w/w measured at 100 s <sup>-1</sup> (e) and 1200 s <sup>-1</sup> (f). .	181

## List of tables

Table 1.1	Characteristics of mucoadhesive polymers.....	25
Table 1.2	Typical viscosity values for 2% (w/v) aqueous solutions of Methocel. Viscosities measured at 20°C. Reproduced from Handbook of Pharmaceutical Excipients (5th Edition)* .....	26
Table 2.1	Composition details of placebo nasal formulation ee521730 (Information supplied by GlaxoSmithKline R&D, Ware, UK). .....	45
Table 2.2	Composition details of placebo nasal formulation ee521950 (Information supplied by GlaxoSmithKline R&D, Ware, UK). .....	45
Table 2.3	Composition details of placebo nasal formulation ee522260 (Information supplied by GlaxoSmithKline R&D, Ware, UK). .....	46
Table 2.4	Mucoadhesive polymer content of placebo nasal formulations (Data supplied from GlaxoSmithKline R&D, Ware, UK).....	55
Table 2.5	Flow behaviour index ( $n$ ) and consistency index ( $K_c$ ) derived from the power law model of mucoadhesive polymeric nasal formulations measured at $100 \text{ s}^{-1}$ ( $n=3$ ).....	72
Table 2.6	Flow behaviour index ( $n$ ) and consistency index ( $K_c$ ) derived from .....	73
Table 2.7	Flow behaviour index ( $n$ ) and consistency index ( $K_c$ ) derived from the power law model of placebo nasal formulations measured at $100 \text{ s}^{-1}$ ( $n=3$ ).....	73
Table 2.8	Flow behaviour index ( $n$ ) and consistency index ( $K_c$ ) derived from the power law model of placebo nasal formulations measured at $1200 \text{ s}^{-1}$ ( $n=3$ ).....	74
Table 2.9	Mean loss tangent ( $\tan \delta$ ) values $\pm$ S.D. for mucoadhesive polymeric nasal formulations at five representative frequencies ( $n=3$ ). .....	79
Table 2.10	Mean loss tangent ( $\tan \delta$ ) values $\pm$ S.D. for mucoadhesive polymeric nasal formulations at five representative frequencies ( $n=3$ ). .....	80
Table 2.11	Mean loss tangent ( $\tan \delta$ ) values $\pm$ S.D. for placebo nasal formulations at five representative frequencies ( $n=3$ ). .....	81

Table 3.1	Summary of the advantages and disadvantages of the optical trap system to measure microrheology*.....	105
Table 4.1	KBR buffer solution composition (Hall <i>et al.</i> , 2002) .....	129

## List of equations

$\tau = K\gamma^n$ [Equation 2.1].....	47
$\Delta G' = G'_{(mix)} - (G'_{(polymer)} + G'_{(mucin)})$ [Equation 3.1] .....	110
$\Delta G'' = G''_{(mix)} - (G''_{(polymer)} + G''_{(mucin)})$ [Equation 3.2] .....	110

## **Publications and presentations**

**Armstrong, M.**, Mains, J., Wilson, C. (2013) The impact of spray device actuation on the apparent viscosity and rheological behaviour of polymeric nasal sprays. (Submitted).

**Armstrong, M.**, Walker, S., Mains, J., Wilson, C. (2013) Drug Delivery Across the Nasal Mucosa in Mucoadhesive Materials and Drug Delivery Systems [Book Chapter] (Published May 2014).

**Armstrong, M.**, Mains, J., Wilson, C. Rheological characterisation of polymeric nasal sprays and the impact of spray device actuation. [Poster Presentation] In AAPS 2012, Chicago, USA.

**Mathie, M.**, Bone, G., Boyter, A., McInnes F. Effect of spray device actuation on rheological flow behavior and mucoadhesive strength of placebo nasal formulations. [Poster Presentation] In AAPS 2011, Washington, USA.

**Mathie, M.**, Bone, G., Boyter, A., McInnes F. Effect of spray device actuation on rheological flow behavior and mucoadhesive strength of placebo nasal formulations. [Poster Presentation] In UKPharmSci 2011, Nottingham, UK.